



DUR
NAVAL
MONTEREY 1943

NAVAL POSTGRADUATE SCHOOL

Monterey, California



THESIS

DESIGN AND ANALYSIS OF COORDINATED
BANK-TO-TURN (CBTT) AUTOPILOTS FOR
BANK-TO-TURN (BTT) MISSILES

by

Ioannis S. Lioulis

December 1983

Thesis Advisor:

Daniel J. Collins

Approved for public release, distribution unlimited

REPORT DOCUMENTATION PAGE

READ INSTRUCTIONS
BEFORE COMPLETING FORM

1. REPORT NUMBER		2. GOVT ACCESSION NO.	3. RECIPIENT'S CATALOG NUMBER
4. TITLE (and Subtitle) Design and Analysis of Coordinated Bank-To-Turn (CBTT) Autopilots for Bank-To-Turn (BTT) Missiles			5. TYPE OF REPORT & PERIOD COVERED Master's Thesis December 1983
7. AUTHOR(s) Ioannis S. Lioulis			6. PERFORMING ORG. REPORT NUMBER
9. PERFORMING ORGANIZATION NAME AND ADDRESS Naval Postgraduate School Monterey, California 93943			8. CONTRACT OR GRANT NUMBER(s)
11. CONTROLLING OFFICE NAME AND ADDRESS Naval Postgraduate School Monterey, California 93943			10. PROGRAM ELEMENT, PROJECT, TASK AREA & WORK UNIT NUMBERS
14. MONITORING AGENCY NAME & ADDRESS (if different from Controlling Office)			12. REPORT DATE December 1983
			13. NUMBER OF PAGES 309
			15. SECURITY CLASS. (of this report) Unclassified
			15a. DECLASSIFICATION/DOWNGRADING SCHEDULE
16. DISTRIBUTION STATEMENT (of this Report) Approved for public release, distribution unlimited			
17. DISTRIBUTION STATEMENT (of the abstract entered in Block 20, if different from Report)			
18. SUPPLEMENTARY NOTES			
19. KEY WORDS (Continue on reverse side if necessary and identify by block number) Coordinated Bank-to-turn Autopilots Nonlinear CBTT autopilots Pitch-Yaw-Roll uncoupled autopilots Control laws Elliptical and Circular airframe Linear CBTT autopilots			
20. ABSTRACT (Continue on reverse side if necessary and identify by block number) This work addresses the design and analysis of the Pitch, Yaw and Roll autopilot for application to the Bank-To-Turn (BTT) missiles. At first, the linear uncoupled channels were designed and analyzed according to the desired requirements. Utilizing the uncoupled channels, the linear coupled autopilots were designed, not including the inertial, kinematic and aerodynamic cross-coupling. Then, the nonlinear CBTT autopilots were designed and			

20. Continuation

analyzed, using the linear CBTT (coordinated Bank-To-Turn) models, which now have coupled with kinematic, inertial and aerodynamic cross-coupling. The minimization of the above kinematic and inertial coupling and their effects were completed using feedbacks of angle-of-attack and rate of angle-of-attack in the Pitch autopilot.

Approved for public release, distribution unlimited

Design and Analysis of Coordinated Bank-to-Turn
(CBTT) Autopilots for Bank-To-Turn (BTT) Missiles

by

Ioannis S. Lioulis
Lieutenant, Hellenic Navy
B.S.E.E, Naval Postgraduate School, 1983

Submitted partial fulfillment of the
requirements for the degree of

MASTER OF SCIENCE IN ENGINEERING SCIENCE

from the

NAVAL POSTGRADUATE SCHOOL
December 1983

ABSTRACT

This work addresses the design and analysis of the Pitch, Yaw and Roll autopilot for application to the Bank-To-Turn (BTT) missiles. At first, the linear uncoupled channels were designed and analyzed according to the desired requirements. Utilizing the uncoupled channels, the linear coupled autopilots were designed, not including the inertial, kinematic and aerodynamic cross-coupling. Then, the nonlinear CBTT autopilots were designed and analyzed, using the linear CBTT (coordinated Bank-To-Turn) models, which now have coupled with kinematic, inertial and aerodynamic cross-coupling. The minimization of the above kinematic and inertial coupling and their effects were completed using feedbacks of angle-of-attack and rate of angle-of-attack in the Pitch autopilot.

TABLE OF CONTENTS

I.	INTRODUCTION	22
II.	LINEAR DESIGN AND ANALYSIS OF UNCOUPLED AUTOPILOT FOR CIRCULAR AND ELLIPTICAL AIRFRAME .	25
A.	GENERAL	25
B.	AIRFRAME CONFIGURATIONS	26
C.	UNCOUPLED LINEAR PITCH CHANNEL	31
D.	UNCOUPLED LINEAR YAW CHANNEL	55
E.	UNCOUPLED LINEAR ROLL CHANNEL.	75
III.	LINEAR DESIGN AND ANALYSIS OF COUPLED AUTOPILOTS FOR CIRCULAR AND ELLIPTICAL AIRFRAMES.	88
A.	GENERAL	88
B.	AERODYNAMIC MODELS FOR THE CIRCULAR AIRFRAME	88
C.	CBTT AUTOPILOT CONTROL LAWS FOR CIRCULAR AIRFRAME	93
D.	ANALYSIS OF LINEAR CBTT AUTOPILOTS FOR CIRCULAR AIRFRAME.	101
E.	AERODYNAMIC MODEL FOR ELLIPTICAL AIRFRAME .	104
F.	CBTT AUTOPILOTS CONTROL LAWS FOR ELLIPTICAL AIRFRAME	105
G.	ANALYSIS OF LINEAR CBTT AUTOPILOTS FOR ELLIPTICAL AIRFRAME.	108
H.	RELATIVE STABILITY OF CBTT AUTOPILOTS OF CIRCULAR AND ELLIPTICAL AIRFRAMES	111
I.	CONCLUSIONS	114
IV.	NONLINEAR ANALYSIS OF CBTT AUTOPILOT FOR CIRCULAR AND ELLIPTICAL AIRFRAMES.	115
A.	GENERAL	115



B.	CONTROL LAWS FOR ELLIPTICAL AIRFRAMES.	118
C.	AERODYNAMIC MODELS FOR ELLIPTICAL AIRFRAMES.	124
D.	ANALYSIS OF NONLINEAR CBTT AUTOPILOTS FOR ELLIPTICAL AIRFRAME.	127
E.	CBTT PERFORMANCE WITH IDEAL AIRFRAME DYNAMICS FOR ELLIPTICAL AIRFRAME	131
F.	CONTROL LAWS FOR CIRCULAR AIRFRAME	142
G.	AERODYNAMIC MODELS FOR CIRCULAR AIRFRAME	156
H.	ANALYSIS OF NONLINEAR CBTT AUTOPILOT FOR CIRCULAR AIRFRAME.	158
I.	EFFECT OF INCREASING PITCH CHANNEL SPEED OF RESPONSE	161
J.	EFFECT OF INERTIAL AND KINEMATIC CROSS-COUPLING IN PITCH CHANNEL	175
K.	CONCLUSIONS	179
V.	MINIMIZATION OF THE KINEMATIC AND INERTIAL CROSS COUPLING EFFECTS	187
A.	GENERAL	187
B.	CROSS-COUPLING OF CBTT AUTOPILOTS.	187
C.	KINEMATIC AND INERTIAL CROSS-COUPLING IN PITCH AUTOPILOT.	190
D.	MINIMIZATION OF THE KINEMATIC AND INERTIAL CROSS-COUPLING EFFECTS IN ELLIPTICAL AIRFRAME	192
E.	MINIMIZATION OF KINEMATIC AND INERTIAL COUPLING IN ELLIPTICAL AIRFRAME.	209
F.	MINIMIZATION OF THE KINEMATIC AND INERTIAL CROSS-COUPLING EFFECTS IN CIRCULAR AIRFRAME.	220
G.	MINIMIZATION OF KINEMATIC AND INERTIAL COUPLING IN CIRCULAR AIRFRAME	238
H.	CONCLUSIONS AND RECOMMENDATIONS.	241



APPENDIX A:	MISSILE SIZING AND MASS PROPERTIES . . .	247
APPENDIX B:	NONLINEAR AERODYNAMIC DATA	248
APPENDIX C:	REQUIREMENTS FOR UNCOUPLED AUTOPILOTS .	249
APPENDIX D:	CSMP PROGRAMS FOR PITCH UNCOUPLED AUTOPILOT	250
APPENDIX E:	CSMP PROGRAMS FOR YAW UNCOUPLED AUTOPILOT	253
APPENDIX F:	CSMP PROGRAMS FOR ROLL UNCOUPLED AUTOPILOT	256
APPENDIX G:	CSMP PROGRAM FOR LINEAR CBTT AUTOPILOTS.	259
APPENDIX H:	CSMP PROGRAMS FOR NONLINEAR CBTT AUTOPILOTS OF ELLIPTICAL AIRFRAME. . . .	263
APPENDIX I:	CSMP PROGRAMS FOR NONLINEAR CBTT AUTOPILOTS OF CIRCULAR AIRFRAME	272
APPENDIX J:	CSMP PROGRAMS FOR MINIMIZATION OF KINEMATIC AND INERTIAL COUPLING EFFECTS	287
APPENDIX K:	CSMP PROGRAMS FOR MINIMIZATION OF KINEMATIC AND INERTIAL COUPLING	297
LIST OF REFERENCES		307
BIBLIOGRAPHY		308
INITIAL DISTRIBUTION LIST		309



LIST OF TABLES

I.	Linearized Aerodynamic Derivatives ($M=3.95$) . . .	34
II.	CBTT Performance of Elliptical Airframe	152
III.	CBTT Performance of Circular Airframe	173
IV.	Kinematic and Inertial Cross-Coupling for Elliptical Airframe	218
V.	Characteristics of the Achieved Inertial Acceleration (n_z) for Circular Airframe	237
VI.	Kinematic and Inertial Coupling for Circular Airframe	239



LIST OF FIGURES

2.1	Bank-To-Turn Autopilot (BTT)	27
2.2	Model of Circular Configuration - 1/6 Scale .	28
2.3	Model of Elliptical Configuration - 1/6 Scale	29
2.4	Aerodynamic Sign Convention and Axis	32
2.5	Uncoupled Pitch Channel Autopilot	33
2.6	Pitch Control Laws	36
2.7	Pitch Normal Acceleration vs Time; Uncoupled Pitch Channel; Circular Airframe.	45
2.8	Pitch Angular Rate vs Time; Uncoupled Pitch Channel; Circular Airframe.	46
2.9	Pitch Tail Incidence vs Time; Uncoupled Pitch Channel; Circular Airframe.	47
2.10	Pitch Normal Acceleration vs Time; Uncoupled Pitch Channel; Elliptical Airframe.	52
2.11	Pitch Angular Rate vs Time; Uncoupled Pitch Channel; Elliptical Airframe.	53
2.12	Pitch Tail Incidence vs Time; Uncoupled Pitch Channel; Elliptical Airframe.	54
2.13	Uncoupled Yaw channel	57
2.14	Yaw Control Laws	58
2.15	Yaw Normal Acceleration vs Time; Uncoupled Yaw Channel; Elliptical Airframe.	65
2.16	Yaw Angular Rate (r) vs Time; Uncoupled Yaw Channel; Circular Airframe.	67
2.17	Yaw Tail Incidence vs Time; Uncoupled Yaw Channel; Circular Airframe.	68
2.18	Yaw Acceleration vs Time; Uncoupled Yaw Channel; Elliptical Airframe.	72



2.19	Yaw Angular Rate vs Time; Uncoupled Yaw Channel; Elliptical Airframe.	73
2.20	Yaw Tail Incidence vs Time; Uncoupled Yaw Channel; Elliptical Airframe.	74
2.21	Uncoupled Roll channel.	76
2.22	Roll Control laws	77
2.23	Roll Angle vs Time; Uncoupled Roll Channel; Circular or Elliptical Airframe	83
2.24	Roll Angular Rate vs Time; Uncoupled Roll Channel; Circular or Elliptical Airframe	84
2.25	Roll Tail Incidence vs Time; Uncoupled Roll Channel; Circular Airframe.	85
2.26	Roll Tail Incidence vs Time; Uncoupled Roll Channel; Elliptical Airframe	86
3.1	Linear Pitch Channel Dynamic Model.	90
3.2	Linear Lateral (Roll/Yaw) Dynamic Model	92
3.3	CBTT Lateral Control law	94
3.4	Coordinated Missile Motion for Coordinated Bank-To-Turn (CBTT) and Limited Bank-To-Turn (LBTT) Control Policies	96
3.5	Sideslip Angle vs Time; Linear CBTT Autopilot; Circular Airframe	102
3.6	Roll Angle vs Time; Linear CBTT Autopilot; Circular Airframe	103
3.7	Sideslip Angle vs Time; Linear CBTT Autopilot Elliptical Airframe	109
3.8	Roll Angle vs Time; Linear CBTT Autopilot; Elliptical Airframe	110
3.9	Major Contributors to the Quality of Sideslip Control of CBTT Autopilot	112
4.1	Nonlinear Pitch Channel Dynamic Model	116



4.2	Nonlinear Lateral (Roll/Yaw) Channel Dynamics Model	117
4.3	Nonlinear Pitch Control Law	119
4.4	CBTT Nonlinear Lateral Control Laws	120
4.5	Achieved Inertial Acceleration vs Time; CBTT of Elliptical Airframe.	128
4.6	Achieved Body-fixed Acceleration (n_{z_B}) vs Time; CBTT of Elliptical Airframe	129
4.7	Achieved Body-Fixed Acceleration (n_{y_B}) vs Time; CBTT of Elliptical Airframe	130
4.8	Angle of Attack vs Time; CBTT of Elliptical Airframe	132
4.9	Sideslip Angle vs Time; CBTT of Elliptical Airframe	133
4.10	Body Pitch Angular Rate vs Time; CBTT of Elliptical Airframe	134
4.11	Roll Angular Rate vs Time; CBTT of Elliptical Airframe	135
4.12	Yaw Angular Rate vs Time; CBTT of Elliptical Airframe	136
4.13	Roll Angle vs Time; CBTT of Elliptical Airframe	137
4.14	Pitch Tail Incidence vs Time; CBTT of Elliptical Airframe	138
4.15	Yaw Tail Incidence vs Time; CBTT of Elliptical Airframe	139
4.16	Roll Tail Incidence vs Time; CBTT of Elliptical Airframe	140
4.17	Achieved Inertial Acceleration vs Time; CBTT of Elliptical Airframe; Ideal Airframe Dynamics	143



4.18	Angle of Attack vs Time; CBTT of Elliptical Airframe; Ideal Airframe Dynamics	144
4.19	Sideslip Angle vs Time; CBTT of Elliptical Airframe; Ideal Airframe Dynamics	145
4.20	Body Pitch Angular Rate vs Time; CBTT of Elliptical Airframe; Ideal Airframe Dynamics.	146
4.21	Body Yaw Angular Rate vs Time; CBTT Elliptical Airframe; Ideal Airframe Dynamics.	147
4.22	Pitch Tail Incidence vs Time; CBTT of Elliptical Airframe; Ideal Airframe Dynamics .	148
4.23	Yaw Tail Incidence vs Time; CBTT of Elliptical Airframe; Ideal Airframe Dynamics	149
4.24	Roll Tail Incidence vs Time; CBTT of Elliptical Airframe; Ideal Airframe Dynamics .	150
4.25	Critical Feedback Loops for CBTT	151
4.26	Nonlinear Pitch Control Law	154
4.27	CBTT Nonlinear Lateral Control Laws.	157
4.28	Achieved Inertial Acceleration vs Time; CBTT of Circular Airframe	160
4.29	Achieved Body-Fixed Acceleration (n_{z_B}) vs Time; CBTT of Circular Airframe	162
4.30	Achieved Body-Fixed Acceleration (n_{y_B}) vs Time; CBTT of Circular Airframe	163
4.31	Angle of Attack vs Time; CBTT of Circular Airframe $K_{A_1} = -0.0274$	164
4.32	Sideslip Angle vs Time; CBTT of Circular Airframe $K_{A_1} = -0.0274$	165
4.33	Pitch Body Angular Rate vs Time; CBTT of Circular Airframe; $K_{A_1} = -0.0274$	166



4.34	Yaw Body Angular rate vs Time; CBTT of Circular Airframe; $K_{A_1} = -0.0274$	167
4.35	Roll Body Angular Rate vs time; CBTT of Circular Airframe; $K_{A_1} = -0.0274$	168
4.36	Roll Angle vs Time; CBTT of Circular Airframe; $K_{A_1} = -0.0274$	169
4.37	Pitch Tail Incidence vs Time; CBTT of Circular Airframe; $K_{A_1} = -0.0274$	170
4.38	Yaw Tail Incidence vs Time; CBTT of Circular Airframe; $K_{A_1} = -0.0274$	171
4.39	Roll Tail Incidence vs Time; CBTT of Circular Airframe; $K_{A_1} = -0.0274$	172
4.40	Achieved Inertial Acceleration vs Time; CBTT of Circular Airframe with Faster Responding Pitch Channel; $K_{A_2} = -0.0387$	174
4.41	Achieved Body-Fixed Acceleration (n_{Z_B}) vs Time; CBTT of Circular Airframe with Faster Responding Pitch Channel; $K_{A_2} = -0.0387$	176
4.42	Achieved Inertial Acceleration vs Time; CBTT of Circular Airframe; Faster Pitch Channel; Inertial and Kinematic Cross-Coupling into Pitch Channel Removed	177
4.43	Achieved Body-Fixed Acceleration (n_{Z_B}) vs Time; CBTT of Circular Airframe; Faster Pitch Channel; Inertial and Kinematic Cross-Coupling into Pitch Channel Removed	178



4.44	Achieved Body-Fixed Acceleration (n_{YB}) vs Time (t); CBTT of Circular Airframe; Faster Pitch Channel; Inertial and Kinematic Cross-Coupling into Pitch Channel Removed	180
4.45	Angle of Attack vs Time; CBTT of Circular Airframe; Faster Pitch Channel; Inertial and Kinematic Cross-Coupling into Pitch channel Removed	181
4.46	Sideslip Angle vs Time; CBTT of Circular Airframe; Faster Pitch Channel; Inertial and Kinematic Cross-Coupling into Pitch Channel Removed	182
4.47	Pitch Body Angular Rate vs Time; CBTT of Circular Airframe; Faster Pitch Channel; Inertial and Kinematic Cross-Ccoupling into Pitch Channel Removed	183
4.48	Yaw Body Angular Rate vs Time; CBTT of Circular Airframe; Faster Pitch Channel; Inertial and Kinematic Cross-Coupling into Pitch Channel Removed	184
4.49	Pitch Tail Incidence vs Time CBTT of Circular Airframe; Faster Pitch Channel; Inertial and Kinematic Cross-Coupling into Pitch Channel Removed	185
4.50	Yaw Tail Incidence vs Time CBTT of Circular Airframe; Faster Pitch Channel; Inertial and Kinematic Cross-Coupling into Pitch Channel Removed	186
5.1	Stability Augmentation Systems (SAS) with q/δ_p of Pitch Channel; CBTT of Elliptical Airframe .	194
5.2	Root Locus of SAS with q/δ_p , of Pitch Channel; CBTT of Elliptical Airframe	196
5.3	Stability Augmentation System (SAS) with a/δ_p , of Pitch Channel; CBTT of Elliptical Airframe .	198
5.4	Root Locus of SAS with a/δ_p , of Pitch Channel; CBTT of Elliptical Airframe	200



5.5	Modified Nonlinear Pitch Autopilot; CBTT of Elliptical Airframe	202
5.6	Achieved Inertial Acceleration vs Time; Modified Pitch Channel; CBTT of Elliptical Airframe; $K = -3.07$	204
5.7	Achieved Inertial Acceleration vs Time; Modified Pitch Channel; CBTT of Elliptical Airframe; $K = -19.37$	207
5.8	Kinematic Coupling vs Time; CBTT of Elliptical Airframe.	210
5.9	Inertial Coupling vs Time; CBTT of Elliptical Airframe.	211
5.10	Kinematic Coupling vs Time; CBTT of Elliptical Airframe; Modified Pitch Channel for Minimization of Coupling Effects	212
5.11	Inertial Coupling vs Time; CBTT of Elliptical Airframe; Modified Pitch Channel for Minimization of Coupling Effects	213
5.12	Modified Pitch Control Law for Minimization of Kinematic and Inertial Cross-Coupling; CBTT of Elliptical Airframe	215
5.13	Kinematic Coupling vs Time; Modified Pitch Channel for Minimization of Kinematic Coupling; CBTT of Elliptical Airframe	216
5.14	Inertial Coupling vs Time; Modified Pitch Channel for Minimization of Inertial Coupling; CBTT of Elliptical Airframe	217
5.15	Achieved Inertial Acceleration vs Time; Modified Pitch Channel for Minimization of Couplings; CBTT of Elliptical Airframe.	219
5.16	Stability Augmentation System SAS with q/δ_p ; CBTT of Circular Airframe	221
5.17	Root Locus of SAS with q/δ_p ; CBTT of Circular Airframe.	223



5.18	Stability Augmentation System SAS with a/δ_p ; CBTT of Circular Airframe	224
5.19	Root Locus of SAS with a/δ_p ; CBTT of Circular Airframe.	226
5.20	Modified Pitch Channel for Circular Airframe.	227
5.21	Achieved Inertial Acceleration vs Time; CBTT of Circular Airframe; $K = -15.6, K_{A_2} = -0.0387$	230
5.22	Achieved Inertial Acceleration vs Time; CBTT of Circular Airframe; $K = -70.88, K_{A_2} = -0.0387$	232
5.23	Achieved Inertial Acceleration vs Time CBTT of Circular Airframe; $K = -15.6, K_{A_1} = -0.0274$	233
5.24	Achieved Inertial Acceleration vs Time CBTT of Circular Airframe; $K = -70.88, K_{A_1} = -0.0274$	234
5.25	Achieved Inertial Acceleration vs Time; CBTT of Circular Airframe $K = -70.88, K_{A_1} = -0.0274,$ $K_{yp}=1.0$	235
5.26	Modified Pitch Control Law for Minimization of the Cross-Coupling; CBTT of Circular Airframe	240
5.27	Minimized Inertial Coupling vs Time; CBTT of Circular Airframe	242
5.28	Minimized Kinematic Coupling vs Time; CBTT of Circular Airframe	243
5.29	Achieved Inertial Acceleration vs Time; Modified Pitch Channel for Minimization of Coupling; CBTT of Circular Airframe	244



TABLES OF SYMBOLS AND ABBREVIATION

BTT	Bank-to-Turn
CBTT	coordinated Bank-to-Turn, minimum sideslip, positive α , ϕ_e 180 deg
CRDT	coordinated Roll-During-Turn
C_l	rolling moment coefficient
C_{l_β}	slope of curve of rolling moment coefficient, C_l vs β
$C_{l_{\delta_R}}$	change in C_l per degree roll control incidence, δ_R
$C_{l_{\delta_Y}}$	change in C_l per degree yaw control incidence, δ_Y
C_m	pitching moment coefficient
C_{m_α}	slope of curve of pitching moment coefficient C_m vs α
$C_{m_{\delta_P}}$	change in C_m per degree pitch control incidence, δ_P
C_N	normal force coefficient
C_{N_α}	slope of curve of normal force coefficient C_N vs α
$C_{N_{\delta_P}}$	change in C_N per degree pitch control incidence, δ_P
C_n	yawing moment coefficient
C_{n_β}	slope of curve of yawing moment coefficient, C_n vs β



q	pitch angular acceleration about Y_B
Q_e	constant or equilibrium pitch angular rate
r	yaw angular rate about Z_B
r_c	yaw angular rate command (coordination command)
r	yaw angular acceleration about Z_B
S	reference area for coefficients = $\pi \text{ ft}^2$
STT	Skid-to-Turn, roll attitude stabilized
u	velocity component in X_B direction
v	velocity component in Y_B direction. assumed to be constant
V	constant missile flight path velocity
V	missile velocity vector
w	velocity component in Z_B direction
X_B	body-fixed roll axis, along axis of symmetry, positive forward
Y_B	body-fixed pitch axis, positive starboard
Y_V	vehicle axis in local horizontal direction, approximated as inertial axis
Z_B	body-fixed yaw axis, forms right handed orthogonal system with X_B and Y_B
Z_V	vehicle axis in downward direction along local gravity vector, approximated as inertial axis
n_z	achieved normal acceleration in Z_V direction
n_{z_c}	commanded normal acceleration in Z_B direction
n_{Y_B}	achieved normal acceleration in Y_B direction
n_{Z_B}	achieved normal acceleration in Z_B direction



$C_{n\delta_Y}$	change in C_n per degree yaw control incidence, δ_Y
$C_{n\delta_R}$	change in C_n per degree yaw control incidence, δ_R
C_Y	side force coefficient
$C_{Y\beta}$	slope of curve of side force coefficient C_Y vs β
$C_{Y\delta_Y}$	change in C_Y per degree yaw control incidence, δ_Y
$C_{Y\delta_R}$	change in C_Y per degree roll control incidence, δ_R
d	reference length for coefficients = 2 ft.
I_{YY}	moment of inertia about Y_B axis
I_{ZZ}	moment of inertia about Z_B axis
I_{XX}	moment of inertia about X_B axis
K_A	autopilot pitch acceleration error gain
K_{YP}	CBTT autopilot coordination branch gain
LBTT	limited Bank-to-Turn may or may not be coordinated, positive and negative α , $\phi_e \leq 90$ or 45 degrees
P	roll rate about X_B
P	roll acceleration about X_B
P_e	constant or equilibrium roll angular rate
POC	preferred orientation control
q	dynamic pressure
q	pitch rate about Y_B

n_Y	achieved normal acceleration in Y_V direction
n_C	normal acceleration command from guidance computer in Z_V direction plus anti-gravity bias command
ϕ_C	roll attitude command from guidance computer, zero degrees in Z_V direction and 90 degrees in Y_V direction
ϕ	roll attitude, zero degrees in $-Z_V$ direction and 90 degrees in Y_V direction
θ	Elevation Euler Angle, second rotation, $(q \cos\phi - r \sin\phi) dt$
δ_P	pitch control incidence (positive tail incidence produces negative pitching moment)*
δ_{P_C}	commanded pitch control incidence, δ_P
δ_Y	yaw control incidence (positive tail incidence produces negative yawing moments)*
δ_{Y_C}	commanded yaw control incidence, δ_Y
δ_R	roll control incidence (positive tail incidence produces positive rolling moment)
δ_{R_C}	commanded roll control incidence, δ_R
α_e	constant or equilibrium angle-of-attack
α	angle-of-attack
$\dot{\alpha}$	angle-of-attack rate
$\bar{\alpha}$	modified form of estimated angle-of-attack for autopilot coordination command
β	angle of sideslip
$\dot{\beta}$	sideslip angular rate



ACKNOWLEDGEMENT

I would like to express my gratitude to Dr. D. J. Collins, for his valuable assistance during the course of this work. To my wife I would like to offer my thanks and love for her patience and understanding.



I. INTRODUCTION

In recent years, the application of Bank-to-turn guidance to missiles has generated considerable interest. This interest has been motivated by the drag reduction, which the Bank-to-turn (BTT) controlled missiles offer, over the conventional cruciform roll stabilized, skid-to-turn controlled missiles.

Bank-to-turn steering may provide improved performance for missile systems. In addition, the ramjet engine inlet configuration is believed to provide a greater range capability than other inlet configurations. BTT control is required to satisfy the sideslip constraints imposed by chin inlets. Despite these facts, there are unanswered questions concerning BTT systems stability during homing, guidance performance, autopilot and guidance logic design and subsystem requirements which must be investigated before Bank-to-turn steering can be considered a viable method of control for high performance missiles.

Many missile programs were initiated during the past decade to improve their capability via Bank-to-turn control. The results have advanced the understanding of the different missile subsystems. In the autopilot area, many types of autopilots have been found which force the missile to roll or bank so that the steering maneuver



occurs with the airframe oriented in a specified or preferred direction with respect to the incoming airstream. This entire class of autopilots may be referred to as preferred orientation control autopilots.

Also, simplified guidance studies which neglect radome effects and assume coordinated missile motion have shown that CBTT can provide acceptable performance with roll rates that are not excessive for autopilot control. These studies were made for a medium range area defense mission and a long range suppression mission and considered both high lift and moderate lift configurations [Ref. 1].

The present work reviews the design and analysis of the pitch, Yaw and Roll autopilot for application to the Bank-to-turn (BTT) missiles developed in [Ref. 2]. At first, the linear model of the uncoupled autopilot channels will be designed and analysed in the critical areas of concern regarding the response of CBTT control for the circular and elliptical airframes. Then, the designed autopilot channels will be coupled using suitable aerodynamic models and a measure of sideslip control is obtained by roll command to the linearized CBTT autopilot. The relative stability of the autopilot branches and means for improving stability will be discussed. In a later chapter the non-linear three dimensional model will be designed, using a three dimensional aerodynamic model and

the same control laws described in the linear studies, except for a minor modification to the coordinating branch dependence on Angle-of-Attack and also the inclusion of Anti-Gravity Bias. Next, the kinematic and inertial coupling effects between pitch and yaw dynamics will be studied. Transients in maneuver plane acceleration are caused in the above cross-coupling effects and are in the form of overshoots and undershoots. Coupling transients will be reduced by increasing pitch stability. The technique of feedbacks of Angle-of-Attack and rate of Angle-of-Attack for the pitch autopilot, will be considered, in order to decrease kinematic and inertial cross-coupling effects. Finally conclusions and recommendations for future study will be stated.

II. LINEAR DESIGN AND ANALYSIS OF UNCOUPLED AUTOPILOTS FOR CIRCULAR AND ELLIPTICAL AIRFRAME

A. GENERAL

The linear design and analysis started with uncoupled autopilot channels, i.e. aerodynamic, kinematic and control law cross-coupling between Pitch, Yaw and Roll channels were removed. The autopilot design technique was classical, using a combination of frequency response and root locus techniques [Ref. 2], providing the range of required missile body angular rates, control motions and minimizing the influence of aerodynamic variations on desired responses. To achieve the desired maneuver plane acceleration response for the CBTT autopilot, both Pitch and Roll uncoupled autopilots were designed to have a time constant of 0.5 sec in order to achieve the desired maneuver plane speed of response. The Yaw channel which follows the Roll channel motion to produce desired coordination (i.e. minimization of sideslip angles), was designed to have a more rapid response than the Roll channel, having 0.39 sec for circular and 0.36 sec for elliptical time constant in the maneuver plane acceleration response. The whole design was done for the constant flight condition of 60 KFT altitude and mach number 3.95. The design discussed here was developed by Arrow [Ref. 2].

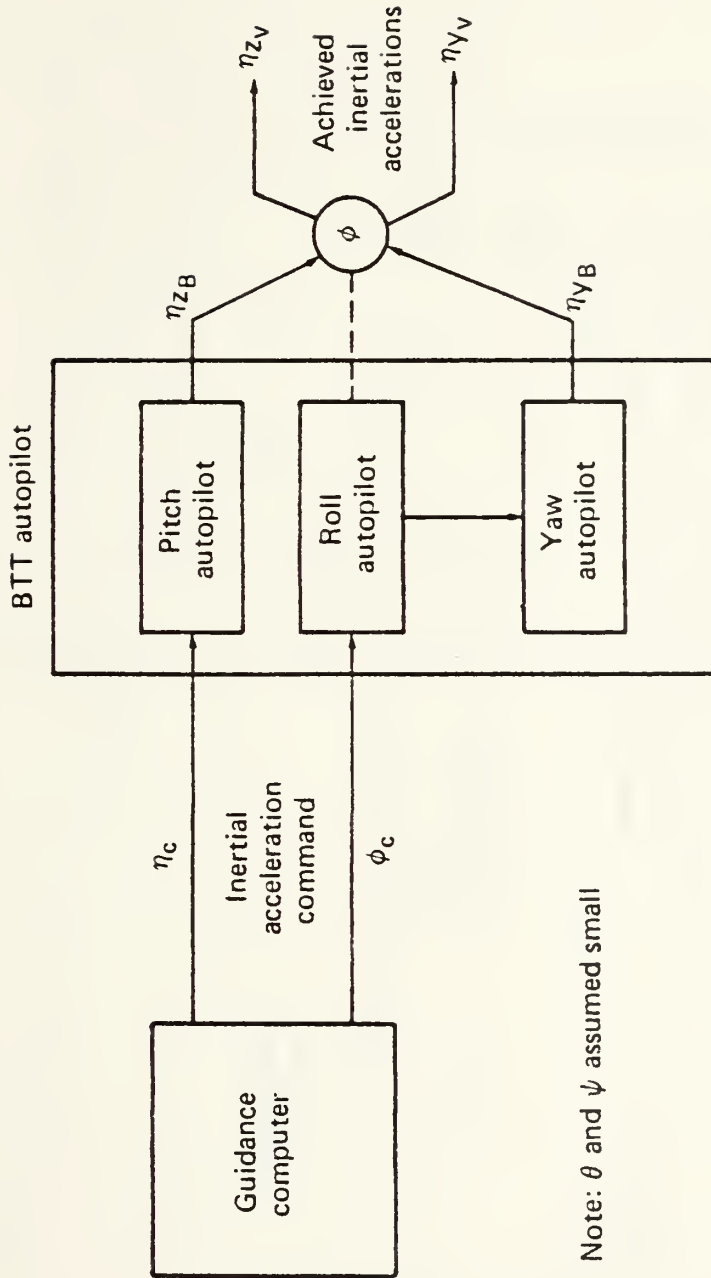
In this chapter the airframe configurations, the aerodynamic models and control laws for the Pitch, Yaw and Roll channel are reviewed. The transfer functions for both circular and elliptical configuration are derived. An analysis for every channel in regard to the acceleration responses, the body angular rates and control surface deflection is made. Also, a comparison of airframe responses for every channel is made, considering the relative stability and required control surfaces.

A general block diagram, of the channels and the command, which are applied to the control laws is shown in Figure 2.1. A number of the Figures shown in this report have been taken from [Ref. 2].

B. AIRFRAME CONFIGURATIONS

The U.S. National Aeronautics and Space Administration maintains a continuing research effort in missile related aerodynamics. In this effort monoplanar missile concepts have been considered, in part, because of the relatively low geometric profile that can be achieved for convenient carriage [Ref. 1]. The two Airframe Configurations studied in this research were taken from [Ref. 1] and are shown in Figure 2.2 and Figure 2.3. The circular cross sectional body has a closure ratio $A_{\text{base}}/A_{\text{max}}$ of 0.69 and the A_{max} occurs at 68.0% body. The Elliptical has an exact 3:1





Note: θ and ψ assumed small

Fig. 2.1 Bank-to-Turn Autopilot (BTT)

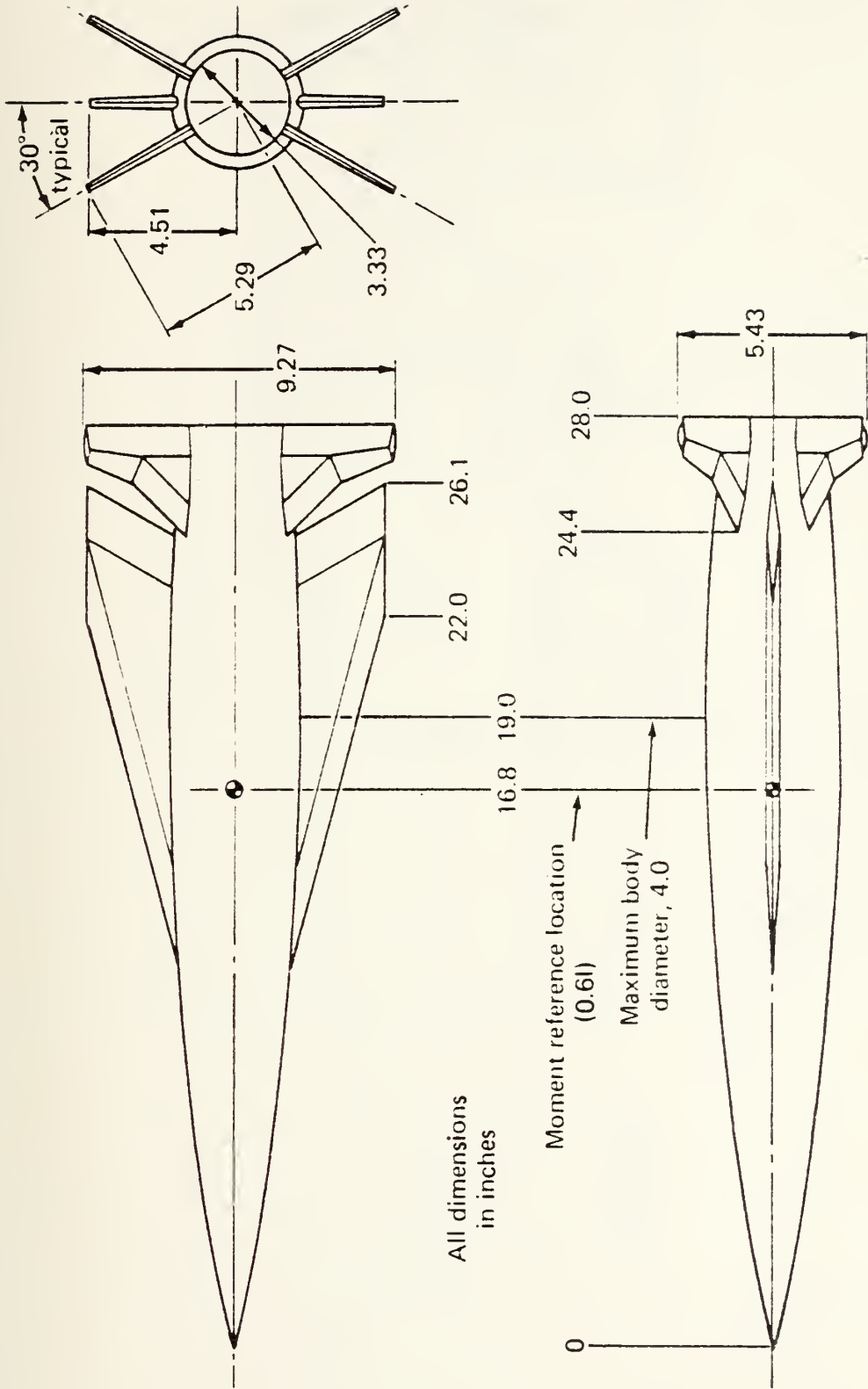


Fig. 2.2 Model of Circular Configuration - 1/6 Scale

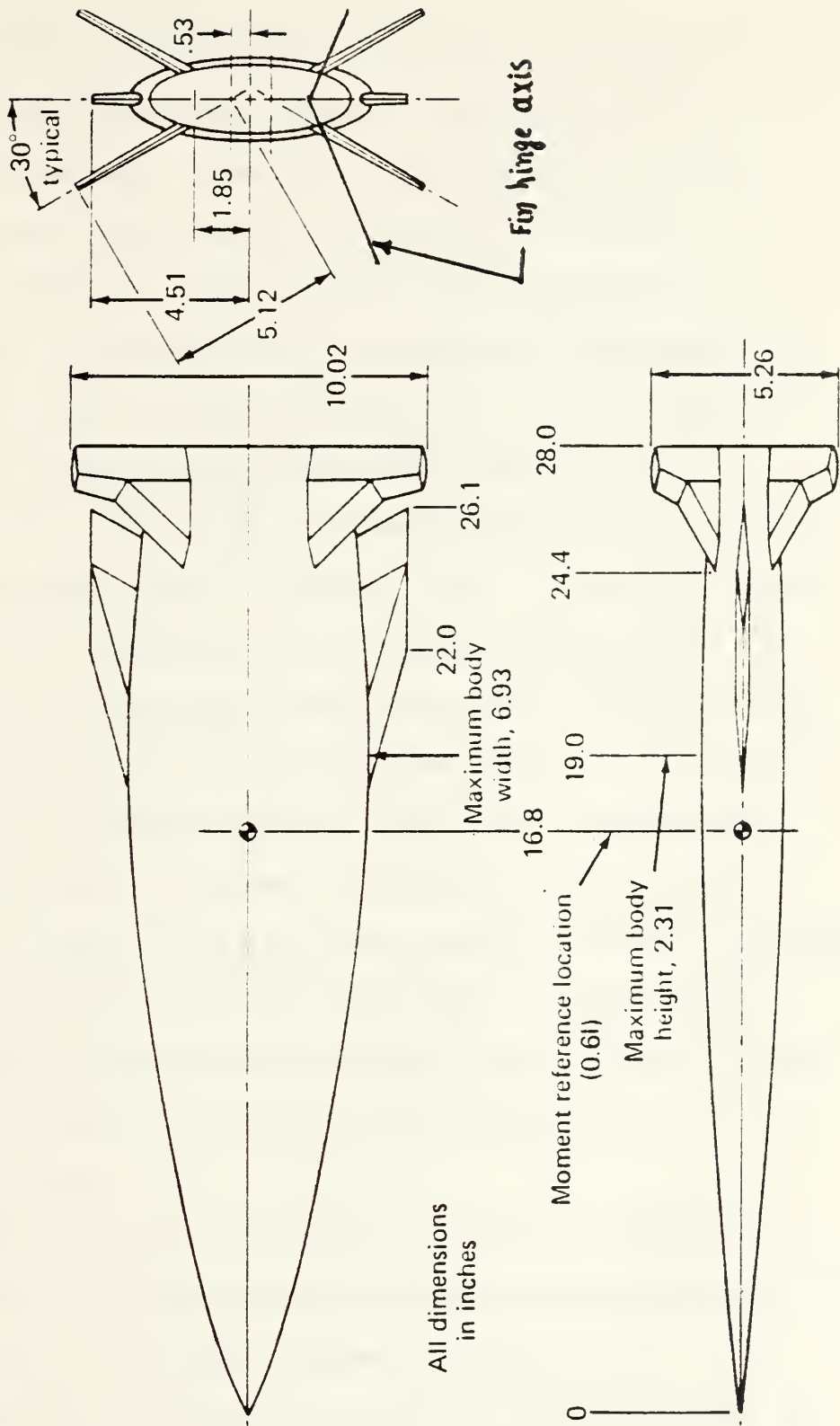


Fig. 2.3 Model of Elliptical Configuration - 1/6 Scale

elliptical cross section, and its cross section area is the same as the area of circular body. The span of both airframes is the same. The wing area and span for the circular concept were chosen as typical of current maneuvering missiles. The wing for the elliptical configuration was determined by projecting the elliptical body on the circular bodywing planform. The resultant exposed wing planform then became the wing for the elliptical body. The tails for each design had a dihedral of 30° degrees as shown in Figure 2.2. In order for tail deflection to be compatible with complex surfaces of the afterbody of the elliptical configuration, the tail hinge line was skewed such that a 10° degrees deflection measured at the body-tail juncture had a resultant 7.04° degrees surface deflection, as shown in Figure 2.3 and [Ref. 1]. Comparison of the elliptical cross section concept with the circular cross section concept indicates the following:

1. About 25 percent more normal force, that is nearly independent of angle of attack can be achieved at supersonic speeds.

2. Values of the longitudinal stability parameter C_{m_a} are more positive, with more pronounced nonlinearities in pitching moment occurring at subsonic speeds.

3. Levels of directional stability are increased and are more compatible with levels of longitudinal stability.

4. Noticeably more yaw control is available, although suitable locations for tails on the body are more limited because of the geometry of the elliptical body.

C. UNCOUPLED LINEAR PITCH CHANNEL

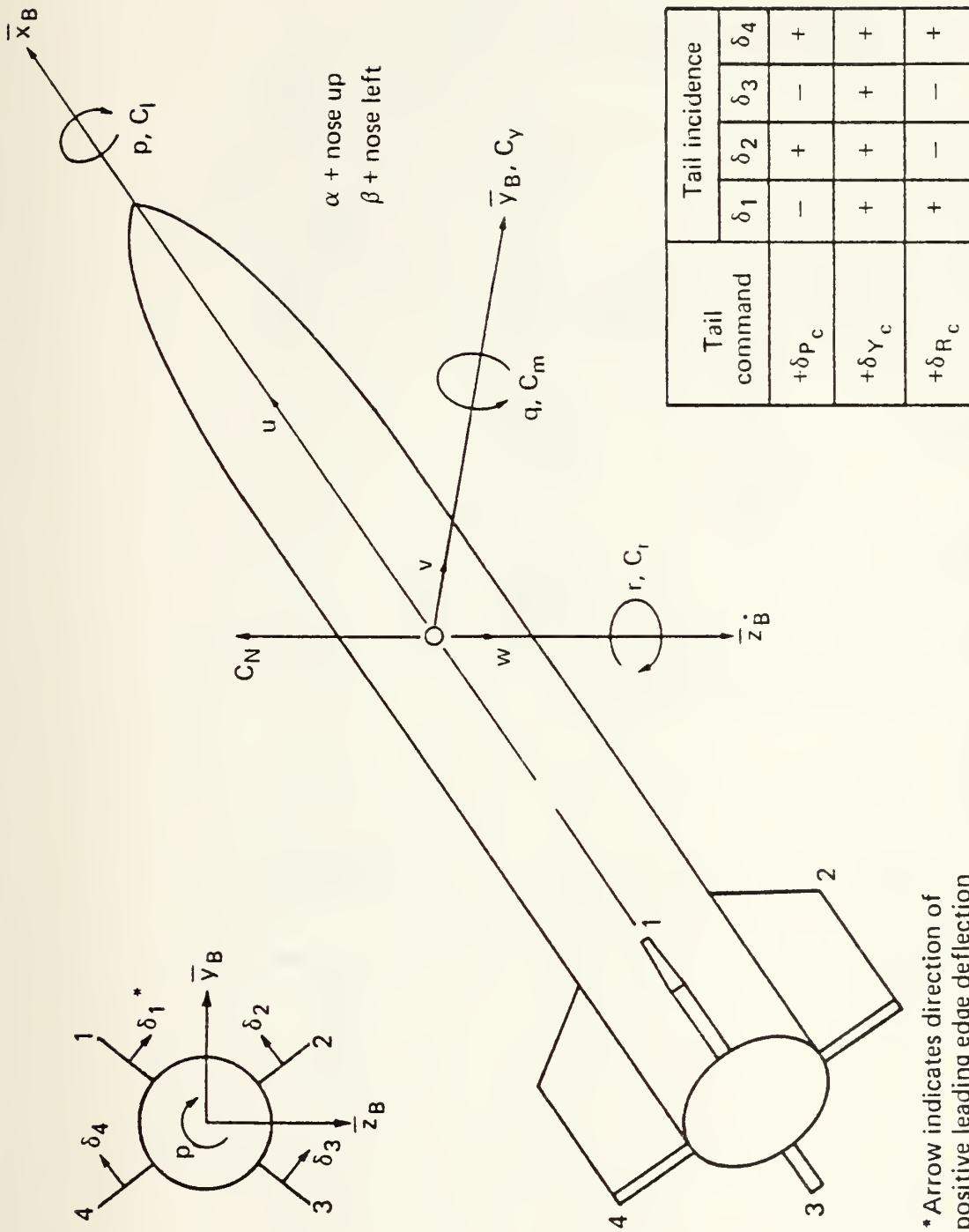
1. Aerodynamic Model

The initial phase in the design of the CBTT autopilots involves the design of the uncoupled pitch channel. The linear pitch channel dynamic model which is used, is shown in Figure 2.5.

This figure is taken from [Ref. 2]. The above model is linearized for stability studies. The following three assumptions were made:

- a. Plane $X_\beta - Z_\beta$ is the maneuver plane, shown in figure 2.4
- b. Missile is trimmed in pitch, that is $M_y = 0$, at fixed values of α , q and δ_p .
- c. Missile roll rate is constant. Using the foregoing assumptions, and the approximation that the variation in forward velocity (u), is equal to zero, a simplified set of longitudinal equations of motion are constructed applicable to short period motion. These equations describe the two degree of freedom, short period mode longitudinal motion.

Linearized aerodynamic derivatives for $M=3.95$ are provided in Table I.



* Arrow indicates direction of positive leading edge deflection

Fig. 2.4 Aerodynamic Sign Convection And axis.

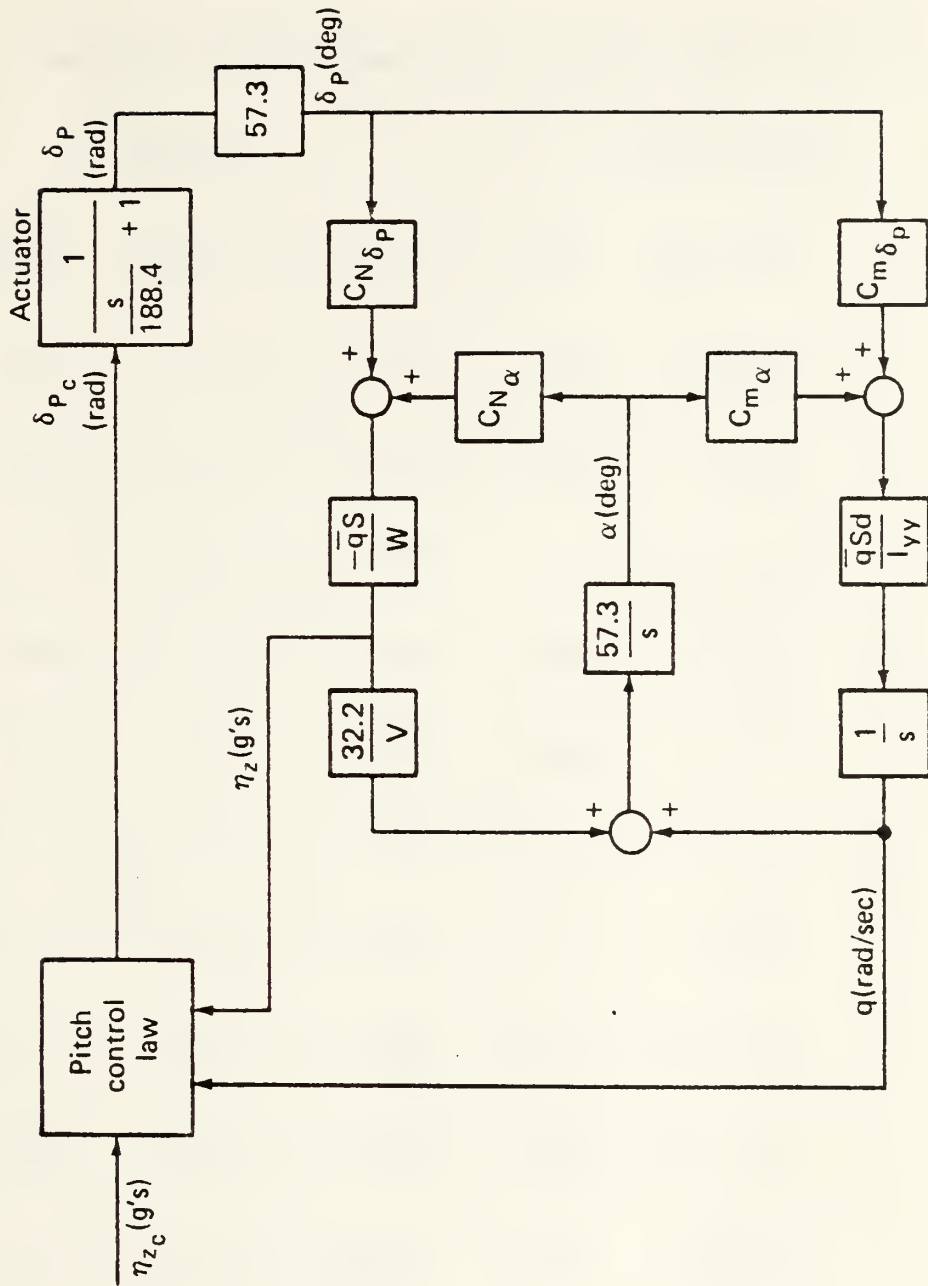


Fig. 2.5 Uncoupled Pitch Channel Autopilot

TABLE I

Linearized Aerodynamic Derivatives (M = 3.95)

	<u>Circular</u>			<u>Elliptical</u>		
	<u>$\alpha = 0^\circ$</u>	<u>$\alpha = 10^\circ$</u>	<u>$\alpha = 20^\circ$</u>	<u>$\alpha = 0^\circ$</u>	<u>$\alpha = 10^\circ$</u>	<u>$\alpha = 20^\circ$</u>
C_{Y_β}	- .065	- .082	- .111	- .043	- .054	- .064
C_{n_β}	- .025	- .019	- .003	+ .024	+ .024	+ .032
C_{l_β}	0	- .009	- .020	0	- .027	- .040
$C_{Y_{\delta_Y}}$	+ .021	+ .022	+ .028	+ .016	+ .015	+ .019
$C_{n_{\delta_Y}}$	- .050	- .053	- .062	- .042	- .039	- .045
$C_{l_{\delta_Y}}$	0	- .016	- .038	0	- .010	- .023
$C_{Y_{\delta_R}}$	0	- .009	- .022	0	- .006	- .014
$C_{n_{\delta_R}}$	0	+ .018	+ .044	0	+ .014	+ .032
$C_{l_{\delta_R}}$	+ .031	+ .035	+ .044	+ .023	+ .023	+ .029
C_{N_α}	+ .15	+ .17	+ .22	+ .18	+ .22	+ .30
$C_{N_{\delta_P}}$	+ .04	+ .04	+ .05	+ .02	+ .02	+ .025
C_{m_α}	- .060	- .065	- .118	+ .015	+ .0137	- .125
$C_{m_{\delta_P}}$	- .080	- .095	- .115	- .055	- .055	- .075

Reference C.G. at 0.6

2. Pitch Control Law

The pitch control laws for the circular and elliptical airframes are shown in Figure 2.6 as given in the [Ref. 2]. Lag-Leads were used to prevent guidance noise saturation problems. An integrator was used in the acceleration error branch of the circular control law to satisfy the guidance requirement of zero steady state error. In the elliptical control law, an integrator was placed in the rate error path (i.e path after the adder $(q+y)$, as shown in Figure 2.6) for reduction of the acceleration response overshoot below 10 percent and a gain $K=1.1053$ was placed in series with the acceleration command for zero steady state acceleration error.

A normal acceleration command n_{z_c} equal to 1 gee, is applied to the pitch control law which uses measurements of missile body pitch angular rate (q) and pitch normal acceleration (n_z) to determine the required actuator command (δ_{p_c}) . The actuator is modeled as a first order lag at 188.4 rad/sec and is shown in Figure 2.5.

3. Transfer Functions of Aerodynamic Models for Circular Airframe

The equations which are represented by the block diagram of the aerodynamic model, of the uncoupled Pitch channel (Figure 2.5) are:

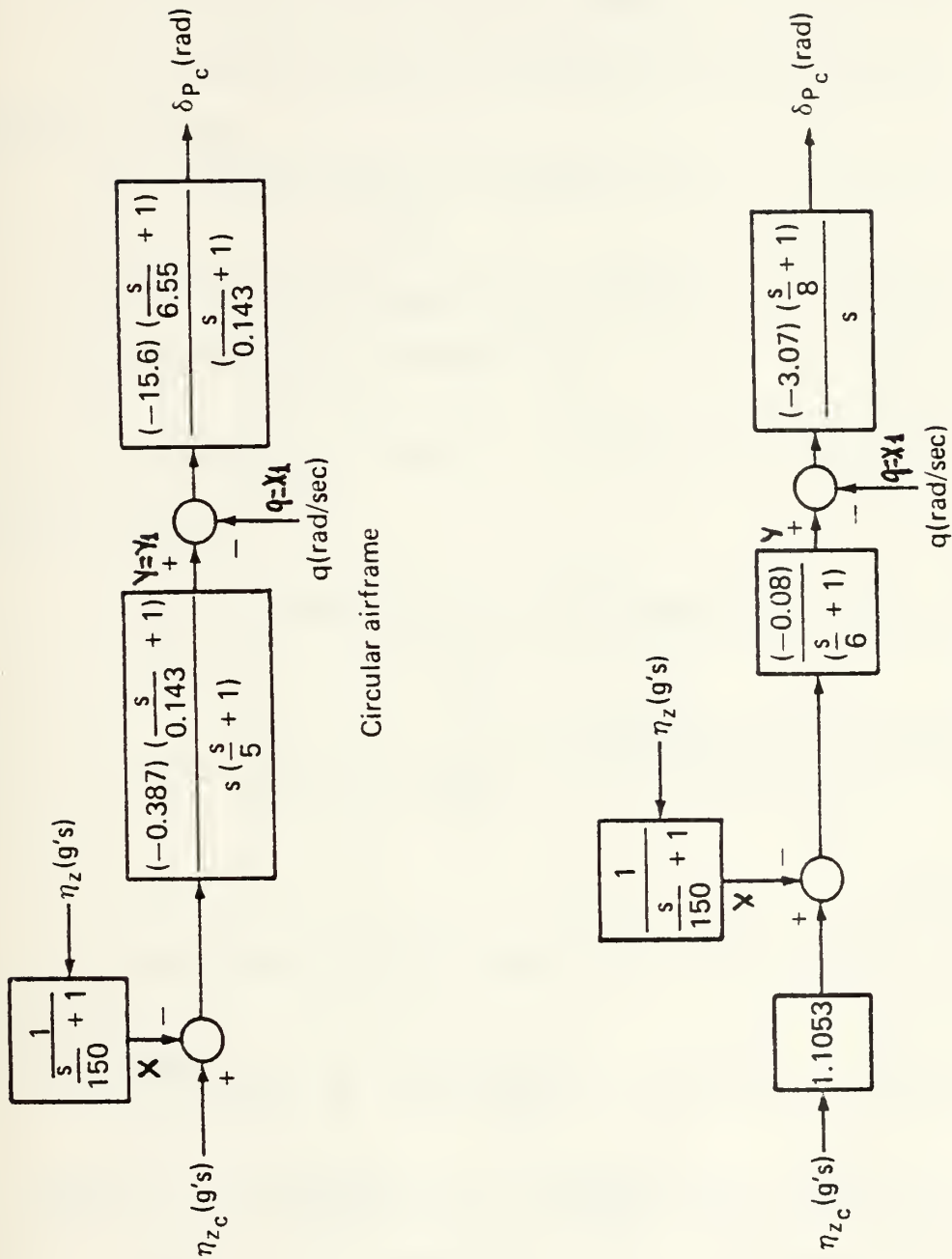


Fig. 2.6 Pitch Control Laws

$$\dot{q} = \bar{q} s d [C_{m\alpha} \cdot \alpha + 57.3 C_{m\delta_p} \cdot \delta_p] / I_{yy} \quad [\text{rad/sec}] \quad (\text{II.C.3-1})$$

$$\eta_z = -\bar{q} s [57.3 C_{N\delta_p} \delta_p + C_{N\alpha} \alpha] / W \quad [\text{gees}] \quad (\text{II.C.3-2})$$

$$\dot{\alpha} = 57.3 [q + 32.2 \eta_z / V] \quad [\text{deg}] \quad (\text{II.C.3-3})$$

Utilizing Laplace Transformation, the above equation becomes:

$$s q = \frac{\bar{q} s d (C_{m\alpha} \alpha + 57.3 C_{m\delta_p} \delta_p)}{I_{yy}} \quad (\text{II.C.3-4})$$

$$\eta_z = -\bar{q} s (57.3 C_{N\delta_p} \delta_p + C_{N\alpha} \alpha) / W \quad (\text{II.C.3-2})$$

$$s \alpha = 57.3 (q + 32.2 \eta_z / V) \quad (\text{II.C.3-5})$$

Introducing equation II.C.3-2 to II.C.3-5 the last equation yields.

$$s q = \frac{\bar{q} s d (C_{m\alpha} \alpha + 57.3 C_{m\delta_p} \delta_p)}{I_{yy}} \quad (\text{II.C.3-6})$$

$$s \alpha = 57.3 \left[q + \frac{32.2}{V} \left(- \frac{\bar{q} s (57.3 C_{N\delta_p} \delta_p + C_{N\alpha} \alpha)}{W} \right) \right] \quad (\text{II.C.3-7})$$

Rearranging above equations, in terms of q and a, we obtain:

$$s q - \left(\frac{\bar{q} s d}{I_{yy}} \cdot C_{m\alpha} \right) \cdot \alpha = \left(\frac{57.3 \bar{q} s d}{W} C_{N\delta_p} \right) \cdot \delta_p \quad (\text{II.C.3-8})$$

$$-57.3 q + \left(s + \frac{k \bar{q} s C_{N\alpha}}{W} \right) \alpha = \left(- \frac{57.3 k \bar{q} s}{W} \cdot C_{N\delta_p} \right) \cdot \delta_p \quad (\text{II.C.3-9})$$

Applying the Cramer's rule in the system of equation II.C.3-8 and II.C.3-9 the transfer functions q/δ_p and α/δ_p are obtained.

$$\frac{q}{\delta_P} = \frac{\left(\frac{57.3 \bar{q} S d}{I_{yy}} \cdot C_{m\delta_P} \right) S + \left(\frac{57.3 K (\bar{q} S)^2 d (C_{N\alpha} C_{m\delta_P} - C_{m\alpha} C_{N\delta_P})}{W \cdot I_{yy}} \right)}{S^2 + \left(\frac{K \bar{q} S C_{N\alpha}}{W} \right) S - \frac{57.3 \bar{q} S d C_{m\alpha}}{I_{yy}}}$$

(II.C.3-10)

And:

$$\frac{\alpha}{\delta_P} = \frac{\left(-\frac{57.3 K \bar{q} S C_{N\delta_P}}{W} \right) S + \left(\frac{3283.29 \bar{q} \cdot S \cdot d \cdot C_{m\delta_P}}{I_{yy}} \right)}{S^2 + \left(\frac{K \bar{q} S C_{N\alpha}}{W} \right) \cdot S - \frac{57.3 \bar{q} S d C_{m\alpha}}{I_{yy}}}$$

(II.C.3-11)

Where:

$$K = \frac{(57.3)(32.2)}{1000} = 0.48$$

$$S = 3.14159 \text{ (ft}^2\text{)}$$

$$d = 2 \text{ (ft)}$$

$$\bar{q} = 1650 \text{ (lbs/ft}^2\text{)}$$

$$I_{yy} = 804 \text{ (slug-ft}^2\text{)}$$

$$W = 2525 \text{ (lbs)}$$

$$C_{m\alpha} = -0.06$$

$$C_{m\delta_P} = -0.08$$

$$C_{N\alpha} = 0.15$$

$$C_{N\delta_P} = 0.04$$

$$a_e = 0$$

As referred to in Appendix A and Table I. After substituting the aforementioned values into equation II.C.3-10, it becomes:

$$\frac{q}{\delta_P} = \frac{-1.3361 \cdot s - 0.159}{22.545 \times 10^{-3} \cdot s^2 + 3.3633 \times 10^{-3} s + 1} \quad (1/sec) \quad (II.C.3-12)$$

Introducing equation II.C.3-12 into equation

II.C.3-2 the last equation yields:

$$\frac{\eta_z}{\delta_P} = \frac{\left(\frac{57.3 K (\bar{q} s)^2 C_{N\delta_P} C_{N\alpha}}{W^2} \right) \cdot s - \frac{3283.29 (\bar{q} s)^2 d C_{m\delta_P} C_{N\alpha}}{I_{yy} \cdot W}}{s^2 + \left(\frac{K \cdot \bar{q} s C_{N\alpha}}{W} \right) \cdot s - \frac{57.3 \bar{q} s d C_{m\alpha}}{I_{yy}}} - \frac{57.3 \bar{q} s}{W} \quad (II.C.3-13)$$

Substituting the above mentioned values into equation II.C.3-13 and minor manipulating, it yields:

$$\frac{\eta_z}{\delta_P} = \frac{106.074 \times 10^{-3} \cdot s^2 - 18.82}{22.545 \times 10^{-3} \cdot s^2 + 3.3633 \times 10^{-3} s + 1} \quad (gees/rad) \quad (II.C.3-14)$$

The equations II.C.3-12 and II.C.3-14 are the pitch aerodynamic transfer functions for the pitch angular rate q about the Y_B and the achieved maneuver acceleration in the z_B direction (n_z).

4. Design Approach and Analysis For Circular Airframe

A Fixed Flight condition was selected for these preliminary performance studies of circular and elliptical airframes. The selected flight condition, at 60KFT altitude and mach 3.95, provides a sufficiently low dynamic

pressure, so that missile maneuvers will result in large enough angles-of-attack, to exercise side slip control. The above fixed condition was selected, in order to reduce the complexities of design of the CBTT autopilots.

The uncoupled autopilot design technique was classical, using a combination of frequency response and root locus technique [Ref. 2] to achieve practical bandwidths (i.e., sufficient high frequency attenuation) and therefore provides the range of required missile body angular rates and control motions. The analysis of the CBTT autopilot channels is based, on the time responses of maneuver plane acceleration, body angular rates and tail incidence angles.

For purposes of analysis, a CSMP program was written (Appendix D) using the equations which are represented by the block diagrams of aerodynamic model and linear uncoupled pitch control law, as are shown in figures 2.4 and 2.6.

The equations of the uncoupled linear pitch aerodynamic model and control law are:

a. Equations of Control Law

(1) Acceleration Filter Equation

$$X = \frac{1}{\frac{s}{150} + 1} \cdot \eta_2 \quad (\text{II.C.4-1})$$

Rearranging above equation II.C.4-1 one obtains:

$$\dot{X} = -150X + 150\eta_2 \quad (\text{II.C.4-2})$$

(2) Acceleration Compensator Equation

$$Y = \frac{-0.387 \cdot \left(\frac{s}{0.143} + 1\right)}{s \cdot \left(\frac{s}{5} + 1\right)} \cdot (\eta_{2c} - X) \quad (\text{II.C.4-3})$$

Utilizing inverse Laplace Transformation and rearranging the above equation, it becomes:

$$\ddot{Y} + 5\dot{Y} = -1.3531(\dot{\eta}_{2c} - \dot{X}) - 193.5 \times 10^{-3}(\eta_{2c} - X) \quad (\text{II.C.4-4})$$

Using state-space representation of a system, in which the forcing function involves derivative terms [Ref. 5: pp. 675-678] one obtains:

$$\dot{Y}_1 = Y_2 - 1.3531(\eta_{2c} - X) \quad (\text{II.C.4-5})$$

$$\dot{Y}_2 = -5Y_2 + 6.572 \cdot (\eta_{2c} - X) \quad (\text{II.C.4-6})$$

$$Y = Y_1 \quad (\text{II.C.4-7})$$

(3) Rate Compensator Equation

$$\delta P_c = \frac{-15.6 \left(\frac{s}{6.55} + 1\right)}{\left(\frac{s}{0.143} + 1\right)} (Y_1 - X_1) \quad (\text{II.C.4-8})$$

Using Inverse Laplace Transformation, it yields:

$$\dot{\delta P}_c = -0.143 \cdot \delta P_c - 340.58 \times 10^{-3}(\dot{Y}_1 - \dot{X}_1) - 2.2308 \cdot (Y_1 - X_1) \quad (\text{II.C.4-8a})$$

b. Actuator Equation (Figure 2.5):

$$\delta P = \frac{1}{\frac{s}{188.4} + 1} \cdot \delta P_c \quad (\text{II.C.4-9})$$

or

$$\dot{\delta}_p = -188.4 \delta_p + 188.4 \delta_{p_c} \quad (\text{II.C.4-10})$$

c. Equations of Aerodynamic Model

In order to achieve the plots of the time response of q , n_z , δ_p in the linear uncoupled pitch channel, the transfer functions which are represented by the aerodynamic model and derived in section II.C.3, were used:

$$\frac{q}{\delta_p} = \frac{-1.3361s - 0.159}{25.545 \times 10^{-3} s^2 + 3.3633 \times 10^{-3} s + 1} \quad (\text{II.C.4-11})$$

or

$$q (25.545 \times 10^{-3} s^2 + 3.3633 \times 10^{-3} s + 1) = (-1.3361 \cdot s - 0.159) \cdot \delta_p \quad (\text{II.C.4-11a})$$

Rearranging and minor manipulating equation

II.C.4-11a it yields:

$$\ddot{q} + 149.182 \times 10^{-3} \dot{q} + 44.3556 q = -59.2635 \dot{\delta}_p - 7.052 \cdot \delta_p \quad (\text{II.C.4-12})$$

Utilizing state representation of a system in

which the forcing function involves derivative terms, as in section II.C.4, one obtains:

$$\dot{X}_1 = X_2 - 59.2635 \cdot \delta_p \quad (\text{II.C.4-13})$$

$$\dot{X}_2 = -44.3556 X_1 - 149.182 \times 10^{-3} X_2 + 1.789 \delta_p \quad (\text{II.C.4-14})$$

$$q = X_1 \quad (\text{II.C.4-15})$$

Also, rearranging and manipulating in the same

way, equation II.C.3-12 yields:

$$\dot{z}_1 = z_2 - 701.901 \times 10^3 \cdot \delta_p \quad (\text{II.C.4-16})$$

$$\dot{z}_2 = -44.3356 z_1 - 149.182 \times 10^{-3} z_2 - 1.0433 \times 10^{-3} \cdot \delta_p \quad (\text{II.C.4-17})$$

$$\eta_z = - (z_1 + 4.705 \delta_p) \quad (\text{II.C.4-18})$$

Utilizing state-space representation, all the aforementioned equations can be modeled in the following ninth order system:

$$\begin{bmatrix} \dot{X}_1 \\ \dot{X}_2 \\ \dot{Z}_1 \\ \dot{Z}_2 \\ \dot{X} \\ \dot{Y}_1 \\ \dot{Y}_2 \\ \dot{\delta}_{Pc} \\ \dot{\delta}_p \end{bmatrix} = \begin{bmatrix} 0 & 1 & 0 & 0 & 0 & 0 & 0 & 0 & -59.26 \\ -44.34 & -0.15 & 0 & 0 & 0 & 0 & 0 & 0 & 1.7885 \\ 0 & 0 & 0 & 1 & 0 & 0 & 0 & 0 & -0.702 \\ 0 & 0 & -44.34 & -0.15 & 0 & 0 & 0 & 0 & -1.043 \\ 0 & 0 & +150 & 0 & -150 & 0 & 0 & 0 & 4.705 \\ 0 & 0 & 0 & 0 & 0 & 1.353 & 1 & 0 & 0 \\ 0 & 0 & 0 & 0 & 0 & 6.572 & -5 & 0 & 0 \\ 2.231 & 0.341 & 0 & 0 & 0 & -0.461 & -0.341 & -0.143 & -20.2 \\ 0 & 0 & 0 & 0 & 0 & 0 & 0 & 188.4 & -188.4 \end{bmatrix} \begin{bmatrix} X_1 \\ X_2 \\ Z_1 \\ Z_2 \\ X \\ Y_1 \\ Y_2 \\ \delta_{Pc} \\ \delta_p \end{bmatrix} + \begin{bmatrix} 0 \\ 0 \\ 0 \\ 0 \\ 0 \\ -1.35 \\ 6.57 \\ 0.461 \\ 0 \end{bmatrix} \eta_{zc}$$

(II.C.4-19)

where the state variables are:

X_1, X_2 : pitch angular rate state variables
(section II.C.4)

Y_1, Y_2 : Achieved Body Acceleration state variables (section II.C.4)

X : output of Acceleration filter

δ_{Pc} : input command in actuator network

δ_p : tail incidence angle

The state X, X_1, Y_1, δ_{Pc} of control law are shown in figure 2.6.

Executing the program of Appendix D, using an input step function which represents the "1Gee Command" and trim angle of attack $\alpha_e = 0$, the time response plots of pitch normal acceleration n_z , pitch angular rate q and pitch tail incidence δ_p for circular airframe are obtained.

Figure 2.7 shows the pitch acceleration response of the circular airframe due to a one Gee acceleration command, when the Missile Aerodynamic Models are linearized about zero angle of attack (α). The response has a 0.5 seconds time constant, steady state error 0.005 and 2.5% overshoot, which are according to the requirements referred to in appendix C.

Figures 2.8 and 2.9 show the required body angular rate and control surface deflection, to achieve the acceleration response. These responses matched those presented in [Ref 2].

5. Design Approach and Analysis For Elliptical Airframe

The design technique used for the elliptical airframe, is the same as that of the circular airframe. The analysis of the Pitch channel for the elliptical airframe was based again, on the time response plots.

For the above purposes, a CSMP program was written, as in the case of circular airframe, referred to in Appendix D.

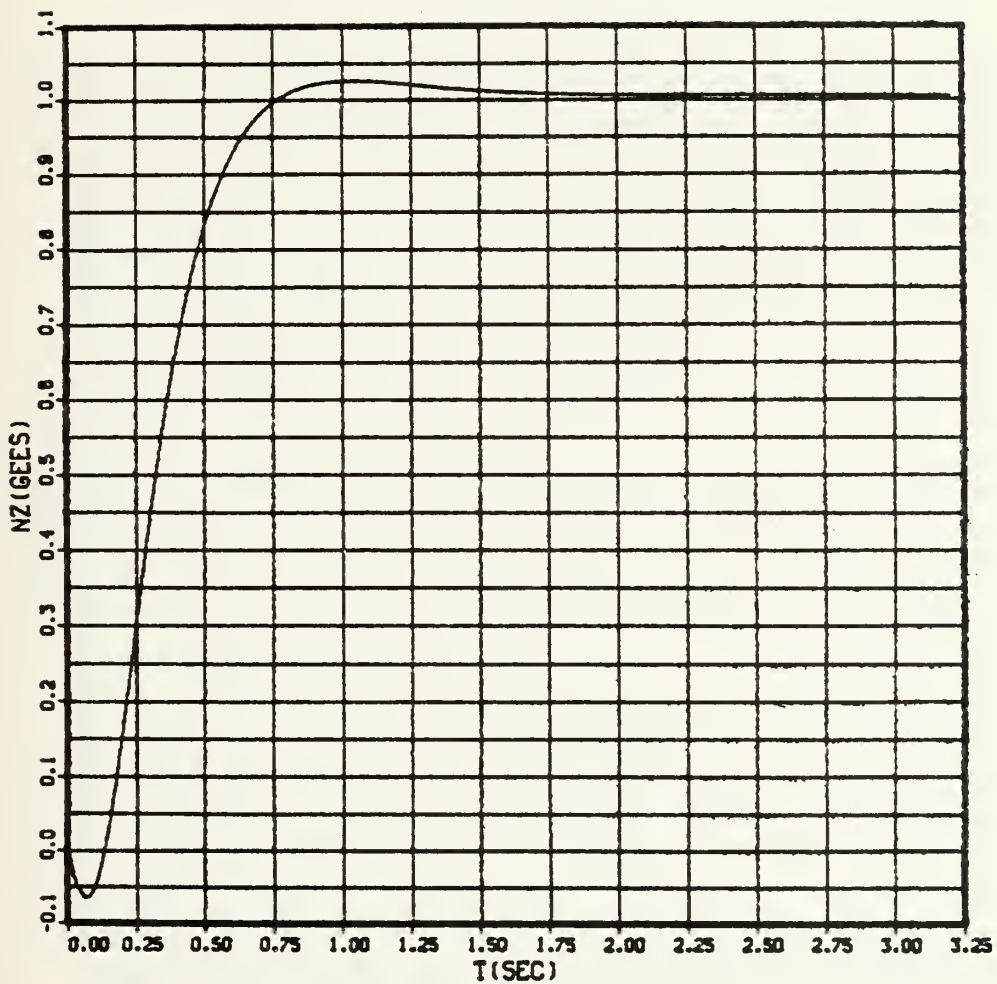


Fig. 2.7 Pitch Normal Acceleration (n_z) vs Time (t)
 Uncoupled Pitch Channel
 Circular airframe (1Gee Command, $a_e = 0$).

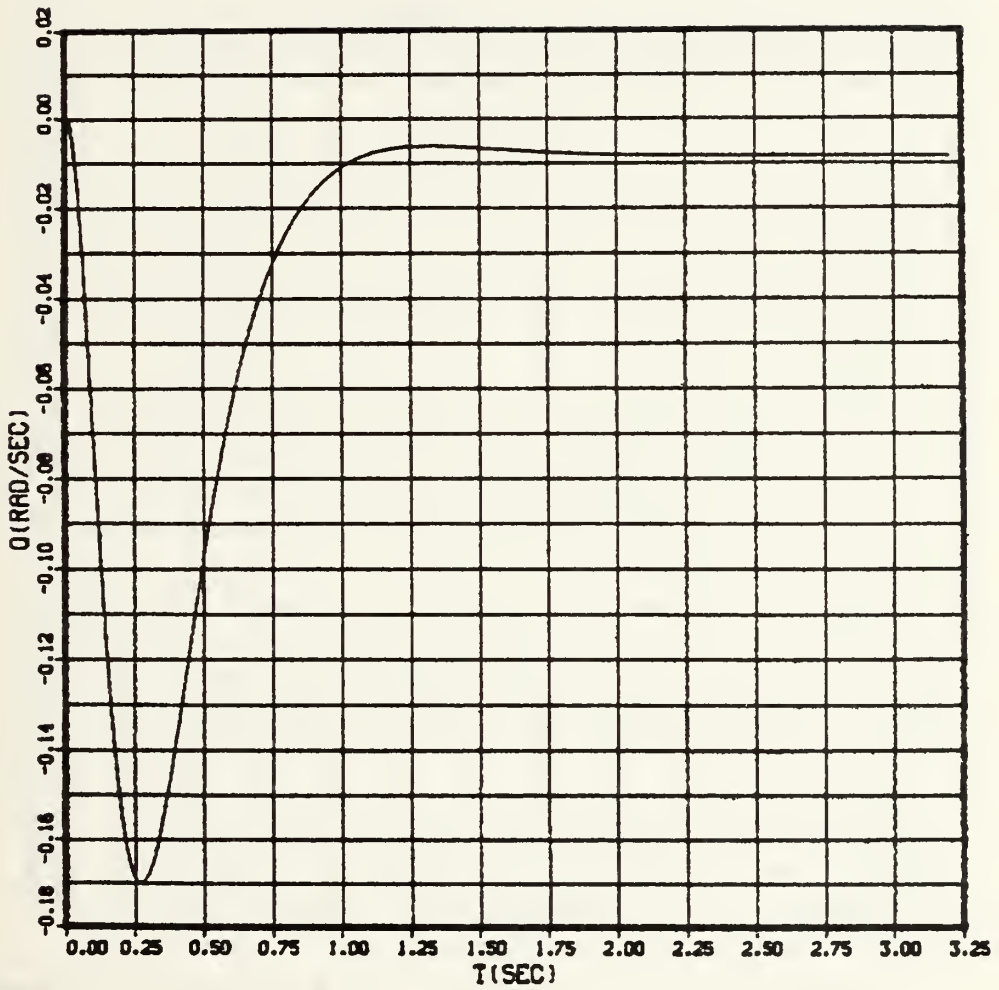


Fig 2.8 Pitch Angular Rate (q) vs Time (t)
 Uncoupled Pitch Channel
 Circular airframe (1Gee Command, $a_e = 0$)

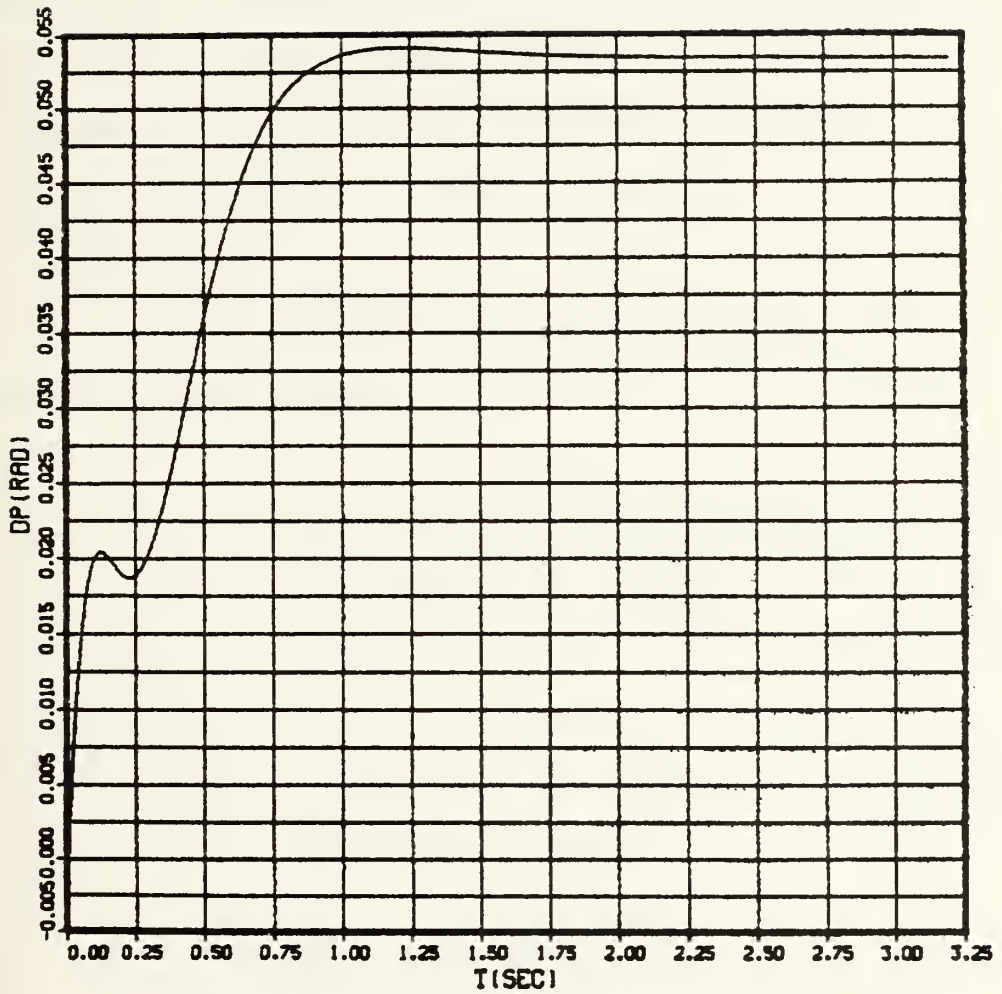


Fig. 2.9 Pitch Tail Incidence (δ_p) vs Time (t)
 Uncoupled Pitch Channel
 Circular airframe (1Gee Command, $a_e = 0$).

The equations of the uncoupled linear Pitch channel for elliptical airframe, which are used in the above CSMP program, are:

a. Equation of Control Law

The control law of the uncoupled linear Pitch channel for the elliptical airframe is very similar to the control law for the circular airframe, with only differences in the gain of acceleration and rate compensators. Elliptical control law is shown in figure 2.6., taken from [Ref. 2].

(1) Acceleration Filter Equation. The Acceleration filter equation is the same as in section II.C.4

(2) Acceleration Compensator Equation

$$Y = \left(-0.008/\frac{s}{6} + 1\right) \cdot (1.1053\eta_{2c} - X) \quad (\text{II.C.5-1})$$

Utilizing, inverse Laplace Transformation and rearranging II.C.5-1 it becomes:

$$\dot{Y} = -6Y - 530.544 \times 10^{-3} \eta_{2c} + 0.48 \cdot X \quad (\text{II.C.5-2})$$

(3) Compensator Equation

$$\frac{\delta P_c}{Y - X_1} = \frac{-3.07 \cdot \left(\frac{s}{8} + 1\right)}{s}$$

(II.C.5-3)

Using inverse Laplace Transformation, it yields:

$$\delta \dot{P}_c = -383.75 \times 10^{-3} (\dot{Y} - \dot{X}_1) - 3.07 (Y - X_1) \quad (\text{II.C.5-4})$$

b. Actuator Equation (Figure 2.5).

As in section II.C.4,b

c. Equation of Uncoupled Linear Pitch
Aerodynamic Model

The equation for pitch angular rate was derived, as in section II.C.3, the only differences are in the constants $W=2475$ (lbs),

$I_{yy}=790$ (Slug-ft²), $C_{m_\alpha}=0.015$, $C_{m_{\delta_p}}=-0.055$, $C_{n_{\delta_p}}=0.02$ and

$C_{n_a}=0.18$, as referred in the Appendix A and Table I.

Manipulating according to the inverse Laplace Transformation rules and rearranging, one obtains.

$$\frac{q}{\delta_p} = (3.66s + 0.688) / (-88.64 \times 10^{-3} s^2 + 15.95 \times 10^{-3} s + 1) \quad (\text{II.C.5-5})$$

Using state-space representation of a system, in which forcing function involves derivative terms [Ref. 5: pp. 675-678.] It yields:

$$\dot{x}_1 = x_2 - 41.29 \cdot \delta_p \quad (\text{II.C.5-7})$$

$$\dot{x}_2 = 11.2815 \cdot x_1 + 179.94 \times 10^{-3} x_2 - 15.1914 \cdot \delta_p \quad (\text{II.C.5-8})$$

$$q = x_1 \quad (\text{II.C.5-8a})$$

Also, Manipulating with same way the equation:

$$\frac{\eta_z}{\delta_p} = \frac{-212.411 \times 10^{-3} s^2 + 81.6}{-88.64 \times 10^{-3} s^2 + 15.95 \times 10^{-3} s + 1} \quad (\text{II.C.5-9})$$

Yielding

$$\dot{z}_1 = z_2 + 528.3 \times 10^{-3} \delta_p \quad (\text{II.C.5-10})$$

$$\dot{z}_2 = 11.2815 \cdot z_1 + 179.94 \times 10^{-3} z_2 - 887.35 \cdot \delta_p \quad (\text{II.C.5-11})$$

$$\eta_z = - (z_1 + 2.936 \cdot \delta_p) \quad (\text{II.C.5-12})$$

Utilizing state-space representation, all of the above equation can be modeled in the following eighth-order system:

$$\begin{array}{c|cccccccc|c|c}
 \dot{X}_1 & 0 & 1 & 0 & 0 & 0 & 0 & 0 & -41.29 & X_1 & 0 \\
 \dot{X}_2 & 11.28 & 0.18 & 0 & 0 & 0 & 0 & 0 & -15.19 & X_2 & 0 \\
 \dot{Z}_1 & 0 & 0 & 0 & 1 & 0 & 0 & 0 & 0.5283 & Z_1 & 0 \\
 \dot{Z}_2 & 0 & 0 & 11.28 & 0.18 & 0 & 0 & 0 & -887.3 & Z_2 & 0 \\
 \dot{X} & 0 & 0 & -150 & 0 & -150 & 0 & 0 & -4.705 & X & 0 \\
 \dot{Y} & 0 & 0 & 0 & 0 & 0.48 & -6 & 0 & 0 & Y & -0.53 \\
 \dot{\delta}_{P_c} & 3.07 & 0.384 & 0 & 0 & -0.184 & -0.768 & 0 & -15.84 & \delta_{P_c} & -0.203 \\
 \dot{\delta}_P & 0 & 0 & 0 & 0 & 0 & 0 & 188.4 & -188.4 & \delta_P & 0
 \end{array}
 \cdot m_{2c}$$

(II.C.5-13)

where the state variables are:

X_1, X_2 : pitch angular rate state variables
(section II.C.4)

Y_1, Y_2 : Achieved Body Acceleration state variables (section II.C.4)

X : output of Acceleration filter

δ_{P_c} : input command in actuator network

δ_P : tail incidence angle

The state $X, X_1, Y_1, \delta_{P_c}$ of control law are shown in Figure 2.6

Utilizing, the above state variables system, a CSMP program was written (Appendix D) to achieve the time response plots of η_z , q and δ_p . As input a step function is used, which represents a one gee command. The trim angle of attack (a_e) is equal to zero.

Figure 2.10 shows the pitch acceleration response of the elliptical airframe due to the command. The response has a time constant of about 0.5, steady state equal to zero, and overshoot 0%, keeping the requirements referred to in Appendix C.

Figures 2.11 and 2.12 show the required body angular rate and control surface deflection, to achieve the acceleration response.

6. Comparison of Airframe Response

Figures 2.7 and 2.10 show that the Pitch acceleration response of the circular and elliptical airframe are approximately the same having a 0.5 second time constant and negligible overshoots.

Figures 2.8, 2.9, 2.11 and 2.12 show that to achieve the acceleration response the elliptical airframe requires less body angular rate and control surface deflection. The elliptical airframe requires less control surface incidences, because the transfer functions have a higher DC gain and poles which are located at a lower frequency due mainly to a more neutrally stable airframe.

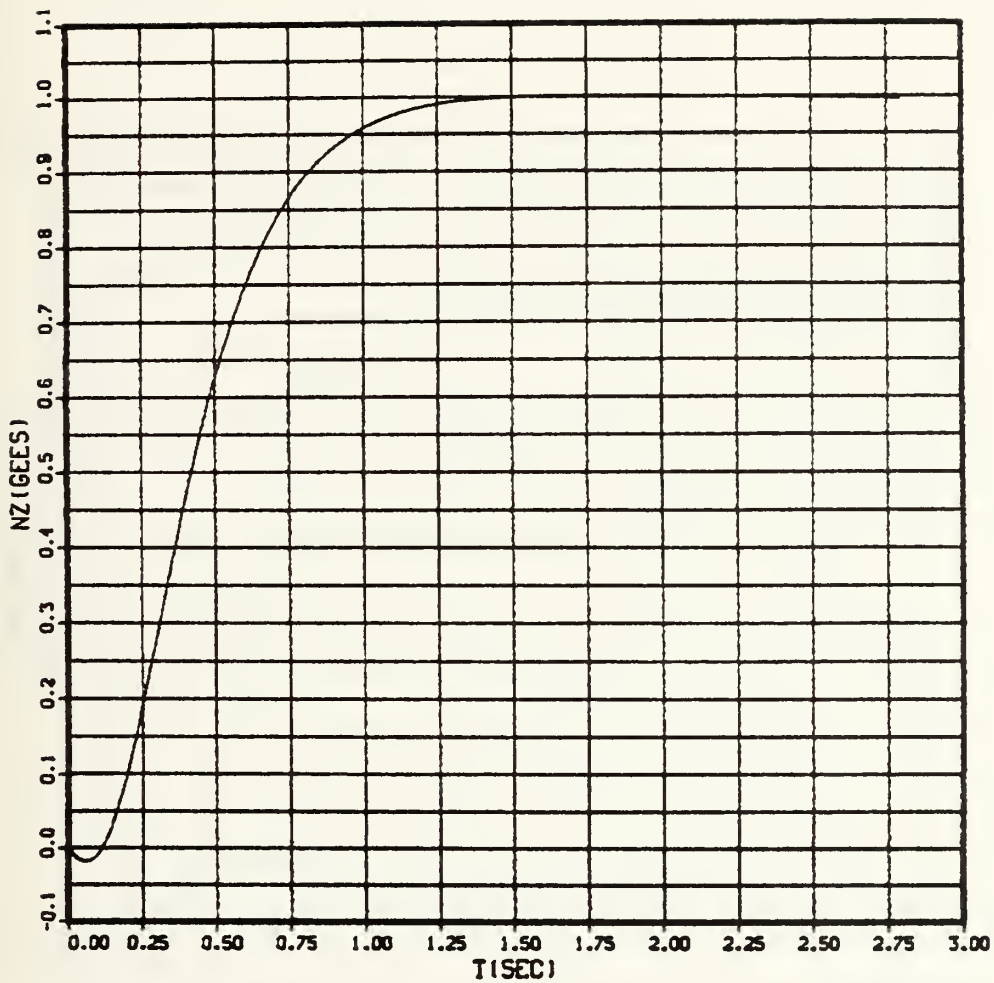


Fig. 2.10 Pitch Normal Acceleration (n_z) vs Time (t)
 Uncoupled Pitch Channel
 Elliptical airframe (1Gee Command, $a_e = 0$)

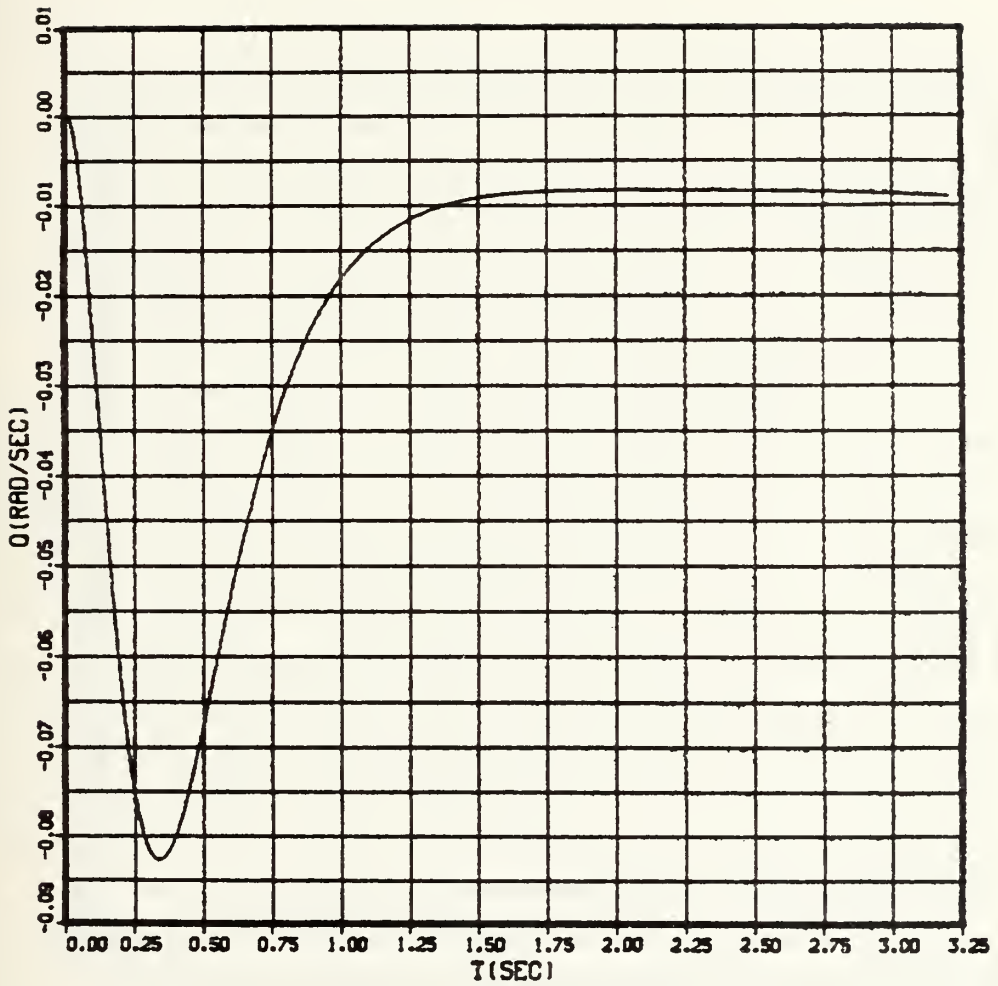


Fig. 2.11 Pitch angular rate (q) vs Time (t)
 Uncoupled Pitch Channel
 Elliptical airframe (1Gee Command, $a_e = 0$)

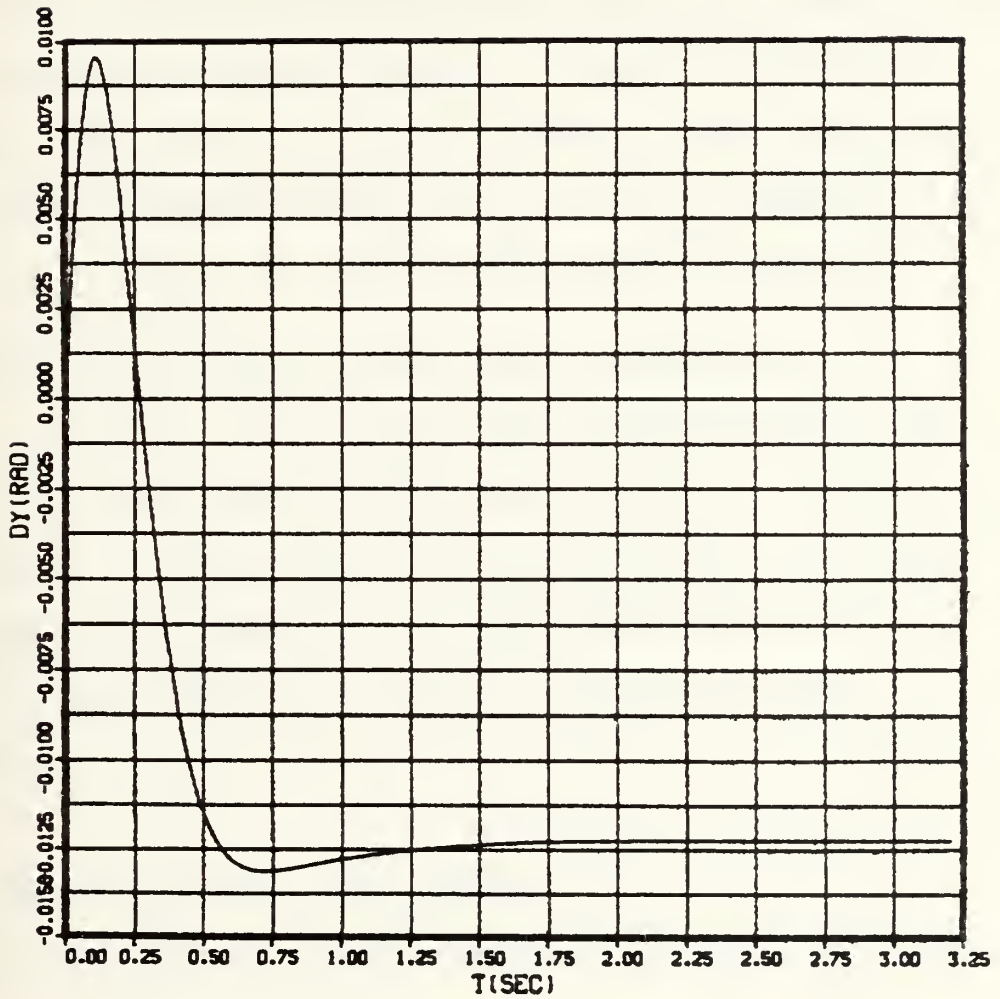


Fig. 2.12 Pitch tail incidence (δ_p) vs Time (t)
 Uncoupled Pitch Channel^P
 Elliptical airframe (1Gee Command, $a_e=0$)

The DC gain $[(qS/w) \cdot (C_{N_\alpha} \cdot C_{m_{\delta p}} / C_{m_a} - C_{N_{\delta p}})]$ is directly proportional to pitch control moment $C_{m_{\delta p}}$ and inversely proportional to magnitude of stability margin in Pitch (i.e., C_{m_a} / C_{N_a} or distance from center of pressure to center of gravity). Thus the nearly neutrally stable elliptical airframe is expected to have a higher gain than the stable circular airframe even though its control moment coefficient is slightly smaller. Higher DC gain will require less control surface incidence. The zeros of n_z / δ_p are directly proportional to C_{N_α} and the location of the ratio $C_{m_{\delta p}} / C_{N_{\delta p}}$ or the distance from the point of action of tail forces to the center of gravity.

Hence, for the elliptical airframe which has larger C_{N_α} the zeros of n_z / δ_p are located at a higher frequency. Lower control surface incidences and higher frequency n_z / δ_p zeros of the elliptical airframe will simplify the design of a rapidly responding Pitch autopilot.

D. UNCOUPLED LINEAR YAW CHANNEL

The purpose of the Yaw channel autopilot of a CBTT autopilot is to minimize sideslip angle or provide coordinated motion between Roll and Yaw channels. This was accomplished in two ways. First, the uncoupled Yaw channel

autopilot, (i.e, Roll and Pitch dynamic effect neglected) was designed as a regulator (i.e no guidance command and with rate and acceleration feedback) to help minimize sideslip angle. Second, to aid in sideslip control, the regulator was commanded from the Roll channel as explained in chapter III.

1. Aerodynamic Model Control Law

A block diagram of the uncoupled Yaw channel is shown in Figure 2.13, taken from [Ref. 2]. In this diagram the aerodynamic model and the Yaw control law are involved. Also, the Yaw control law without the accelerator is shown in Figure 2.14. These figures were abstracted from [Ref. 2].

The normal acceleration n_{y_c} is not used to command the CBTT autopilot. Instead, it is used for the design and analysis of the uncoupled channel. The command used by the coupled system is shown in dashed lines and is a yaw angular rate command, r_c .

The yaw control law is governed by missile body yaw angular rate (r) and yaw normal acceleration n_y . The yaw control law determines the required command δ_{y_c} to an actuator, which is approximated as a first order lag at 30 Hz (188.4 rad/sec).

The aerodynamics, linearized about a trim a_e angle-of-attack equal to zero.

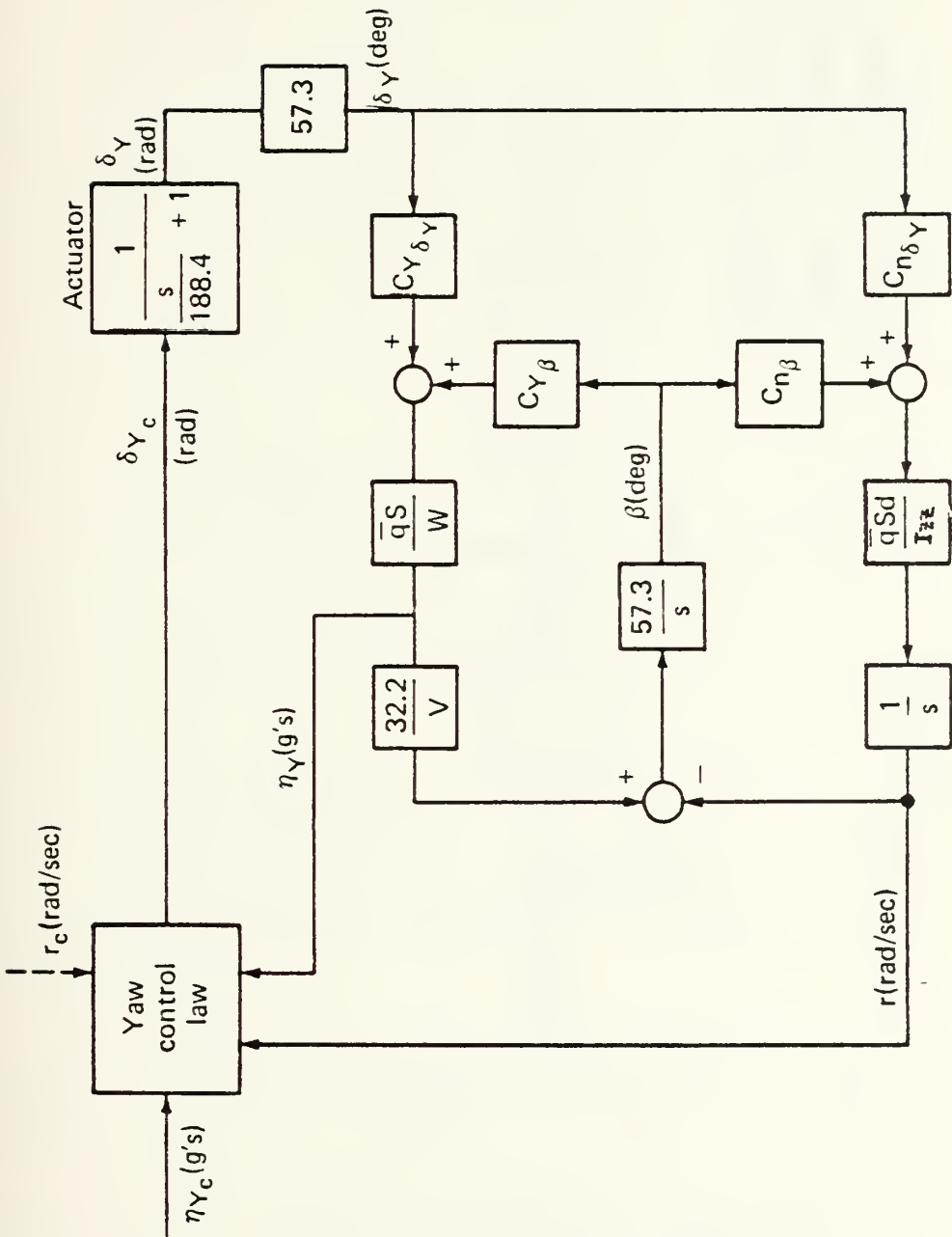
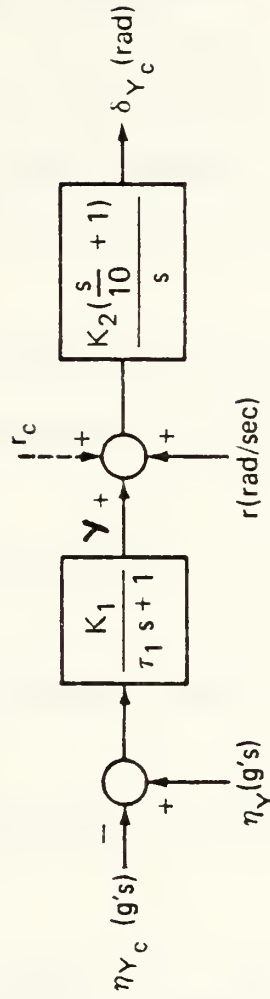


Fig. 2.13 Uncoupled Yaw Channel



Airframe	K_1	τ_1	K_2
Circular	0.31946	0.2	4.85
Elliptical	0.83935	0.25	6.08

Fig. 2.14 Yaw Control Laws

2. Transfer Functions of Aerodynamic Model

The aerodynamic characteristic of the Yaw channel are modeled by a second-order system, by the following equation, where the states are r , yaw angle and β , sideslip angle:

$$\dot{r} = (\bar{q} S d / I_{zz}) \cdot (c_{n\beta} \cdot \beta + 57.3 c_{n\delta y} \cdot \delta y) \quad (\text{rad/sec}) \quad (\text{II.D.2-1})$$

$$\dot{\beta} = 57.3 \left(-r + \frac{32.2}{V} \cdot \eta_y \right) \quad (\text{deg}) \quad (\text{II.D.2-2})$$

and also, by the equation:

$$\eta_y = (\bar{q} S' / W) \cdot (c_{y\beta} \cdot \beta + 57.3 c_{y\delta y} \cdot \delta y) \quad (\text{gees}) \quad (\text{II.D.2-3})$$

substituting equations II.D.2-3 into II.D.2-2, the

last equation becomes:

$$\dot{\beta} = 57.3 \left[-r + \frac{32.2}{V} \left(\frac{\bar{q} S'}{W} (c_{y\beta} \cdot \beta + 57.3 \cdot c_{y\delta y} \cdot \delta y) \right) \right] \quad (\text{II.D.2-4})$$

Taking the Laplace Transform of the equations, one

obtains

$$rs = \frac{\bar{q} S d}{I_{zz}} \cdot (c_{n\beta} \cdot \beta + 57.3 c_{n\delta y} \cdot \delta y) \quad (\text{II.D.2-5})$$

$$\beta s = 57.3 \left(-r + \frac{32.2}{V} \left(\frac{\bar{q} S'}{W} (c_{y\beta} \cdot \beta + 57.3 c_{y\delta y} \cdot \delta y) \right) \right) \quad (\text{II.D.2-6})$$

Rearranging above equations, in terms of q and α ,

they become:

$$rs - \frac{\bar{q} S d}{I_{zz}} \cdot c_{n\beta} \cdot \beta = \frac{57.3 k \bar{q} S'}{I_{zz}} c_{n\delta y} \cdot \delta y \quad (\text{II.D.2-7})$$

$$57.3 \cdot r + \left(s - \frac{k \bar{q} S'}{W} \cdot c_{y\beta} \right) \cdot \beta = \frac{57.3 k \bar{q} S'}{W} \cdot c_{y\delta y} \cdot \delta y \quad (\text{II.D.2-8})$$

Applying the Cramer's rule in the system of the equations II.D.2-7 and II.D.2-8 the transfer functions r/δ_y and β/δ_y are obtained.

$$\frac{r}{\delta_y} = \frac{\left(\frac{57.3 K (\bar{q} S')^2 d}{I_{zz}} \cdot C_{n\delta_y} \right) \cdot s + \frac{57.3 K (\bar{q} S')^2}{W I_{zz}} \left(-C_{n\delta_y} \cdot C_{Y\beta} + C_{n\beta} \cdot C_{Y\delta_y} \right)}{s^2 - \left(\frac{K \bar{q} S'}{W} C_{Y\beta} \right) \cdot s + \left(\frac{57.3 \bar{q} S' d}{I_{zz}} \right) \cdot C_{n\beta}} \quad (\text{II.D.2-9})$$

and

$$\frac{\beta}{\delta_p} = \frac{\left(\frac{57.3 K \bar{q} S'}{W} C_{Y\delta_y} \right) \cdot s - \frac{3283.29 \cdot \bar{q} S' d \cdot C_{n\delta_y}}{I_{yy}}}{s^2 + \left(\frac{K \bar{q} S' C_{m\alpha}}{W} \right) \cdot s - \frac{57.3 \bar{q} S' d C_{m\alpha}}{I_{yy}}} \quad (\text{II.D.2-10})$$

$$K = \frac{(57.3) \cdot (32.3)}{V} = 0.48$$

$$\bar{q} = 1650 \text{ (lbs/ft}^2\text{)}$$

$$S = 3.14159 \text{ (ft}^2\text{)}$$

$$d = 2 \text{ (ft)}$$

$$I_{zz} = 810 \text{ (slug-ft}^2\text{)}$$

$$W = 2525 \text{ (lbs)}$$

$$C_{n\beta} = -0.025$$

$$C_{n\delta_y} = -0.050$$

$$C_{Y\beta} = -0.065$$

$$C_{Y\delta_y} = 0.021$$

$$\alpha_e = 0^\circ$$

As referred to in Appendix A and Table I.

Substituting the aforementioned values into equation

(II.D.2-9), it becomes:

$$\frac{r}{\delta p_y} = \frac{2.005 \cdot s + 0.16}{-54.54 \times 10^{-3} s^2 - 2.8 \times 10^{-3} s + 1} \quad (1/\text{sec}) \quad (\text{II.D.2-11})$$

Introducing equation II.D.2-10 into II.D.2-3 and rearranging the last one, the transfer function of yaw normal acceleration in terms of the yaw control incidence, is obtained:

$$\frac{n_y}{\delta y} = \frac{\left(\frac{57.3 k (\bar{q} s)^2}{W^2} C_{y\delta y} \cdot C_{y\theta} \right) \cdot s - \frac{3283.29 (\bar{q} s)^2 d}{I_{yy} W} C_{n\delta y} \cdot C_{y\theta}}{s^2 + \left(\frac{k \bar{q} s}{W} \cdot C_{W\alpha} \right) \cdot s - \frac{57.3 \bar{q} s d C_{m\alpha}}{I_{yy}}} - \frac{57.3 \bar{q} s}{W} \cdot C_{y\delta y} \quad (\text{II.D.2-12})$$

After substituting the values into the equation (II.D.2-12), one obtains:

$$\frac{n_y}{\delta y} = \frac{-13.474 s^2 + 17.76}{-54.54 \times 10^{-3} s^2 - 2.8 \times 10^{-3} s + 1} \quad (\text{gees/rad}) \quad (\text{II.D.2-13})$$

The above transfer functions are used for finding the time responses of the yaw angular rate r and the yaw normal acceleration.

Using inverse Laplace transformation, the equation II.D.2-11 and II.D.2-13 become:

$$\ddot{r} + 51.338 \times 10^{-3} \dot{r} - 18.3335 \cdot r = -36.761 \cdot \delta \dot{y} - 2.75 \cdot \delta y \quad (\text{II.D.2-14})$$

$$\ddot{n}_y + 51.338 \times 10^{-3} \dot{n}_y - 18.3335 n_y = 2.387 \delta \dot{y} - 325.629 \cdot \delta y \quad (\text{II.D.2-15})$$

The equations II.D.2-14 and II.D.2-15 involve derivative terms in the forcing function. Using rules of state-space representation of a system [Ref. 5: pp 675-678], they turn:

$$\dot{X}_1 = X_2 - 36.761 \cdot \delta y \quad (\text{II.D.2-16})$$

$$\dot{X}_2 = 18.335 \cdot X_1 - 51.338 \times 10^{-3} \cdot X_2 - 863.014 \times 10^{-3} \cdot \delta y \quad (\text{II.D.2-17})$$

$$r = X_1 \quad (\text{II.D.2-18})$$

$$\dot{z}_1 = z_2 - 122.544 \times 10^{-3} \cdot \delta y \quad (\text{II.D.2-19})$$

$$\dot{z}_2 = 18.335 \cdot z_1 - 51.338 \times 10^{-3} \cdot z_2 - 281.857 \cdot \delta y \quad (\text{II.D.2-20})$$

$$n_y = z_1 + 2.387 \cdot \delta y \quad (\text{II.D.2-21})$$

3. Equations of Yaw Control Law

As mentioned before, the yaw control law is governed by missile body yaw angular rate (r) and yaw normal acceleration n_y and it is used to determine the required command δ_{y_c} to the actuator. The yaw control law at the flight condition of interest (i.e, Mach 3.95, 60kft) is shown in Figure 2.14, taken from [Ref. 2]. The rate compensation determines the high frequency attenuation and is used to minimize aerodynamic variations on the quality of regulation. The acceleration compensation determines the acceleration bandwidth via the time constant of the acceleration response due to a step command of acceleration at n_{y_c} .

a. Acceleration Compensator Equation:

$$Y = \frac{0.31946}{0.25 + 1} (-n_{y_c} + n_y) \quad (\text{II.D.3-1})$$

Inverse transforming and rearranging the II.D.3-1, it turns into:

$$\dot{Y} = -5Y + 1.5973 (n_y - n_{y_c}) \quad (\text{II.D.3-2})$$

b. Rate Compensator Equation:

$$\delta y_c = \frac{4.85 \left(\frac{s}{10} + 1 \right)}{s} (\gamma + r) \quad (\text{II.D.3-3})$$

Utilizing inverse Laplace Transformation and introducing equation II.D.2-16, the equation II.D.3-3 turns into:

$$\delta \dot{y}_c = 0.485 (\dot{\gamma} + \dot{x}_1) + 4.85 (\gamma + x_1) \quad (\text{II.D.3-3a})$$

c. Actuator Equation:

$$\delta \gamma = \frac{1}{\frac{s}{188.4} + 1} \delta y_c \quad (\text{II.D.3-4})$$

Inverse transforming and rearranging the equation II.D.3-4, it turns into:

$$\delta \dot{\gamma} = -188.4 \delta \gamma + 188.4 \delta y_c \quad (\text{II.D.3-5})$$

Using state-space representation, all the aerodynamic model and control laws can be modeled in the following seventh order system:

$$\begin{array}{c|cccccc|c|c|c} \begin{array}{l} \dot{x}_1 \\ \dot{x}_2 \\ \dot{z}_1 \\ \dot{z}_2 \\ \dot{\gamma} \\ \delta \dot{y}_c \\ \delta \dot{\gamma} \end{array} & = & \begin{array}{cccccc} 0 & 1 & 0 & 0 & 0 & 0 \\ 18.335 & -0.514 & 0 & 0 & 0 & 0 \\ 0 & 0 & 0 & 1 & 0 & 0 \\ 0 & 0 & 18.335 & -0.514 & 0 & 0 \\ 0 & 0 & 1.597 & 0 & -5 & 0 \\ 4.85 & 0.485 & 0.775 & 0 & 2.425 & 0 \\ 0 & 0 & 0 & 0 & 0 & 188.4 \end{array} & \begin{array}{l} -36.761 \\ -0.863 \\ -0.1226 \\ -281.86 \\ 3.8127 \\ -17.829 \\ -188.4 \end{array} & \begin{array}{l} X_1 \\ X_2 \\ Z_1 \\ Z_2 \\ Y \\ \delta y_c \end{array} & + & \begin{array}{l} 0 \\ 0 \\ 0 \\ 0 \\ -1.597 \\ 0.775 \end{array} & \eta y_c \end{array}$$

(II.D.3-6)

where the state variables are:

x_1, x_2 : pitch angular rate state variables
(section II.D.2)

Y_1, Y_2 : yaw acceleration state variables
(section II.D.2)

Y : output of acceleration compensator

δ_{P_C} : input command in the actuator

δ_P : yaw tail incidence

The state X_1, Y, δ_{Y_C} of control law are shown in

Figure 2.14.

4. Design Approach and Analysis of Circular Airframe

The design technique used for the Yaw channel is the same as the technique used in the Pitch channel. The analysis of it, for circular airframe is based, on the time responses of the yaw angular rate r , the yaw normal acceleration n_y and yaw tail incidence δ_y .

For purposes of analysis, a CSMP program was written (Appendix E) using the state-variable system which is represented by the block diagram of the yaw aerodynamic model and control law.

Executing the referred program, using as input a step function, which represents the "one Gee Command" and trim angle of attack $a_e = 0$, the time response plots are obtained.

Figure 2.15 shows the yaw acceleration response of the circular airframe. The response has a 0.39 seconds time constant, 7% overshoot and steady state error 0.018

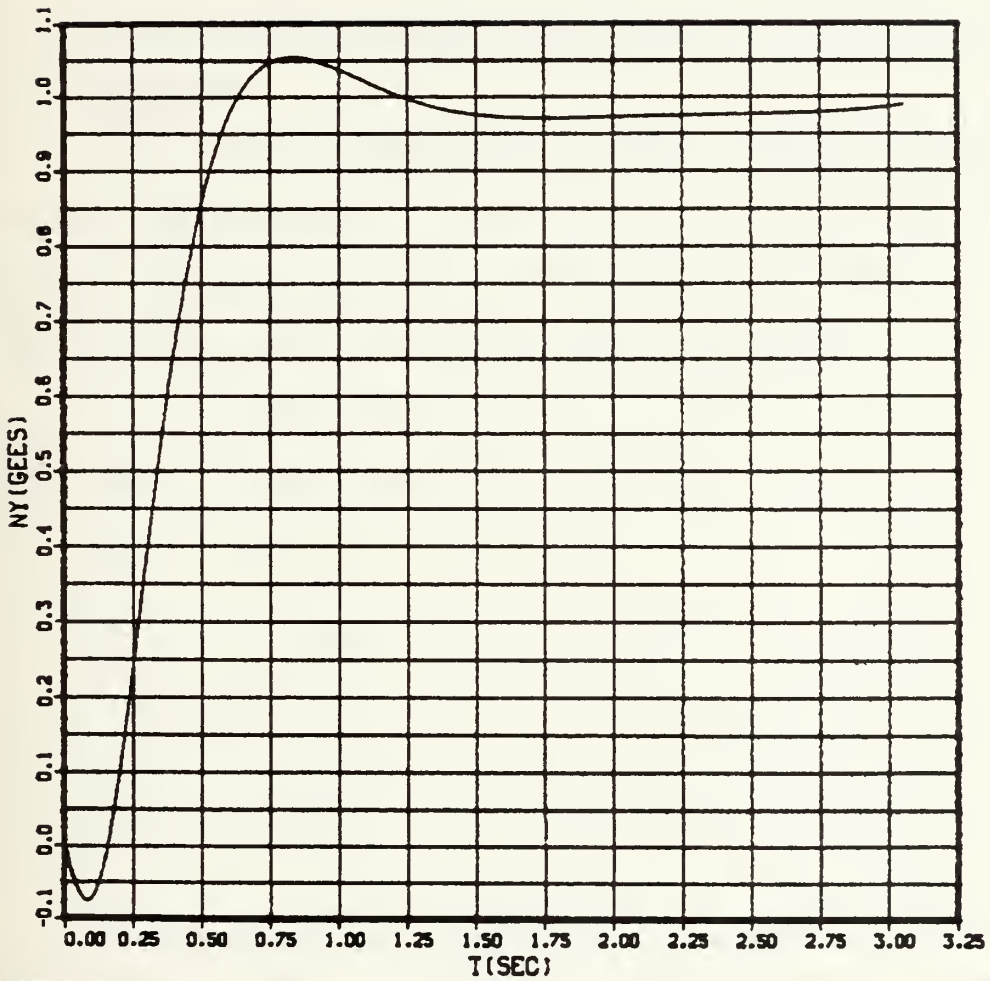


Fig. 2.15 Yaw normal acceleration (n_y) vs time (t)
 Uncoupled Yaw Channel
 Elliptical airframe (1Gee Command, $a_e = 0$)

which are according to the requirements referred in Appendix C.

Figures 2.16 and 2.17 show the required body yaw angular rate and control surface deflection, to achieve the acceleration response. Again these results matched those of [Ref. 2].

5. Aerodynamic Transfer Function for Elliptical Airframe

The transfer functions for yaw angular rate and yaw normal acceleration for the elliptical airframe, were derived in the same way as in section II.D.2. The only differences are in the following constants

$$w = 2475 \text{ (lbs)}$$

$$I_{zz} = 853 \text{ (slug-ft}^2\text{)}$$

$$C_{n_{\beta}} = 0.024$$

$$C_{n_{\delta_Y}} = -0.042$$

$$C_{Y_{\beta}} = -0.043$$

$$C_{Y_{\delta_Y}} = 0.016$$

As referred to in Appendix A and table I.

a. Transfer function of yaw angular rate r .

$$\frac{r}{\delta_Y} = \frac{-1.7485 \cdot s - 0.0598}{59.838 \times 10^{-3} \cdot s^2 + 2.593 \times 10^{-3} \cdot s + 1} \left(\frac{1}{\text{sec}} \right) \text{ (II.D.5-1)}$$

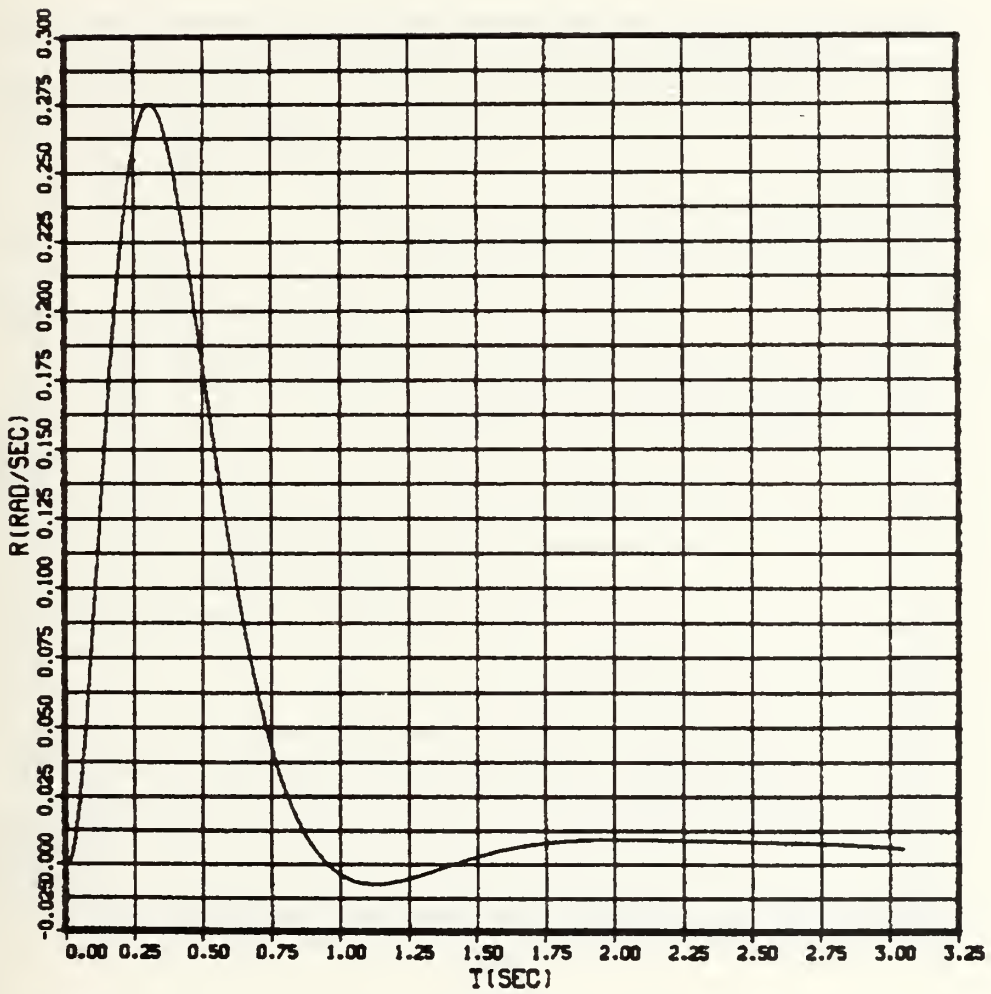


Fig. 2.16 Yaw angular rate (r) vs Time (t)
 Uncoupled Yaw Channel
 Circular airframe (1Gee Command, $a_e = 0$)

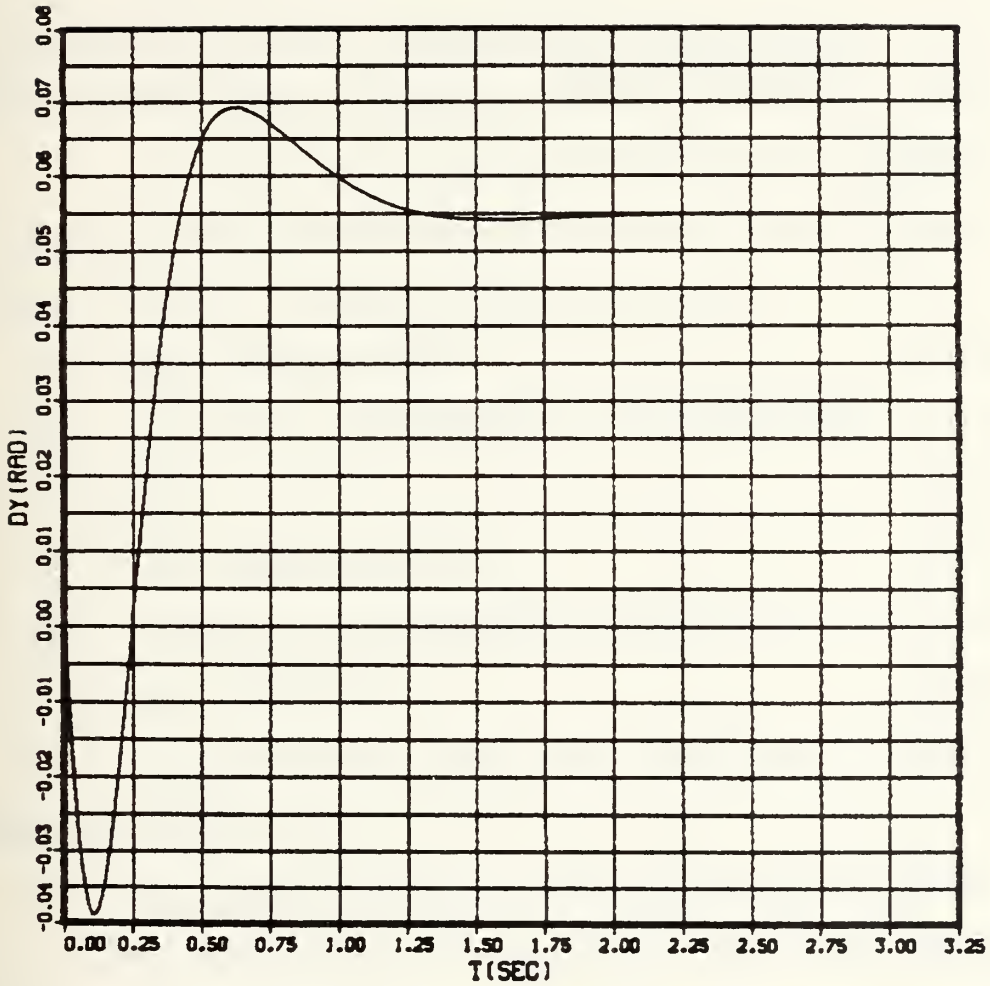


Fig. 2.17 Yaw tail incidence (δ_Y) vs Time (t)

Uncoupled Yaw Channel
 Circular airframe (1Gee Command, $a_e = 0$)

b. Transfer function of yaw normal acceleration n_Y

$$\frac{n_Y}{\delta_Y} = \frac{114.633 \times 10^{-3} s^2 - 7.1}{59.838 \times 10^{-3} s^2 + 2.593 \times 10^{-3} s + 1} \left(\frac{\text{gees}}{\text{rad}} \right) \quad (\text{II.D.5-2})$$

Using inverse Laplace transformation, the equation II.D.5-1 and II.D.5-2 becomes:

$$\ddot{Y} + 43.333 \times 10^{-3} \dot{Y} + 16.7117 \cdot Y = -29.213 \cdot \delta_Y - 999.36 \times 10^{-3} \delta_Y \quad (\text{II.D.5-3})$$

$$\ddot{n}_Y + 43.333 \times 10^{-3} \dot{n}_Y + 16.7117 \cdot n_Y = 1.9157 \cdot \delta_Y - 118.653 \cdot \delta_Y \quad (\text{II.D.5-4})$$

Utilizing state representation of a system in which the forcing functions involve derivative terms, as in section II.D.2, the above equations yield:

$$\dot{X}_1 = X_2 - 29.221 \cdot \delta_Y \quad (\text{II.D.5-5})$$

$$\dot{X}_2 = -16.7117 X_1 - 43.333 \times 10^{-3} X_2 + 266.874 \times 10^{-3} \delta_Y \quad (\text{II.D.5-6})$$

$$Y = X_1 \quad (\text{II.D.5-7})$$

$$\dot{Z}_1 = Z_2 - 83.013 \times 10^{-3} \delta_Y \quad (\text{II.D.5-8})$$

$$\dot{Z}_2 = -16.7117 \cdot Z_1 - 43.333 \times 10^{-3} Z_2 - 150.6637 \cdot \delta_Y \quad (\text{II.D.5-9})$$

$$n_Y = Z_1 + 1.9517 \cdot \delta_Y \quad (\text{II.D.5-10})$$

The aerodynamic model for elliptical airframe is shown in Figure 2.13.

6. Yaw Control Equation for Elliptical Airframe

The control law of uncoupled linear Yaw channel for elliptical airframe, is similar to the control law for circular airframe. There are differences in the gains of the acceleration and rate compensators, as is shown in Figure 2.14.

a. Acceleration Compensator Equation

$$Y = (0.8393/0.25 \cdot s + 1) \cdot (-\eta_{Y_c} + \eta_Y) \quad (\text{II.D.6-1})$$

Utilizing inverse laplace transformation and rearranging the equation II.D.6-1, it turns into:

$$\dot{Y} = -4 Y + 3.3574 \cdot (-\eta_{Y_c} + \eta_Y) \quad (\text{II.D.6-2})$$

b. Rate Compensator Equation

$$\delta_{Y_c} = \frac{6.08 \cdot (\frac{s}{10} + 1)}{s} (Y - r) \quad (\text{II.D.6-3})$$

Inverse Laplace transforming and introducing the equation (II.D.5-7) into the equation (II.D.6-3), it turns into:

$$\delta_{Y_c} = 0.608 (\dot{Y} + \dot{X}_1) + 6.08 (Y + X_1) \quad (\text{II.D.6-4})$$

c. Actuator Equation

Same as the equation II.D.3-5.

Using state-space representation all equations of the aerodynamic model and control law, can be modeled in the follow seventh-order system:

\dot{X}_1	0	1	0	0	0	0	-29.22	X_1	0
\dot{X}_2	-16.72	-0.433	0	0	0	0	0.267	X_2	0
\dot{Z}_1	0	0	0	1	0	0	-0.83	Z_1	0
\dot{Z}_2	0	0	-16.72	-0.433	0	0	-150.6	Z_2	0
\dot{Y}	0	0	3.36	0	-4	0	6.553	Y	-3.36
δ_{Y_c}	6.08	0.608	2.041	0	-2.432	0	3.984	δ_{Y_c}	-2.04
$\delta \dot{Y}$	0	0	0	0	0	188.4	-188.4	$\delta \dot{Y}$	0

(II.D.6-5)

where the state variables are:

X_1, X_2 : yaw angular rate state variables
(section II.D.5)

Z_1, Z_2 : yaw normal Acceleration state
variables (section II.D.5)

Y : output of acceleration compensator network

δ_{Y_c} : input command in the actuator

δ_Y : yaw tail incidence

The state X_1, Y, δ_{Y_c} of control law are shown in Figure 2.14.

7. Design Approach and Analysis for Elliptical Airframe

The design technique and analysis for elliptical airframe is the same as that, in section II.D.4. Again, for purposes of analysis, a CSMP program was written (Appendix E) using equations of aerodynamic model and control law.

Figure 2.18 shows the yaw acceleration response of the elliptical airframe. The response has 0.35 second time constant, overshoot about 6% and steady state error 0.01 which are according to the requirements, (Appendix C).

Figures 2.19 and 2.20 show the required body yaw angular rate and control surface deflection, to achieve the acceleration response.

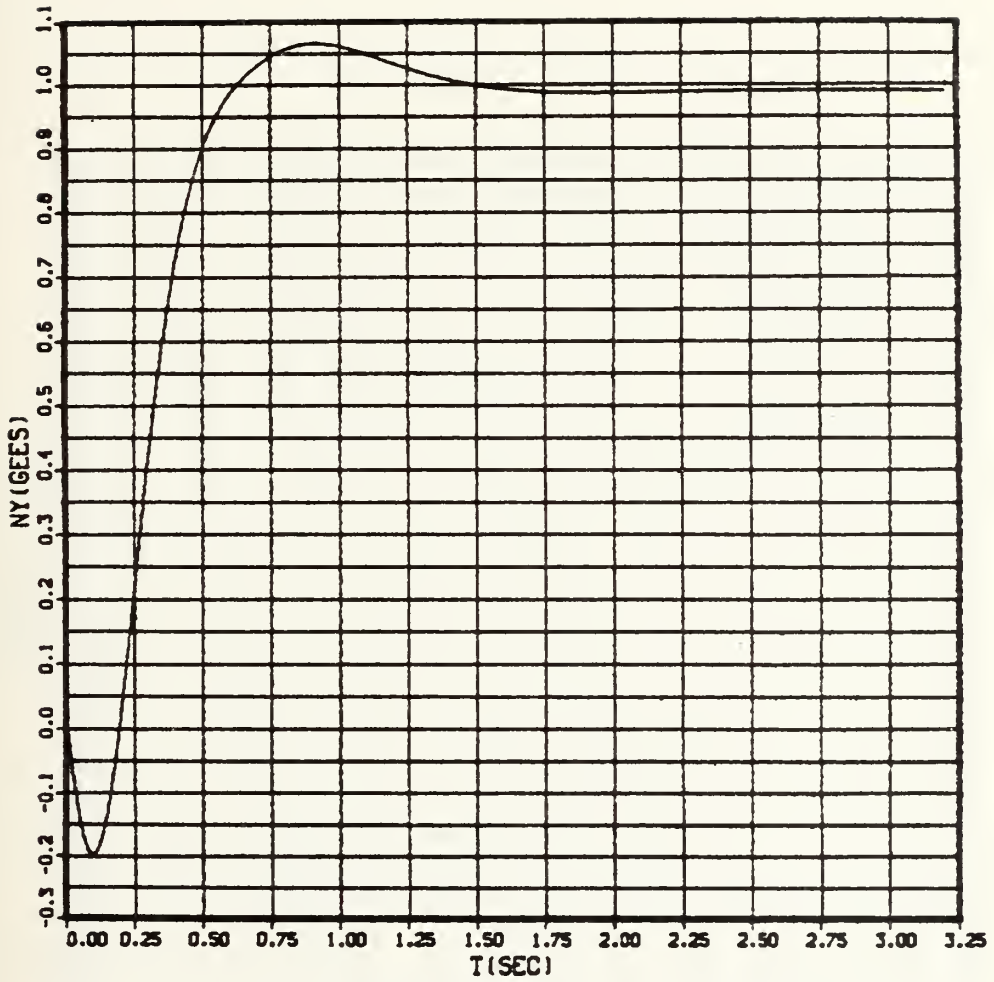


Fig. 2.18 Yaw Acceleration (n_y) vs Time (t)

Uncoupled Yaw channel

Elliptical airframe (1Gee Command. $a_e = 0$)

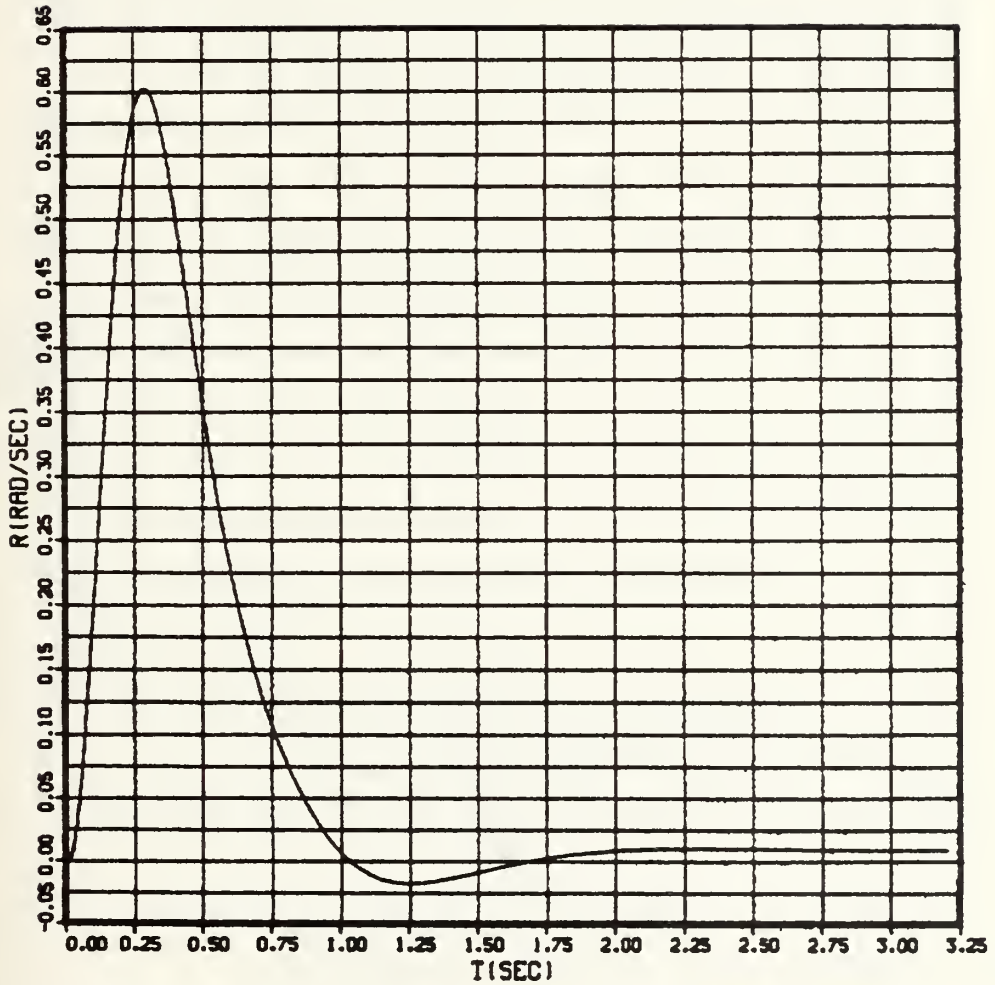


Fig. 2.19 Yaw Angular Rate (r) vs Time (t)
 Uncoupled Yaw Channel
 Elliptical airframe (1Gee Command, $a_e = 0$)

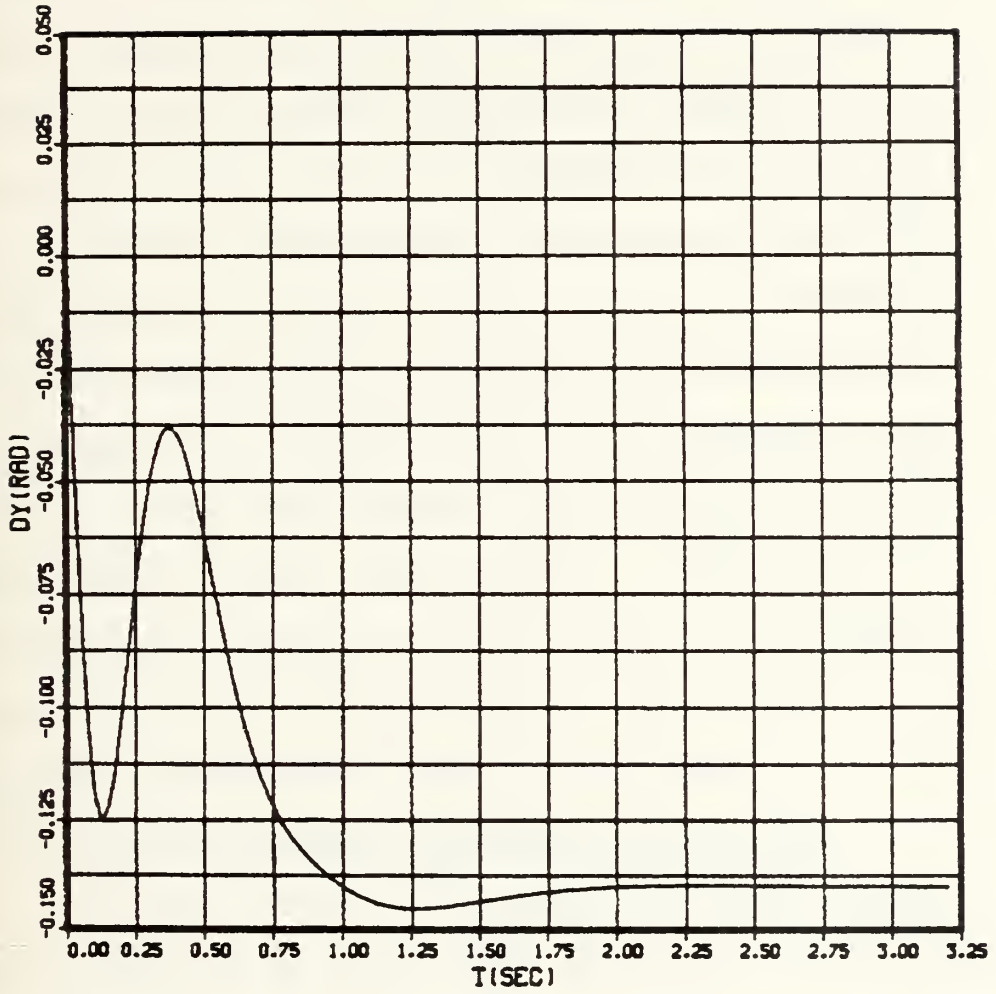


Fig. 2.20 Yaw Tail Incidence (δ_y) vs Time (t)
 Uncoupled Yaw Channel^y
 Elliptical airframe (1Gee Command, $a_e = 0$)

E. LINEAR UNCOUPLED ROLL CHANNEL

Generally, the purpose of a roll channel autopilot is to command the ϕ signal, in order to roll the missile through an angle ϕ , measured from the vertical axis.

The roll channel of a coordinated bank-to-turn autopilot is commanded to roll the missile so as to put the preferred maneuver direction of the missile in the direction of the guidance acceleration command, while the pitch channel acceleration is commanded to produce the total magnitude of the guidance acceleration command.

The desired maneuver plane acceleration should be attained as rapidly as the achieved body-fixed pitch acceleration. To accomplish this, the uncoupled roll channel autopilot was designed to have the roll angle time constant equal to the time constant of the normal acceleration achieved by the uncoupled pitch channel autopilot. This is not necessarily the optimal relationship between the two time constants.

1. Roll Aerodynamic Model and Control Law

A block diagram of the uncoupled Roll channel is shown in Figure 2.21, taken from [Ref. 2]. In this diagram the aerodynamic model is involved. Also, the roll control law is shown in Figure 2.22. These figures were taken from [Ref. 2].

The roll control law is commanded by roll angle ϕ_c is governed by roll angular rate p and roll angle ϕ and

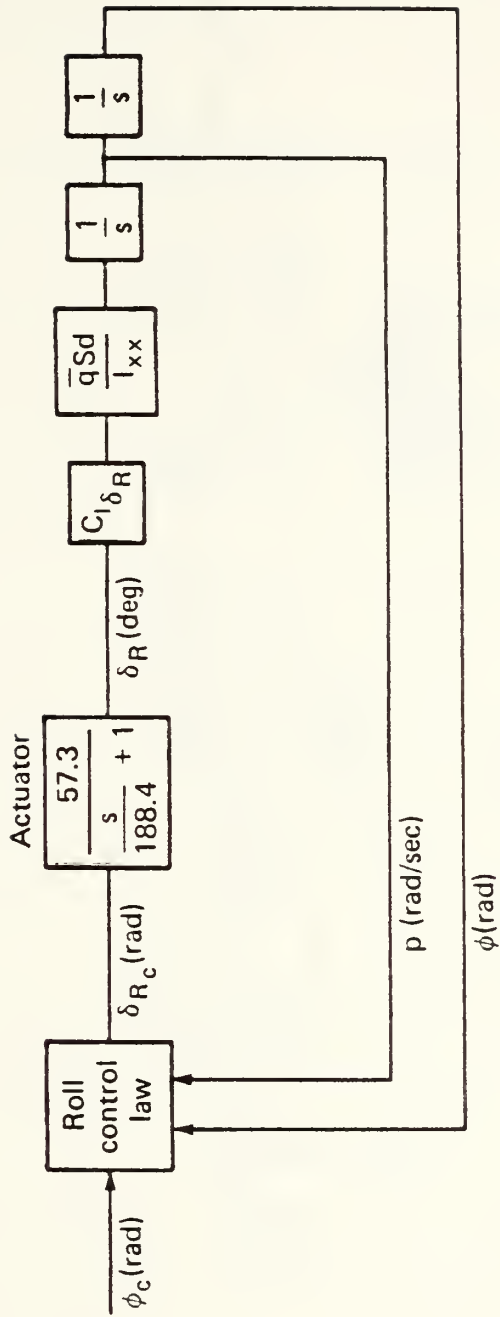


Fig. 2.21 Uncoupled Roll Channel

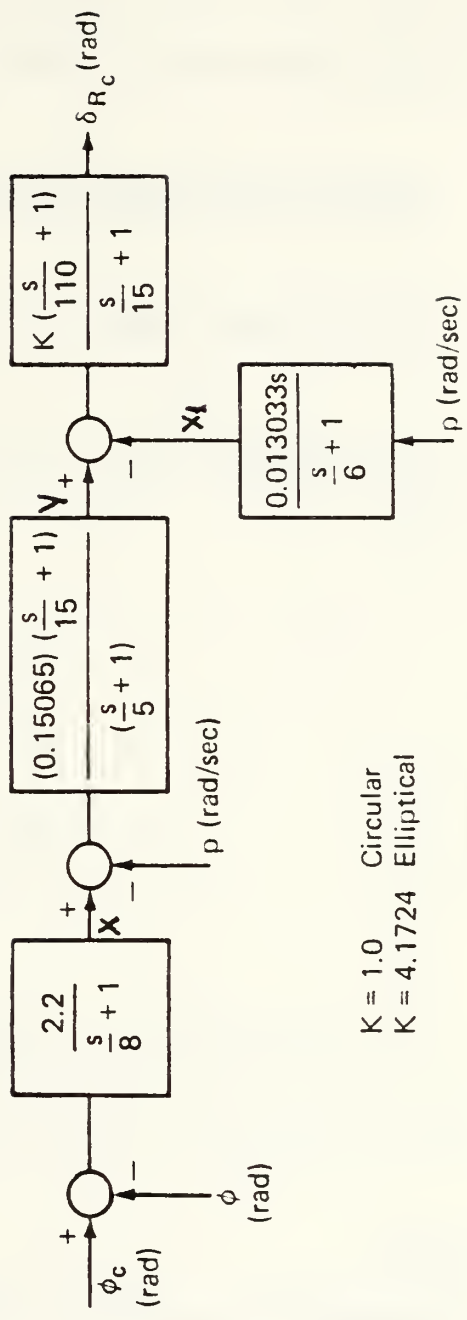


Fig. 2.22 Roll Control Laws

determines the required command δ_{Rc} to an actuator which is approximated as a first order lag at 30Hz (188.4 rad/sec). The aerodynamics, linearized about a trim angle-of-attack (α_e) equal to zero.

2. Equations of Aerodynamic Model for Circular Airframe

The aerodynamic model is represented by the following equations:

$$\dot{P} = (\bar{q} S d / I_{xx}) \cdot (c_{\delta R} \cdot \delta_R \text{ (rad/sec}^2\text{)}) \quad (\text{II.E.2-1})$$

$$\dot{\phi} = P \text{ (rad/sec)} \quad (\text{II.E.2-2})$$

where:

$$\bar{q} = 1650 \text{ (lbs/ft}^2\text{)}$$

$$S = 3.14159 \text{ (ft}^2\text{)}$$

$$d = 2 \text{ (ft)}$$

$$I_{xx} = 40 \text{ (slug-ft}^2\text{)}$$

$$C_{\delta R} = 0.031$$

As referred to in Appendix A and Table I.

Substituting the above values in equation II.E.2-1, it yields:

$$\dot{P} = 8.0346 \cdot \delta_R \quad (\text{II.E.2-3})$$

3. Equations of Aerodynamic Model for Elliptical Airframe

The aerodynamic model equations are similar to those for the circular airframe, with the only differences

in the constant $I_{xx} = 110 \text{ (slug-ft}^2\text{)}$ and $C_{\delta_R} = 0.023$.

Hence they are:

$$\dot{p} = 2.1677 \cdot \delta_R \text{ (rad/sec}^2\text{)} \quad (\text{II.E.3-1})$$

$$\dot{\phi} = P \text{ (rad/sec)} \quad (\text{II.E.3-2})$$

4. Equations of Control Law for Circular and Elliptical Airframe

The yaw control law for circular and elliptical airframe is shown in Figure 2.22.

a. Roll Angle Compensator Equation

$$x = \frac{2.2}{\frac{s}{8} + 1} \cdot (\phi_c - \phi) \quad (\text{II.E.4-1})$$

inverse Laplace transforming the equation II.E.4-1

it becomes:

$$\dot{x} = -8x + 17.6 (\phi_c - \phi) \quad (\text{II.E.4-2})$$

b. Rate Compensator Equation

$$y = \frac{0.15065 \cdot \left(\frac{s}{15} + 1\right)}{\left(\frac{s}{5} + 1\right)} (x - p) \quad (\text{II.E.4-3})$$

Utilizing inverse Laplace transformation, and minor manipulating the equation II.E.4-3, one obtains:

$$\dot{y} = -5y + 50.333 \times 10^{-3} \cdot (\dot{x} - \dot{p}) + 0.7555 (x - p) \quad (\text{II.E.4-4})$$

c. Pseudo Differentiator Equation

$$x_1 = \frac{0.01303}{\frac{s}{6} + 1} \cdot p \quad (\text{II.E.4-5})$$

Using inverse Laplace transformation and rearranging the equation II.E.4-5, it becomes:

$$\dot{x}_1 = -6x_1 + 0.0782 \cdot \dot{p} \quad (\text{II.E.4-6})$$

d. Equation of Actuator Compensator

This network of roll control law is different for circular and elliptical airframe.

(1) Circular Airframe

$$\delta_{R_c} = \left(\frac{s}{110} + 1 \right) \cdot (Y - X_1) / \left(\frac{s}{15} + 1 \right) \quad (\text{II.E.4-7})$$

Using, inverse Laplace transformation and

rearranging the equation II.E.4-7, it yields:

$$\dot{\delta}_{R_c} = -15\delta_{R_c} + 0.1363 (\dot{Y} - \dot{X}_1) + 15(Y - X) \quad (\text{II.E.4-8})$$

(2) Elliptical Airframe

$$\delta_{R_c} = \frac{4.1724 \cdot \left(\frac{s}{110} + 1 \right)}{\frac{s}{15} + 1} (Y - X_1) \quad (\text{II.E.4-9})$$

Inverse Laplace transforming and

rearranging the above equation, it becomes:

$$\dot{\delta}_{R_c} = -15\delta_{R_c} + 0.56993 (\dot{Y} - \dot{X}_1) + 62.536 (Y - X_1)$$

(II.E.4-10)

e. Actuator Equation

$$\delta_{R_c} = \frac{57.3}{\frac{s}{188.4} + 1} \delta_{R_c} \text{ (deg)} \quad (\text{II.E.4-11})$$

Utilizing inverse Laplace transformation, the equation II.E.4-11 becomes:

$$\dot{\delta}_R = -188.4 \cdot \delta_R + 10795.32 \delta_{R_c} \text{ (deg/sec)} \quad (\text{II.E.4-12})$$

Utilizing state-space representation, all the aforementioned equation of the aerodynamic models and

control laws for the circular and elliptical airframes, can be modelled in the state variables systems given below:

(1) For the circular airframe

$$\begin{array}{c} \dot{P} \\ \dot{\phi} \\ \dot{X} \\ \dot{Y} \\ \dot{X}_1 \\ \dot{\delta}_{Rc} \\ \dot{\delta}_R \end{array} = \begin{array}{ccccccc} 0 & 0 & 0 & 0 & 0 & 0 & 8.0345 \\ 1 & 0 & 0 & 0 & 0 & 0 & 0 \\ 0 & 17.6 & -8 & 0 & 0 & 0 & 0 \\ -0.756 & 0.886 & 0 & -5 & 0 & 0.353 & -0.4044 \\ 0 & 0 & 0 & 0 & -6 & 0 & 6.283 \\ -0.103 & 0.121 & 0.483 & 14.319 & -14.182 & -5 & -0.038 \\ 0 & 0 & 0 & 0 & 0 & 10795.32 & -188.4 \end{array} \cdot \begin{array}{c} P \\ \phi \\ X \\ Y \\ X_1 \\ \delta_{Rc} \\ \delta_R \end{array} + \begin{array}{c} 0 \\ 0 \\ -17.6 \\ -0.886 \\ 0 \\ -0.121 \\ 0 \end{array} \phi_c$$

(II.E.4-13)

(2) For the elliptical airframe

$$\begin{array}{c} \dot{P} \\ \dot{\phi} \\ \dot{X} \\ \dot{Y} \\ \dot{X}_1 \\ \dot{\delta}_{Rc} \\ \dot{\delta}_R \end{array} = \begin{array}{ccccccc} 0 & 0 & 0 & 0 & 0 & 0 & 2.1677 \\ 1 & 0 & 0 & 0 & 0 & 0 & 0 \\ 0 & 17.6 & -8 & 0 & 0 & 0 & 0 \\ -0.756 & 0.886 & 0 & -5 & 0.353 & 0 & -0.4044 \\ 0 & 0 & 0 & 0 & -6 & 0 & 6.283 \\ -4.248 & -0.504 & 0.208 & -3.141 & 59.7413 & -15 & -0.588 \\ 0 & 0 & 0 & 0 & 0 & 10795.3 & -188.4 \end{array} \cdot \begin{array}{c} P \\ \phi \\ X \\ Y \\ X_1 \\ \delta_{Rc} \\ \delta_R \end{array} + \begin{array}{c} 0 \\ 0 \\ -17.6 \\ -0.856 \\ 0 \\ -0.504 \\ 0 \end{array} \phi_c$$

(II.E.4-14)

where the state variables are:

P : roll angular rate

ϕ : roll angle

X : output of roll angle compensator

Y : output of rate compensator network

X_1 : output of pseudo differentiator

δ_{R_C} : input command in the actuator

δ_R : roll tail incidence

The state $\phi, X, P, Y, X_1, \delta_{Y_C}$ are shown in Figure 2.22.

5. Design Approach and Analysis of Uncoupled Linear Roll Channel for Circular and Elliptical Airframe

The design technique and analysis is the same as that which was used for the Pitch and Yaw channel.

For purposes of analysis, two CSMP program were written (Appendix F) using the state variable system represented by the aerodynamic model and control law, Block diagram.

Figures 2.23 shows the roll angle response of both elliptical and circular airframe. The time constant of the roll angle response is 0.55 seconds, the overshoot 3% and the steady state roll angle error equal to zero.

Figure 2.24 shows the required body roll angular rate for both elliptical and circular airframes. Only the roll tail angular deflection figures 2.25 and 2.26 is different for the airframes, due to the method of compensating for a reduction in the elliptical aerodynamic roll gain. This is desirable for the aerodynamic roll gain $(57.3qsdC_{L_{\delta_R}} / I_{XX})$ to be as large as possible to minimize

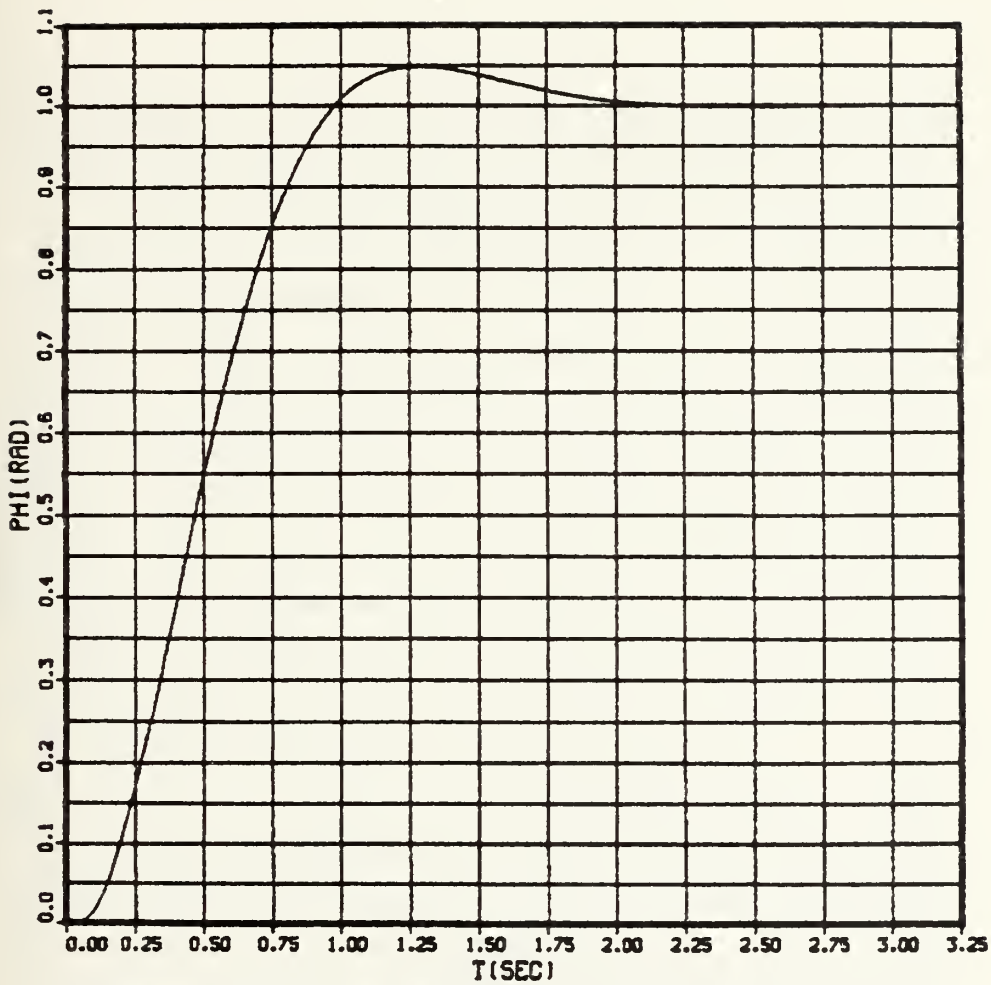


Fig. 2.23 Roll Angle (ϕ) vs Time (t)
 Uncoupled Roll Channel
 Circular or Elliptical airframe
 (1 RAD Command, $a_e = 0$)

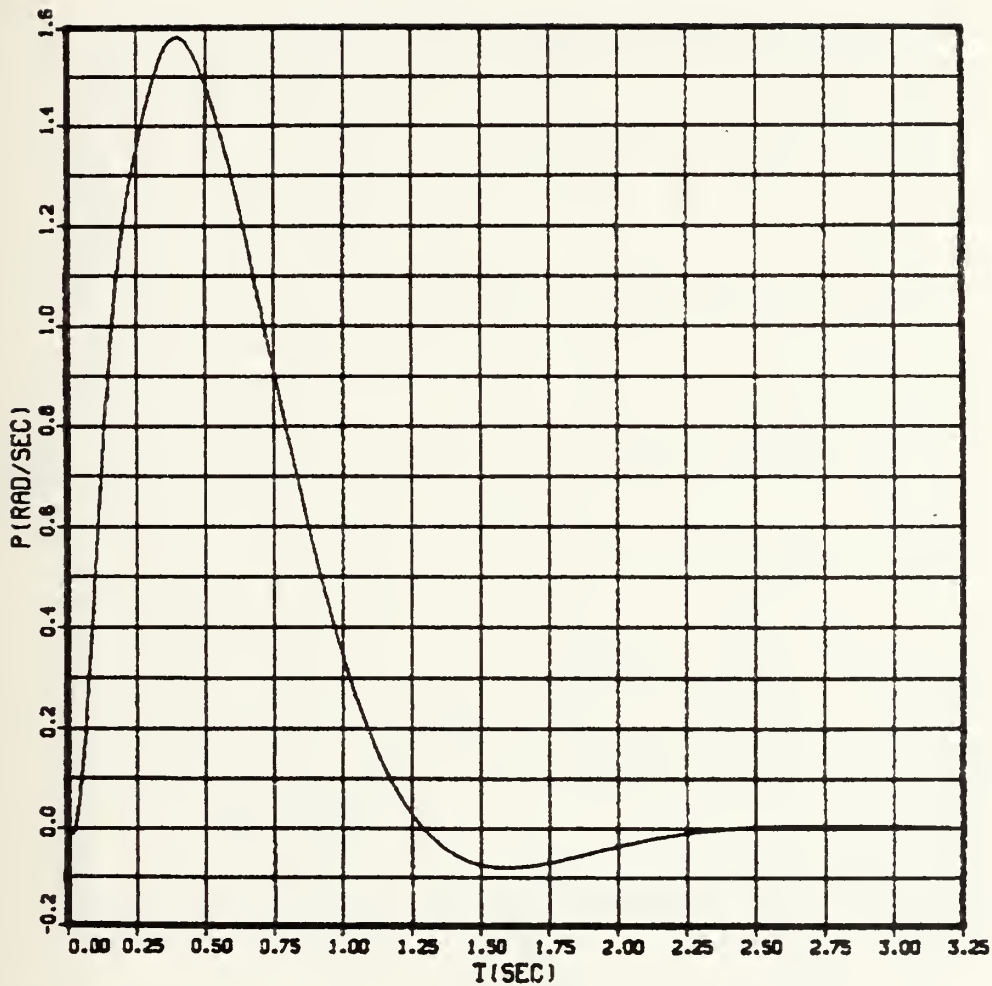


Fig. 2.24 Roll Angular Rate (p) vs Time (t)
 Uncoupled Roll Channel
 Circular or Elliptical airframe
 (1 RAD Command. $a_e = 0$)

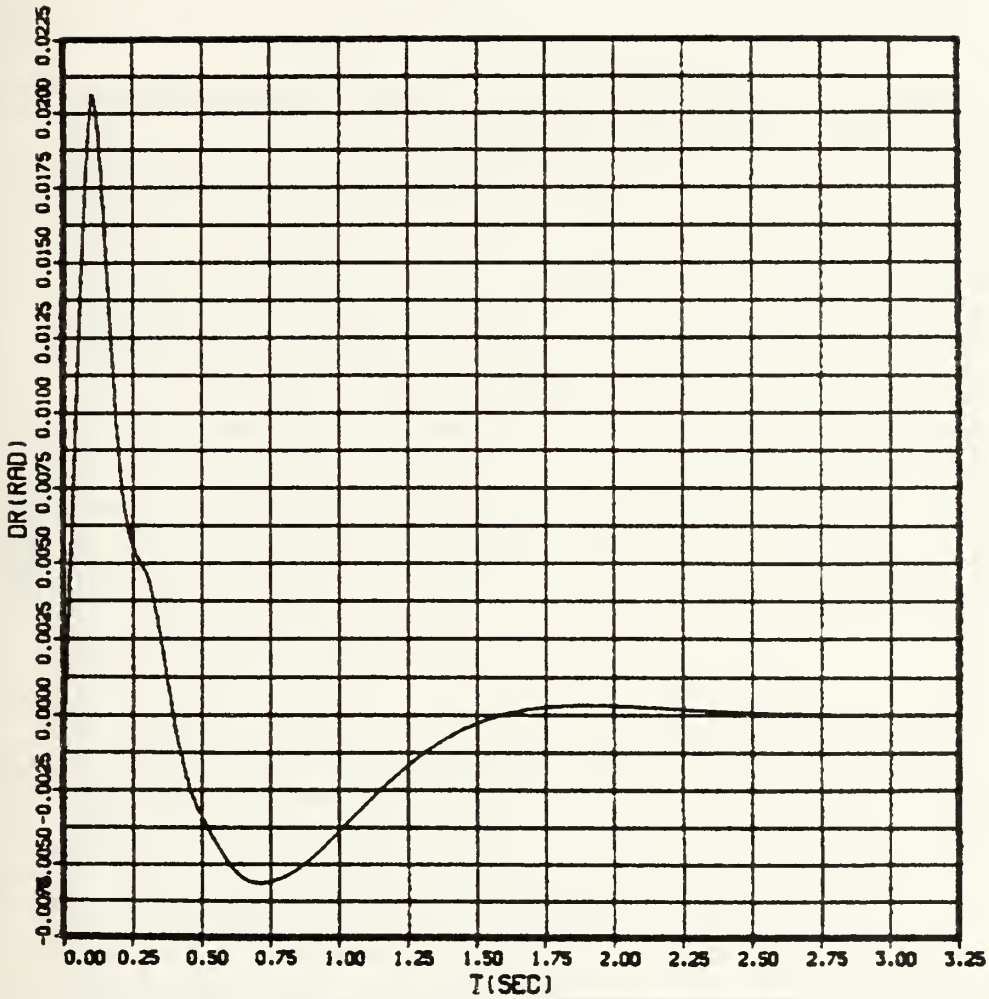


Fig. 2.25 Roll tail incidence (δ_R) vs Time (t)

Uncoupled Roll Channel
 Circular airframe (1 RAD Command,
 $a_e = 0$)

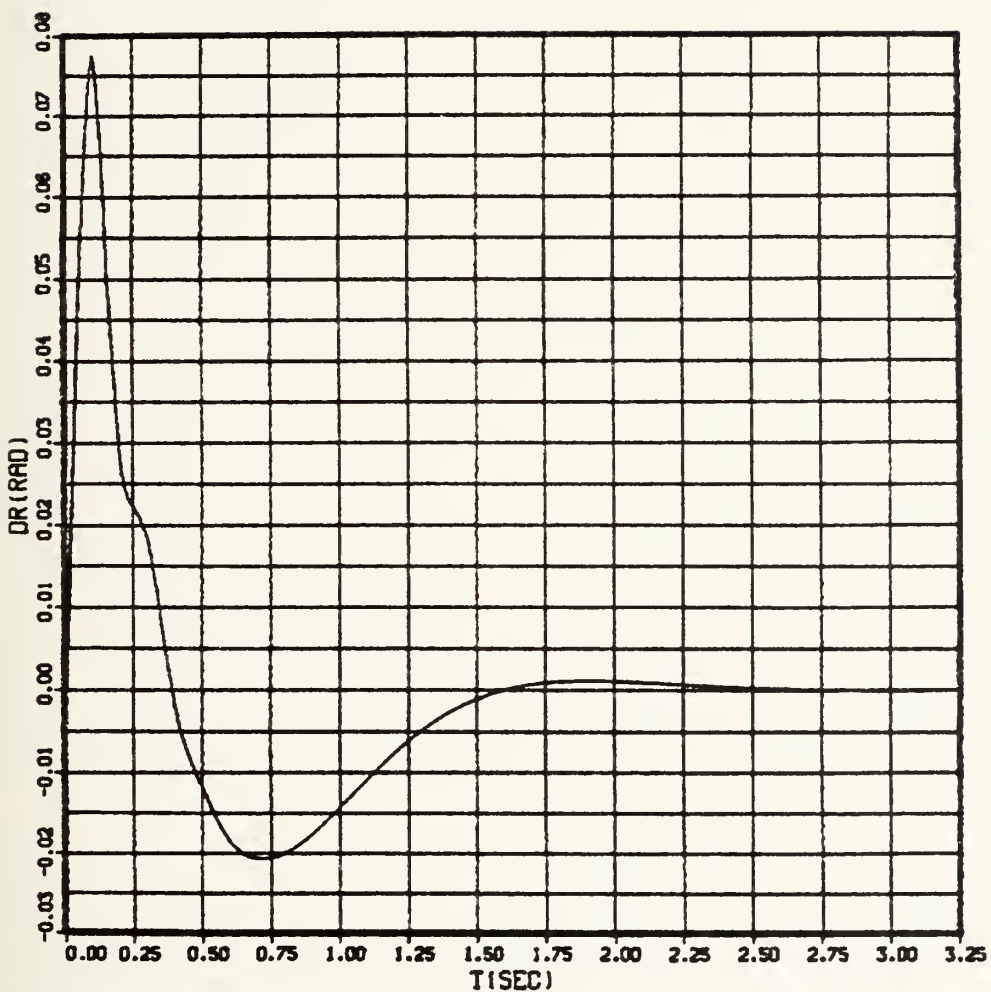


Fig. 2.26 Roll tail incidence (δ_R) vs Time (t)
 Uncoupled Roll Channel
 Elliptical airframe (1 RAD Command, $a_e = 0$)

control surface motion. It is also desirable to have as large $C_{l\delta_R}$ as possible to minimize the effects of aerodynamic control cross coupling. The circular airframe has a considerably larger aerodynamic roll gain due to a much smaller roll inertia and a larger control derivative

$C_{l\delta_R}$.

III. LINEAR DESIGN AND ANALYSIS OF COUPLED AUTOPILOTS FOR CIRCULAR AND ELLIPTICAL AIRFRAMES

A. GENERAL

The linear design and analysis technique began with uncoupled autopilot channels. The uncoupled autopilot design technique was classical, using a combination of frequency response and root locus techniques [Ref. 2], to achieve practical bandwidths (i.e, sufficient high frequency attenuation) and in turn provides the range of required missile body angular rates and control motions, as mentioned in section II.

In this section, CBTT control laws are analyzed to add control coupling for coordinated missile motion. A measure of sideslip control is obtained by applying a roll angle command to the linearized CBTT autopilot. The relative stability of the autopilot branches and means for improving stability are discussed. An examination of the autopilot sensitivity to aerodynamic cross-coupling is made.

B. AERODYNAMIC MODELS FOR THE CIRCULAR AIRFRAME

The aerodynamic models of pitch and roll-yaw channels for the circular airframe are shown in Figures 3.1 and 3.2, taken from [Ref. 2]. The models are linearized and were developed for stability studies in the frequency domain.

The assumptions for linearization are the same, as those in section II.C.1.

Pitch and Lateral channels are coupled via constant missile roll rate P_e . Also, the linear model has inertial, kinematic and aerodynamic cross couplings, which will be discussed further, in the non-linear model.

1. Pitch Channel

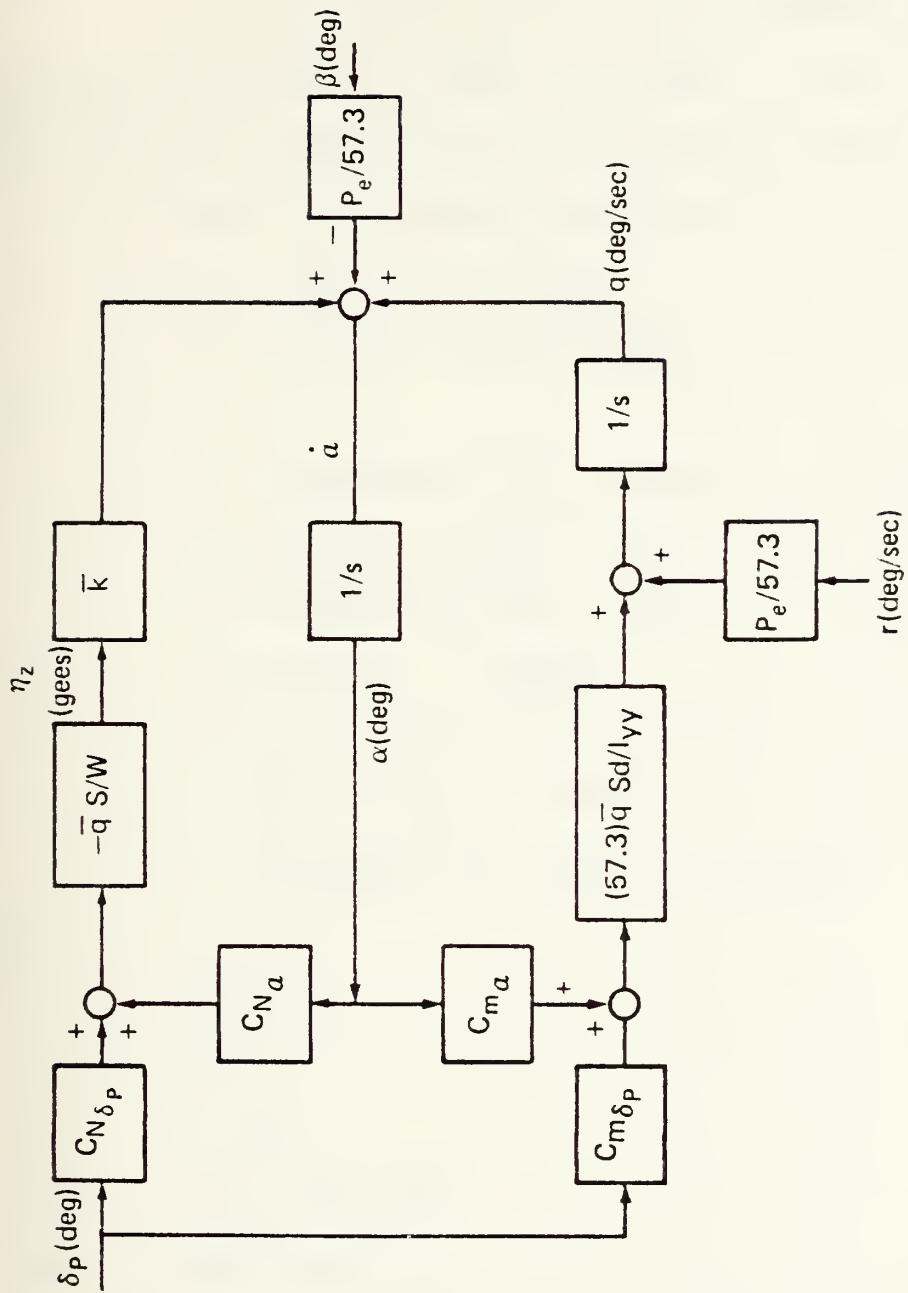
The linear aerodynamic model of the pitch channel consisted of the uncoupled model mentioned in chapter II, which is coupled with the Roll-Yaw channels via constant roll rate (P_e), as shown in Figure 3.1.

In this work, the P_e was set to zero, because when $P_e=0$, the Q_e (i.e equilibrium pitch rate) has been found to have negligible influence in the lateral model (i.e roll-yaw).

The equations, which represent the pitch aerodynamic model given in [Ref. 2] are the same as the equations of the uncoupled linear model, mentioned in chapter II.

2. Lateral Channels

The linear lateral aerodynamic model consisted of the uncoupled roll and yaw aerodynamic channel, coupled via the linearized aerodynamic derivatives $C_{l\beta}$, $C_{l\delta_Y}$ and $C_{n\delta_R}$. Also, it is coupled with the pitch dynamic model via



- Note: 1. P_e = constant roll rate (deg/sec).
 2. $\eta_z, \alpha, \beta, q, r$ are perturbation of missile from trim.

Fig. 3.1 Linear Pitch channel dynamic model

the P_e , as previously mentioned. The lateral dynamic model is shown in Figure 3.2, as given in [Ref. 2].

To find the equations which represent the lateral dynamic model, P_e and Q_e are set to zero because of their negligible influence in the lateral channel.

The aforementioned equations are as follows:

$$\eta_Y = \bar{q} \cdot S \cdot E_1 / W \quad (\text{gees}) \quad (\text{II.B.2-1})$$

$$E_1 = \beta \cdot C_{Y\beta} + C_{Y\delta_Y} \cdot \delta_Y \quad (\text{deg}) \quad (\text{III.B.2-2})$$

where:

$$\dot{r} = 57.3 \bar{q} S d \cdot E_2 / I_{zz} \quad (\text{deg/sec}^2) \quad (\text{III.B.2-3})$$

$$E_2 = \beta \cdot C_{n\beta} + C_{n\delta_R} \cdot \delta_R + C_{n\delta_Y} \cdot \delta_Y \quad (\text{deg}) \quad (\text{III.B.2-4})$$

$$\dot{p} = 57.3 \bar{q} S d E_4 / I_{xx} \quad (\text{deg/sec}^2) \quad (\text{III.B.2-5})$$

$$\dot{\phi} = P/57.3 \quad (\text{rad/sec}) \quad (\text{III.B.2-6})$$

$$E_3 = C_{e\delta_Y} \cdot \delta_Y + C_{e\delta_R} \cdot \delta_R \quad (\text{deg}) \quad (\text{III.B.2-7})$$

$$E_4 = E_3 + C_{e\beta} \cdot \beta \quad (\text{deg}) \quad (\text{III.B.2-8})$$

$$\dot{\beta} = P \cdot A / 57.3 - Y + K \cdot (\bar{q} S E_1 / W) \quad (\text{deg/sec}) \quad (\text{III.B.2-9})$$

where:

$$k = 0.48$$

$$S = \pi (\text{ft})^2$$

$$d = 2.0 (\text{ft})$$

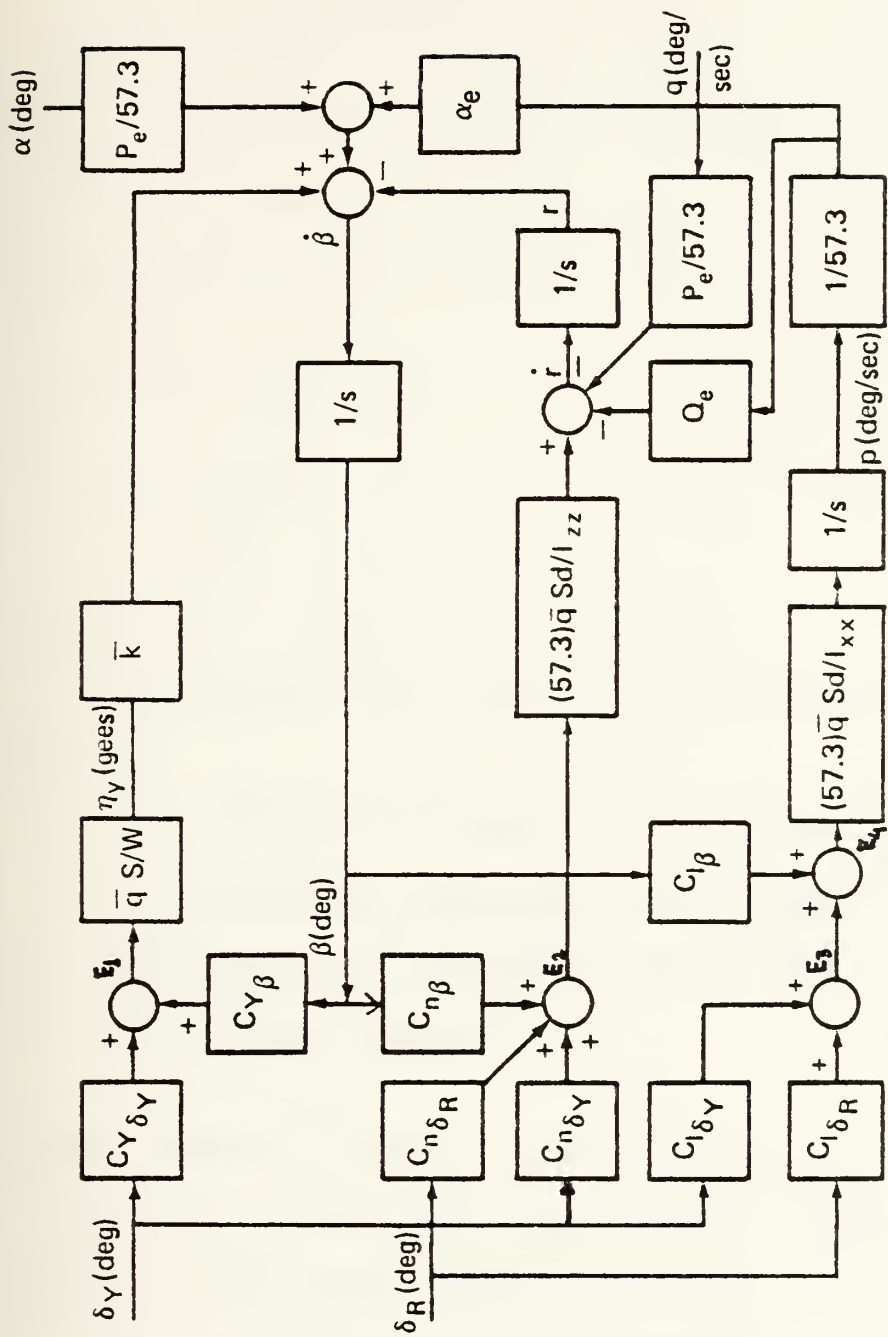
$$\bar{q} = 1650 \quad (\text{lb/ft}^2)$$

$$W = 2525 \quad (\text{lb})$$

$$I_{xx} = 40.0 \quad (\text{slug-ft}^2)$$

$$I_{zz} = 810.0 \quad (\text{slug-ft}^2)$$

$$C_{Y\delta_Y} = 0.22$$



Note: 1. P_e = constant roll rate (deg/sec).

2. α_e = constant angle of attack (deg).

3. O_e = constant pitch rate (deg/sec)

Fig. 3.2 Linear lateral (Roll/Yaw) dynamic model

$$C_{Y\beta} = -0.082$$

$$C_{n\delta_R} = 0.018$$

$$C_{n\beta} = -0.019$$

$$C_{n\delta_Y} = -0.053$$

$$C_{l\delta_Y} = -0.016$$

$$C_{l\beta} = -0.009$$

$$C_{l\delta_R} = 0.035$$

$$A = 10^0$$

As referred to in Appendix A and Table I.

Substituting the values into the above equations, they yield:

$$\dot{\gamma} = -13.934 \cdot \beta + 13.934 \cdot \delta_R - 38.87 \cdot \delta_Y \text{ (deg/sec}^2\text{)} \quad (\text{III.B.2-10})$$

$$\dot{p} = -133.66 \cdot \beta + 519.788 \cdot \delta_R - 237.618 \cdot \delta_Y \text{ (deg/sec}^2\text{)} \quad (\text{III.B.2-11})$$

$$\dot{\beta} = 0.01745 P - r - 0.0808 \beta + 0.217 \cdot \delta_Y \text{ (deg/sec)} \quad (\text{III.B.2-12})$$

$$\dot{\phi} = P/57.3 \text{ (rad/sec)} \quad (\text{III.B.2-13})$$

C. CBTT AUTOPILOT CONTROL LAWS FOR CIRCULAR AIRFRAME

The control laws, which were used by the CBTT autopilots of the circular and elliptical airframe, are shown in Figures 2.6 and 3.3, as given in [Ref. 2].

The pitch control law for the circular airframe is the same as determined in the uncoupled pitch channel study

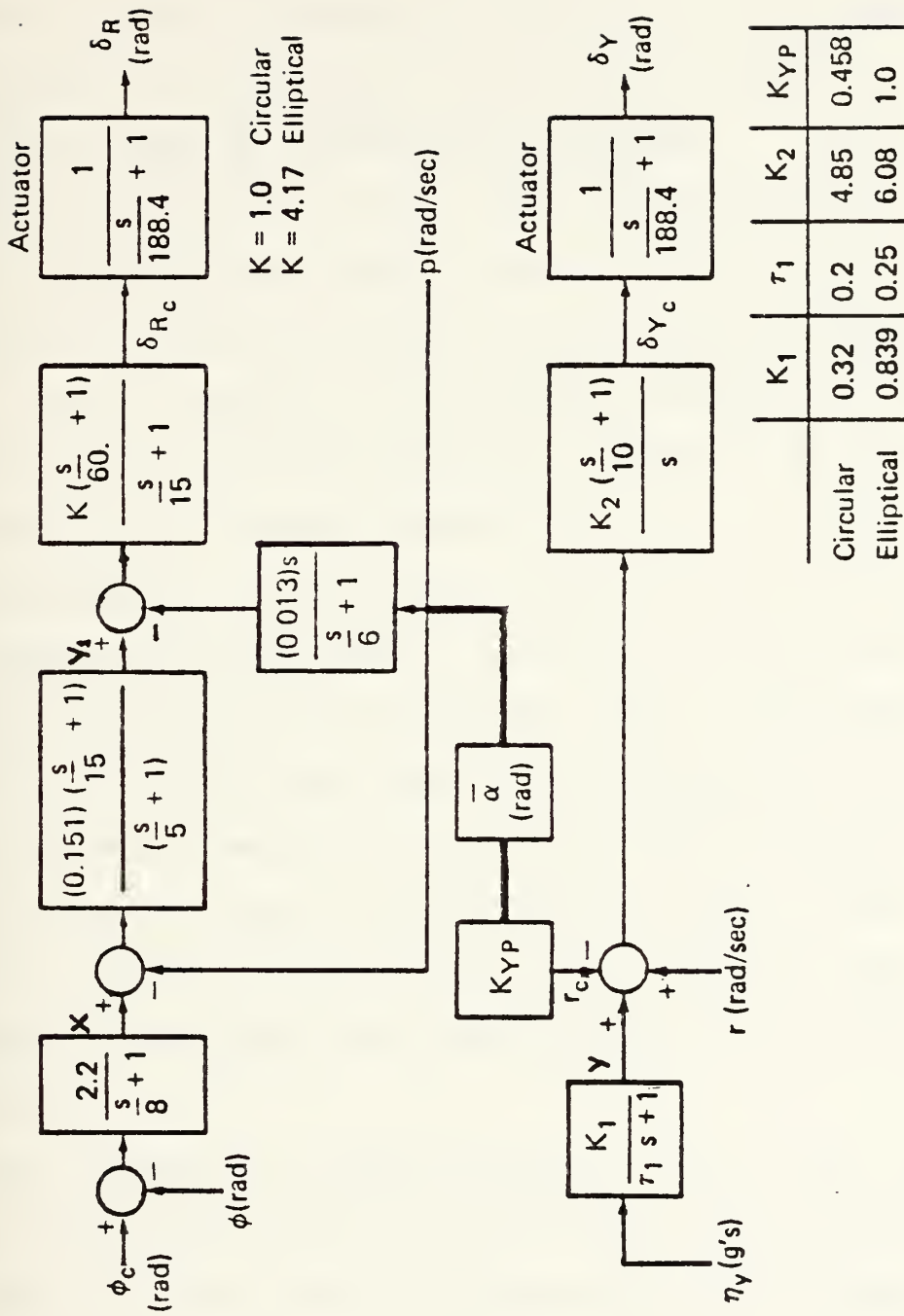


Fig. 3.3 CBTT lateral control law

section II.B.2, and therefore, the equations which represent it, are the same as in section II.B.3., except the equation for pitch tail incidence angle which is:

$$\dot{\delta}_p = -188.4 \cdot \delta_p + 10795.3 \cdot \delta_{p_c} \text{ (deg/sec)} \quad (\text{III.C.1})$$

The uncoupled roll and yaw laws are coupled via a cross-coupling branch, shown in solid line in Figure 3.3, in order to consist the linear coupled lateral control law.

In the roll actuator of the lateral control law, the frequency has been changed from 110 rad/sec to 60 rad/sec, for improving of autopilot stability.

The autopilot cross-coupling branch between Roll and Yaw channels has been added to provide coordinated motion. Coordinated motion or zero sideslip angle is achieved by directing the body fixed pitch axis of the missile of the missile velocity vector, so that there is no component of missile velocity along the body fixed yaw axis of the missile. Figure 3.4, as given in [Ref. 2] shows the attitude of the missile body with respect to its velocity vector V.

When commanding an upward maneuver (i.e, $\phi = 0$), the missile body moves upward with its pitch axis directed at the velocity vector until it reaches the desired maneuver level or angle-of-attack. No roll motion is required to maintain coordination for this maneuver.

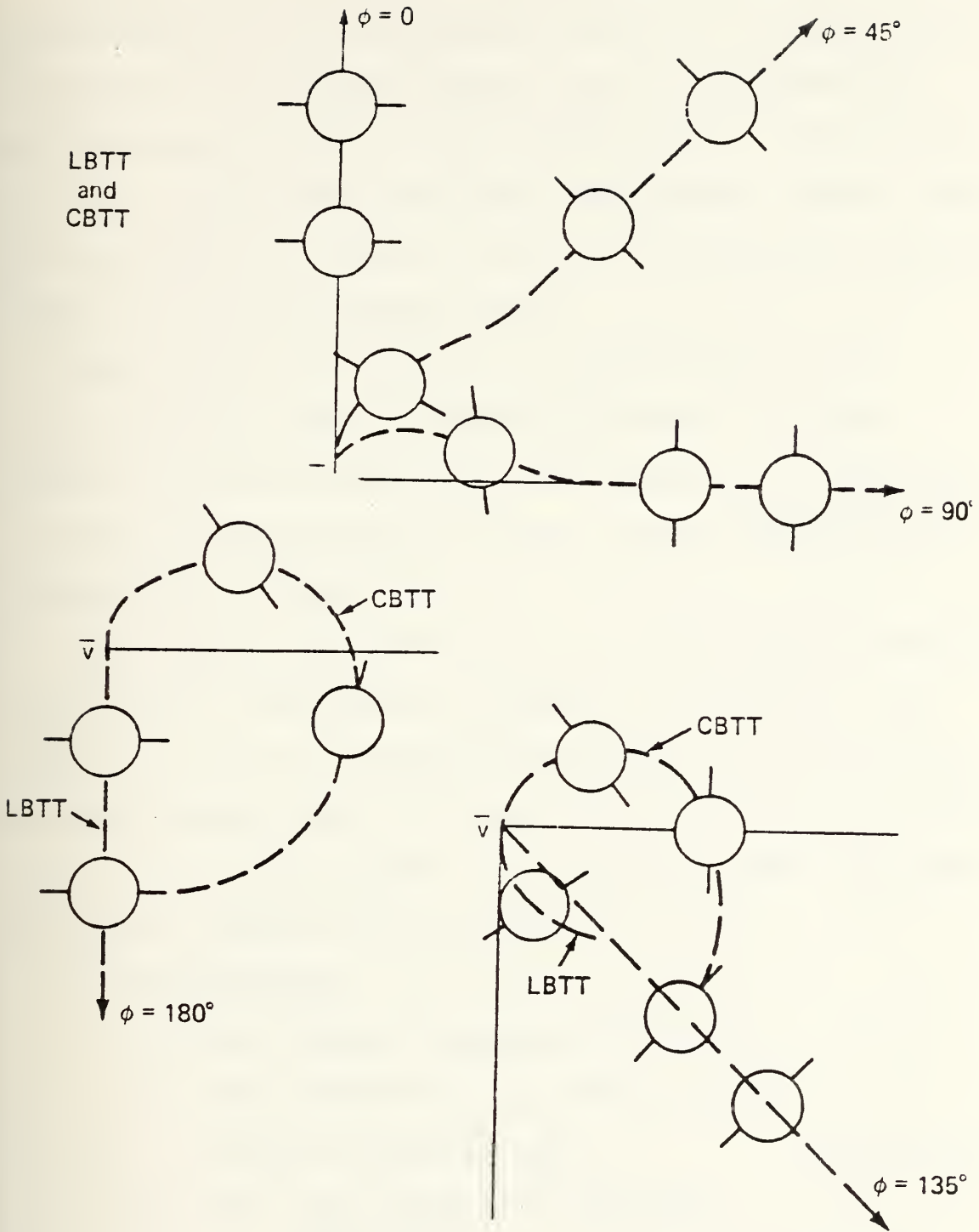


Fig. 3.4 Coordinated Missile Motion for Coordinated bank-to-turn (CBTT) and limited bank-to-turn (LBTT) Control policies

For maneuvers in the $\phi=45$ or 90 degree directions, the missile body rolls the desired ϕ and moves its pitch axis directed at the velocity vector, until it achieves the desired maneuver level. For maneuvers with ϕ higher than 90° , the missile must roll about the velocity vector, while the Yaw channel directs the pitch axis towards the velocity vector for minimum sideslip angle.

The missile is forced to roll about its velocity vector, when the desired maneuver direction is in the negative angle-of-attack direction, because it is desired to avoid negative angles-of-attack. These maneuvers are illustrated in Figure 3.4.

The coordinating command r_c , is a yaw angular rate from a rate gyro. The command is equal to $-Pa_e$, where $a_e=a$ (Figure 3.3) in the coordinating branch is the equivalent angle-of-attack, which is exactly equal to angle of attack (a), in the linear studies. The equations which represent the lateral channel are as follows:

1. Roll Channel

a. Roll Command Compensator Equation

Same equation as in section II.E

$$\dot{\chi} = 8\chi + 17.6 (\phi_c - \phi) \quad (\text{III.C.1-1})$$

b. Roll Rate Compensator Equation

$$Y_1 = \frac{0.151 \cdot \left(\frac{s}{15} + 1 \right)}{\frac{s}{5} + 1} (X - P/57.3) \quad (\text{III.C.1-2})$$

Inverse Laplace transforming and rearranging the equation (III.C.1-2), it becomes:

$$\dot{Y}_1 = -5Y_1 + 0.0503 (\dot{X} - P/57.3) + 0.755 (X - P/57.3) \quad (\text{III.C.1-3})$$

c. Pseudo Differentiator Equation

$$X_1 = \frac{0.013 \cdot S}{\frac{S}{6} + 1} (P/57.3) \quad (\text{III.C.1-4})$$

Utilizing inverse Laplace transformation and minor manipulating the above equation, one has:

$$\dot{X}_1 = -6X_1 + 0.078 (\dot{P}/57.3) \quad (\text{III.C.1-5})$$

d. Actuator's Compensator Equation

The frequency of the compensator was changed from 110 rad/sec to 60 rad/sec for purposes of stability, as referred in section III.C. The equation represents the network is:

$$\delta_{Rc} = \frac{\frac{S}{60} + 1}{\frac{S}{15} + 1} (Y - X_1) \quad (\text{III.C.1-6})$$

Using inverse Laplace transformation, the equation III.C.1-6, one obtains:

$$\dot{\delta}_{Rc} = -15 \delta_{Rc} + 0.25 (\dot{Y} - \dot{X}_1) + 15 (Y - X_1) \quad (\text{III.C.1-7})$$

e. Actuator Equation

$$\delta_R = \frac{57.3}{\frac{S}{188.4} + 1} \delta_{Rc} \text{ (deg)} \quad (\text{III.C.1-8})$$

Utilizing inverse Laplace transformation and rearranging the equation III.C.1-8, it yields.

$$\dot{\delta}_R = -188.4 \delta_R + 10795.32 \delta_{Rc} \quad (\text{III.C.1-9})$$

All the referred to above state variables, are shown in figure 3.3.

2. Yaw Channel

a. Acceleration Compensator Equation

$$Y = \frac{0.32}{0.2s + 1} \eta_Y \quad (\text{III.C.2-1})$$

Inverse Laplace transforming, equation

III.C.2-1 becomes:

$$\dot{Y} = -5Y + 1.6 \eta_Y \quad (\text{III.C.2-2})$$

b. Actuator Compensator Equation

$$\delta_{Yc} = (4.85(\frac{s}{10} + 1)/s) \cdot (Y - 0.458 \bar{\alpha} \cdot P/57.3 + r) \quad (\text{III.C.2-3})$$

Utilizing inverse Laplace transformation and rearranging the equation III.C.2-3, it yields:

$$\delta \dot{Y}_c = 0.485(\dot{Y} + \dot{Y}/57.3 - 0.458 \cdot \bar{\alpha} \cdot \dot{P}/57.3) + 4.85(Y + r/57.3 - 0.458 \cdot \bar{\alpha} \cdot P/57.3) \quad (\text{III.C.2-4})$$

c. Actuator Equation

$$\delta \dot{Y} = -188.4 \cdot \delta Y + 10795.3 \cdot \delta Y_c \quad (\text{III.C.2-5})$$

Making use the state-variable representation, the above equations, of the aerodynamic models and control laws, can be modelled in the following, state variable equation system:

$$\begin{bmatrix} \dot{r} \\ \dot{p} \\ \dot{\phi} \\ \dot{\beta} \\ \dot{x} \\ \dot{y}_1 \\ \dot{x}_1 \\ \delta_{Rc} \\ \delta_R \\ \dot{y} \\ \delta_{Yc} \\ \dot{\delta}_Y \end{bmatrix} = \begin{bmatrix} 0 & 0 & 0 & -13.934 & 0 & 0 & 0 & 0 & 13201 & 0 & 0 & -38.87 \\ 0 & 0 & 0 & -133.66 & 0 & 0 & 0 & 0 & 519.79 & 0 & 0 & -237.62 \\ 0.0174 & 0 & 0 & 0 & 0 & 0 & 0 & 0 & 0 & 0 & 0 & 0 \\ -1 & 0.1745 & 0 & -0.0808 & 0 & 0 & 0 & 0 & 0 & 0 & 0 & 0.2168 \\ 0 & 0 & -17.6 & 0 & -8 & 0 & 0 & 0 & 0 & 0 & 0 & 0 \\ 0 & 0.0132 & -0.886 & 0.1174 & 0.3523 & -5 & 0 & 0 & -0.457 & 0 & 0 & 0.2088 \\ 0 & 0 & 0 & -0.182 & 0 & 0 & -6 & 0 & 0.7074 & 0 & 0 & -0.323 \\ 0 & 0.0033 & -0.2215 & 0.0748 & 0.0812 & 13.75 & -13.6 & -15 & 0.291 & 0 & 0 & 0.133 \\ 0 & 0 & 0 & 0 & 0 & 0 & 0 & 10795.3 & -188.4 & 0 & 0 & 0 \\ 0 & 0 & 0 & -0.269 & 0 & 0 & 0 & 0 & 0 & -5 & 0 & 0 \\ 0.0174 & -0.0014 & 0 & -0.187 & 0 & 0 & 0 & 0 & 0 & -0.482 & 2.425 & 0.0037 \\ 0 & 0 & 0 & 0 & 0 & 0 & 0 & 0 & 0 & 10795.3 & -188.4 & 0 \end{bmatrix} \cdot \begin{bmatrix} r \\ p \\ \phi \\ \beta \\ x \\ y_1 \\ x_1 \\ \delta_{Rc} \\ \delta_R \\ y \\ \delta_{Yc} \\ \delta_Y \end{bmatrix} + \begin{bmatrix} 0 \\ 0 \\ 0 \\ 0 \\ 17.6 \\ 0.886 \\ 0 \\ 0.2215 \\ 0 \\ 0 \\ 0 \\ 0 \end{bmatrix} \phi_c$$

(III.C.2-6)

where the state variables are:

- r : yaw angular rate
- p : roll angular rate
- ϕ : roll angle
- β : sideslip angle
- x : output of roll command compensator
- y_1 : output of roll rate compensator
- x_1 : output of pseudo differentiator
- δ_{Rc} : input command in roll actuator
- δ_R : roll tail incidence
- y : output of yaw acceleration compensator
- δ_{Yc} : input command in yaw actuator
- δ_Y : yaw tail incidence angle

All the referred before state variables are shown in Figures 3.2 and 3.3.

D. ANALYSIS OF LINEAR CBTT AUTOPILOTS FOR CIRCULAR AIRFRAME

In the analysis of the linear CBTT autopilots it is assumed that the missile is initially in the desired maneuver plane, is trimmed at ten degrees angles-of-attack, the equilibrium roll rate P_e and equilibrium pitch rate Q_e were set equal to zero.

For purposes of analysis, a CSMP program was written (Appendix G) using the equations of the aerodynamic models and control laws of the linear CBTT autopilots for the circular airframe.

Figure 3.5 shows the sideslip angle for the linearized CBTT autopilot, having a maximum value of 2.32° . Since the model is linear, and therefore the magnitude of the sideslip is directly proportional to the magnitude of the input command, a one radian roll angle command was used for convenience.

The coupled autopilots have a roll angle response which is the same, as the uncoupled roll channel response, differing slightly in the overshoot, as shown in Figure 3.6.

The aforementioned values and plots are exactly the same as the plots given in the [Ref. 2] therefore its results are verified.

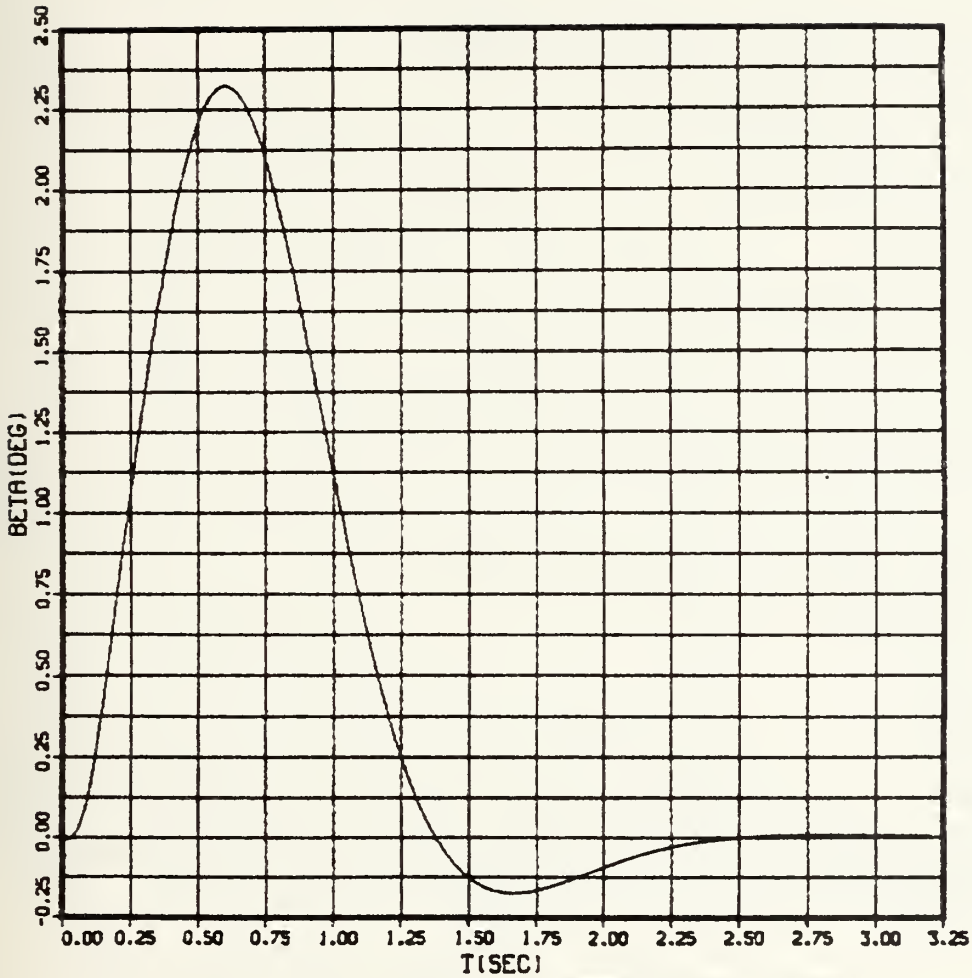


Fig. 3.5 Sideslip angle (β) vs Time (t)
 Linear CBTT Autopilot (1 RAD Roll
 Command); Circular airframe ($a_e=10$ deg,
 $P_e=Q_e=0$ deg)

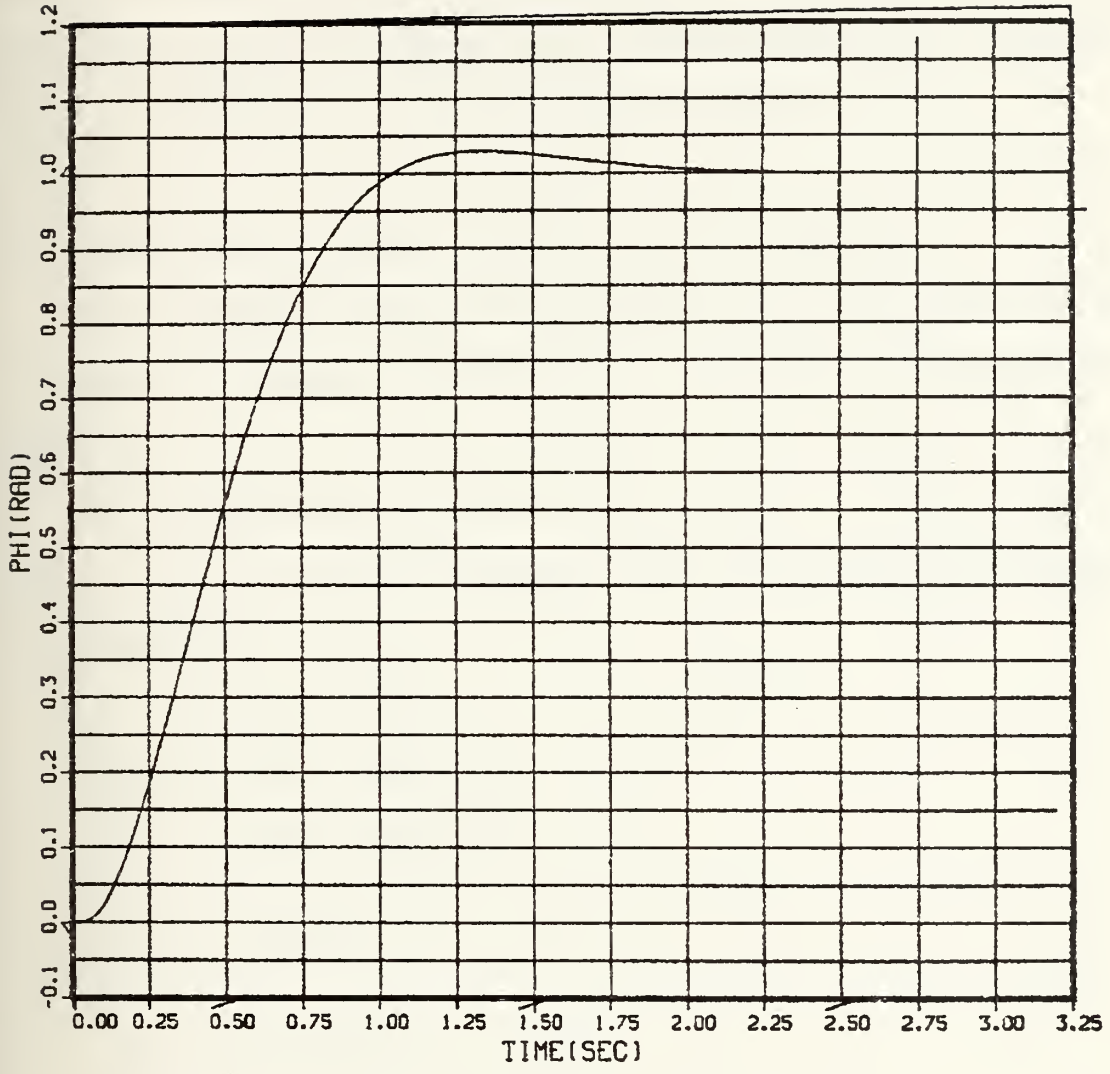


Fig. 3.6 Roll angle (ϕ) vs Time (t)
 Linear CBTT Autopilot (1 RAD Roll
 Command) Circular airframe ($a_e=10$
 deg, $P_e=Q_e=0$ deg)

Comparing the state variable form system with these previous discussed in the section II.D and II.E, this is the twelfth order system because it includes roll and yaw autopilots and the matrices A,B are different than the A,B matrices at the uncoupled roll and yaw autopilot, because of the existence of the coordination branch.

E. AERODYNAMIC MODELS FOR ELLIPTICAL AIRFRAME

The dynamic models for elliptical airframe are the same as those of circular airframe and are shown in Figures 3.1 and 3.2.

The differences of the circular and elliptical models are in the following constants and linearized aerodynamics derivatives:

$$w = 2475 \text{ (lbf)}$$

$$I_{xx} = 110 \text{ (slug-ft}^2\text{)}$$

$$I_{zz} = 790 \text{ (slug-ft}^2\text{)}$$

$$C_{Y_{\delta_Y}} = 0.015$$

$$C_{Y_{\beta}} = -0.054$$

$$C_{n_{\delta_R}} = 0.014$$

$$C_{n_{\beta}} = 0.024$$

$$C_{n_{\delta_Y}} = -0.039$$

$$C_{\ell \delta_Y} = -0.010$$

$$C_{\ell \beta} = -0.027$$

$$C_{\ell \delta_R} = 0.023$$

as referred to in Appendix A and Table I. The equations which represent the aerodynamic model, are as follows:

$$\dot{\gamma} = 18.0469 \cdot \beta + 10.5273 \cdot \delta_R - 29.3262 \cdot \delta_Y \quad (\text{III.E.1})$$

$$\dot{\beta} = -145.8107 \cdot \beta + 124.2091 \cdot \delta_R - 54.04 \cdot \delta_Y \quad (\text{III.E.2})$$

$$\dot{\phi} = P/57.3 \quad (\text{III.E.3})$$

$$\dot{\delta} = 0.17452 P - \gamma + 0.054287 \cdot \beta - 0.01508 \cdot \delta_Y \quad (\text{III.E.4})$$

F. CBTT AUTOPILOTS CONTROL LAWS FOR ELLIPTICAL AIRFRAME

The control laws, which were used by the CBTT autopilots of the elliptical airframe are the same as those of the circular airframe and are shown in Figure 2.6 and 3.3.

The differences which exist in the control laws of the two airframes are the gain K_{YP} of the coordinated branch, and the gains of the actuators.

Hence, the equations that represent the control laws are:

1. Pitch Channel

The linear pitch control law equations for the elliptical airframe, are the equations of the Pitch uncoupled channel, as given in section II.C.5.

2. Roll Channel

Same equations as in par. III.C.

$$a. \dot{\chi} = -8\chi + 17.6 (\phi_c - \phi) \quad (\text{II.C.1-1})$$

$$b. \dot{Y}_1 = -5Y_1 + 0.0503 (\dot{\chi} - \dot{P}/57.3) + 0.755 (\chi - P/57.3) \quad (\text{II.C.1-3})$$

$$c. \dot{X}_1 = -6X_1 + 0.078 (\dot{P}/57.3) \quad (\text{II.C.3-5})$$

d. Actuator Compensator

$$\dot{\delta}_{R_c} = \frac{4.17 \left(\frac{s}{60} + 1 \right)}{\frac{s}{15} + 1} (Y_1 - X_1) \quad (\text{III.F.2-1})$$

Utilizing inverse Laplace transformation and rearranging the equation III.F.2-1, it becomes:

$$\dot{\delta}_{R_c} = -15\delta_{R_c} + 1.0425 (\dot{Y}_1 - \dot{X}_1) + 62.53 (Y_1 - X_1) \quad (\text{III.F.2-2})$$

$$e. \dot{\delta}_R = -188.4 \delta_R + 10.7953 \times 10^3 \delta_{R_c} \quad (\text{III.C.3-8})$$

3. Yaw Channel

a. Acceleration Compensator Equation

$$Y = \frac{0.839}{\frac{s}{4} + 1} n_Y \quad (\text{III.F.3-1})$$

Inverse Laplace transforming and rearranging the equation III.F.3-1, it yields:

$$\dot{Y} = -4Y + 3.356 n_Y \quad (\text{III.F.3-2})$$

b. Actuator Compensator Equation

$$\dot{\delta}_{Y_c} = \frac{0.608s + 6.08}{s} \left(Y + r/57.3 - \bar{\alpha} P/57.3 \right) \quad (\text{III.F.3-3})$$

Utilizing inverse Laplace transformation and rearranging the above equation, one obtains:

$$\dot{\delta}_{Y_c} = 0.608 \left(\dot{Y} + \frac{\dot{r}}{57.3} - \frac{\bar{\alpha} \dot{P}}{57.3} \right) + 6.08 \left(Y + \frac{r}{57.3} - \frac{\bar{\alpha} P}{57.3} \right) \quad (\text{III.F.3-4})$$

c. Actuator Equation

Same as in par. III.F.2.e

Utilizing the state-variable representation, the equation which represent the aerodynamic model and the control laws, can be modelled in the following twelfth-order system:

$$\begin{bmatrix} \dot{\gamma} \\ \dot{p} \\ \dot{\phi} \\ \dot{\beta} \\ \dot{X} \\ \dot{Y}_1 \\ \dot{X}_1 \\ \dot{\delta}_{R_c} \\ \dot{\delta}_R \\ \dot{\gamma} \\ \dot{\delta}_{Y_c} \\ \dot{\delta}_Y \end{bmatrix} = \begin{bmatrix} 0 & 0 & 0 & 18.05 & 0 & 0 & 0 & 0 & 10.53 & 0 & 0 & -29.32 \\ 0 & 0 & 0 & -145.81 & 0 & 0 & 0 & 0 & 124.21 & 0 & 0 & -54.004 \\ 0 & 0.0175 & 0 & 0 & 0 & 0 & 0 & 0 & 0 & 0 & 0 & 0 \\ -1 & 0.175 & 0 & 0.0543 & 0 & 0 & 0 & 0 & 0 & 0 & 0 & -0.0451 \\ 0 & 0 & -17.6 & 0 & -8 & 0 & 0 & 0 & 0 & 0 & 0 & 0 \\ 0 & -0.132 & -0.886 & 0.13 & 0.35 & -5 & 0 & 0 & -0.109 & 0 & 0 & 0.047 \\ 0 & 0 & 0 & -11.37 & 0 & 0 & -6 & 0 & 9.69 & 0 & 0 & -4.212 \\ 0 & -0.0137 & -0.926 & 11.99 & 0.367 & 57.74 & -56.3 & -15 & -10.21 & 0 & 0 & 4.44 \\ 0 & 0 & 0 & 0 & 0 & 0 & 0 & 10795.3 & -188.4 & 0 & 0 & 0 \\ 0 & 0 & 0 & -0.38 & 0 & 0 & 0 & 0 & 0 & -4 & 0 & 0.015 \\ 0.106 & -0.0185 & 0 & 0.156 & 0 & 0 & 0 & 0 & 0.887 & 3.17 & 0 & -0.51 \\ 0 & 0 & 0 & 0 & 0 & 0 & 0 & 0 & 0 & 0 & 10795.3 & -188.4 \end{bmatrix} \cdot \begin{bmatrix} \gamma \\ p \\ \phi \\ \beta \\ X \\ Y_1 \\ X_1 \\ \delta_{R_c} \\ \delta_R \\ \gamma \\ \delta_{Y_c} \\ \delta_Y \end{bmatrix} + \begin{bmatrix} 0 \\ 0 \\ 0 \\ 0 \\ 17.6 \\ 0.886 \\ 0 \\ 0.926 \\ 0 \\ 0 \\ 0 \\ 0 \end{bmatrix} \cdot \phi_c$$

(III.F.3-5)

where the state variables are:

- r : yaw angular rate
- p : roll angular rate
- φ : roll angle
- β : side slip angle
- X : output of roll command compensator
- Y₁ : output of roll rate compensator
- X₁ : output of pseudo-differentiator network
- δ_{R_c} : input command in roll actuator
- δ_R : roll tail incidence angle

Y : output of acceleration compensator in yaw control law

δ_{Y_c} : input command in yaw actuator

δ_y : yaw tail incidence angle

All the state variables are shown in Figure 3.2 and 3.3. The above system is different in the matrix A and B from the system discussed in chapter II for uncoupled Roll and Yaw autopilots, because of the coordination branch equation.

G. ANALYSIS OF LINEAR CBTT AUTOPILOTS FOR ELLIPTICAL AIRFRAME

In the analysis of the linear CBTT for elliptical airframe, the same assumptions, which were made for the circular airframe, are valid.

A CSMP program was written (Appendix G) with the above equations, which represent the aerodynamic models and the control laws of the linear CBTT autopilots.

Figure 3.7 shows the sideslip angle β for the linearized CBTT autopilot, having maximum values of -0.46° and 0.26° .

Figure 3.8 shows the roll angle response which has an overshoot of 4 percent and is about the same with the roll angle of uncoupled roll autopilot. The above plots verify the results, given in the [Ref. 2].

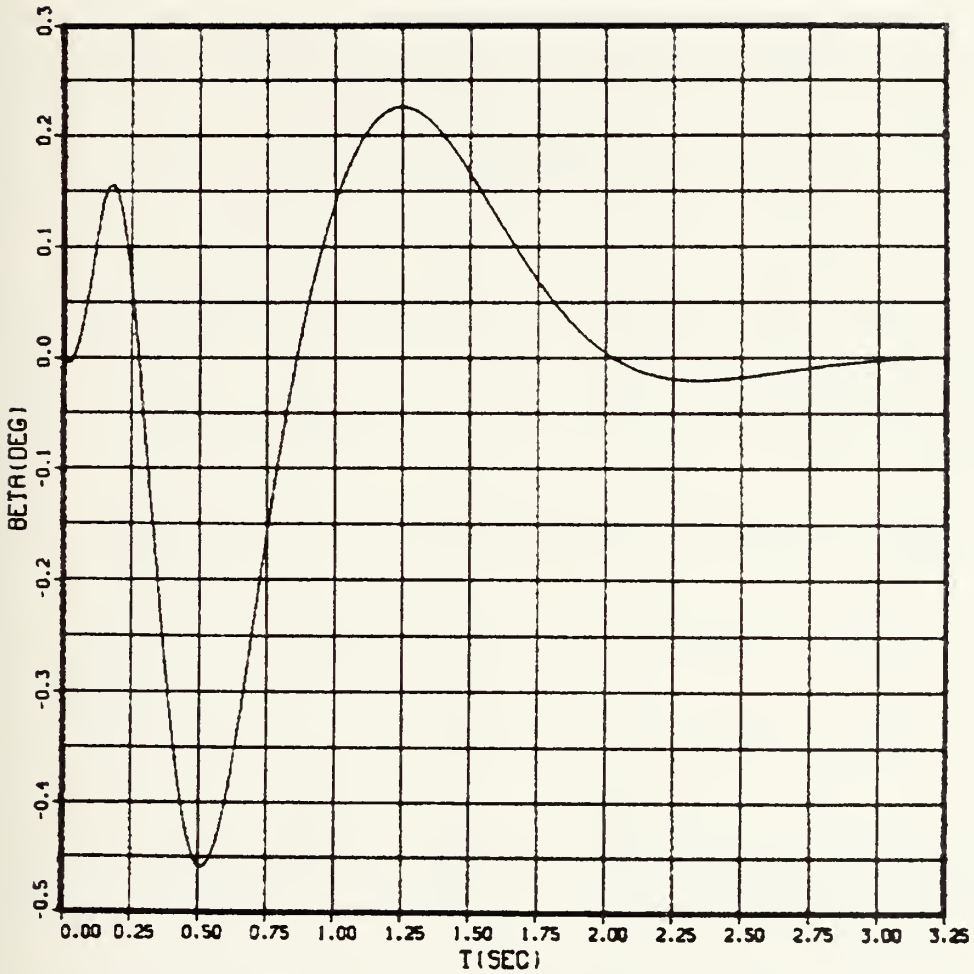


Fig. 3.7 Sideslip angle (β) Vs Time (t)
 Linear CBTT Autopilot (1 RAD Roll
 command) Elliptical airframe ($a_e = 10^\circ$,
 $P_e = Q_e = 0^\circ$)

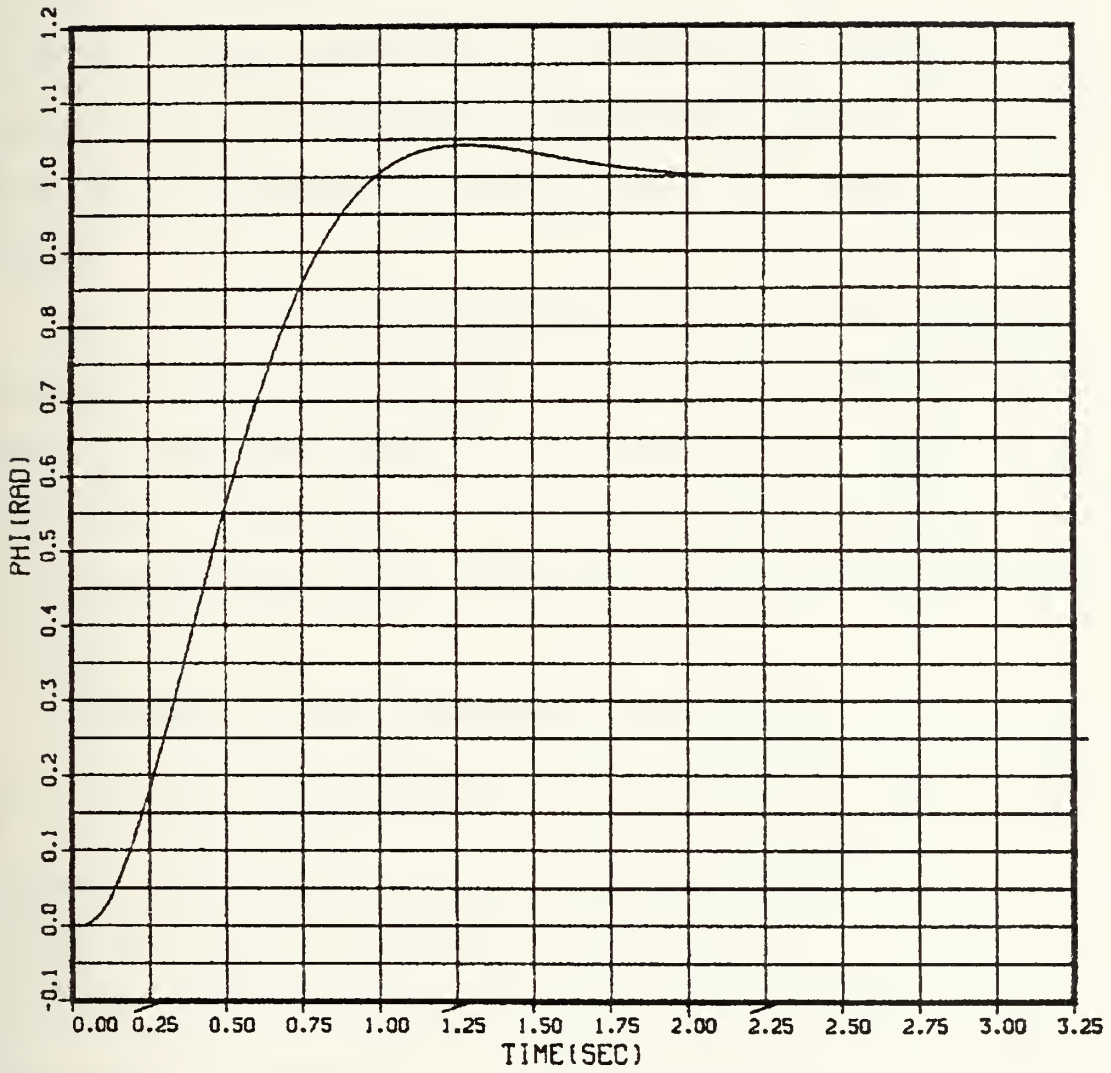


Fig. 3.8 Roll angle (ϕ) vs Time (t)
 Linear CBTT Autopilot (1 RAD Roll
 command) Elliptical airframe
 ($a_e = 10^\circ$, $P_e = Q_e = 0^\circ$)

H. RELATIVE STABILITY OF CBTT AUTOPILOTS OF CIRCULAR AND ELLIPTICAL AIRFRAMES

When the coordinating branch gain K_{yp} was set to zero in CBTT autopilot of the circular airframe, the maximum sideslip angle increased to 2.8 degrees. Therefore, for the circular airframe the coordinating branch is not very effective in helping the yaw autopilot to reduce sideslip angle.

If k_{yp} is increased to unity, as it is for the CBTT autopilot of the elliptical airframe, the maximum sideslip remains below one degree for 3 seconds but the autopilot is unstable. Modifying of the circular airframe will be done in the non-linear CBTT, for minimization of the sideslip angle.

Removal of the aerodynamic cross-coupling (i.e. $C_{n_{\beta}}$, $C_{n_{\delta_R}}$, $C_{n_{\delta_R}}$) had no effect on the sideslip angle. This showed that the aerodynamic cross-coupling plays an indirect role in determining the quality of sideslip control by determining the relative stability of the coordination branch or the magnitude of the coordination gain K_{yp} . The magnitude of sideslip angle is dependent on the nulling effects of two parallel paths shown in Figure 3.9, as given in [Ref. 2].

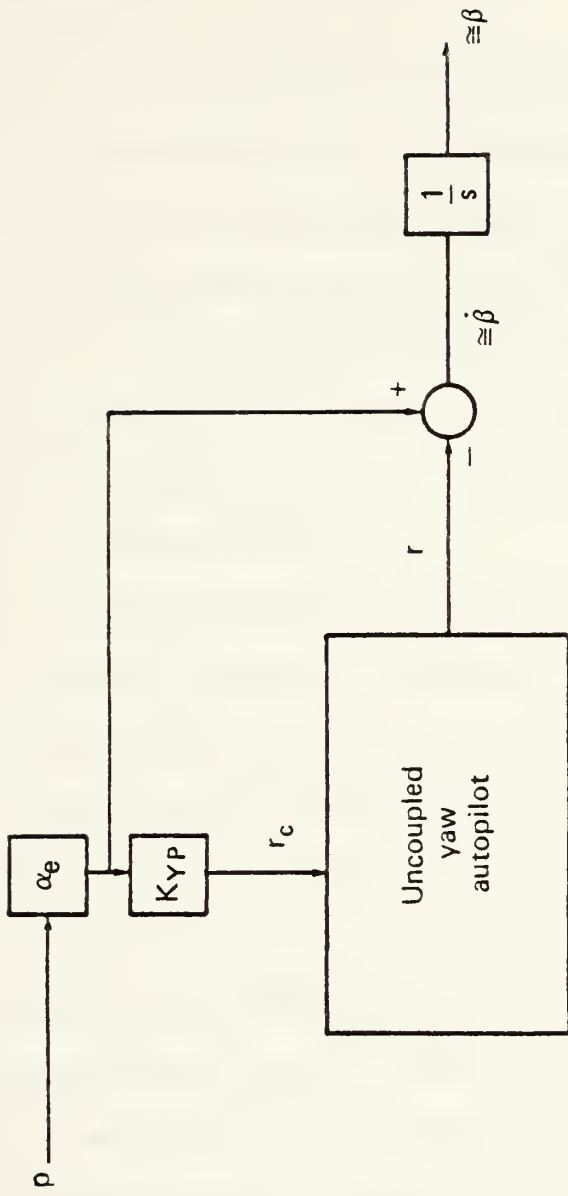


Fig. 3.9 Major Contributors to quality of sideslip control of CBTT autopilot

The contribution of yaw acceleration n_y to the maximum β is negligible and therefore neglected. β is formed mainly by the subtraction of the kinematic paths of $a_{e.p}$ and the yaw angular rate r .

The coordination is obtained in the CBTT control law by commanding the yaw autopilot with a yaw angular rate command r_c (Figure 3.2) of $K_{YP} a_{e.p}$, which forces r to be equal to $a_{e.p}$ and therefore nulling β as shown in Figure 3.9. The nulling process will be accomplished more efficiently if $K_{YP} = 1.0$. The reason the sideslip is not nulled completely is that n_y is not zero and r can not equal r_c over all frequencies.

The linearized CBTT autopilot of the circular airframe was unstable, when the uncoupled channel control laws used with a coordinating branch gain K_{YP} of unity. The autopilot was stabilized by decreasing K_{YP} to 0.458. The actuator of roll control channel has a frequency of 60 rad/sec.

The stability of the CBTT autopilot for the elliptical airframe is considerably better, due to the setting of K_{YP} at unity, which results in a substantial decrease in the magnitude of sideslip angle as shown in Figure 3.9.

I. CONCLUSIONS

1. The linear coupled autopilots verify the results of the uncoupled autopilots and keep the sideslip angle small for coordination motion. (section II.D. and II.E)

2. Further Conclusions about the relative stability of the autopilots, about the gain K_{yp} of the coordination branch and about the sensitivity of the autopilots to the aerodynamic cross-coupling are given in chapter 7 of [Ref. 2].

IV. NONLINEAR ANALYSIS OF CBTT AUTOPILOT FOR CIRCULAR AND ELLIPTICAL AIRFRAME

A. GENERAL

The three dimensional nonlinear aerodynamic models used for the analysis are shown in the Figures 4.1 and 4.2. For the configuration under consideration, the assumptions, which have been found to be consistent are referred to in chapter 5 of [Ref. 2].

Nonlinear aerodynamics and mass parameters values are presented in Appendixes A and B, as taken from the [Ref. 2]. The same flight conditions (i.e 60kft altitude and $M=3.95$) as in linear CBTT.

In this section the control laws for the non-linear CBTT autopilots are discussed. The results for commanding the CBTT autopilots for both airframes are shown and the desired aerodynamic model to enhance CBTT performance is determined. The performance of the CBTT autopilot for the elliptical airframe is determined, when no lateral aerodynamic cross-coupling exists and with ideal airframe dynamics. Also the performance of the q CBTT autopilot for the circular airframe is determined, when no inertial and kinematic cross-coupling exist into the pitch autopilot. The conclusion of the nonlinear analysis are stated.

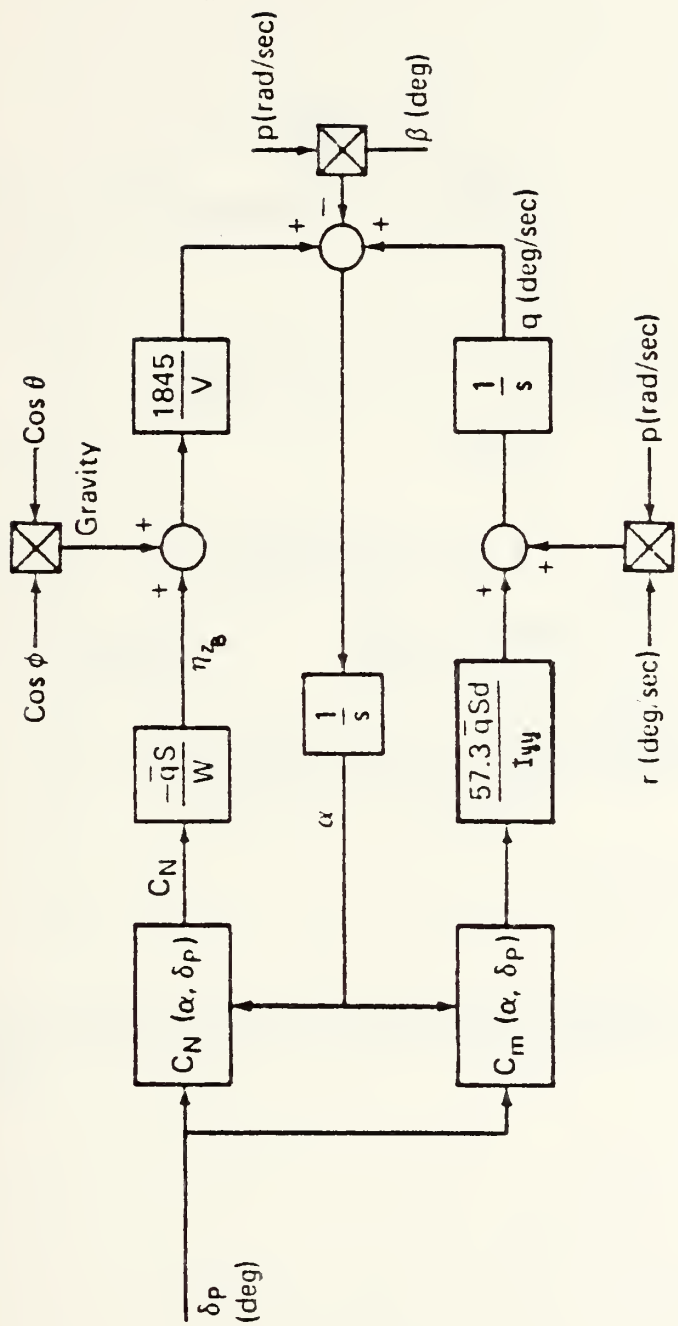


Fig. 4.1 Nonlinear Pitch channel dynamic model

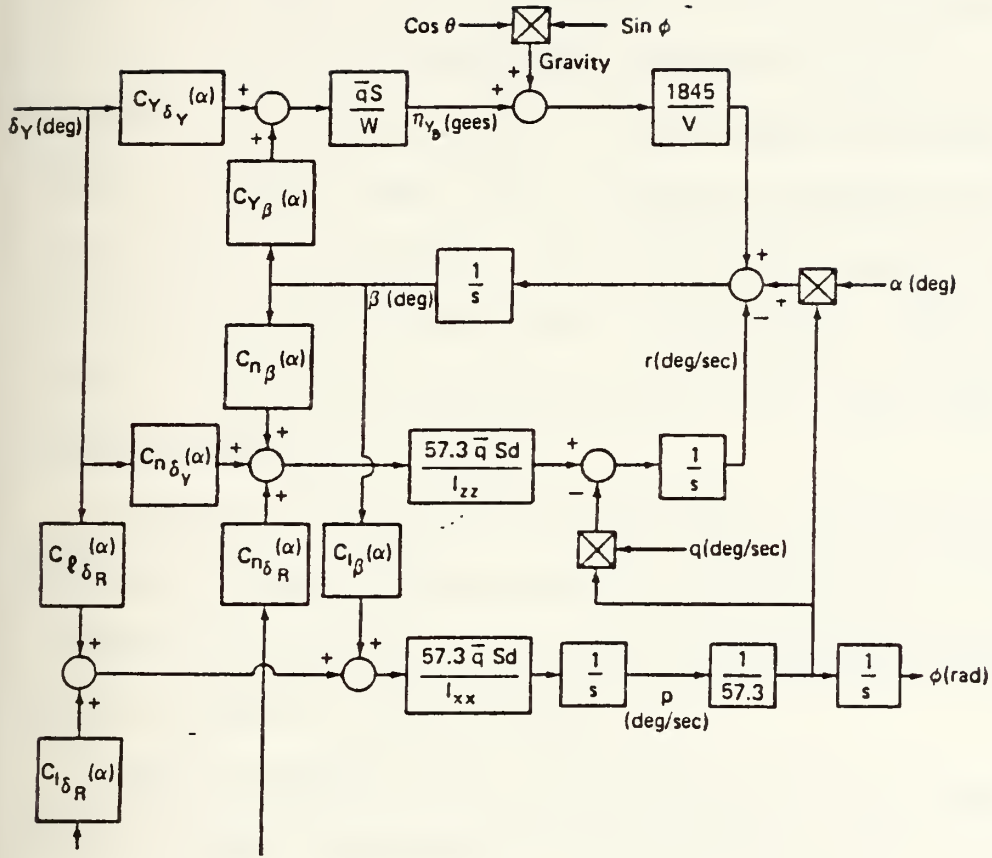


Fig. 4.2 Nonlinear Lateral (Roll/Yaw) channel dynamic model

B. CONTROL LAWS FOR ELLIPTICAL AIRFRAME

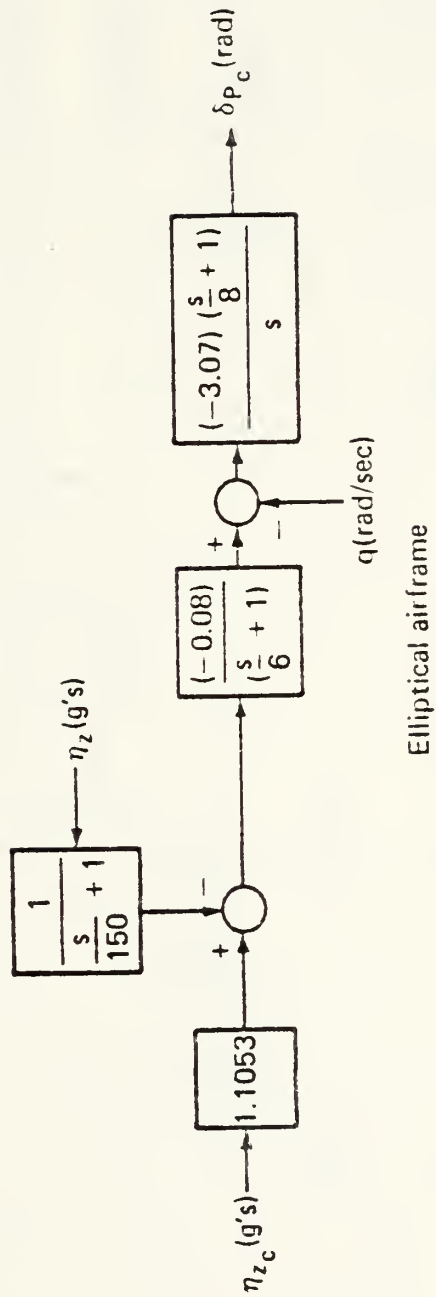
The control laws used for the following nonlinear 3-D studies were the same as those used for the linear studies in section III, which are shown in Figures 4.3 and 4.4 taken from [Ref. 2], except for the gain as shown in the bold line of the coordination branch in Figure 4.4. The new gain a is held constant at one degree magnitude for angles of attack less than one degree positive and greater than negative 5 degrees. For angles-of-attack greater than one degree positive, the gain a is equal to the angle of attack. This maintains coordination for very small angles-of-attack.

Gravity effects were not included in the linear studies, because it was assumed to have a negligible influence on autopilot stability and response perturbations about a missile trim condition.

Gravity effects were included in the nonlinear studies, where the missile body-fixed yaw axis will be subjected to the full force of gravity and may therefore have a significant influence on sideslip.

1. Pitch Control Law

The pitch control law for the elliptical airframe is the same that is used in the linear studies in section III.F., except in the command applied to the channel.



Elliptical airframe

Fig. 4.3 Nonlinear Pitch control law

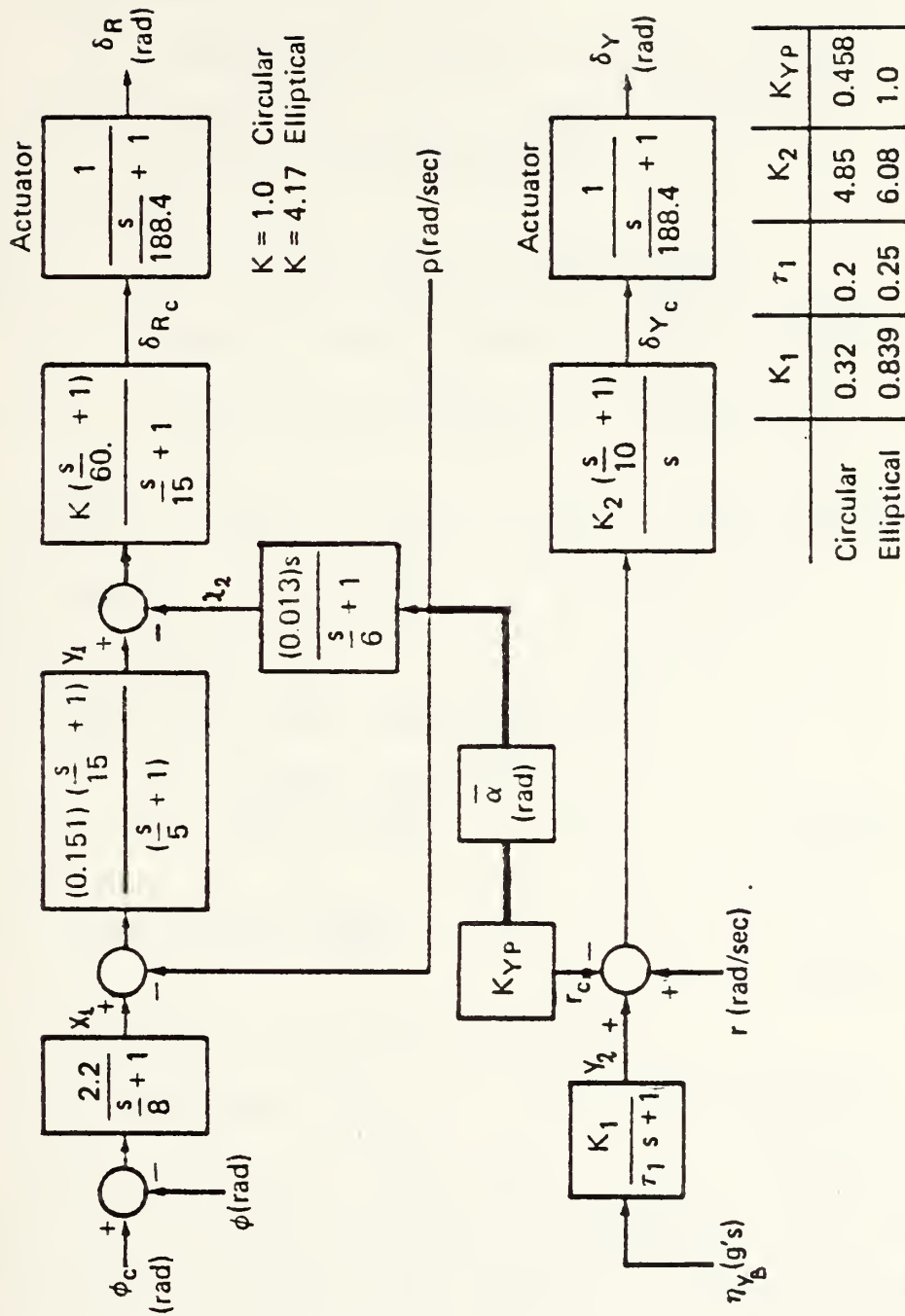


Fig. 4.4 CBTT Nonlinear lateral control laws

In inertial rectangular coordinates, the acceleration commands, are:

a. n_c (acceleration command in inertial Z_Y direction as in figure 2.4) = $n_{z_c} - \cos\phi$ IV.B.1-1

where: n_{z_c} : guidance command (gees)

$-\cos\phi$: anti-gravity bias command (gees)

θ : Elevation Euler angle = $(q\cos\phi - r\sin\phi)dt$

b. n_{Y_c} acceleration command in inertial Y_V

direction, which is equal to zero, because it is desired coordinated motion. In the polar coordinates, the acceleration commands are:

$$\begin{aligned} \text{a. } n_c &= - \left[(n_{z_c} - \cos\theta)^2 + n_{Y_c}^2 \right]^{1/2} \\ &= - \left[(n_{z_c} - \cos\theta)^2 \right]^{1/2} \\ &= - (n_{z_c} - \cos\theta) \end{aligned} \quad (\text{IV.B.1-2})$$

$$\text{b. } \phi_c = \tan^{-1} \left(\frac{n_{Y_c}}{n_{z_c}} \right) \quad (\text{IV.B.1-3})$$

hence $\phi_c = n\pi$ and $n = 0, 1, 2, \dots$

Since the pitch control law of the elliptical airframe does not have an integration in the acceleration error path (i.e. in the acceleration compensator as in the case of circular airframe) and requires a gain in series with the acceleration command shown in Figures 4.3 it was necessary to modify the anti-gravity command as follows to assure an anti-gravity bias of just one gee.

$$n_c \quad (\text{elliptical airframe inertial acceleration command}) = \\ = n_{z_c} - 0.913 \cos \theta \quad (\text{III.B.1.4})$$

The autopilot was tested, using a commanded 2 gee (0° , 180°), that denotes an inertial command of 2 gees, which is first applied in the 0° or upward direction at $\tau = 2$ seconds for 3 seconds and at the fifth second is applied in the 180° or downward direction. Since at first both the missile roll angle and roll angle command are at zero degrees, there is no roll motion and the missile turns upward as a skid-to-turn controlled missile. At fifth second the missile is commanded to roll through 180° degrees while moving in a coordinated manner in yaw and roll to minimize sideslip angle and prevent or minimize negative angle-of-attack.

The other equations, which represent the nonlinear pitch control law are the same as for linear studies section III.C. and the state variables are shown in Figure 4.3.

The equations are:

$$\dot{X} = -150X + 150 \eta_{z_B} \quad (\text{IV.B.1-1})$$

$$\dot{Y} = -6Y - 0.5305 \eta_c + 0.48X \quad (\text{IV.B.1-2})$$

$$\delta \ddot{p}_c = -0.3837 (\dot{Y} + \dot{q} / 57.3) - 3.07 (Y - q / 57.3) \quad (\text{IV.B.1-3})$$

$$\delta \dot{p} = -188.4 \cdot \delta p + 10795.3 \cdot \delta p_c \quad (\text{IV.B.1-4})$$

where:

n_{z_B} : achieved body-fixed acceleration in Z axis

n_c : inertial acceleration command.

2. Lateral Control Laws

The lateral control laws are the same as those used for the linear studies, except the modification in the coordination branch.

The command ϕ_c for the roll control law is zero for the first 5 seconds and 180° afterwards, as derived in IV.B.1.

The equations which represent the lateral control laws are the same those of section III.F.

$$\dot{Y}_2 = -4 Y_2 + 3.356 n_{y_B} \quad (\text{IV.B.2-1})$$

$$\begin{aligned} \delta \dot{Y}_c &= 0.608 \left(\dot{Y}_2 + \frac{\dot{r}}{57.3} - \frac{(\alpha_e \cdot P)'}{(57.3)^2} \right) + 6.08 \left(Y_2 + \frac{r}{57.3} - \frac{\alpha_e \cdot P}{(57.3)^2} \right) \\ &= 0.608 \left(\dot{Y}_2 + \frac{\dot{r}}{57.3} - \frac{\alpha_e \cdot P}{3283.29} - \frac{\dot{\alpha}_e \cdot P}{3283.29} \right) + 6.08 \left(Y_2 + \frac{r}{57.3} - \frac{\alpha_e \cdot P}{3283.29} \right) \end{aligned} \quad (\text{IV.B.2-2})$$

where:

$$\left. \begin{aligned} \alpha_e &= \alpha \\ \dot{\alpha}_e &= \dot{\alpha} \end{aligned} \right\} \alpha > 1^\circ$$

and

$$\left. \begin{aligned} \alpha_e &= 1^\circ \\ \dot{\alpha}_e &= 0 \end{aligned} \right\} \alpha < 1^\circ$$

$$\dot{X}_1 = -8X_1 - 17.6\phi + 17.6\phi_c \quad (\text{IV.B.2-3})$$

$$\delta \dot{Y} = -188.4 \delta Y + 10795.3 \delta Y_c \quad (\text{IV.B.2-4})$$

$$\dot{Y}_1 = -5Y_1 + 0.05033(\dot{X}_1 - \dot{P}/57.3) + 0.755(X_1 - P/57.3) \quad (\text{IV.B.2-5})$$

$$\dot{X}_2 = -6X_2 + 0.078(\dot{P}/57.3) \quad (\text{IV.B.2-6})$$

$$\delta \dot{R}_c = -15\delta R_c + 1.0425(\dot{Y}_1 - \dot{X}_2) + 62.55(Y_1 - X_2) \quad (\text{IV.B.2-7})$$

$$\dot{\delta}_R = -188.4 \cdot \delta_R + 10795.3 \cdot \delta_{RC} \quad (\text{IV.B.2-8})$$

The state variables are shown in Figure 4.4. For purposes of analysis, a CSMP program was written (Appendix H).

C. AERODYNAMIC MODELS FOR ELLIPTICAL AIRFRAME

The aerodynamic models of Pitch and Roll-Yaw channels for the elliptical airframe are shown in Figures 4.1, 4.2. The airframe dynamics under consideration, have a level of complexity sufficient to determine the critical areas of concern regarding the stability and response of CBTT control.

1. Pitch Channel

The nonlinear aerodynamic model of the Pitch channel consisted of the uncoupled model, coupled with the Roll-Yaw channels via the inertial cross-coupling of r_p into q and the kinematic cross-coupling of $-\beta \cdot P$ into a . Also the antigravity command $\cos\phi \cos\theta$ is inserted into n_z . This model is shown in Figure 4.1.

The above terms consist of the nonlinear terms of the pitch channel.

The equations which represent the pitch aerodynamic model are:

$$n_{zB} = -\bar{q} S C_N / W \text{ (gees)} \quad (\text{IV.C.1-1})$$

$$\dot{q} = P \cdot r / 57.3 + 57.3 \bar{q} S d C_M / I_{yy} \quad (\text{IV.C.1-2})$$

$$\dot{\alpha} = q + k \cdot \eta_{z_B} - P \cdot \theta / 57.3 \quad (\text{IV.C.1-3})$$

where:

$$k = \frac{1845}{V} = 0.48$$

$$\bar{q} = 1650 \text{ (lbf/ft}_2\text{)}$$

$$S = \pi \text{ (ft}^2\text{)}$$

$$d = 2 \text{ (ft)}$$

$$w = 2475 \text{ (lbf)}$$

$$I_{yy} = 790 \text{ (slug-ft}^2\text{)}$$

Functions $C_N(a, \delta_p)$ and $C_m(a, \delta_p)$ are nonlinear functions shown in Appendix B that vary with a and δ_p .

Substituting the values into the above equations, they yield:

$$\eta_{z_B} = -1.3333 \cdot C_N \quad (\text{IV.C.1-4})$$

$$\dot{q} = 0.17452 \cdot P \cdot \gamma + 751.9541 C_M \quad (\text{IV.C.1-5})$$

$$\dot{\alpha} = q - 0.63998 C_N - 0.017452 P \cdot \theta \quad (\text{IV.C.1-6})$$

2. Lateral Channels

The nonlinear aerodynamic model consisted of the uncoupled roll and yaw channels, which coupled via C_{η_β} , $C_{\eta_{\delta_Y}}$ and $C_{\eta_{\delta_R}}$. Also the lateral channel coupled with the lateral channel coupled with the pitch channel via the inertial cross-coupling of $-qp$ into r and the kinematic cross-coupling of ap into β . The above term is the nonlinear part the lateral pitch channel. The nonlinear lateral dynamic model is shown in Figure 4.2. The

equations that represent the aforementioned model are as follows:

$$n_{Y\beta} = \bar{q} S (C_{Y\beta} \cdot \beta + C_{Y\delta_Y} \cdot \delta_Y) / W \quad (\text{gees}) \quad (\text{IV.C.2-1})$$

$$\dot{\beta} = K n_{Y\beta} + \alpha \cdot P / 57.3 - r \quad (\text{deg/sec}) \quad (\text{IV.C.2-2})$$

$$\dot{r} = -q \cdot P / 57.3 + 57.3 \bar{q} S d (C_{n\beta} \cdot \beta + C_{n\delta_Y} \cdot \delta_Y + C_{n\delta_R} \cdot \delta_R) / I_{zz} \quad (\text{IV.C.2-3})$$

$$\dot{P} = 57.3 \bar{q} S d (C_{e\beta} \cdot \beta + C_{e\delta_Y} \cdot \delta_Y + C_{e\delta_R} \cdot \delta_R) / I_{xx} \quad (\text{IV.C.2-4})$$

$$\dot{\phi} = P / 57.3 \quad (\text{rad/sec}) \quad (\text{IV.C.2-4a})$$

$$\dot{\phi}_d = P \quad (\text{deg/sec}) \quad (\text{IV.C.2-5})$$

where:

$$K = 0.48$$

$$\bar{q} = 1650 \quad (\text{lbF/ft}_2)$$

$$S = \pi \quad (\text{ft}^2)$$

$$d = 2 \quad (\text{ft})$$

$$W = 2475 \quad (\text{lbF})$$

$$I_{xx} = 110 \quad (\text{slug-ft}^2)$$

$$I_{zz} = 853 \quad (\text{slug-ft}^2)$$

as referred to in Appendix A.

Functions $C_{Y_{\delta_Y}}(a)$, $C_{Y_{\beta}}(a)$, $C_{n_{\beta}}(a)$, $C_{n_{\delta_Y}}(a)$, $C_{l_{\delta_Y}}$

$C_{l_{\beta}}(a)$, $C_{l_{\delta_R}}$ and $C_{n_{\delta_R}}(a)$ are nonlinear functions which

vary with a angle-of-attack and referred in Appendix B.

Substituting the values into the referred before equations one obtains:

$$n_{Y\beta} = 1.3333 (c_{Y\beta} \cdot \beta + c_{Y\delta Y} \cdot \delta Y) \quad (\text{IV.C.2-5})$$

$$\dot{\beta} = 0.63998 (c_{Y\beta} \cdot \beta + c_{Y\delta Y} \cdot \delta Y) + 0.017452 \alpha \cdot P - \gamma \quad (\text{IV.C.2-6})$$

$$\dot{\gamma} = -0.01745 q \cdot P + 696.42 (c_{n\beta} \cdot \beta + c_{n\delta Y} \cdot \delta Y + c_{n\delta R} \cdot \delta R) \quad (\text{IV.C.2-7})$$

$$\dot{p} = 5400.3977 (c_{e\beta} \cdot \beta + c_{e\delta Y} \cdot \delta Y + c_{e\delta R} \cdot \delta R) \quad (\text{IV.C.2-8})$$

$$\dot{\phi}_d = P \quad (\text{IV.C.2-9})$$

D. ANALYSIS OF NONLINEAR CBTT AUTOPILOTS FOR ELLIPTICAL AIRFRAME

For purposes of analysis, a CSMP program was written (Appendix H) with the aforementioned equations of the aerodynamics models and control laws of the nonlinear CBTT autopilots.

To decrease computer time, appropriate initial conditions were inserted. The initial conditions are:

a : angles of attack = 2.41 degrees

δ_p : pitch tail incidence = 0.658 degrees

θ : pitch Euler angle = 0.636 rad

X : output of pitch acceleration feedback lag = 1gee

Y : output of pitch acceleration compensator = -0.0105

δ_{p_c} : pitch actuator command = 0.0148 rad

The achieved maneuver plane acceleration n_z is calculated from the body-fixed accelerations $n_{z\beta}$ (Figure 4.6) and (Figure 4.7) and the roll angle ϕ (Figure 4.13) as follows:

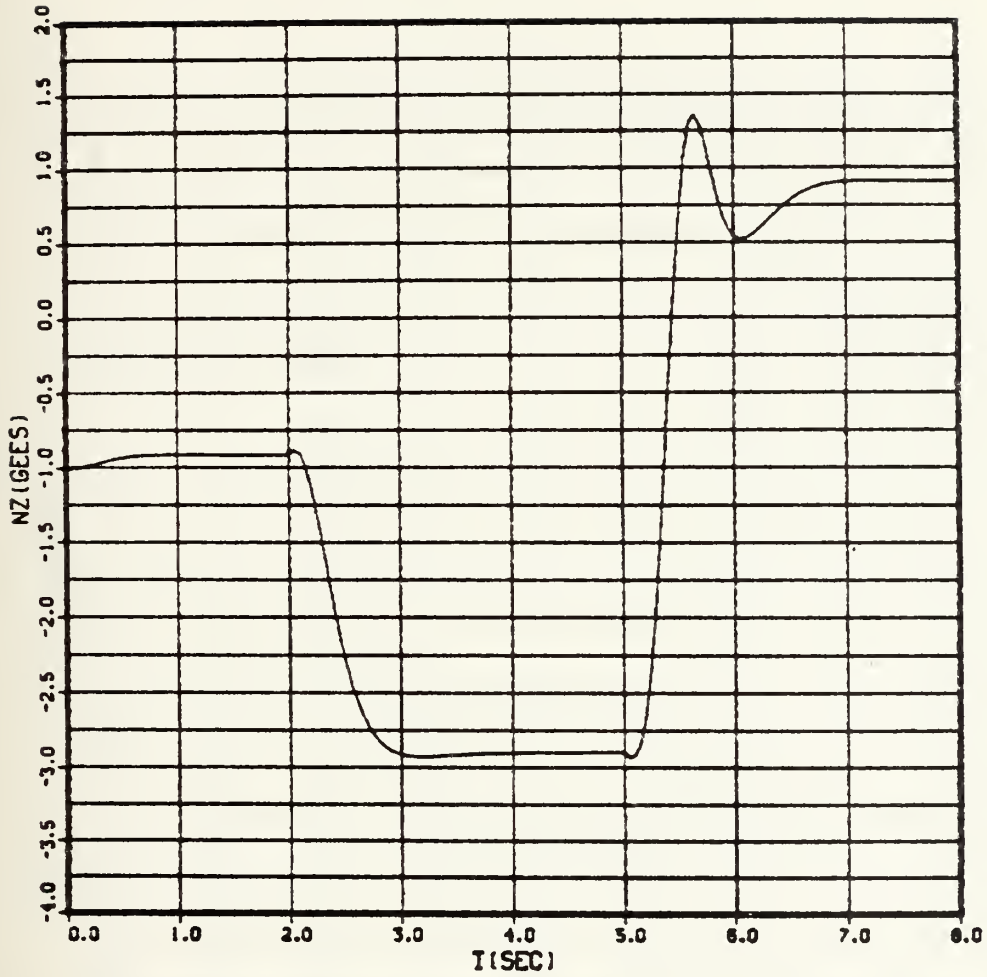


Fig. 4.5 Achieved Inertial Acceleration (n_z) vs Time (t)
 CBTT of Elliptical airframe: 2 Gees (0° , 180°)

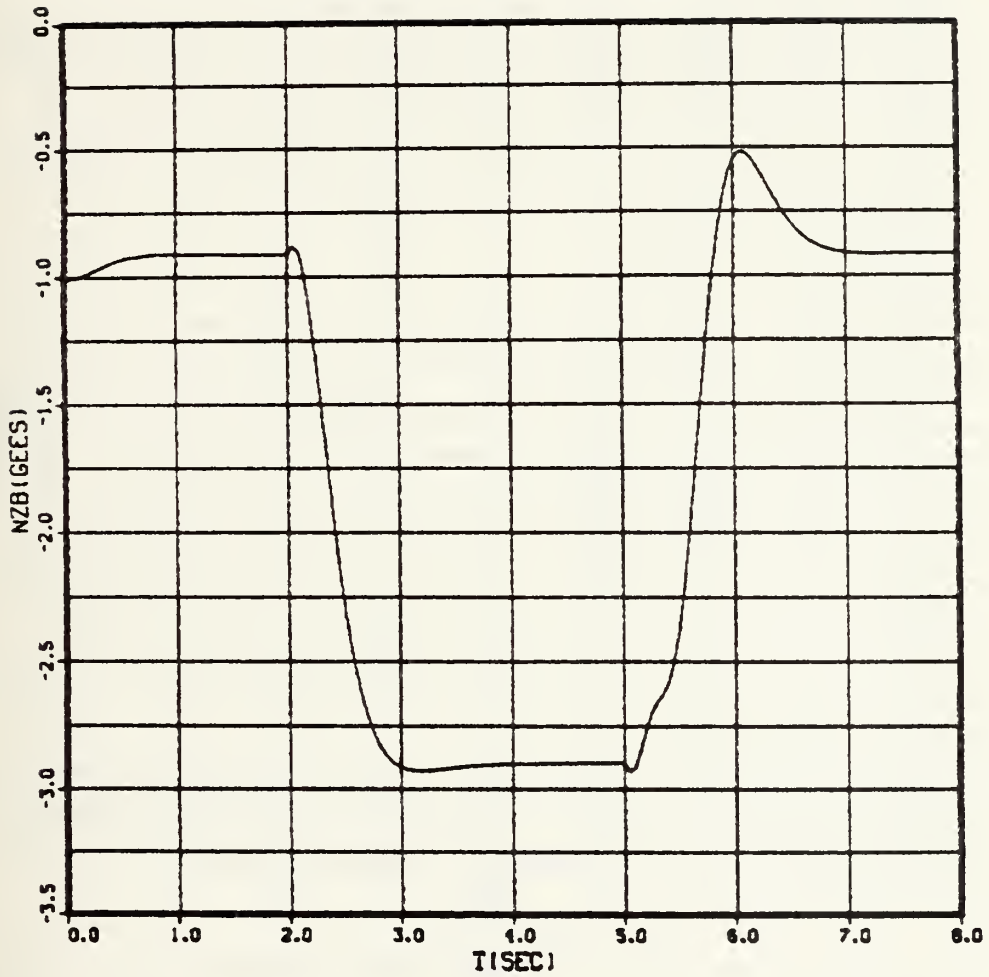


Fig. 4.6 Achieved Body-fixed Acceleration (n_{z_B}) vs Time (t) CBTT of Elliptical airframe; 2 Gees ($0^\circ, 180^\circ$)

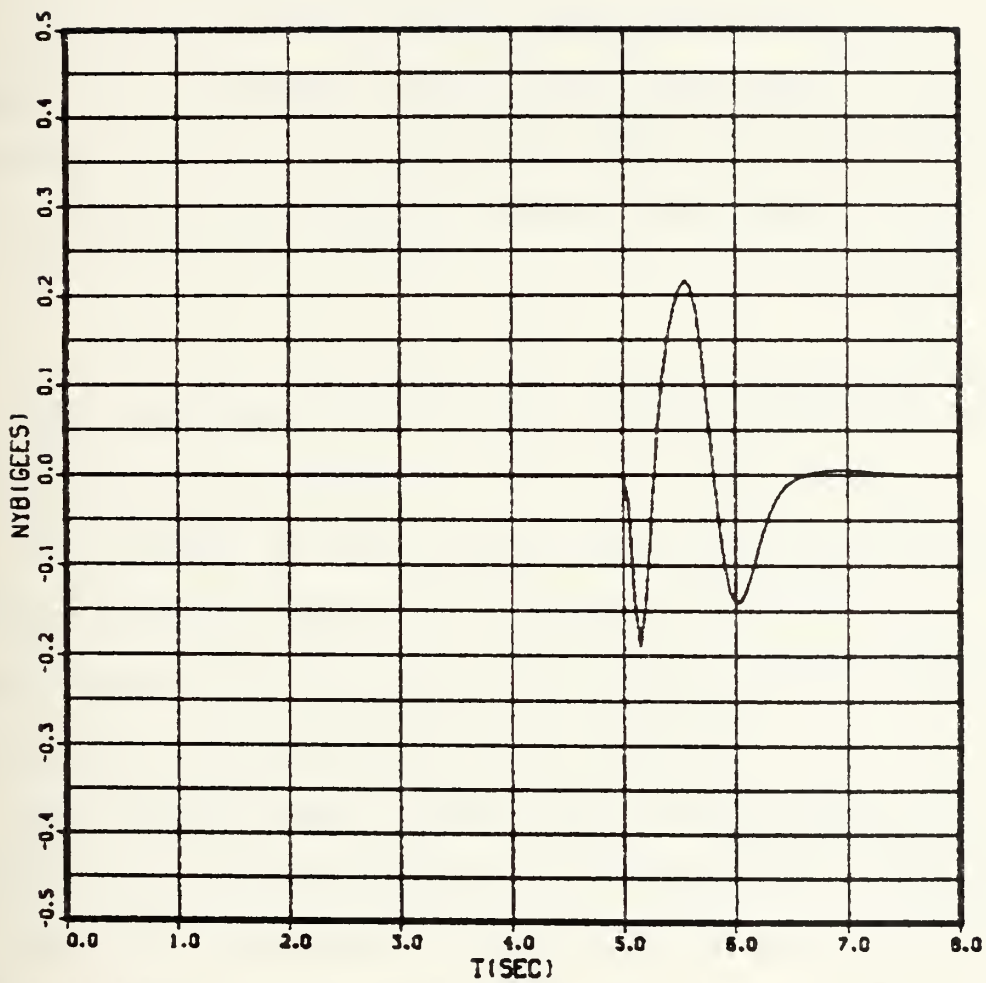


Fig. 4.7 Achieved Body-fixed Acceleration (n_{Y_B}) vs
 Time (t) CBTT of Elliptical airframe; 2
 Gees ($0^\circ, 180^\circ$)

$$n_z = n_{zB} \cdot \cos\phi + n_{yB} \cdot \sin\phi \quad (\text{IV.D-1})$$

Figure 4.5 through 4.16 show the responses of n_z , n_{yB} , a , β , q , p , r , ϕ , δ_p , δ_y and δ_R . Also these figures and table II show the time constants and the overshoots of the referred before variables.

Figure 4.5 shows that the achieved inertial acceleration n_z doesn't satisfy the requirement of the overshoot (i.e below 10 percent) and it is not acceptable. The results of this analysis verify the result of the [Ref. 2].

E. CBTT PERFORMANCE WITH IDEAL AIRFRAME DYNAMICS FOR ELLIPTICAL AIRFRAME

The purpose of the following simplifications to the airframe dynamics model is to isolate the critical cross-coupling paths, which have caused, the transients in the maneuver plane acceleration responses.

The dynamic model without the coupling paths will be referred to as ideal dynamics. Although ideal dynamics are not physically attainable, it is a useful goal for both autopilot and airframe designers.

The same guidance commands are applied to the CBTT autopilot of the elliptical airframe as in par. IV.B.1 (i.e, 2 gees (0° , 180°) but with lateral aerodynamic cross-coupling removed. That means, the aerodynamic

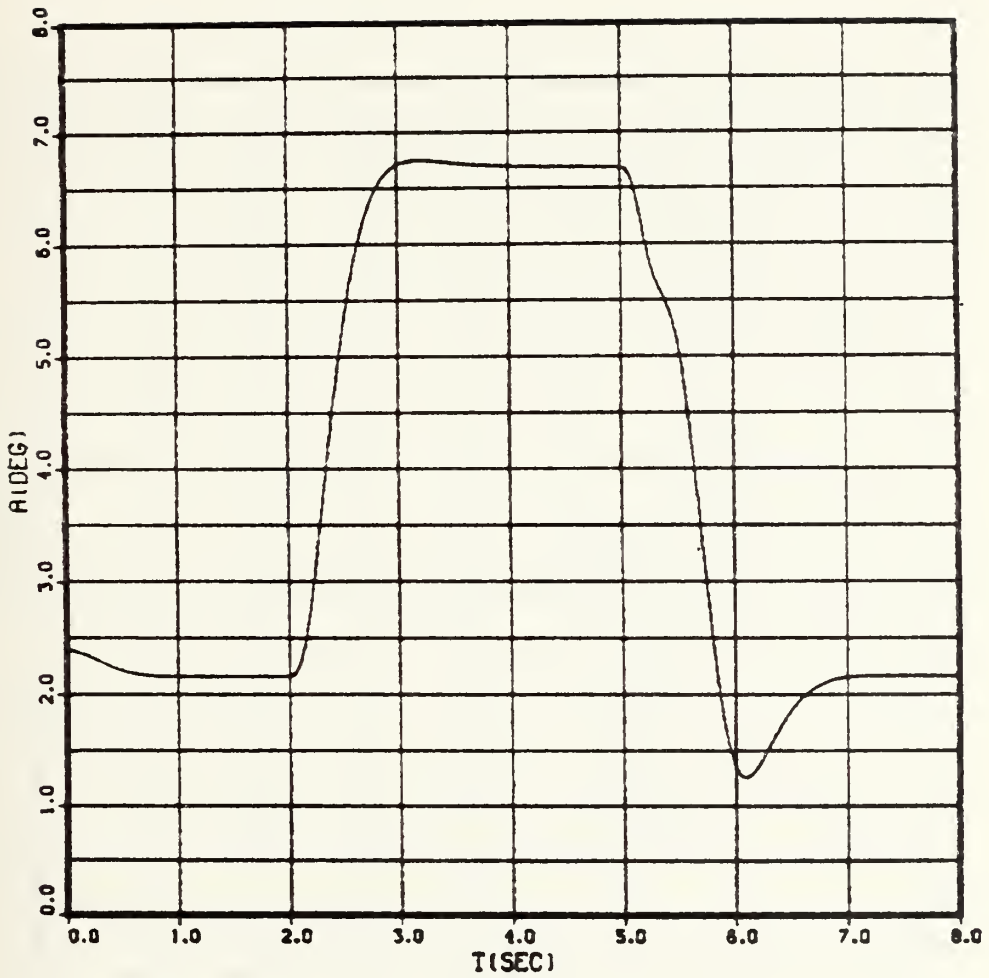


Fig. 4.8 Angle of Attack (α) vs Time (t) CBT of Elliptical airframe; 2 Gees (0° , 180°)

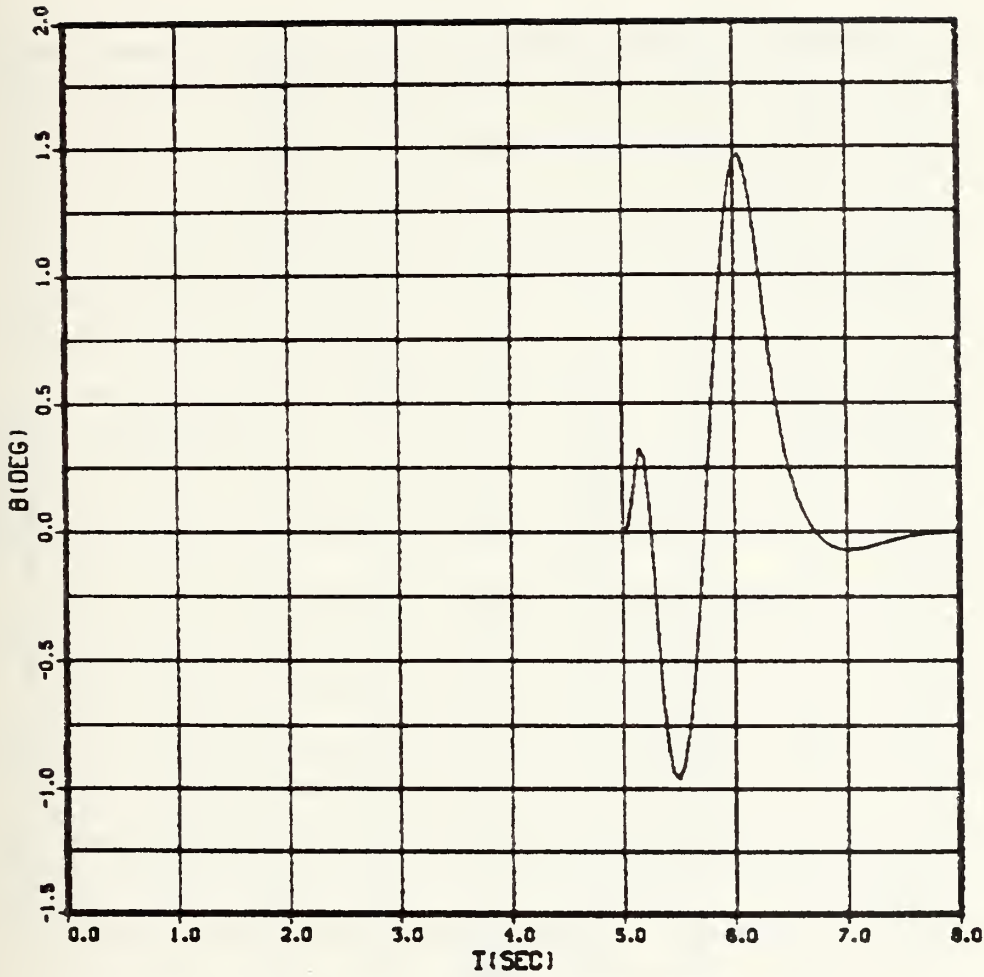


Fig. 4.9 Sideslip angle (β) vs Time (t)
 CBTT of Elliptical airframes; 2 Gees
 ($0^\circ, 180^\circ$)

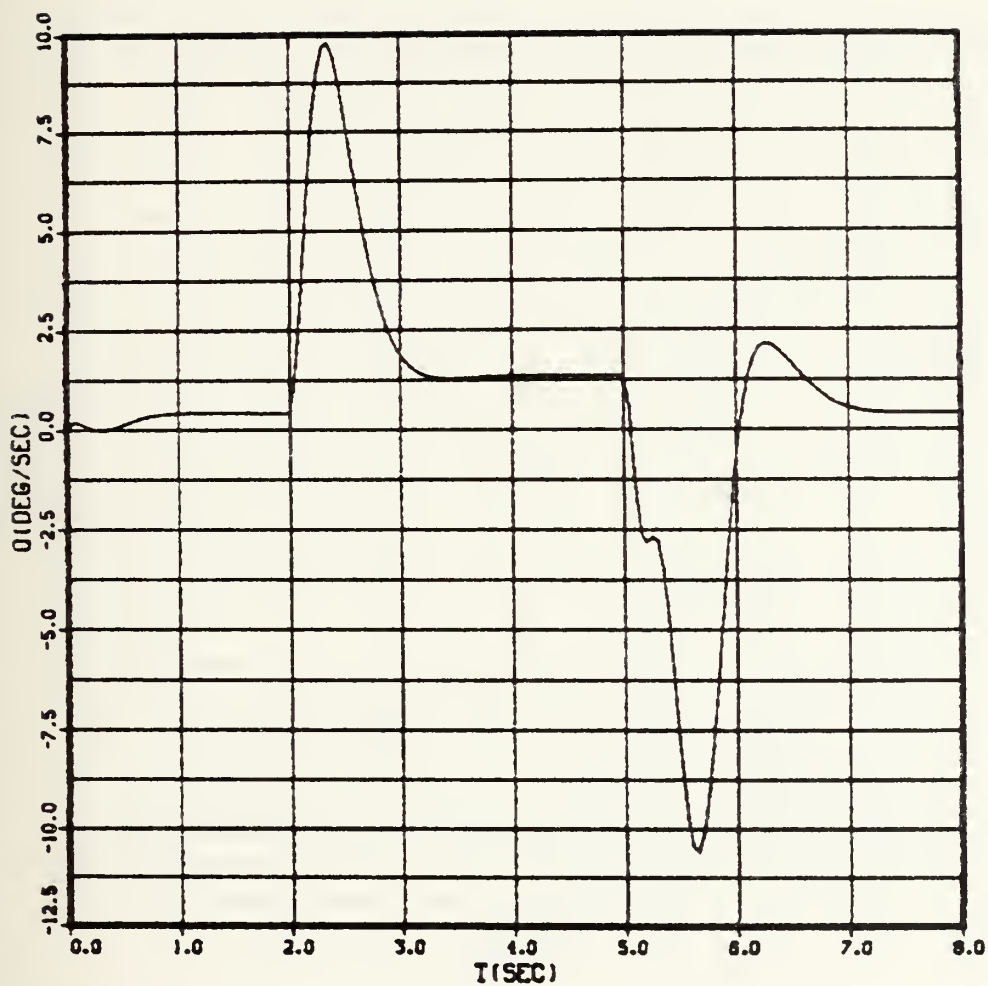


Fig. 4.10 Body pitch Angular rate (q) vs Time (t)
 CBTT of Elliptical airframe; 2 Gees
 ($0^\circ, 180^\circ$)

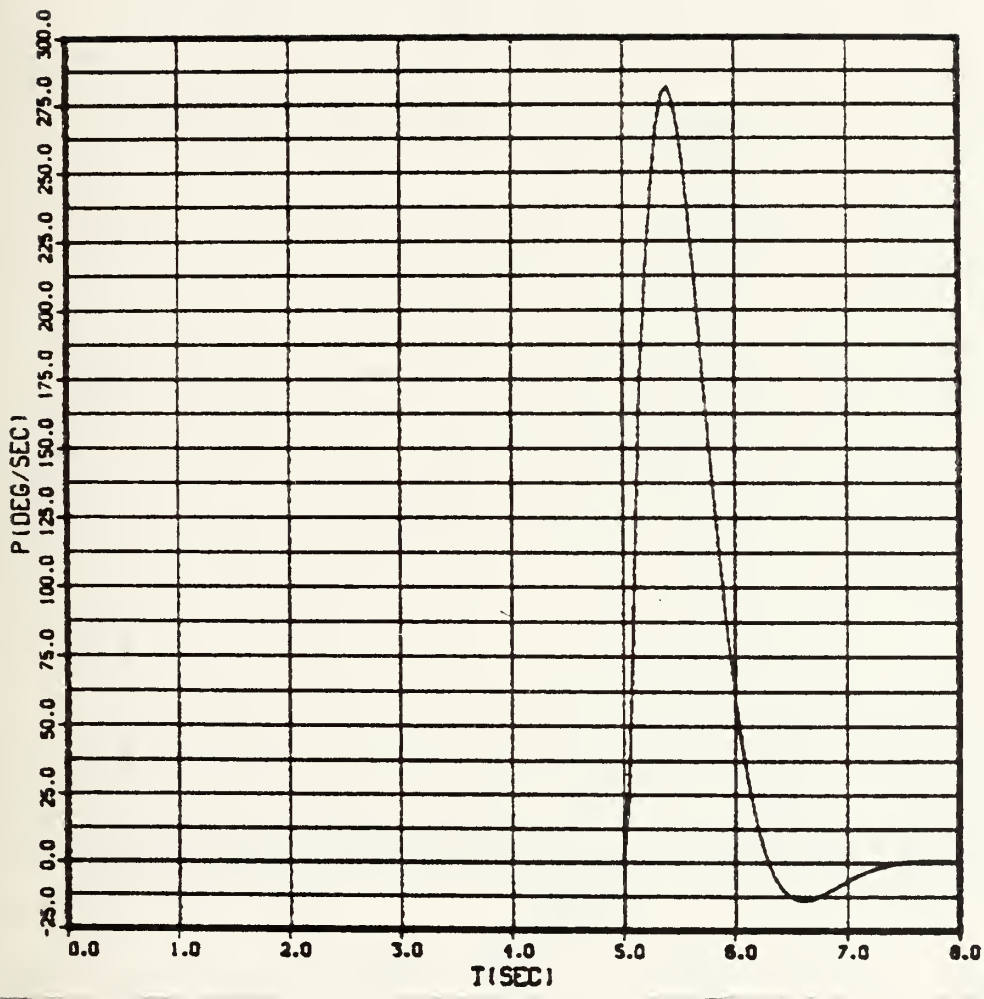


Fig. 4.11 Roll angular rate (p) vs Time (t)
 CBTT of Elliptical airframe; 2 Gees
 (0° , 180°)

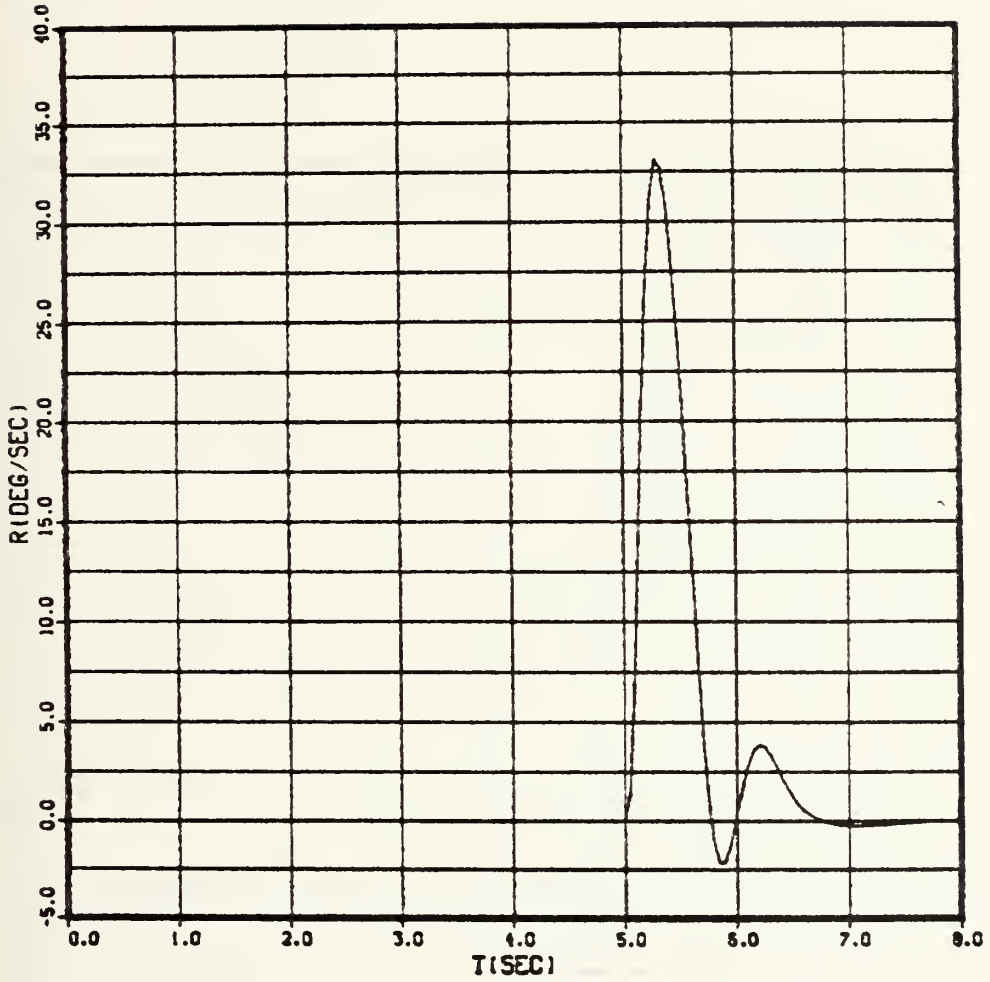


Fig. 4.12 Yaw angular rate (r) vs Time (t)
 CBTT of Elliptical airframe; 2 Gees (0° , 180°)

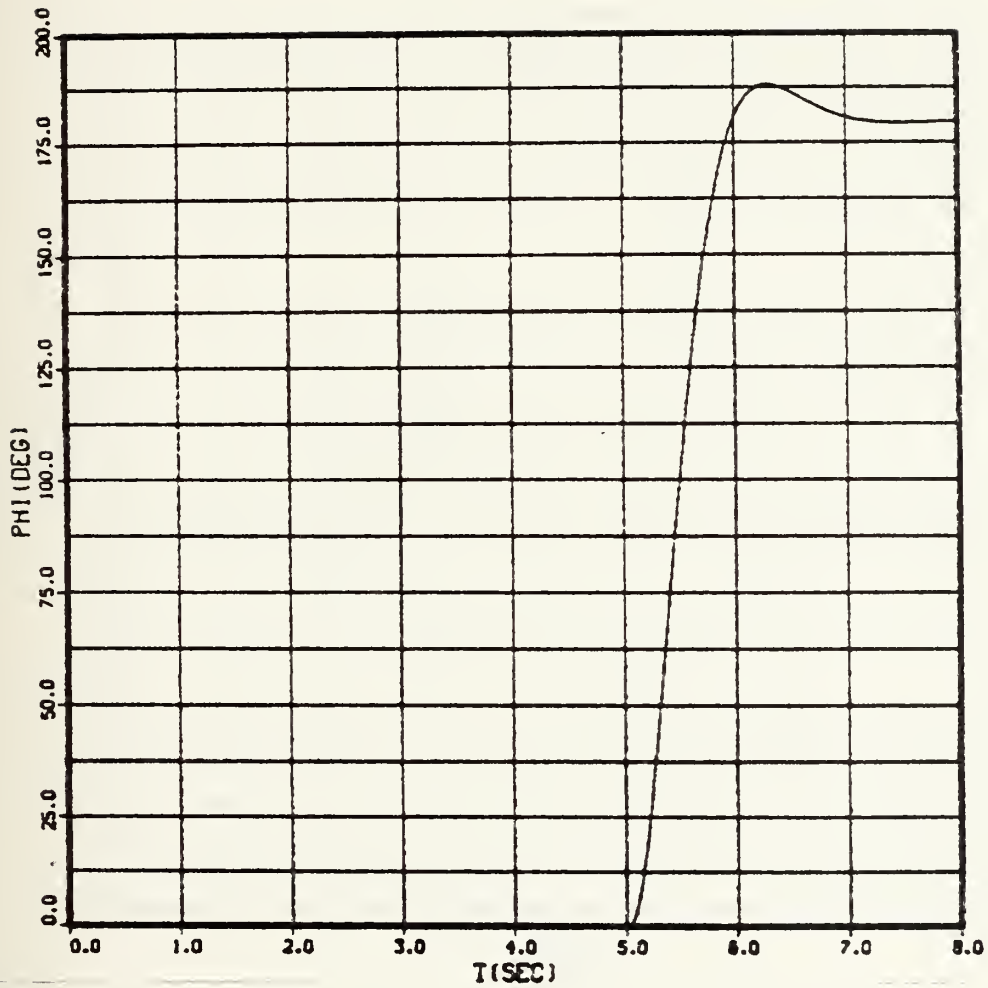


Fig. 4.13 Roll angle (ϕ) vs Time (t)
 CBTT of Elliptical airframe; 2 Gees (0° , 180°)

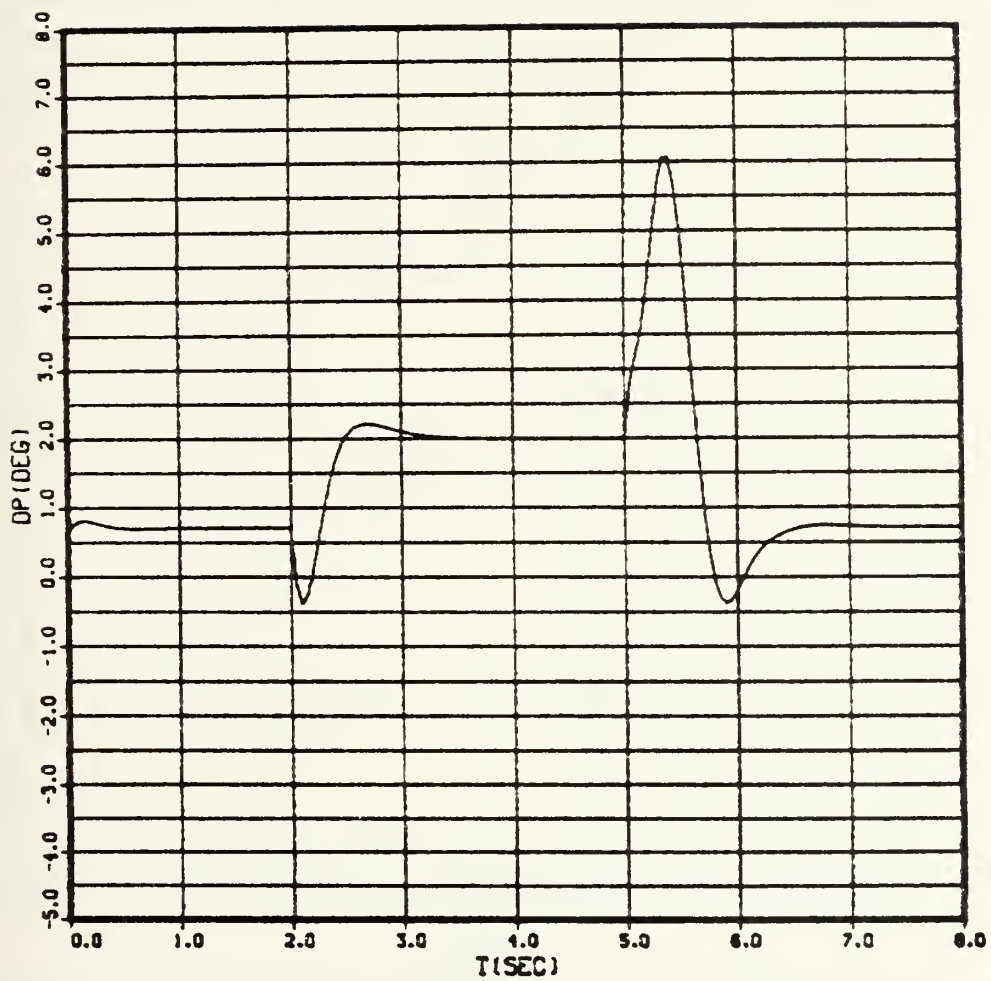


Fig. 4.14 Pitch tail incidence (δ_p) vs Time (t)
 CBTT of Elliptical airframe; 2 Gees (0° , 180°)

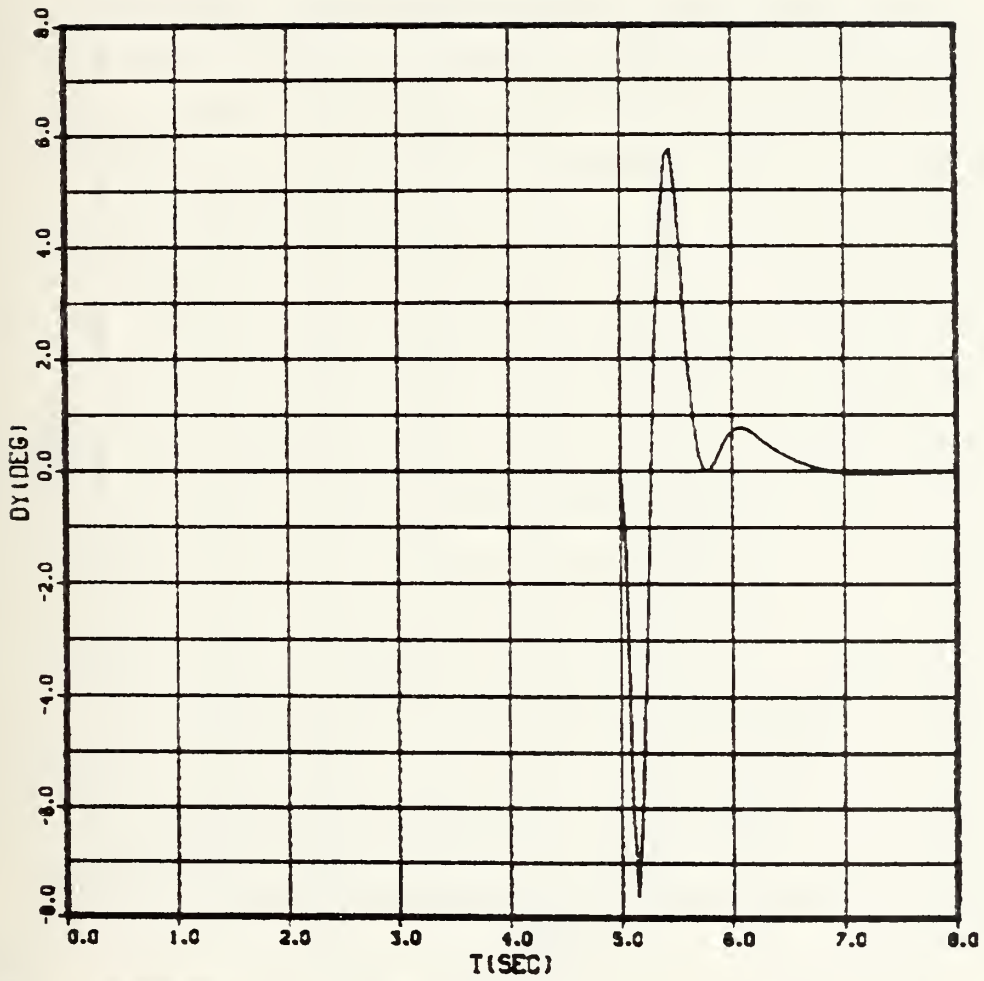


Fig. 4.15 Yaw tail incidence (δ_Y) vs Time (t)
 CBTT of Elliptical airfframe; 2 Gees ($0^\circ, 180^\circ$)

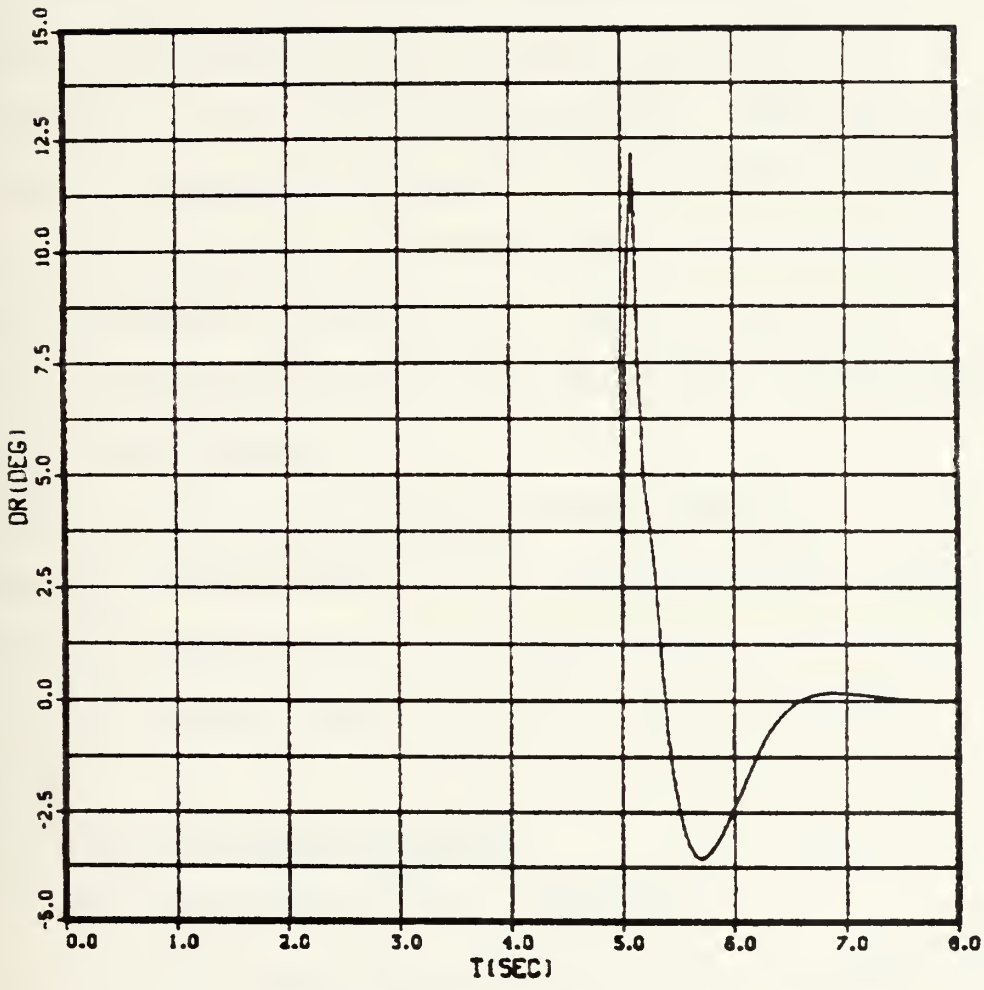


Fig. 4.16 Roll tail incidence (δ_R) vs Time (t)
 CBT of Elliptical airframe; 2 Gees ($0^\circ, 180^\circ$)

cross-coupling was removed. The major influence of the aerodynamic cross-coupling in the elliptical airframe response has been to decrease the overshoot in the achieved maneuver plane acceleration resulting from the second guidance command.

In addition to aerodynamic cross-coupling the kinematic cross-coupling of $-\beta p$ into a and inertial cross-coupling of pr into q were removed. Therefore, the only cross-coupling which exist in the airframe dynamic model are the kinematic coupling of ap into β and the inertial coupling of $-qp$ into r . There is also the autopilot cross-coupling of the coordinating command from the Roll to Yaw channel.

The equations, which represent the modified aerodynamic model by removing the referred cross-coupling are same with those as in paragraphs IV.B.1, IV.B.2, IV.C.1 and IV.C.2, with the only difference in the following equations:

1. Pitch Aerodynamic Model

$$\begin{aligned} \dot{q} &= 57.3 \bar{q} S d C_M / I_{yy} \quad (\text{deg/sec}^2) \\ &= 751.9541 C_M \end{aligned} \quad (\text{IV.E.1-1})$$

and

$$\begin{aligned} \dot{\alpha} &= q + k \cdot \eta_{zB} \\ &= q - (k \bar{q} S C_N / W) \\ &= q - 0.63998 C_N \quad (\text{deg/sec}) \end{aligned} \quad (\text{IV.E.1-2})$$

2. Lateral Aerodynamic Model

$$\begin{aligned}\dot{\gamma} &= -\frac{q \cdot P}{57.3} + \frac{57.3 \bar{q} S d}{I_{zz}} (C_{n\beta} \cdot \beta + C_{n\delta_Y} \cdot \delta_Y) \\ &= -0.017452 q \cdot P + 696.417 (C_{n\beta} \cdot \beta + C_{n\delta_Y} \cdot \delta_Y) \text{ (deg/sec}^2\text{)}\end{aligned}$$

(IV.E.1-3)

and

$$\begin{aligned}\dot{p} &= \frac{57.3 \bar{q} S d}{I_{xx}} \cdot C_{l\delta_R} \cdot \delta_R \\ &= 5400.3977 C_{l\delta_R} \cdot \delta_R \text{ (deg/sec}^2\text{)}\end{aligned}$$

(IV.E.2-2)

For purposes of analysis, a CSMP program (Appendix H) was written, using these equations. Figures 4.17 through 4.24 show the time responses of the n_z , n_{z_B} , a , β , q , r , δ_P , δ_Y , δ_R . The above figures and table II show the time constants and the overshoots of the variables.

Figure 4.17 and Table II show that the achieved inertial maneuver acceleration satisfy the requirements for the time constants and overshoot, when the cross-couplings which were discussed before have been removed.

Figure 4.25 (taken from [Ref. 2]) shows the critical feedback paths which couple the pitch and yaw channels via missile roll rate.

The aforementioned figures and plots verify the results of the [Ref. 2].

F. CONTROL LAWS FOR CIRCULAR AIRFRAME

The control laws used for the circular airframe are the same as those used in the linear studies, except for

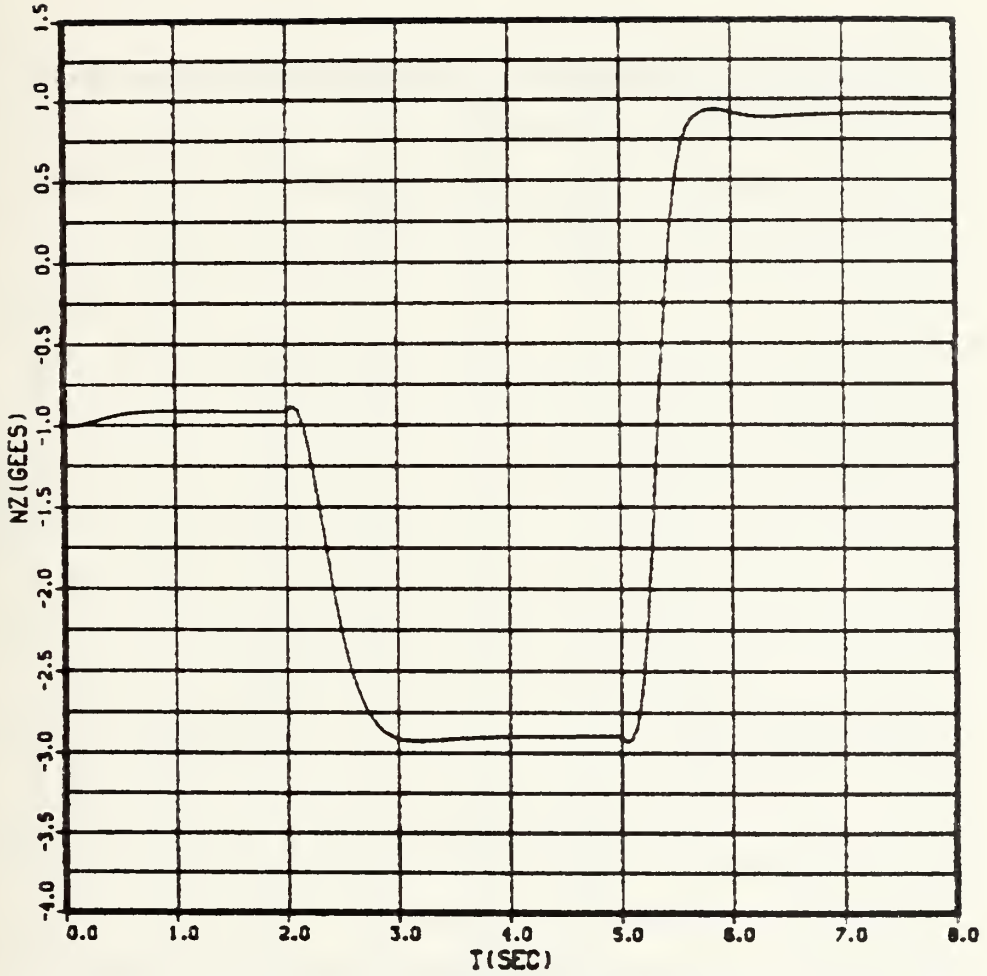


Fig. 4.17 Achieved Inertial Acceleration (n_z) vs Time (t)

CBTT of Elliptical airframe; Ideal
Airframe dynamics; 2 Gees ($0^\circ, 180^\circ$)

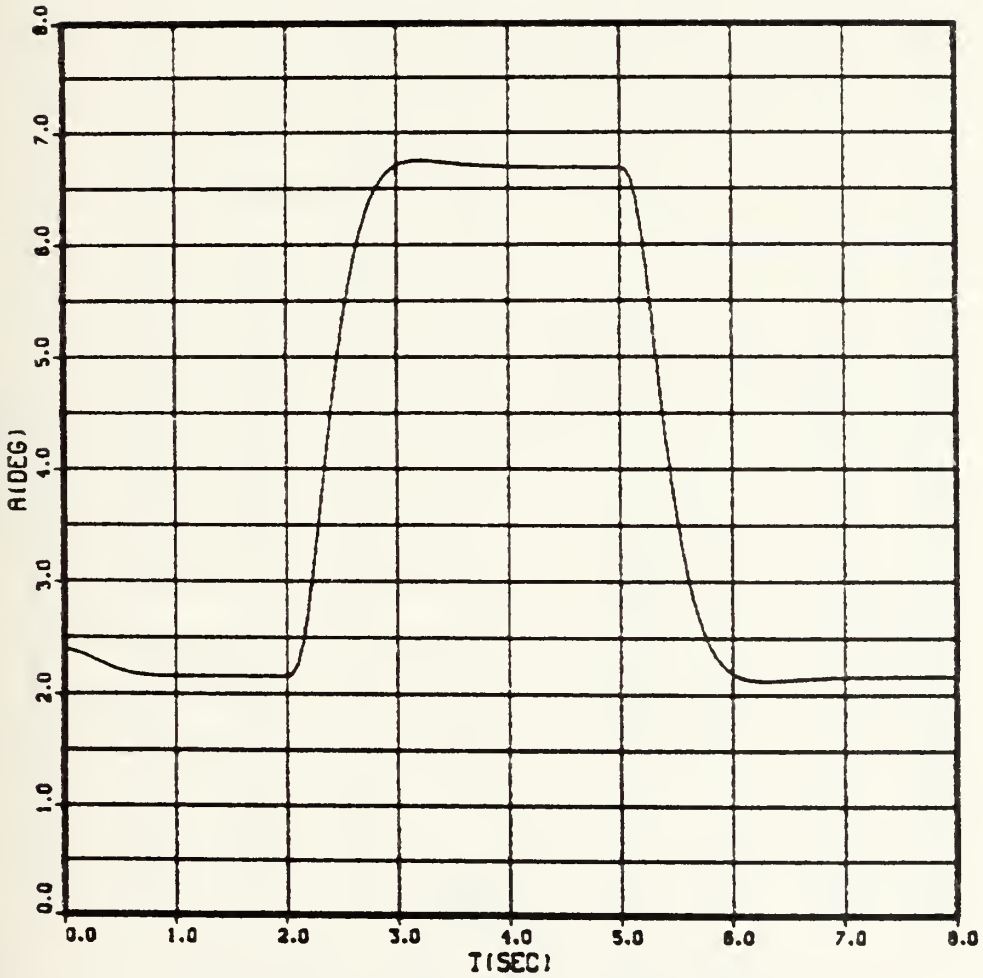


Fig. 4.18 Angle of Attack (a) vs Time (t)
 CBTT of Elliptical airframe; Ideal
 airframe dynamics; 2 Gees (0° , 180°)

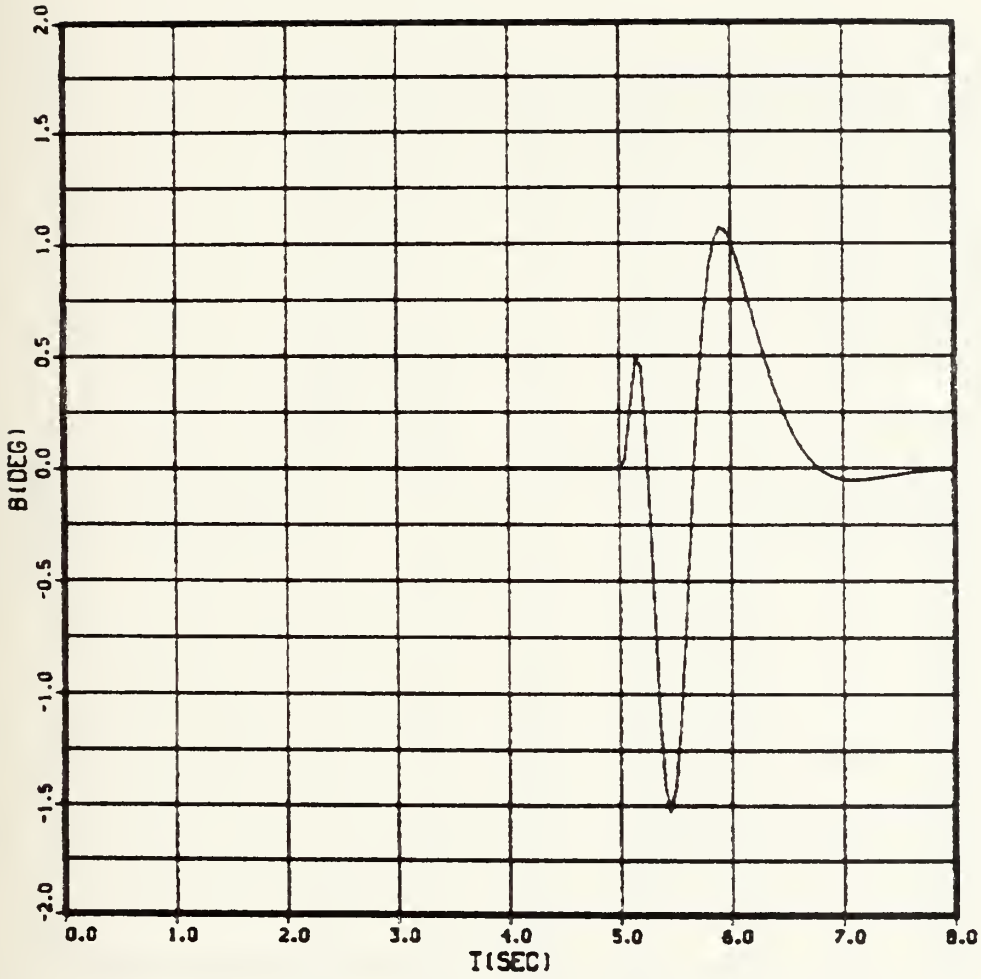


Fig. 4.19 Sideslip angle (β) vs Time (t)
 CBTT of Elliptical airframe; Ideal
 airframe dynamics; 2 Gees (0° , 180°)

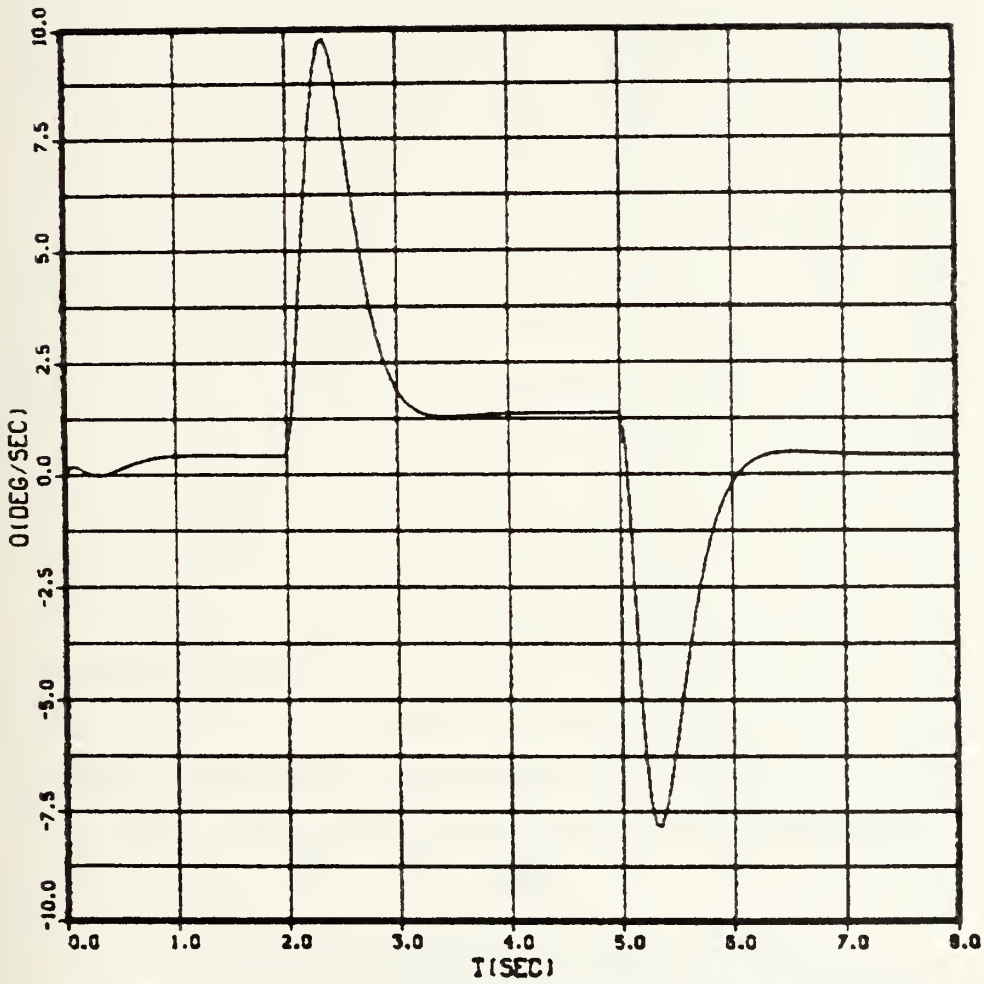


Fig. 4.20 Body pitch angular rate (q) vs Time (t)
 CBTT of Elliptical airframe; Ideal
 airframe dynamics; 2 Gees (0° , 180°)

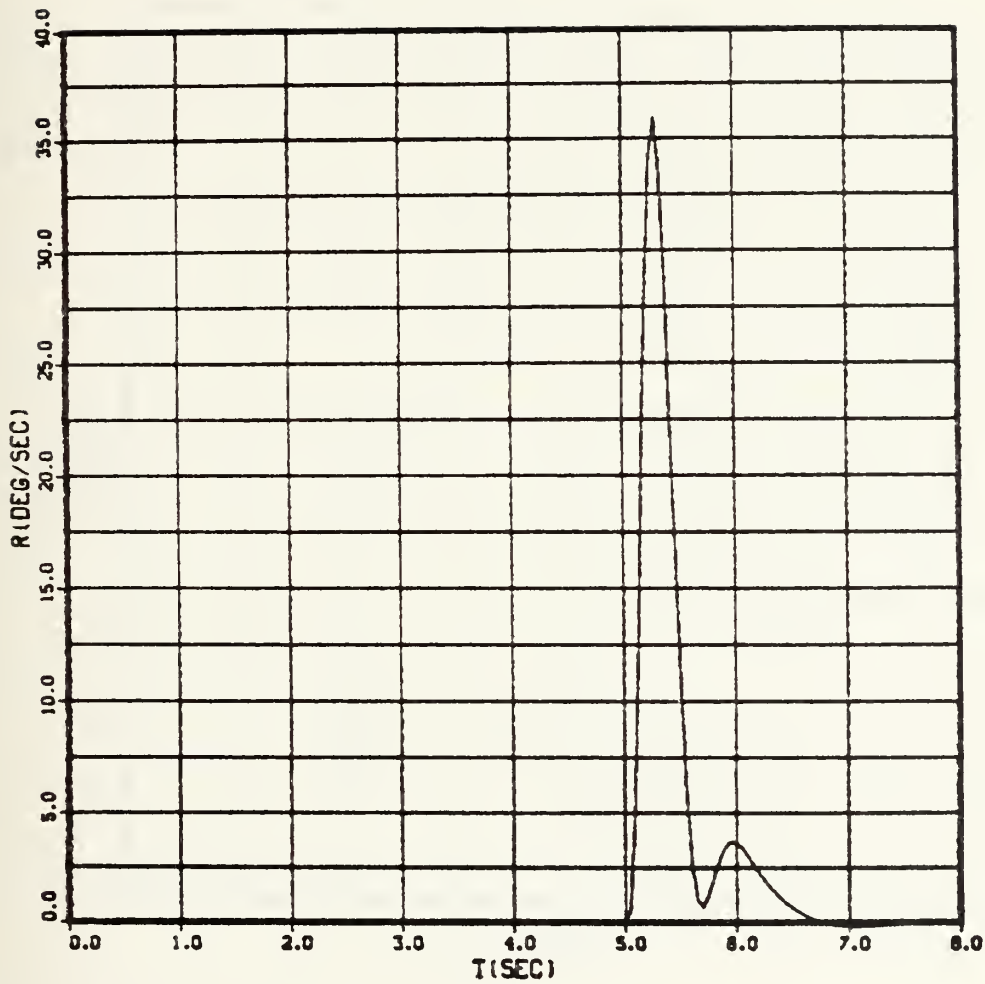


Fig. 4.21 Body Yaw angular rate (r) vs Time (t)
 CBTT Elliptical airframe; Ideal
 airframe dynamics; 2 Gees ($0^\circ, 180^\circ$)

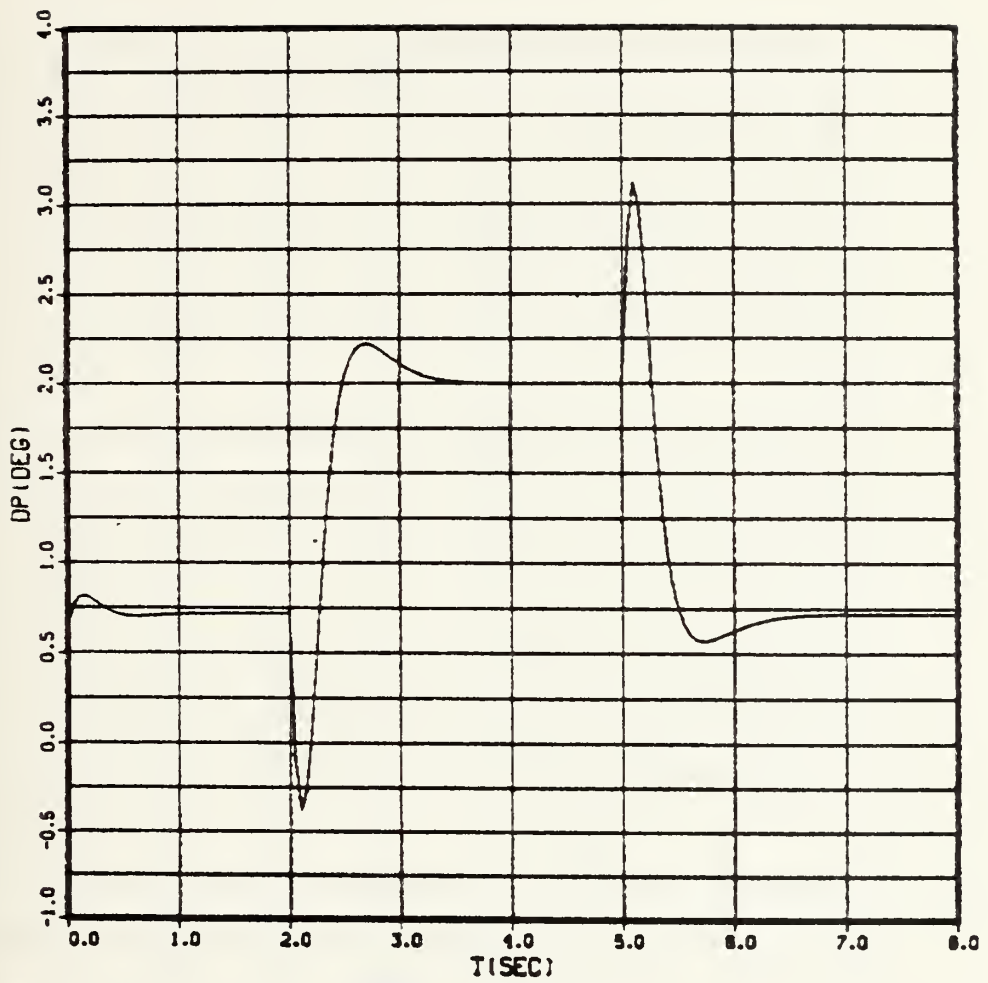


Fig. 4.22 Pitch tail incidence (δ_p) vs Time (t)
 CBTT of Elliptical airframe Ideal
 airframe dynamics; 2 Gees (0° , 180°)

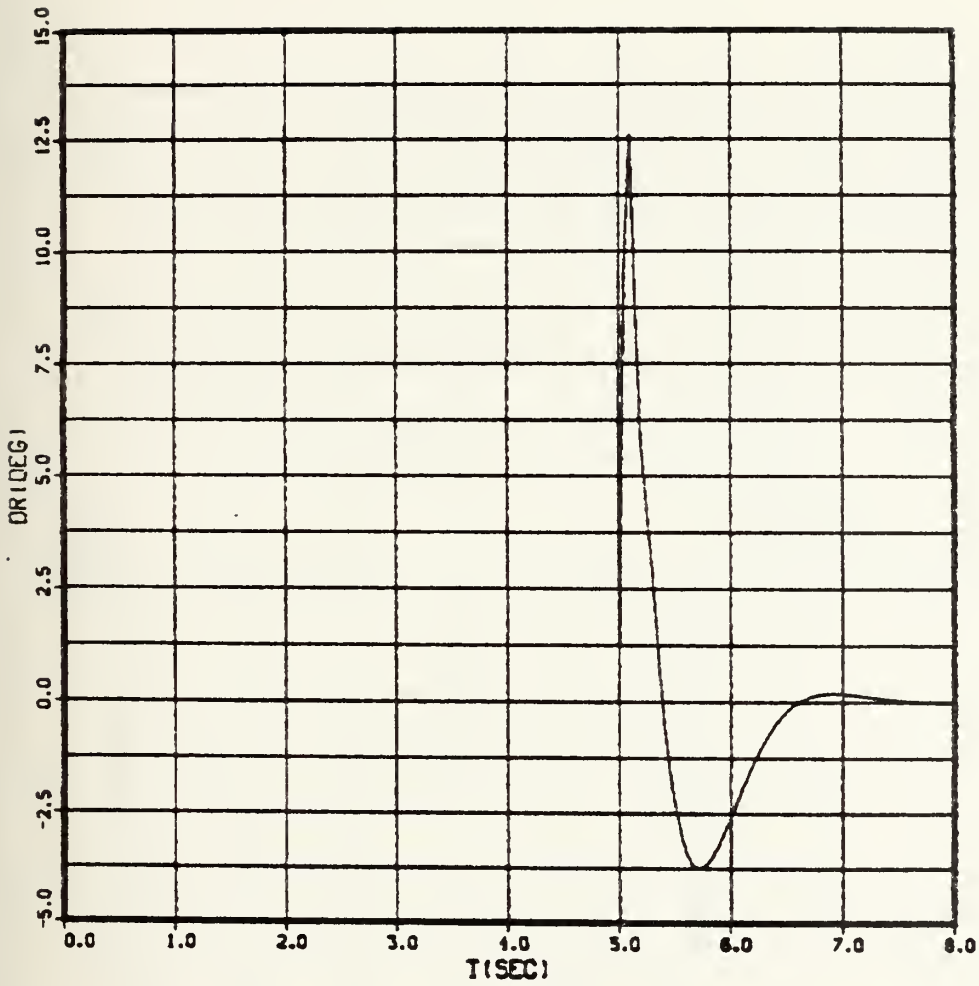


Fig. 4.23 Yaw tail incidence (δ_R) vs Time (t)
 CBTT of Elliptical airframe; Ideal
 airframe dynamics; 2 Gees ($0^\circ, 180^\circ$)

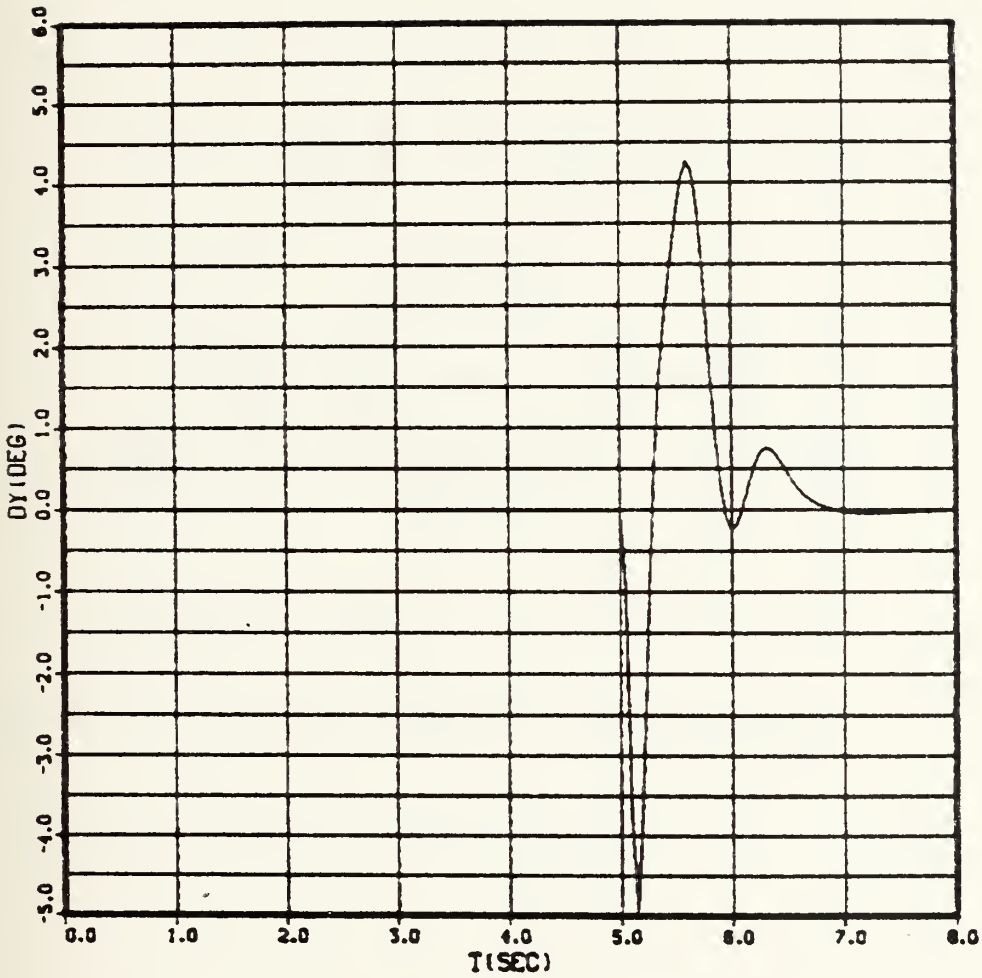


Fig. 4.24 Roll tail incidence (δ_Y) vs Time (t)

CBTT of Elliptical airframe; Ideal
airframe dynamics; 2 Gees ($0^\circ, 180^\circ$)

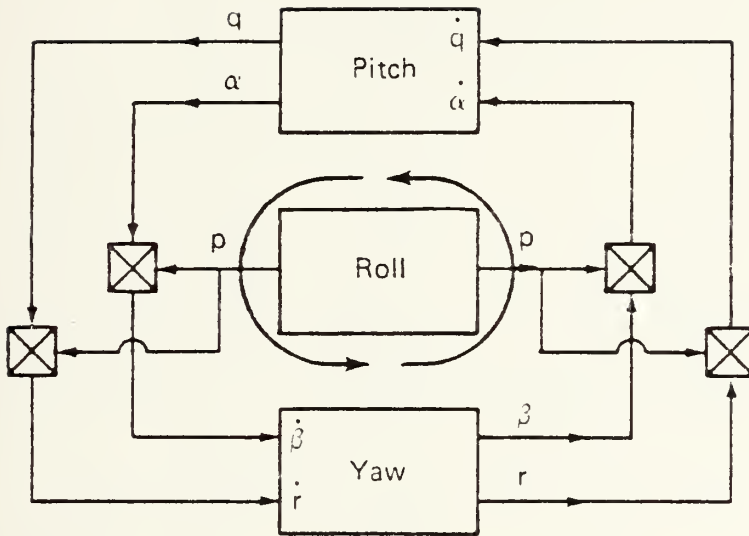


Fig. 4.25 Critical Feedback loop for CBTT

TABLE II. CBTT PERFORMANCE OF ELLIPTICAL AIRFRAME

VARIABLE	VALUE	TIME (sec)	CROSS- COUPLING	τ_1 (sec) Overshoot%	τ_2 (sec) Overshoot%
n_{zmin}	-2.934 (gees)	5.061	All	0.48 and	0.41 and
n_{zmax}	1.351 (gees)	5.661	All	0%	11.25%
n_{zmin}	-2.934 (gees)	5.062	ideal	0.48 and	0.37 and
n_{zmax}	0.937 (gees)	5.853	ideal	0%	0%
a_{min}	1.35 (deg)	6.10	All		
a_{max}	6.75 (deg)	3.10	All		
a_{min}	2.22 (deg)	6.295	ideal		
a_{max}	6.75 (deg)	3.10	ideal		
B_{min}	-0.9 (deg)	5.49	All		
B_{max}	1.49 (deg)	6.05	All		
B_{min}	1.53 (deg)	5.45	ideal		
B_{max}	1.07 (deg)	5.91	ideal		
q_{min}	-10.6 (deg/sec)	5.639	All		
q_{max}	9.5 (deg/sec)	2.337	All		
q_{min}	-7.8 (deg/sec)	5.328	ideal		
q_{max}	9.5 (deg/sec)	2.337	ideal		
p_{min}	-14.115 (deg/sec)	6.600	All		
p_{max}	282.094 (deg/sec)	5.387	All		
p_{min}	-14.29 (deg/sec)	6.600	ideal		
p_{max}	281.928 (deg/sec)	5.387	ideal		
r_{min}	-2.32 (deg/sec)	5.90	All		
r_{max}	33.1 (deg/sec)	5.32	All		
r_{min}	-0.178 (deg/sec)	7.036	ideal		
r_{max}	37.5 (deg/sec)	5.29	ideal		

Note:

All the above referred values are for command 2 (0° , 180°) τ_1 : 62 percent time constant of achieved maneuver plane acceleration due to the first guidance command. τ_2 : 63 percent time constant of achieved maneuver plane acceleration due to the second guidance command.

the gain (a) of the coordination branch of lateral control laws, as mentioned in the study for the elliptical airframe.

The same 2 gees (0° , 180°) guidance commands and flight condition were used for direct comparison with the performance results of the elliptical airframe.

However, to decrease simulation run time, the first guidance command and anti-gravity bias were applied at zero time with no missile or autopilot initial conditions.

1. Pitch Control Law

The pitch control law for the circular airframe is the same as that use in the uncoupled autopilot shown in Figure 4.26. The command used in the autopilot is different than the one used in uncoupled channel and it is as follows:

$$\eta_c = \eta_{z_c} - \cos \Theta \quad (\text{IV.B.1-1})$$

as referred to in section IV.B.1

The equations which represent the nonlinear pitch control law are the same as those in section III.C. of the linear pitch control law, using $K_{A_2} = -0.0387$

The equations are:

$$\dot{X} = -150X + 150\eta_{2B} \quad (\text{IV.F.1-1})$$

$$\dot{Y}_3 = Y_4 - 1.3531 \cdot (\eta_c - X) \quad (\text{IV.F.1-2})$$

$$\dot{Y}_4 = -5Y_4 + 6.572 \cdot (\eta_c - X) \quad (\text{IV.F.1-3})$$

$$\dot{\delta p_c} = -0.143 \cdot \delta p_c - 0.34058(\dot{Y}_3 + \dot{q}/57.3) - 2.2308 \cdot (Y_3 - q/57.3) \quad (\text{IV.F.1-4})$$

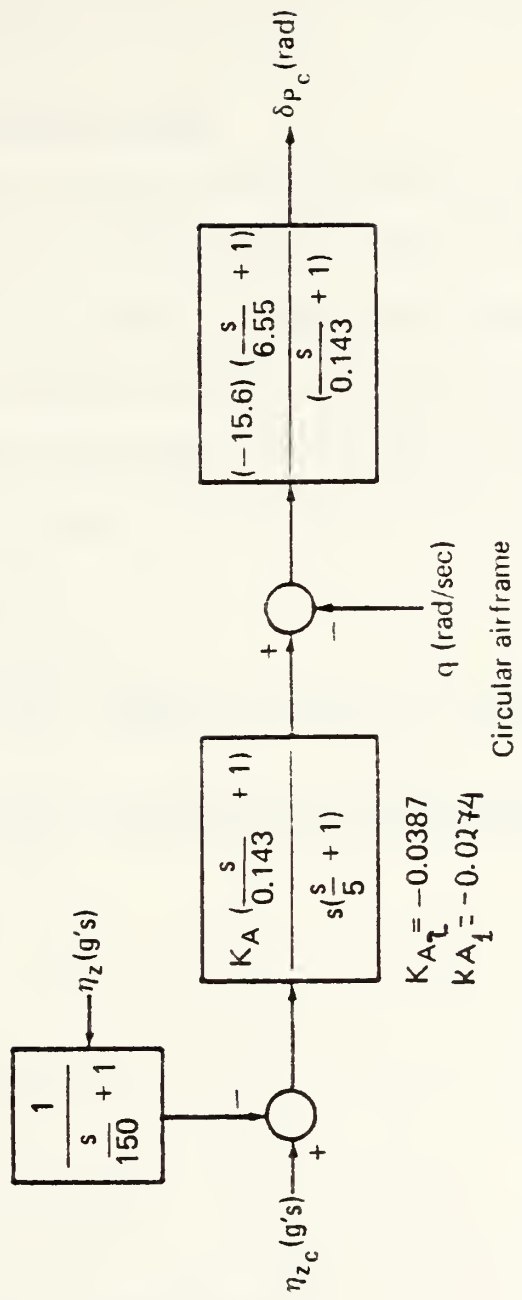


Fig. 4.26 Nonlinear pitch control law

$$\delta \dot{p} = -188.4 \delta p + 10795.3 \cdot \delta p_c \quad (\text{IV.F.1-5})$$

The state variables of the above equation are

shown in Figure 4.26.

2. Lateral Control Laws

The lateral control laws for the circular airframe are the same as those used for the linear studies, except the modification in α_e (or α) which was referred to before.

The same command is used, as in the elliptical airframe. The equations which represent the lateral control laws are the same those of section III.C.1 and III.C.2. and they are:

$$\dot{Y}_2 = -5 Y_2 + 1.6 \eta_{YB} \quad (\text{IV.F.2-1})$$

$$\begin{aligned} \delta \dot{Y}_c &= 0.485 \left[\dot{Y}_2 + \frac{\dot{r}}{57.3} - \frac{0.458}{(57.3)^2} \cdot (\dot{\alpha}_e \cdot P + \alpha_e \dot{P}) \right] + 4.85 \left(Y_2 + \frac{r}{57.3} - \frac{0.458 \alpha_e P}{(57.3)^2} \right) \\ &= 0.485 \left[\dot{Y}_2 + \frac{\dot{r}}{57.3} - 0.000139 (\dot{\alpha}_e \cdot P + \alpha_e \dot{P}) \right] + 4.85 \left(Y_2 + \frac{r}{57.3} - 0.000139 \alpha_e \cdot P \right) \end{aligned}$$

$$(\text{IV.F.2-2})$$

where:

$$\left. \begin{aligned} \alpha_e &= \alpha \\ \dot{\alpha}_e &= \dot{\alpha} \end{aligned} \right\} \alpha > 1^\circ$$

and

$$\left. \begin{aligned} \alpha_e &= 1^\circ \\ \dot{\alpha}_e &= 0 \end{aligned} \right\} \alpha < 1^\circ$$

$$\delta \dot{Y} = -188.4 \delta Y + 10795.3 \delta Y_c \quad (\text{IV.F.2-3})$$

$$\dot{X}_1 = -8 X_1 - 17.6 \phi + 17.6 \phi_c \quad (\text{IV.F.2-4})$$

$$\begin{aligned} \dot{Y}_1 &= -5 Y_1 + 0.05033 (\dot{X}_1 - \dot{P}/57.3) + 0.755 (X_1 - P/57.3) \\ &(\text{IV.F.2-5}) \end{aligned}$$

$$\dot{X}_2 = -6X_2 + 0.078 (\dot{P}/57.3) \quad (\text{IV.F.2-6})$$

$$\delta \dot{R}_c = -15\delta R_c + 0.25 (\dot{Y}_1 - \dot{X}_2) + 15(Y_1 - X_2) \quad (\text{IV.F.2-7})$$

$$\delta \dot{P} = -198.4\delta R_c + 10795.3 \cdot \delta R_c \quad (\text{IV.F.2-8})$$

The above state variables are shown in Figure

4.27.

G. AERODYNAMIC MODELS FOR CIRCULAR AIRFRAME

The aerodynamic models of Pitch and Roll-Yaw channels for the circular airframe are the same as those of the elliptical airframe and are shown in Figures 4.1, 4.2, the only differences which exist between them, are the aerodynamic mass parameters and nonlinear derivatives changes, as referred to in the (Appendices A and B).

Hence, the equations which represent the dynamic models are:

1. Pitch Channel

$$\eta_{z_B} = -\bar{q} S C_N / w \quad (\text{yees}) \quad (\text{IV.C.1-1})$$

$$\dot{q} = \frac{P.R}{57.3} + \frac{57.3 \bar{q} S d C_M}{I_{zz}} \quad (\text{deg/sec}^2) \quad (\text{IV.C.1-2})$$

$$\dot{\alpha} = q + K \cdot \eta_{z_B} - \frac{P.B}{57.3} \quad (\text{deg/sec}) \quad (\text{IV.C.1-3})$$

Substituting the values for aerodynamic and mass parameter for circular airframe, the above equations become:

$$\eta_{z_B} = -2.05292 \cdot C_N \quad (\text{IV.G.1-1})$$

$$\dot{q} = -0.017452 P.R + 736.8604 C_M \quad (\text{IV.G.1-2})$$

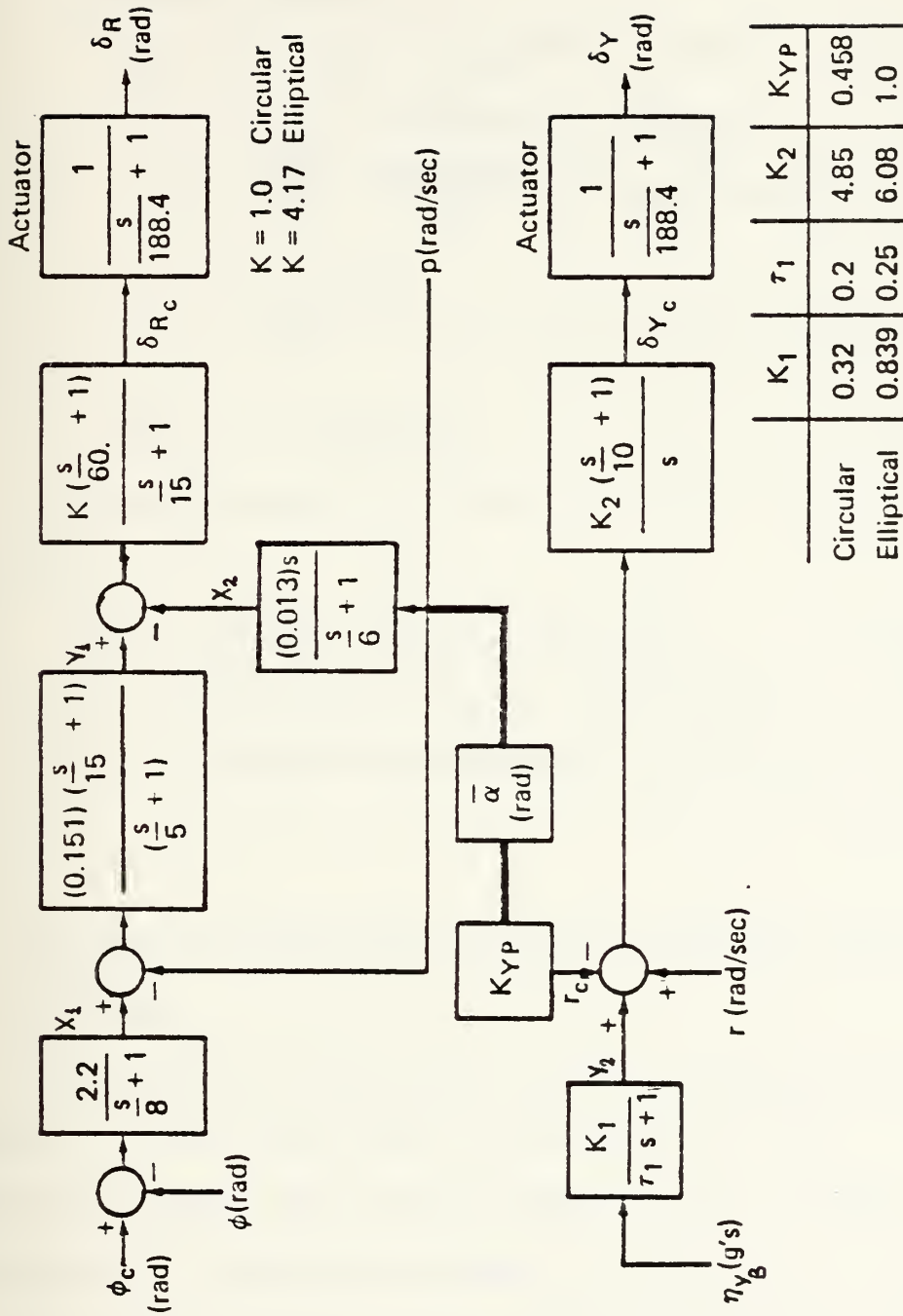


Fig. 4.27 CBTT nonlinear lateral control law

$$\dot{\alpha} = q - 0.9854 C_N - 0.017452 p \cdot \theta \quad (\text{IV.G.1-3})$$

2. Lateral Channels

$$\eta_{Y_B} = \bar{q} S (C_{Y_\theta} \cdot \theta + C_{Y_{\delta Y}} \cdot \delta Y) / W \text{ (gees)} \quad (\text{IV.C.2-1})$$

$$\dot{\theta} = K \cdot \eta_{Y_B} + \alpha \cdot p / 57.3 - r \text{ (deg/sec)} \quad (\text{IV.C.2-2})$$

$$\dot{r} = -\frac{q \cdot P}{57.3} + \frac{57.3 \bar{q} S d}{I_{zz}} (C_{n_\theta} \cdot \theta + C_{n_{\delta Y}} \cdot \delta Y + C_{n_{\delta R}} \cdot \delta R) \quad (\text{IV.C.2-3})$$

$$\dot{p} = \frac{57.3 \bar{q} S d}{I_{xx}} (C_{e_\theta} \cdot \theta + C_{e_{\delta Y}} \cdot \delta Y + C_{e_{\delta R}} \cdot \delta R) \quad (\text{IV.C.2-4})$$

$$\dot{\phi}_d = p \text{ (deg/sec)} \quad (\text{IV.C.2-5})$$

Substituting the values in the above equations,

they yield:

$$\eta_{Y_B} = 2.05292 (C_{Y_\theta} \cdot \theta + C_{Y_{\delta Y}} \cdot \delta Y) \quad (\text{IV.G.2-1})$$

$$\dot{\theta} = 0.9854 (C_{Y_\theta} \cdot \theta + C_{Y_{\delta Y}} \cdot \delta Y) + 0.01745 p \cdot \alpha - r \quad (\text{IV.G.2-2})$$

$$\dot{r} = -0.017452 q \cdot P + 733.3837 (C_{n_\theta} \cdot \theta + C_{n_{\delta Y}} \cdot \delta Y + C_{n_{\delta R}} \cdot \delta R) \quad (\text{IV.G.2-3})$$

H. ANALYSIS OF NONLINEAR CBTT AUTOPILOTS FOR CIRCULAR AIRFRAME

For purposes of analysis, a CSMP program was written (Appendix H) with the equations representing the aerodynamic models and control laws of the nonlinear CBTT autopilots for referred airframe.

At first, in order to understand the effect of faster response, in the reduction of the effect of kinematic and inertial cross-coupling, the pitch acceleration error gain

K_A Figure 4.26 was reduced to $K_{A_1} = 0.0274$ for slower response.

The equation, which represents the acceleration compensator after the above reduction, is:

$$Y_3 = \frac{-0.0274 (s/0.143 - 1)}{s \cdot \left(\frac{s}{5} + 1 \right)} \cdot (\eta_c - X) \quad (\text{IV.H-1})$$

Utilizing method of state-space representation with forcing term derivatives, the equation IV.H-1 yields:

$$\dot{Y}_3 = Y_4 - 0.95804 \cdot (\eta_c - X) \quad (\text{IV.H-2})$$

$$\dot{Y}_4 = -5 \cdot Y_4 + 4.653 \cdot (\eta_c - X) \quad (\text{IV.H-3})$$

Using the above equations, instead of the equation IV.F.1-2 and IV.F.1-3, a new CSMP program (Appendix I) was written.

Figure 4.28 shows that the achieved maneuver plane acceleration has a good response to the first command which is applied at zero time. The missile with the circular airframe moves upward like a skid-to-turn missile, as did the elliptical airframe missile, because the motion is in the desired maneuver direction and therefore the roll channel is not commanded.

The time constant of the achieved maneuver response τ_1 is equal to 0.49 seconds. The achieved maneuver plane response due to the second guidance command applied at 3 seconds, shown in Figure 4.28 is reacting differently to the kinematic and inertial cross-coupling than the

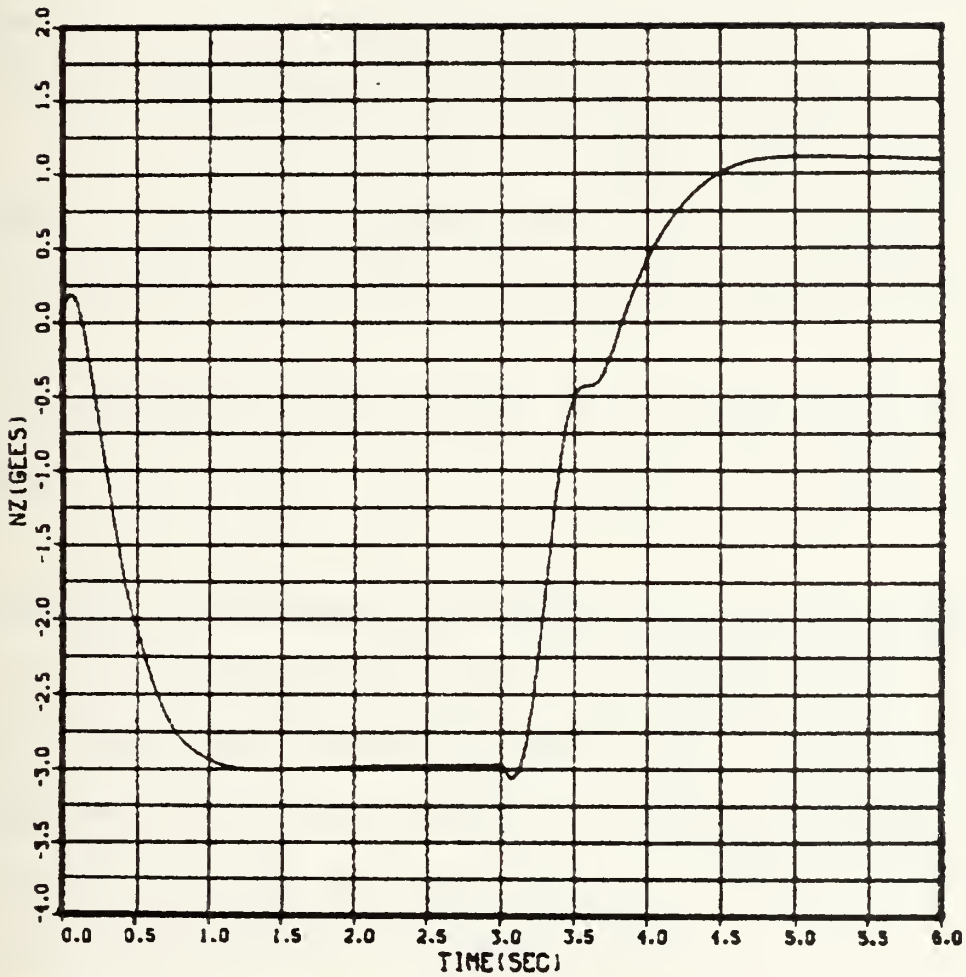


Fig. 4.28 Achieved Inertial Acceleration (n_z) vs Time (t)

CBTT of Circular airframe; 2 Gees (0° , 180°),
 $K_{A_1} = -0.0274$

elliptical airframe in Figure 4.5. Rather than overshoots and undershoots, a slowing transient starts at 3.5 seconds.

Figure 4.29 shows that the overshoot in the body-fixed pitch acceleration, due to the kinematic and inertial cross-coupling during the second command, is 60.8 percent which is substantially more than it was for the elliptical airframe and occurs much sooner at 3.66 second.

Figure 4.29 through 4.39 show the time responses of the n_{y_c} , a , β , q , p , r , ϕ , δp , δ and δ_R . Above figures and table III show the characteristic of the responses of the variables for the circular airframe, when the $K_A = -0.0274$.

The referred results of this study verify the results of [Ref. 2].

I. EFFECT OF INCREASING PITCH CHANNEL SPEED OF RESPONSE

In order to reduce the effect of kinematic and inertial cross-coupling during the second guidance command, the response of the Pitch channel of the CBTT autopilot for the circular airframe was made faster as shown in section

II. This was accomplished by increasing the acceleration error gain $K_{A_2} = -0.0387$.

Using the above gain K_{A_2} the equations represent the acceleration compensator are the IV.F.1-2 and IV.F.1-3.

The effect of the change in K_A on achieved body fixed acceleration (Figure 4.40) results in the achieved maneuver

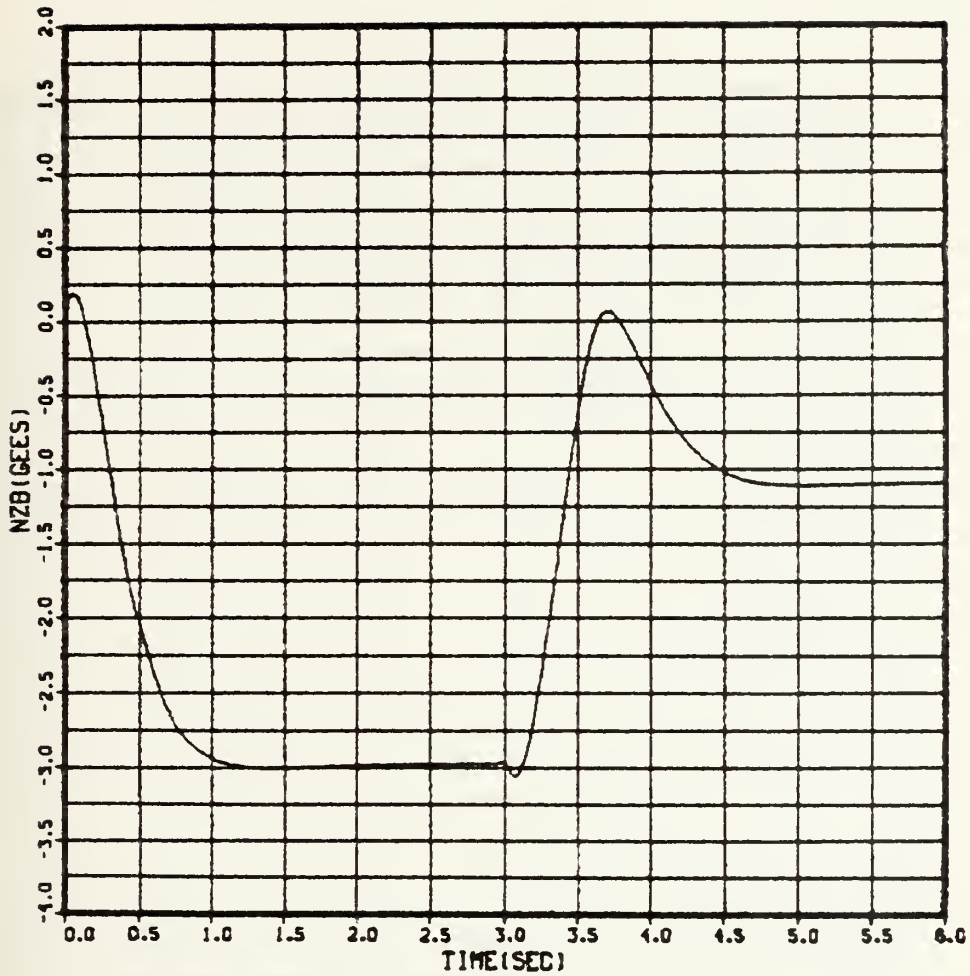


Fig. 4.29 Achieved Body-fixed Acceleration (n_{Z_B}) vs
 Time (t) CBTT of Circular airframe; 2 Gees (0° ,
 180°), $K_A = -0.0274$

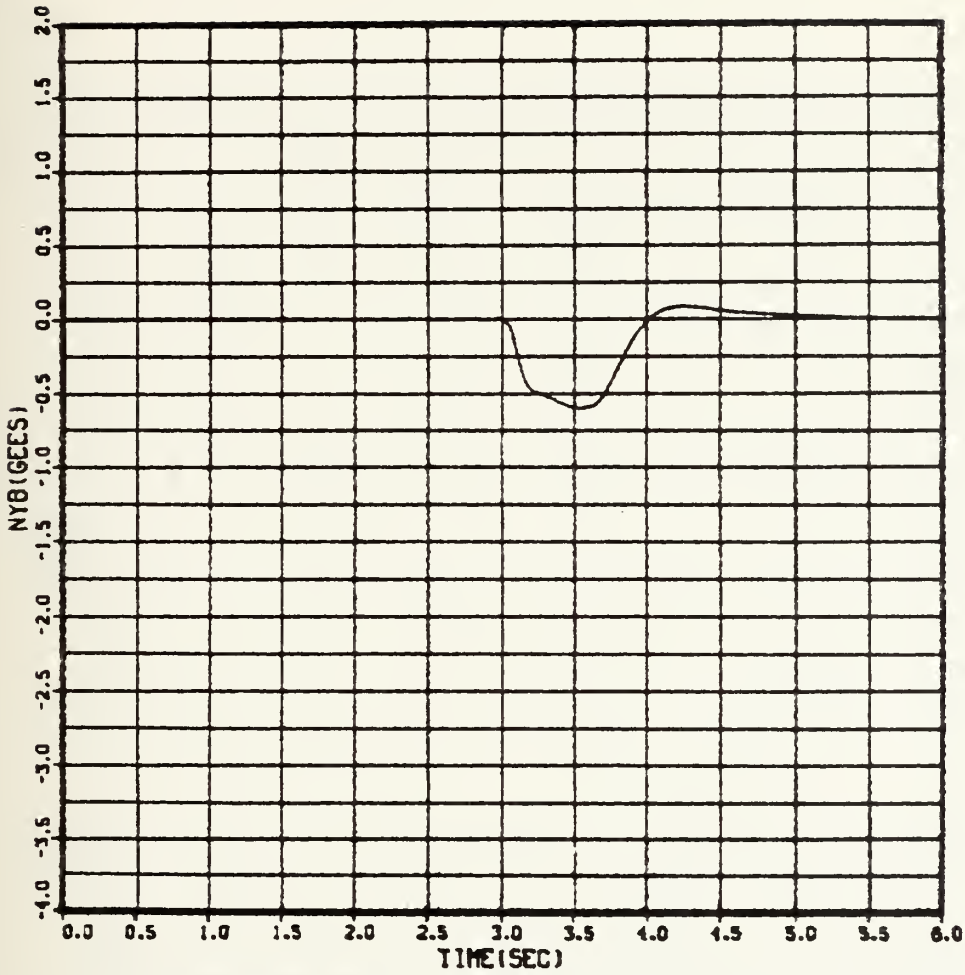


Fig. 4.30 Achieved Body-fixed Acceleration (n_Y) vs Time (t); CBTT of Circular airframe; 2 Gees (0° , 180°), $K_{A_1} = -0.0274$

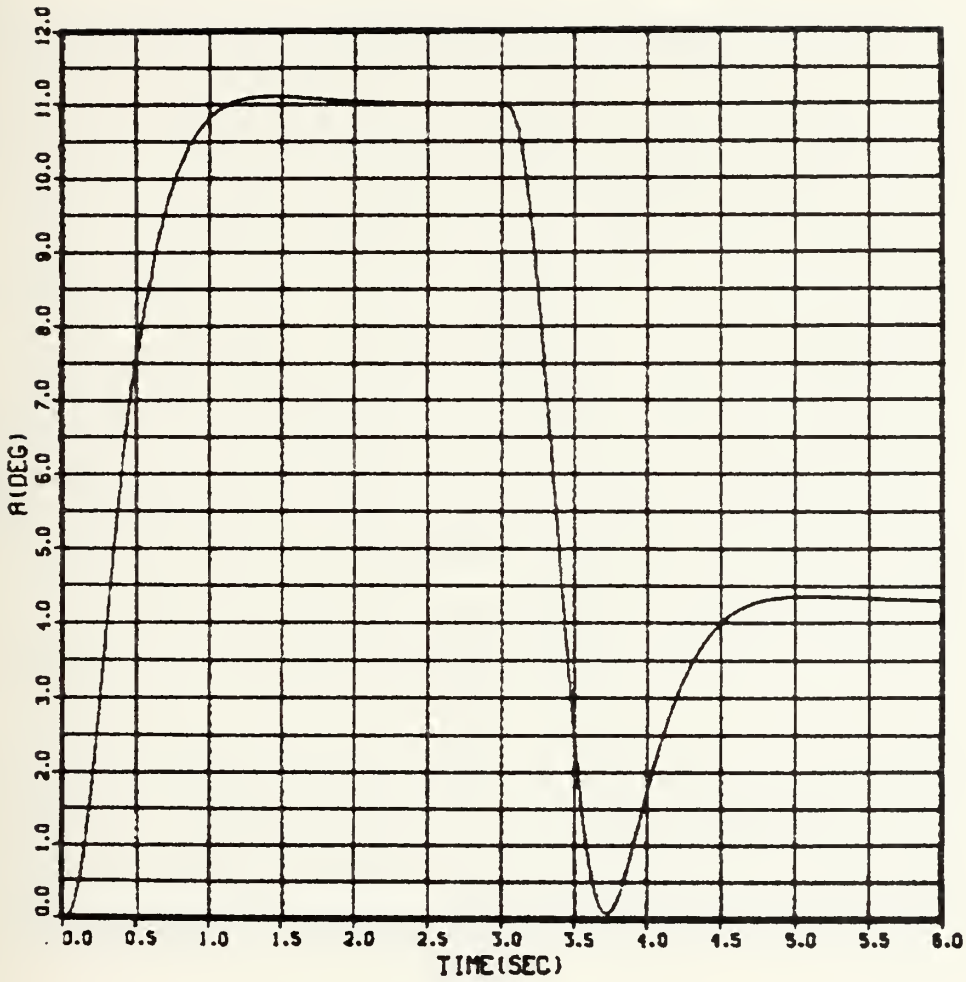


Fig. 4.31 Angle of attack (α) vs Time (t)
 CBTT of Circular airframe;
 2 Gees ($0^\circ, 180^\circ$), $K_{A_1} = -0.0274$

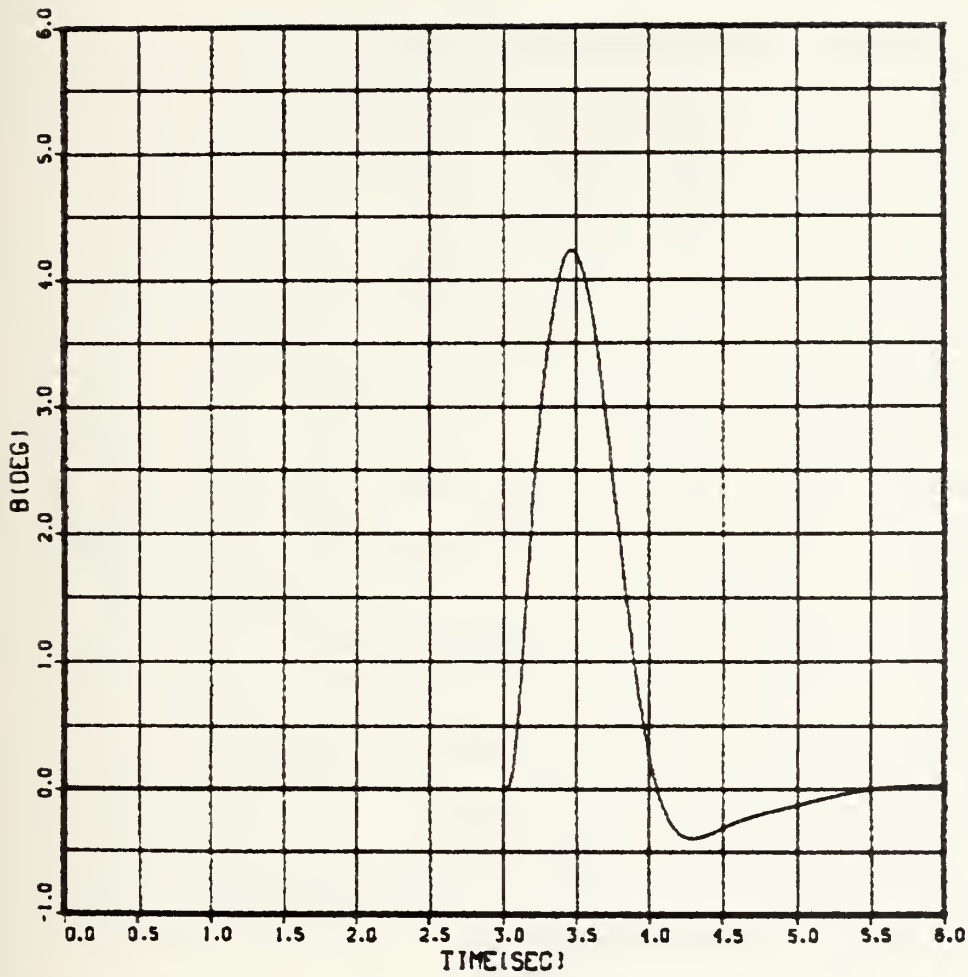


Fig. 4.32 Sideslip angle (β) vs Time (t)
 CBTT of Circular airframe;
 2 Gees ($0^\circ, 180^\circ$), $K_{A_1} = -0.0274$

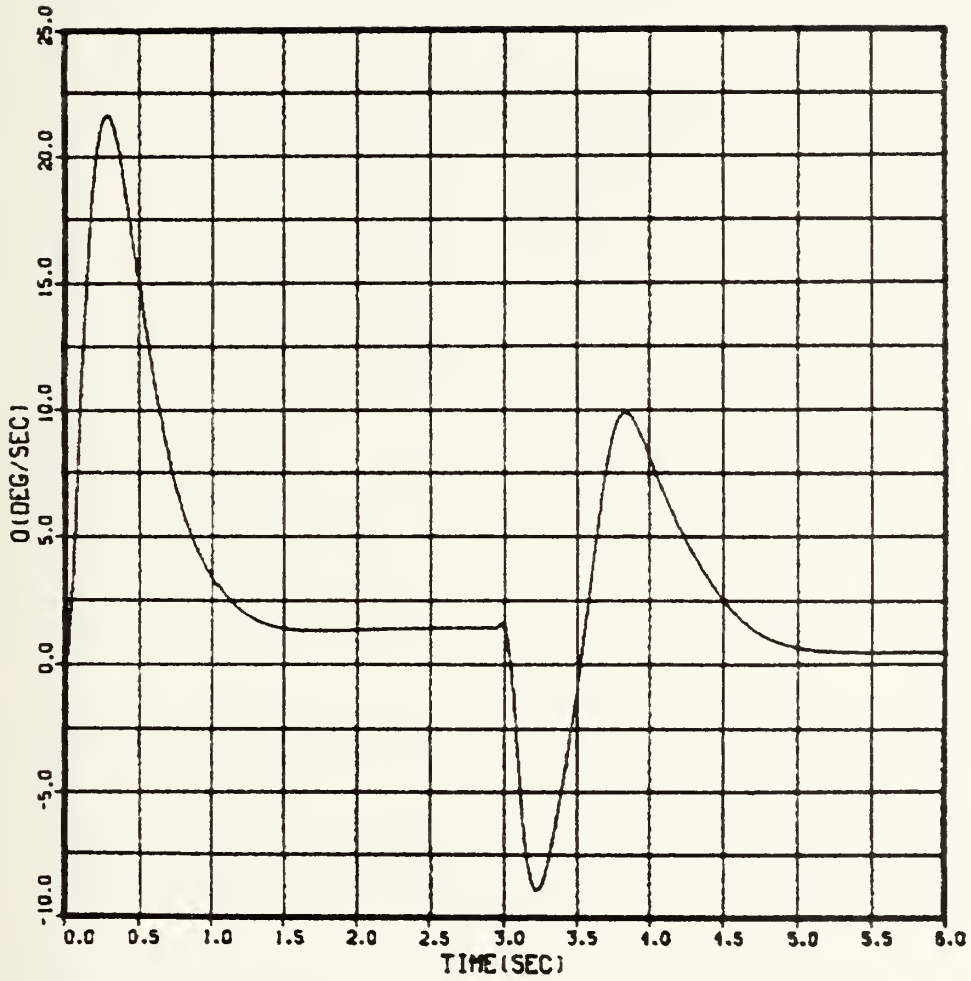


Fig. 4.33 Pitch Body angular rate (q) vs Time (t)
 CBTT of Circular airframe; 2 Gees
 $(0^\circ, 180^\circ)$, $K_{A_1} = -0.0274$

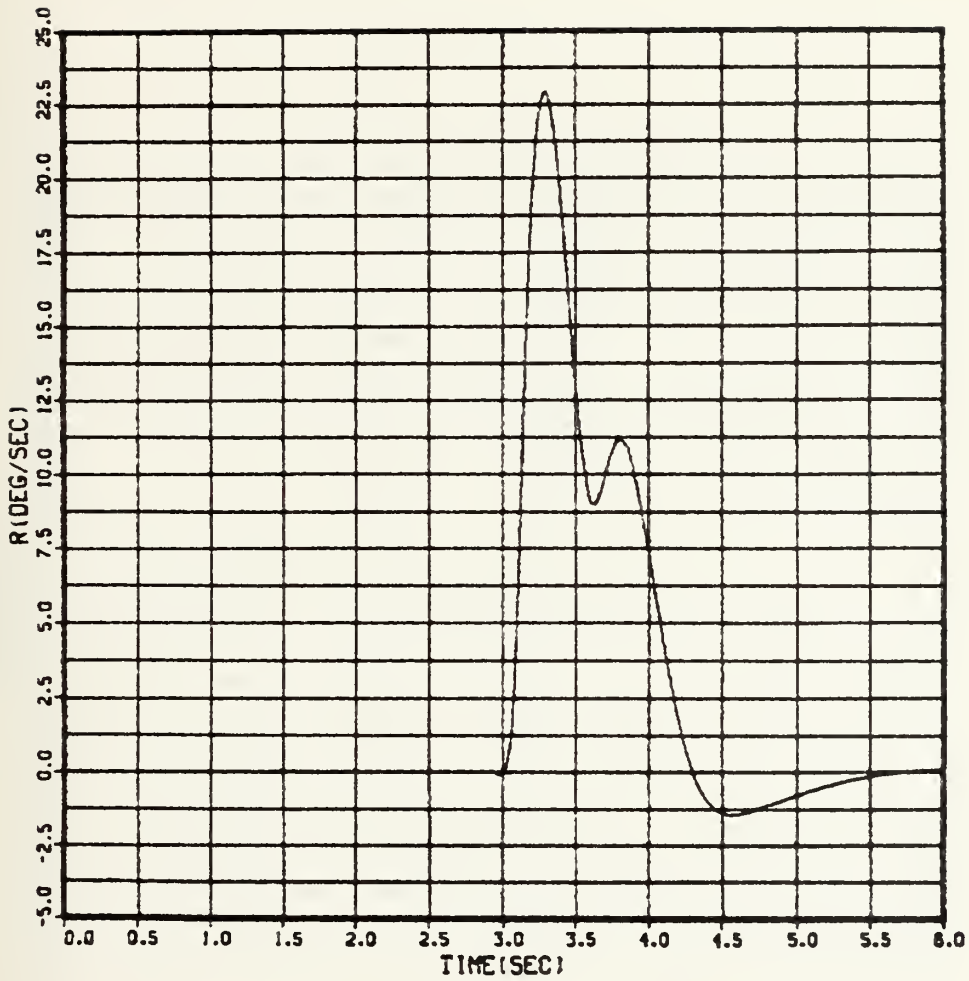


Fig. 4.34 Yaw Body angular rate (r) vs Time (t)
 CBTT of Circular airframe;
 2 Gees ($0^\circ, 180^\circ$), $K_{A_1} = -0.0274$

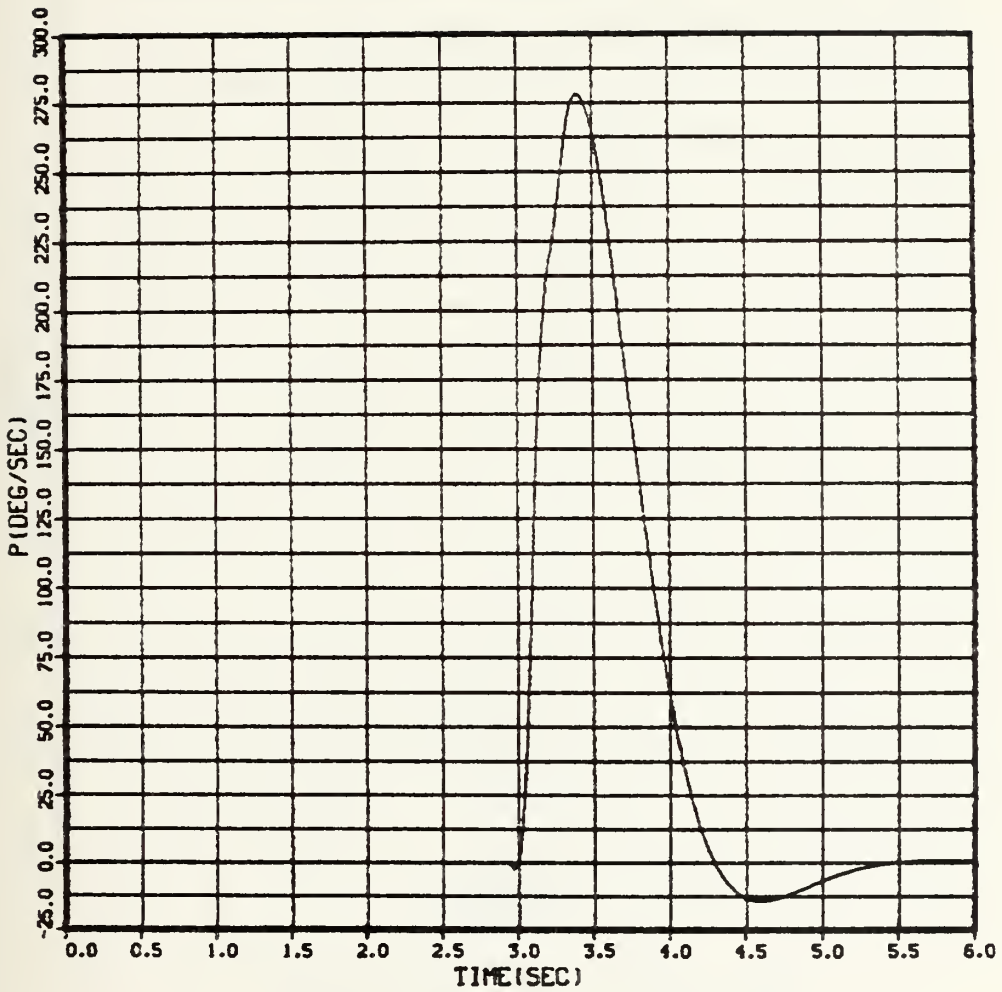


Fig. 4.35 Roll Body angular rate (P) vs Time (t)
 CBTT of Circular airframes;
 2 Gees (0° , 180°), $K_{A_1} = -0.0274$

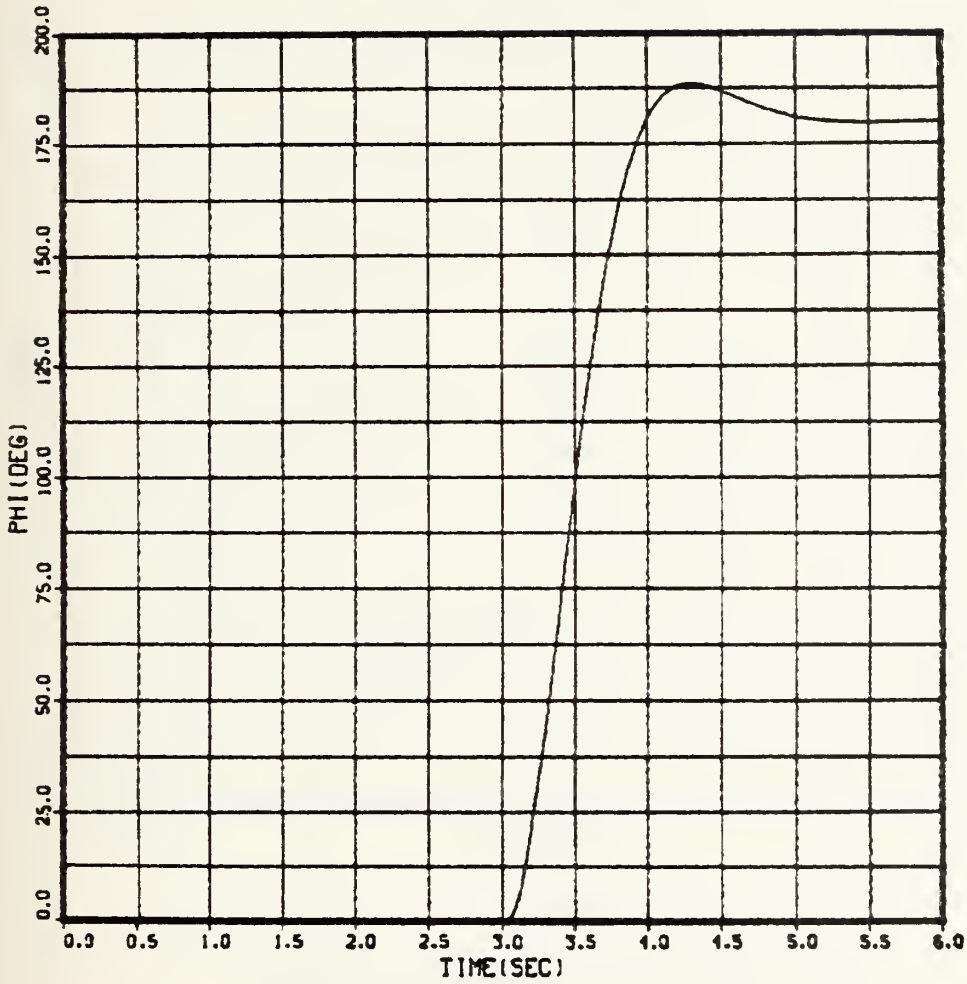


Fig. 4.36 Roll angle (ϕ) vs Time (t)
 CBTT of Circular airframe;
 2 Gees (0° , 180°), $K_{A_1} = -0.0274$

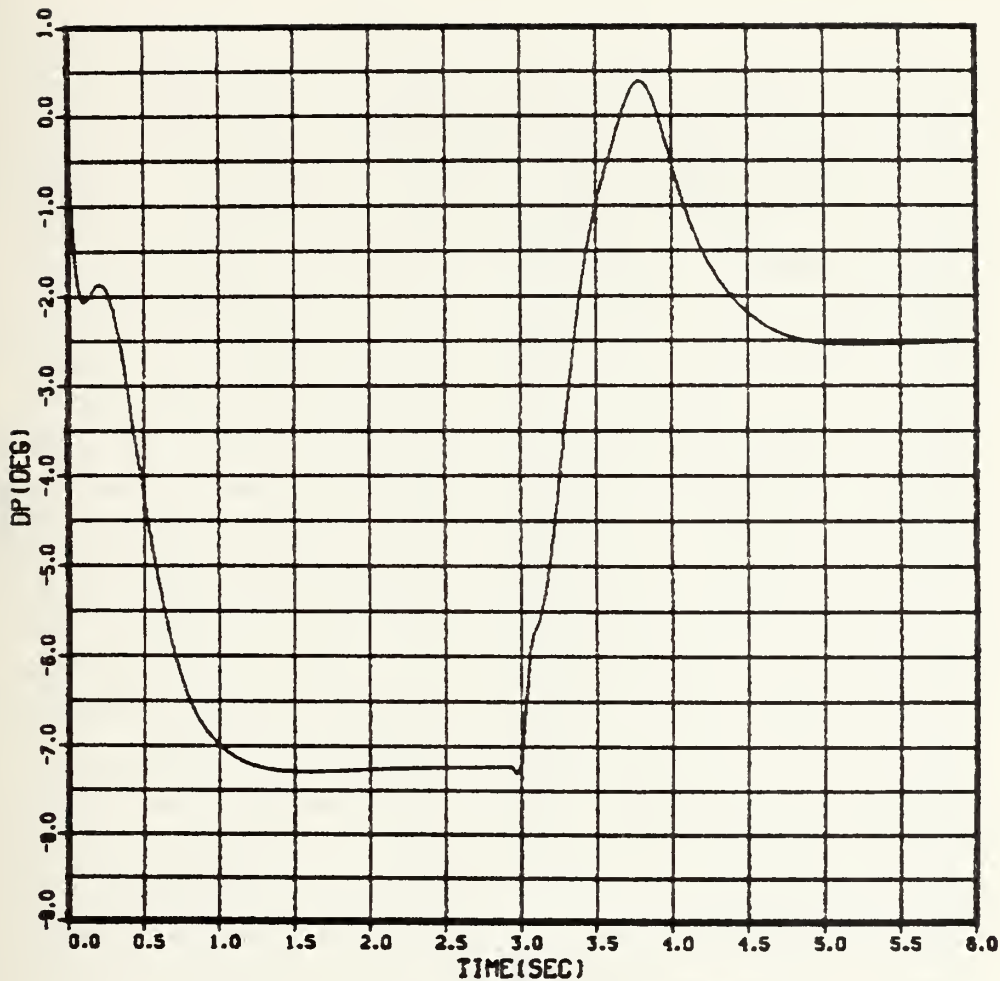


Fig. 4.37 Pitch tail incidence (δ_p) vs Time (t)

CBTT of Circular airframes;
 2 Gees ($0^\circ, 180^\circ$), $K_{A_1} = -0.0274$

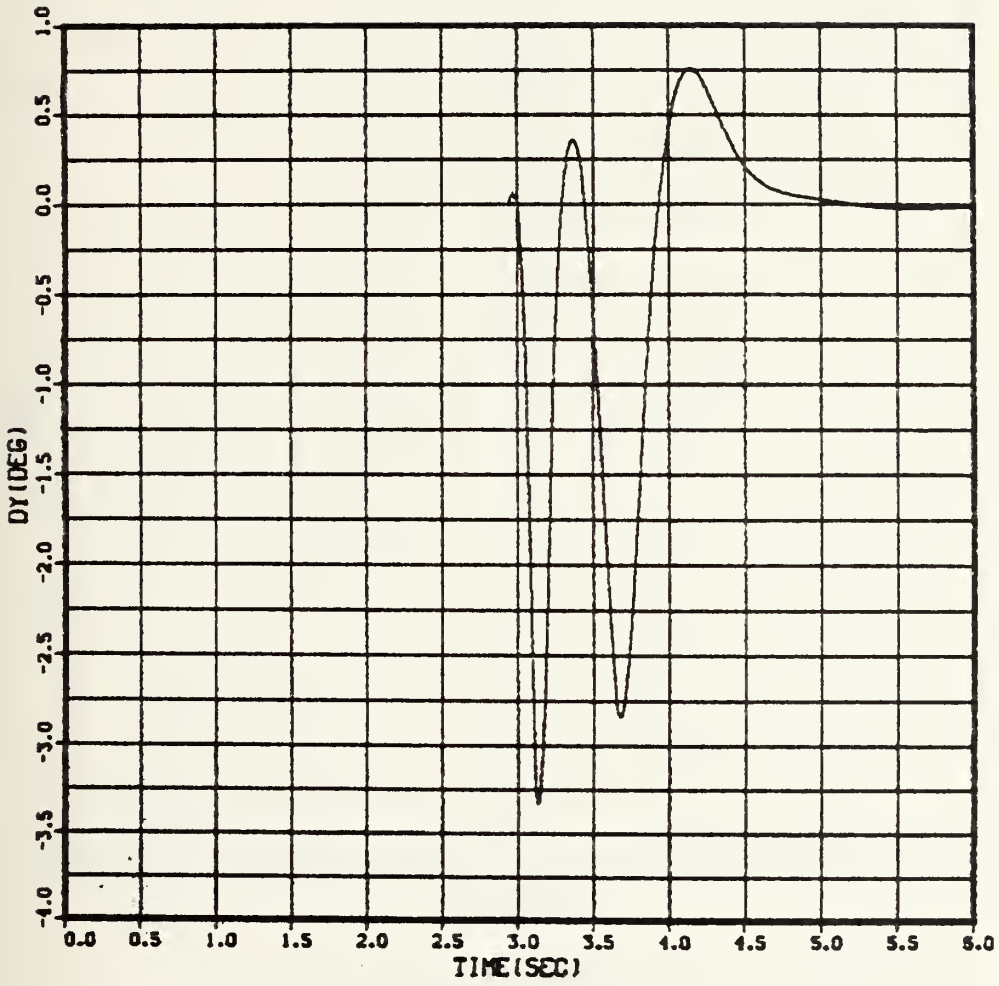


Fig. 4.38 Yaw tail incidence (δ_Y) vs Time (t)
 CBTT Circular airframe;
 2 Gees ($0^\circ, 180^\circ$), $K_{A_1} = -0.0274$

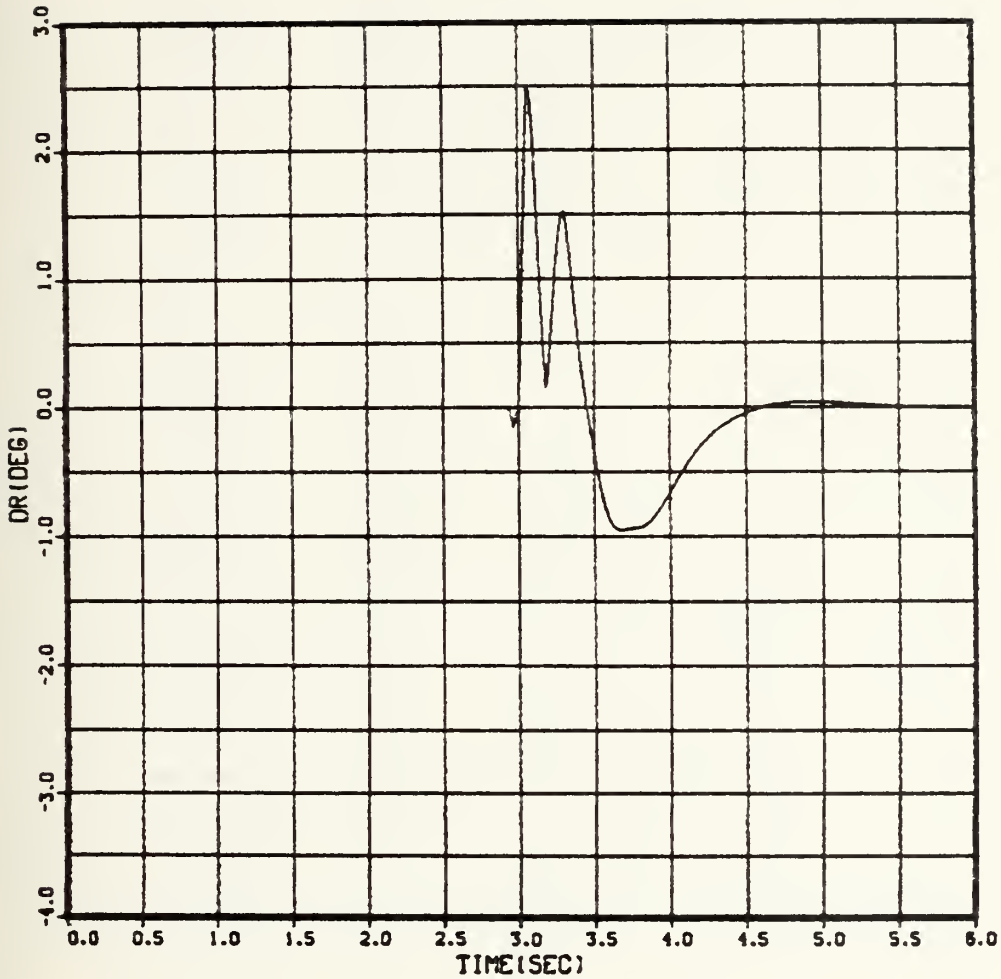


Fig. 4.39 Roll tail incidence (δ_R) vs Time (t)
 CBTT Circular airframe;
 2 Gees ($0^\circ, 180^\circ$), $K_{A_1} = -0.0274$

TABLE III. CBTT PERFORMANCE OF CIRCULAR AIRFRAME

VARIABLE	VALUE	TIME(sec)	CONDITION	τ_1 (sec); overshoot%	τ_2 (sec); overshoot%
n_{zmax}	1.092 (gees)	5.10	K_{A_1}	0.46 and	0.52 and
n_{zmin}	-3.044 (gees)	3.060		%	%
n_{zmax}	1.109 (gees)	4.540	K_{A_2}	0.34 and	0.62 and
n_{zmin}	-3.125 (gees)	0.825		5%	0.05%
n_{zmax}	1.002 (gees)	5.040	K_{A_3}	0.34 and	0.53 and
n_{zmin}	-3.125 (gees)	0.825		5%	0%
a_{max}	11.15 (deg)	1.432	K_{A_1}		
a_{min}	0 (deg)	0			
a_{max}	11.489 (deg)	0.862	K_{A_2}		
a_{min}	0.053 (deg)	3.656			
a_{max}	11.488 (deg)	0.862	K_{A_3}		
a_{min}	0 (deg)	0			
B_{max}	4.25 (deg)	3.461	K_{A_1}		
B_{min}	-0.399 (deg)	4.286			
B_{max}	3.633 (deg)	3.458	K_{A_2}		
B_{min}	-0.326 (deg)	4.290			
B_{max}	5.114 (deg)	3.608	K_{A_3}		
B_{min}	-0.414 (deg)	4.620			
q_{max}	21.39 (deg/sec)	0.285	K_{A_1}		
q_{min}	-8.84 (deg/sec)	3.220			
q_{max}	29.562 (deg/sec)	0.261	K_{A_2}		
q_{min}	-14.323 (deg/sec)	3.225			
q_{max}	29.562 (deg/sec)	0.261	K_{A_3}		
q_{min}	-17.575 (deg/sec)	3.251			
p_{max}	278.5 (deg/sec)	3.394	K_{A_1}		
p_{min}	-14.166 (deg/sec)	4.6			
p_{max}	279.487 (deg/sec)	3.4	K_{A_2}		
p_{min}	-14.071 (deg/sec)	4.6			
p_{max}	277.574 (deg/sec)	3.4	K_{A_3}		
p_{min}	-13.798 (deg/sec)	4.597			
r_{max}	22.66 (deg/sec)	3.28	K_{A_1}		
r_{min}	-1.456 (deg/sec)	4.56			
r_{max}	21.406 (deg/sec)	3.262	K_{A_2}		
r_{min}	-1.322 (deg/sec)	4.537			
r_{max}	23.159 (deg/sec)	3.287	K_{A_3}		
r_{min}	-1.364 (deg/sec)	4.818			

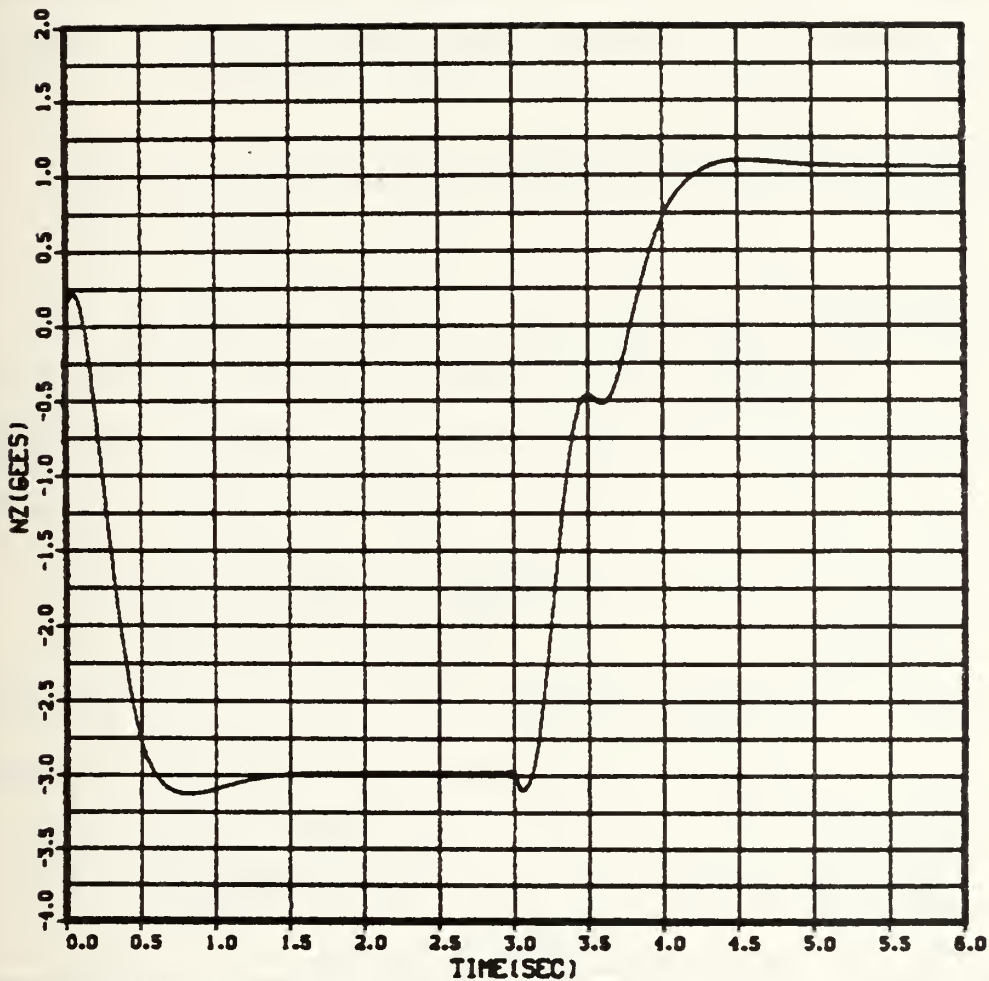


Fig. 4.40 Achieved Inertial Acceleration (n_z) vs

Time (t) CBTT of Circular airframe with faster
 responding Pitch channel; $K_{A_2} = -0.0387$, 2 Gees
 ($0^\circ, 180^\circ$)

plane acceleration response (Figure 4.41). Figure 4.41 shows that the achieved maneuver plane acceleration response during the first guidance command has improved.

Table III shows that increasing the K_A resulted in a decreasing in maximum sideslip angle 3.66 and a slight decrease in yaw angular rates (maximum 21.4 degrees).

J. EFFECT OF INERTIAL AND KINEMATIC CROSS-COUPLING IN PITCH CHANNEL

The cross-couplings, $(-BP)$ into a and (rP) into q , were removed in order to assess their effect on performance. Hence, the equations for a and q in the pitch aerodynamic model becomes:

$$\dot{\alpha} = q + k \cdot \eta_{zB} \quad (\text{deg/sec}) \quad (\text{IV.J-1})$$

$$\dot{q} = 57.3 \bar{q} S d C_M / I_{yy} \quad (\text{IV.J-2})$$

Replacing the values to the parameters of the above equations, they yield:

$$\dot{\alpha} = q - 0.9854 C_N \quad (\text{IV.J-3})$$

$$\dot{q} = 738.860 C_M \quad (\text{IV.J-4})$$

where C_N , C_M nonlinear functions which vary with a and δ_p referred to in (Appendix B). The lateral aerodynamic cross-coupling was retained. For purpose of analysis, a CSMP program (Appendix I) was written.

Comparing Figures 4.42 and 4.43 with figures 4.40 and 4.41 it is concluded that the undersirable transients are gone.

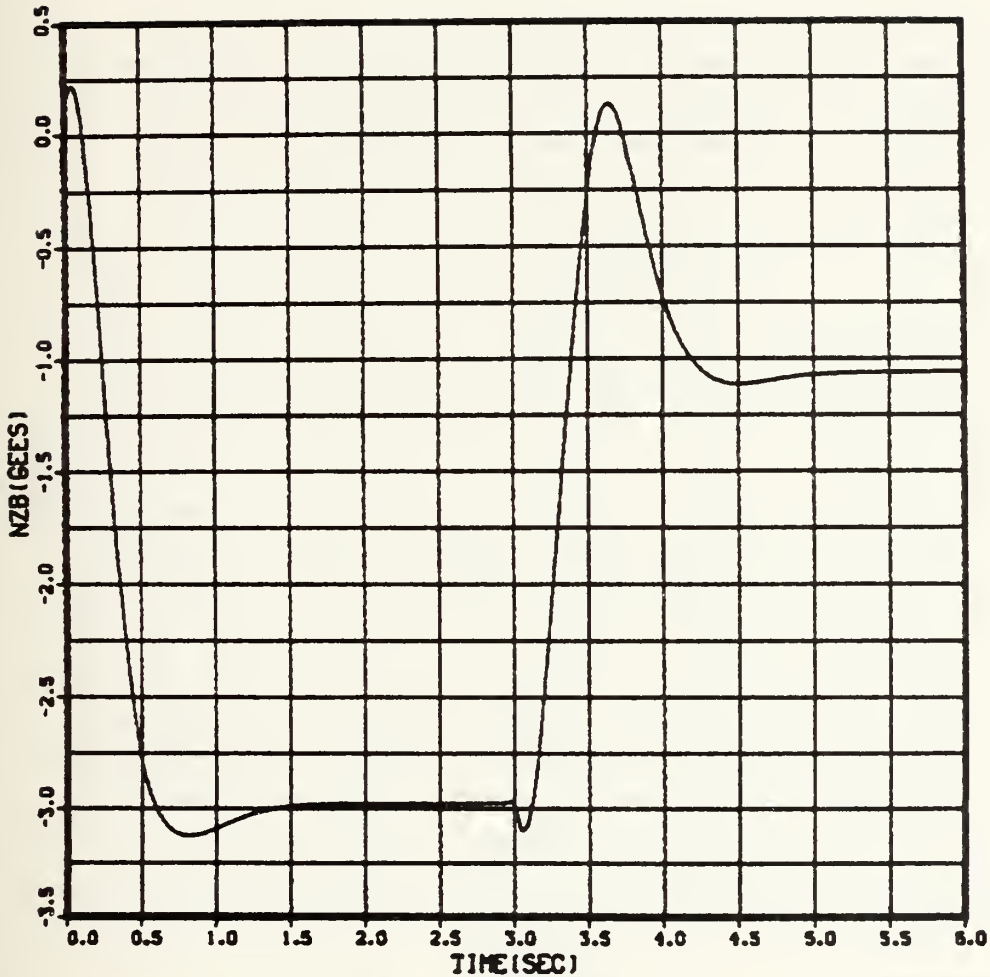


Fig. 4.41 Achieved body-fixed Acceleration (n_{z_B}) vs Time
 (t) CBTT of Circular airframe; Faster responding
 Pitch channel; 2 Gees ($0^\circ, 180^\circ$) $K_{A_2} = -0.0387$

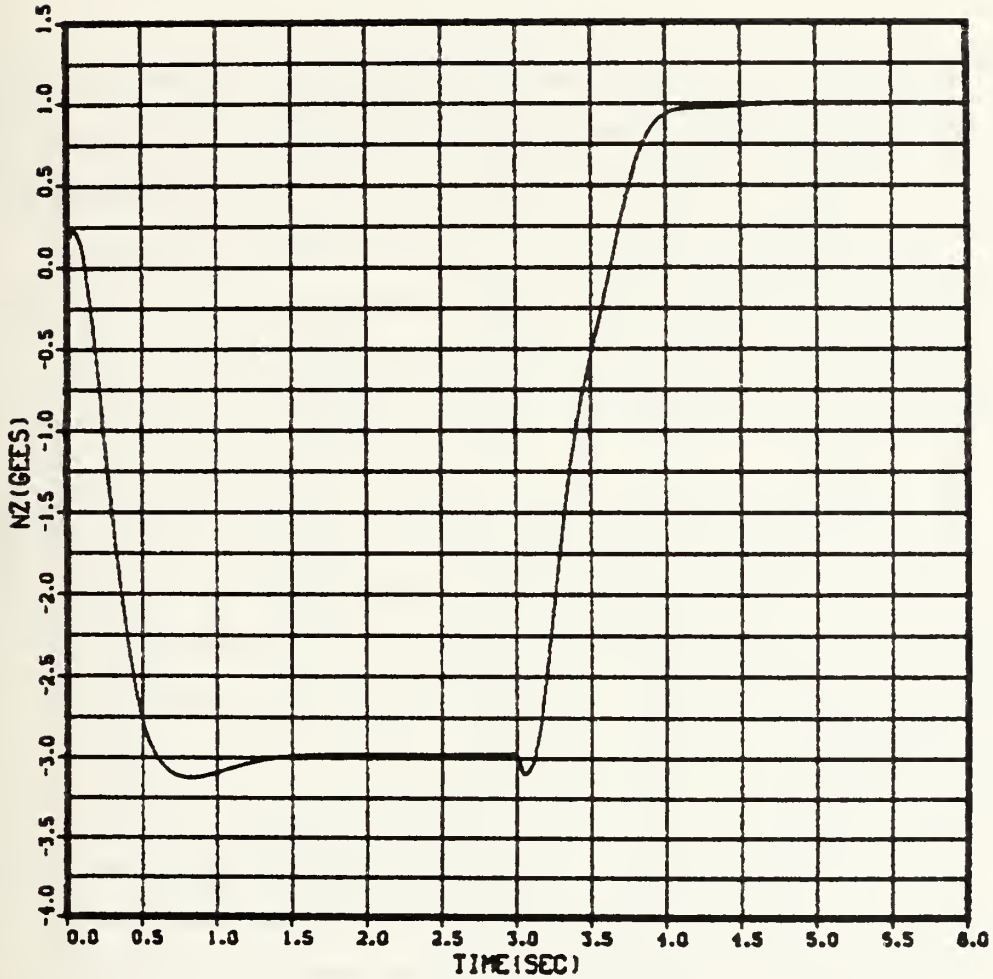


Fig. 4.42 Achieved Inertial Acceleration (n_z) vs Time (t)

CBTT of Circular airframe; Faster Pitch channel; inertial and kinematic cross-coupling into Pitch channel removed; 2 Gees ($0^\circ, 180^\circ$), $K_{A_3} = -0.0387$

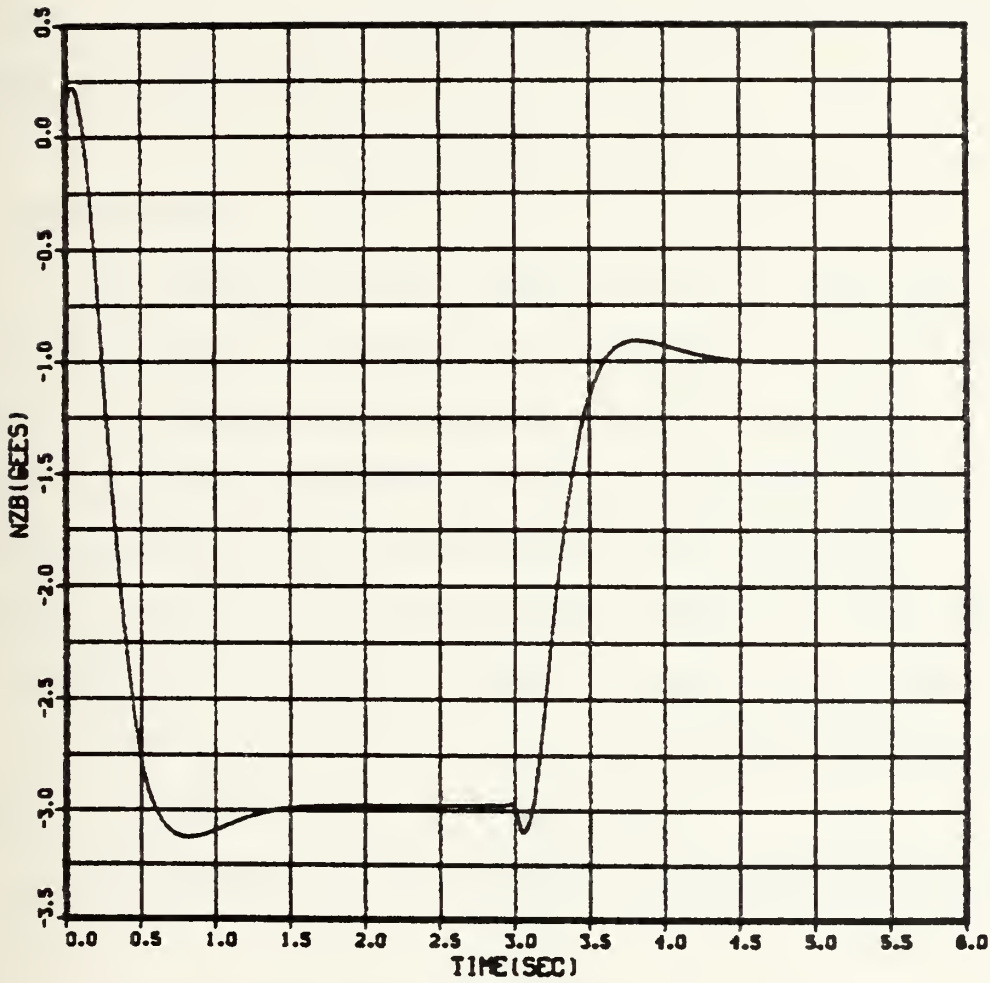


Fig. 4.43 Achieved Body-fixed Acceleration (n_{z_B}) vs Time (t); CBTT of Circular airframe; Faster Pitch channel; inertial and kinematic cross-coupling into Pitch channel removed; 2 Gees ($0^\circ, 180^\circ$), $K_{A_3} = -0.0387$

Table III shows that the achieved maneuver plane acceleration time constant for the second guidance command has decreased.

Figures 4.44 through 4.50 show the time responses for a , β , q , r , δ_p , δ_y , and δ_R when the K_A is equal $K_{A_3} = -0.0387$ and the kinematic and inertial cross-coupling of the Pitch channel have removed.

K. CONCLUSIONS

1. The maneuver plane responses have transients, which may have to be reduced, are caused by inertial and kinematic coupling between pitch and yaw dynamics. Transients cause excessive overshoots and undershoots in achieved maneuver plane acceleration for elliptical airframe (Figure 4.6) and excessive slowdown in the speed of response for circular airframe (Figure 4.28, 4.40).

2. The result of the nonlinear 3-D performance study verify the linear study of chapter III.

3. The results of this study verify the results of [Ref. 2].

Further analysis and conclusion about a , q , r , p and β are discussed in [Ref. 2].

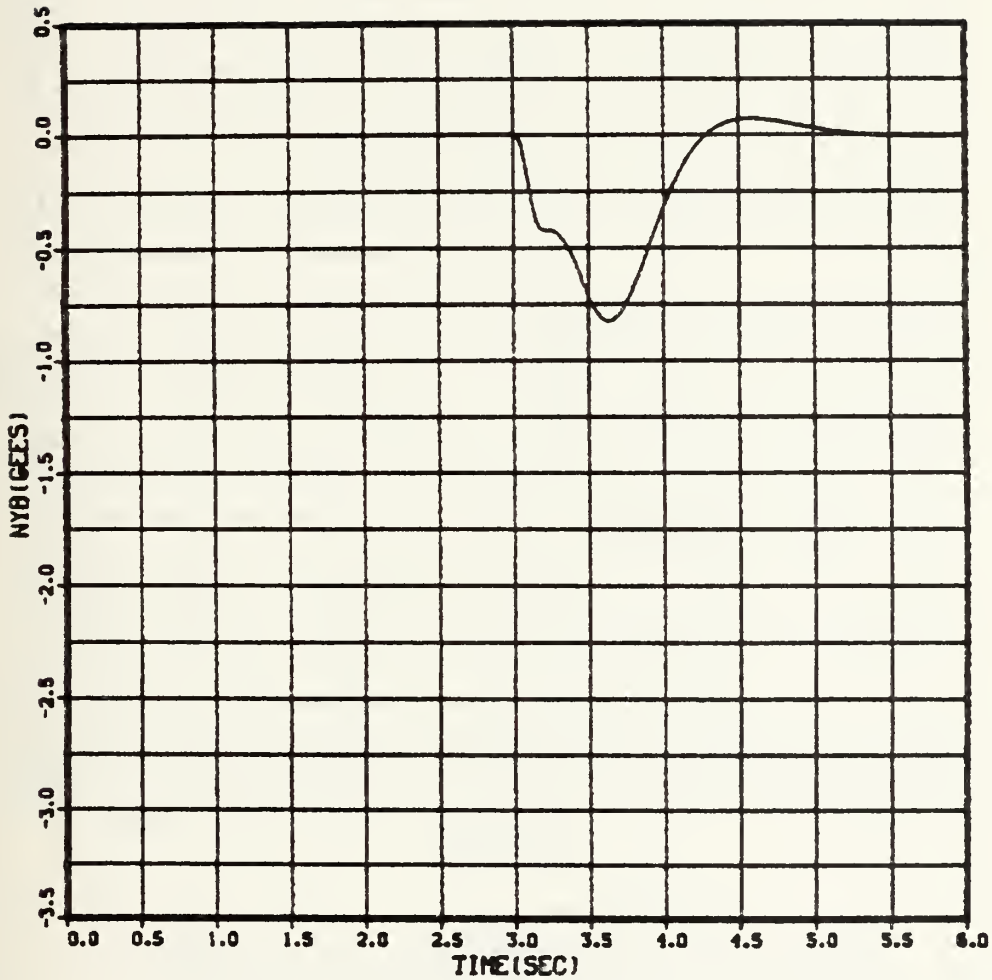


Fig. 4.44 Achieved Body-fixed Acceleration (n_{y_B}) vs Time

(t) CBTT of Circular airframe; Faster pitch channel; inertial and kinematic cross-coupling into pitch channel removed; 2 Gees ($0^\circ, 180^\circ$), $K_{A_3} = -0.0387$

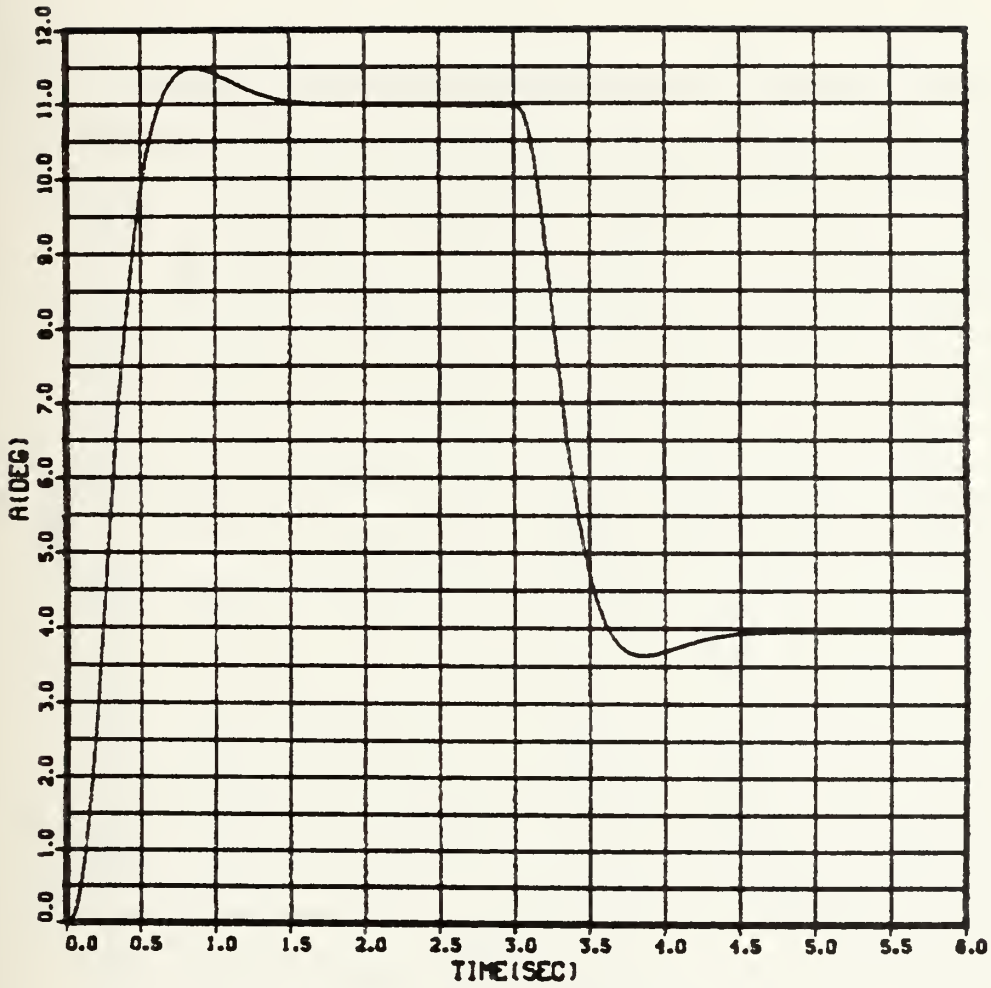


Fig. 4.45 Angle of Attack (α) vs Time (t)
 CBTT of Circular airframe; Faster Pitch
 channel; inertial and kinematic cross-coupling
 into Pitch channel removed; 2 Gees (0° , 180°),
 $K_{A_3} = -0.0387$

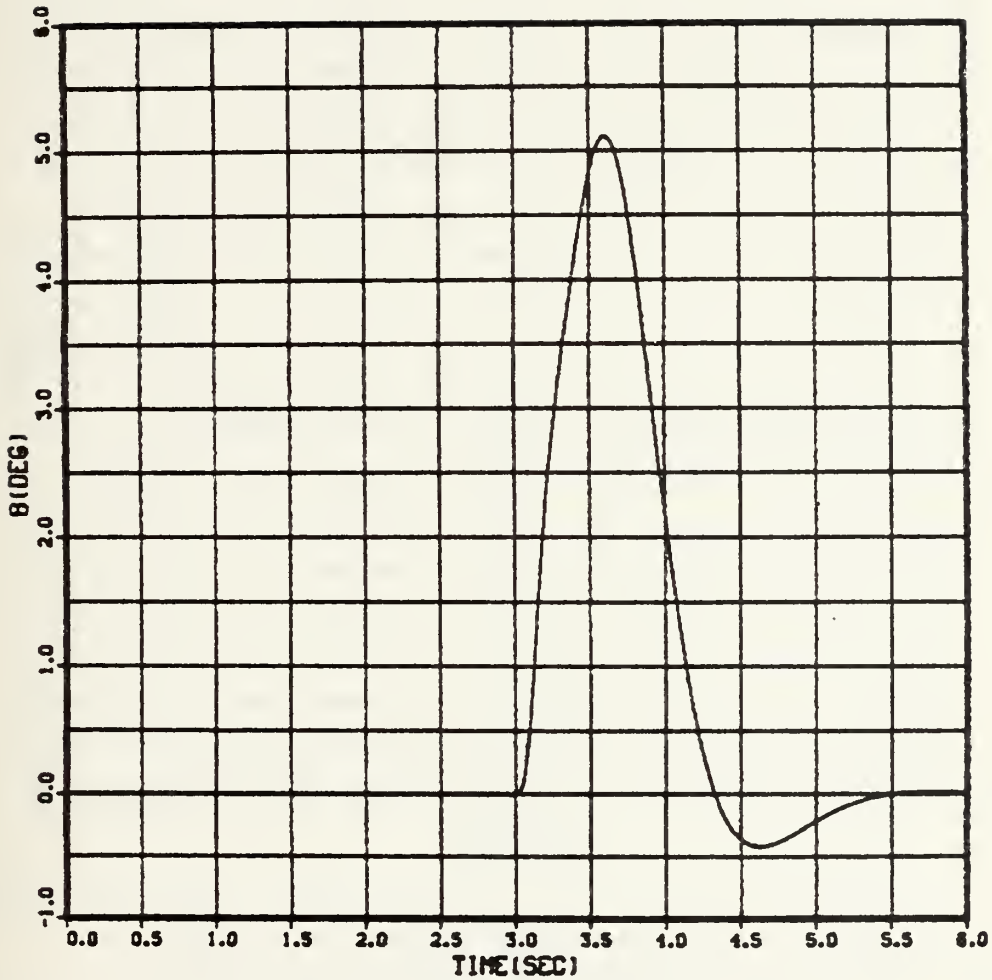


Fig. 4.46 Sideslip angle (β) vs Time (t)
 CBTT of Circular airframe; Faster Pitch
 channel; inertial and kinematic cross-
 coupling into Pitch channel removed;
 2 Gees ($0^\circ, 180^\circ$), $K_{A_3} = -0.0387$

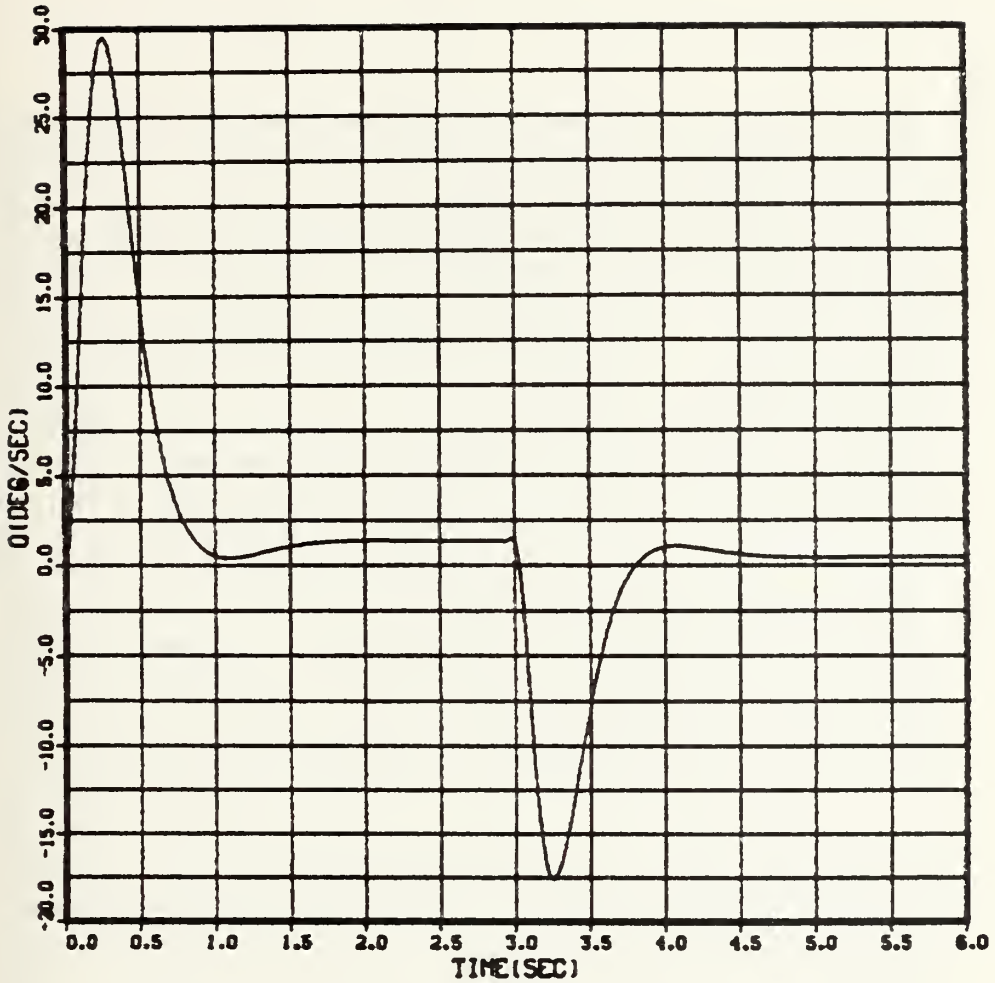


Fig. 4.47 Pitch Body angular rate (q) vs Time (t)
 CBTT of Circular airframe; Faster Pitch
 channel; inertial and kinematic cross-coupling
 into Pitch channel removed; 2 Gees (0° , 180°),
 $K_{A_3} = -0.0387$

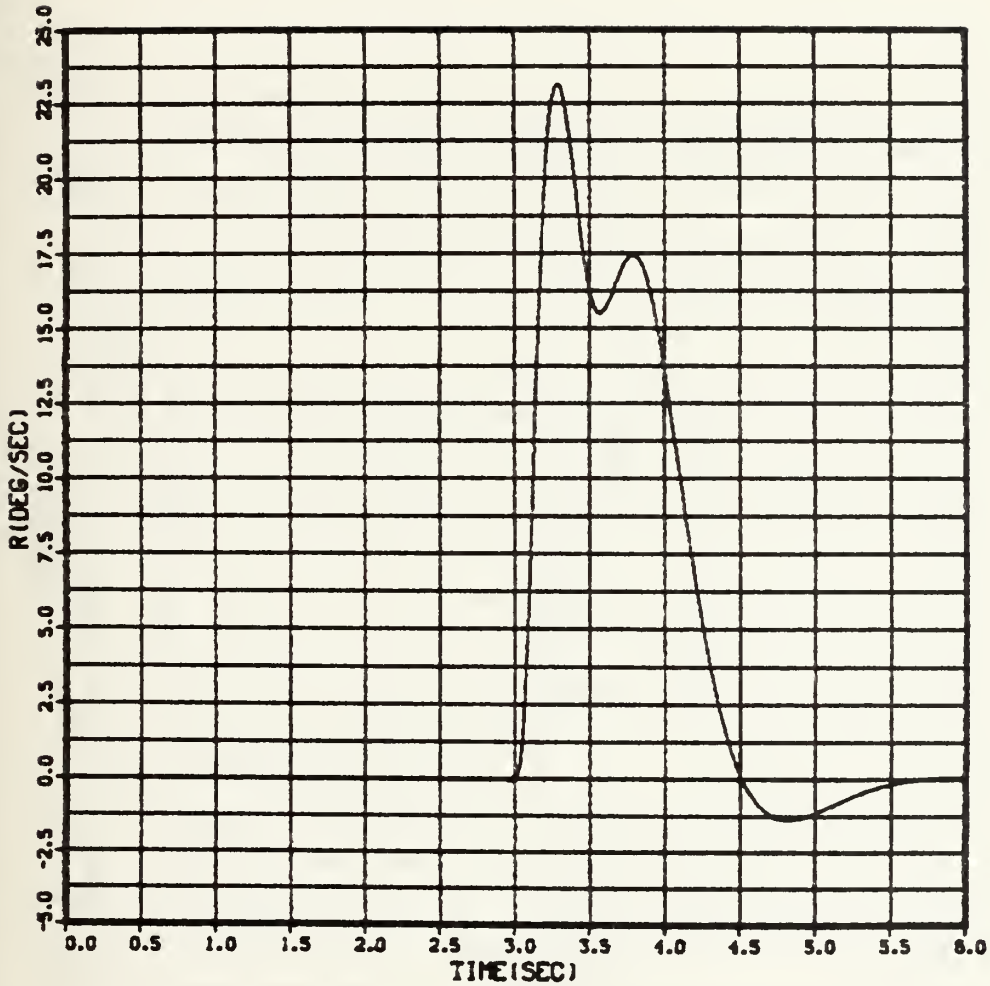


Fig. 4.48 Yaw Body angular rate (r) vs Time (t)
 CBTT of Circular airframe; Faster Pitch
 channel; inertial and kinematic cross-coupling
 into Pitch channel removed; 2 Gees ($0^\circ, 180^\circ$),
 $K_{A_3} = -0.0387$

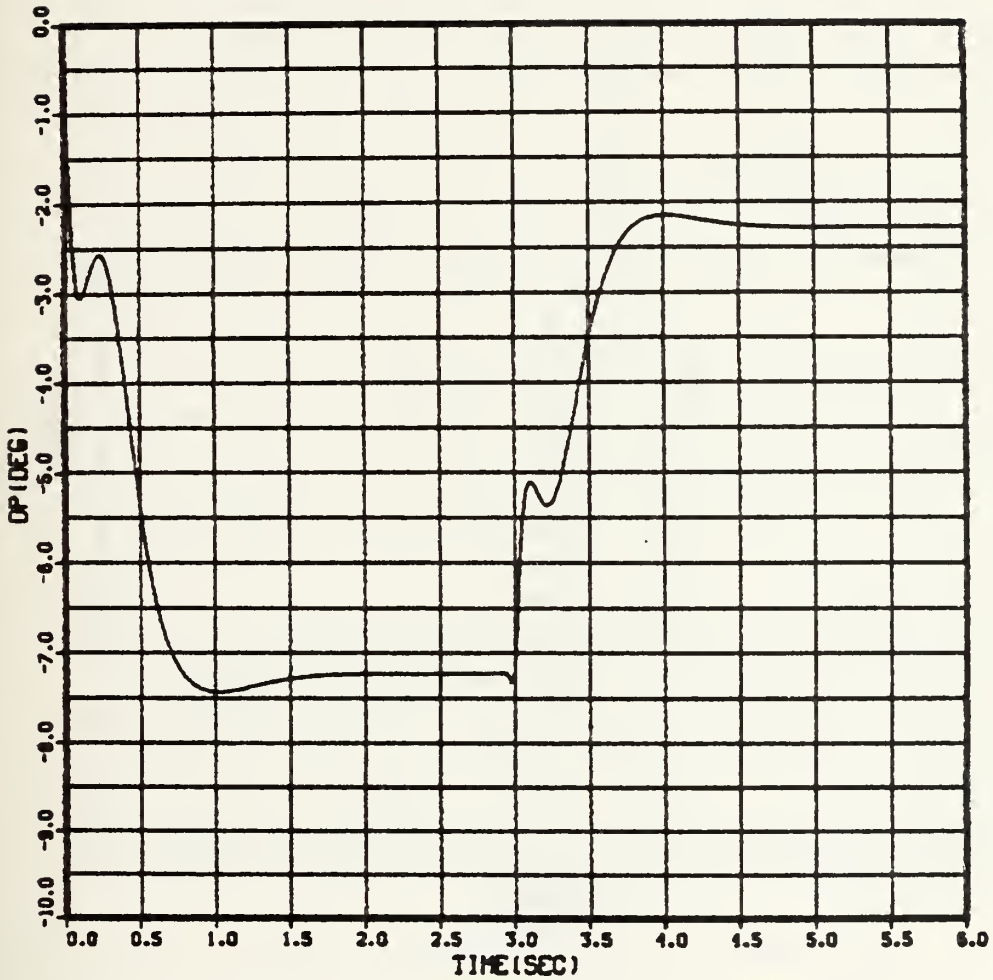


Fig. 4.49 Pitch tail incidence (δ_p) vs Time (t)

CBTT of Circular airframe; Faster Pitch channel; inertial and kinematic cross-coupling into Pitch channel removed; 2 Gees ($0^\circ, 180^\circ$),
 $K_{A_3} = -0.0387$

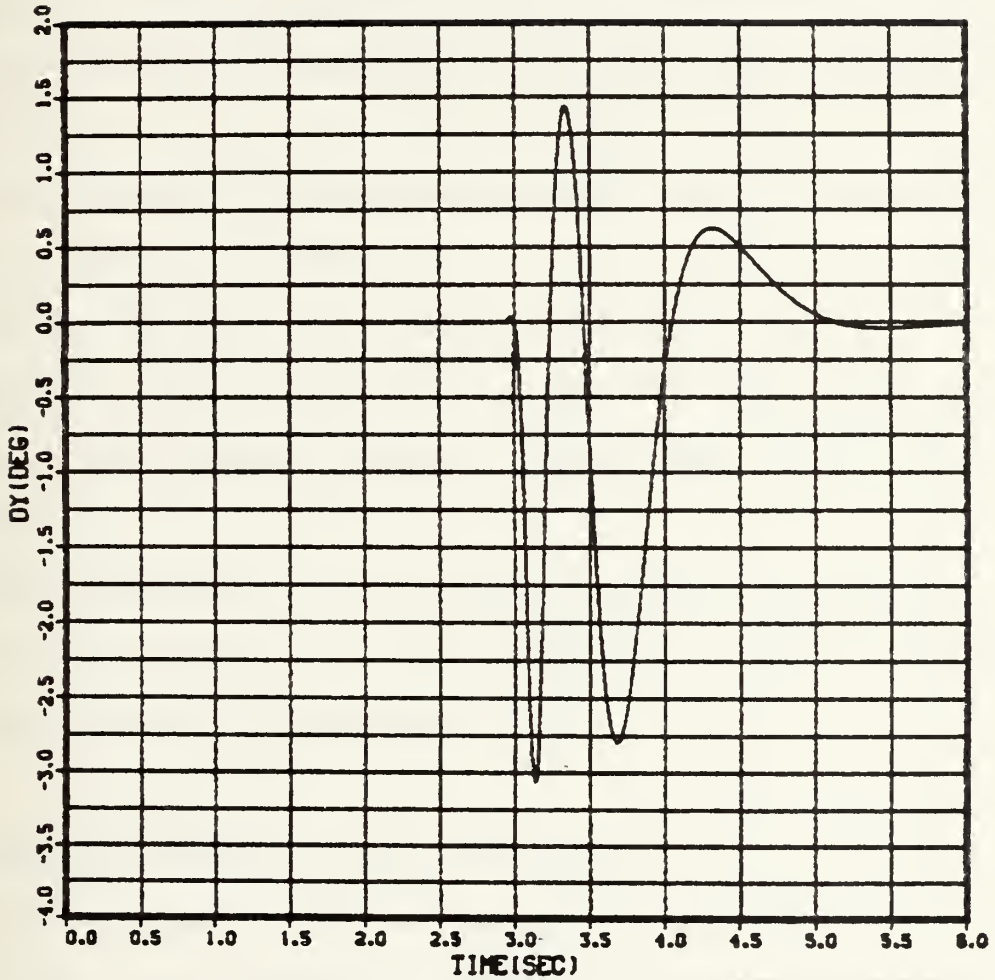


Fig. 4.50 Yaw tail incidence (δ_Y) vs Time (t)

CBTT of Circular airframe; Faster Pitch channel; inertial and kinematic cross-coupling into Pitch channel removed; 2 Gees (0° , 180°),
 $K_{A_3} = -0.0387$

V. MINIMIZATION OF THE KINEMATIC AND INERTIAL
CROSS-COUPLING EFFECTS

A. GENERAL

The nonlinear CBTT autopilot for both airframes, consisted of the uncoupled autopilots discussed in section II, which coupled via inertial, kinematic and aerodynamic couplings.

The effects of the cross-coupling were discussed for both airframes in section IV.

In this section the kinematic, inertial and aerodynamic coupling effects will be summarized. The kinematic and inertial effects in the pitch channel will be analyzed.

The minimization of the above coupling and their effects will be studied, using feedbacks of angle of attack and rate of angle of attacks.

B. CROSS-COUPLING OF CBTT AUTOPILOTS

As discussed in previous sections, the four cross-couplings, between the autopilot channels for both airframes are:

1. Aerodynamic Cross-Coupling

The aerodynamic cross-coupling is the coupling between the Roll and Yaw nonlinear channels, via the

$C_{l_{\beta}}$, $C_{l_{\delta_Y}}$ and $C_{n_{\delta_R}}$ (Figure 4.2). The major effect of the

above coupling in the elliptical airframe response is to decrease the overshoot in the achieved maneuver plane acceleration resulting from the second guidance command, (i.e 2 gee (180°), the other effects on the missile variables were small but in a direction which improves performance (i.e decreased missile body angular rates, less control surface motion, less sideslip variations). In the circular airframe, the effects of the $C_{l_{\beta}}$, $C_{n_{\delta_R}}$ are negligible, the critical coupling coefficient is the $C_{l_{\delta_Y}}$ which effects the stability in the coordination branch, which can be improved by reducing the effect of $C_{l_{\delta_Y}}$ on missile roll angular acceleration. (equation IV.C.2-4)

2. Cross-Coupling Between Roll-Yaw Autopilots for Coordination Motion

This cross-coupling branch, shown in Figure 4.4, has been added between the yaw and roll control laws, in order to provide coordinated motion between these two channels. For purposes of stability the coordinating branch gain K_{YP} was selected for the elliptical airframe $K_{YP} = 1$ and for the circular airframe $K_{YP} = 0.458$. The elliptical airframe is more stable than the circular with the above selected K_{YP} .

3. Kinematic and Inertial Cross-Coupling

The kinematic and inertial cross-coupling exist between the pitch and lateral nonlinear aerodynamic models of the CBTT autopilots. There exist the following cross-coupling paths between pitch and lateral channel.

a. Kinematic cross-coupling path of $(-\beta p)$ into a in the pitch aerodynamic model (Figure 4.3).

b. Kinematic cross-coupling path of (ap) into β in the lateral aerodynamic model (Figure 4.4).

c. Inertial cross-coupling path of (pr) into q in the lateral dynamic model (Figure 4.4).

d. Inertial cross-coupling path of $(-qp)$ into r in the lateral dynamic model (Figure 4.4).

The effects of the inertial and kinematic coupling are the transients in the achieved maneuver plane acceleration response, and have the form of overshoots and undershoots discussed in section III, IV. Transients may also result in a slower maneuver plane acceleration response and are less pronounced at higher acceleration levels.

Coupling transients may be reduced by increasing pitch stability, by decreasing maximum roll rate (section IV), by improving the autopilot coordination technique to minimize sideslip rate β (section IV), by increasing the effects of stabilizing lateral aerodynamic coupling

(negative C_{ℓ_β}), by increasing pitch channel speed of response (section IV) and by increasing the pitch stability C_{m_a} with feedbacks of both angle-of-attack and rate of angle-of-attack for the pitch autopilot.

C. KINEMATIC AND INERTIAL CROSS-COUPLING IN PITCH AUTOPILOT

The kinematic and inertial cross-couplings in the pitch autopilot, are via the pitch angular rate q and the rate of angle-of-attack ($\dot{\alpha}$) (Figure 4.1)).

The equations for q and $\dot{\alpha}$ (figure 27) are:

$$\dot{q} = \frac{57.3 \bar{q} S d}{I_{yy}} \cdot (C_{m\dot{\rho}} \cdot \dot{\rho} + C_{m\alpha} \alpha) + \frac{r \cdot P}{57.3} \quad (\text{V.C.1})$$

$$\dot{\alpha} = q - (P.8/57.3) \quad (\text{V.C.2})$$

where:

$$rP/57.3 = \text{Inertia Cross-Coupling}$$

$$-8P/57.3 = \text{Kinematic Cross-Coupling}$$

Removing C_{m_a} from the parenthesis in (V.C.1) and combining with (V.C.2) to eliminate q , the (V.C.1) results in:

$$\ddot{\alpha} = \frac{57.3 \bar{q} S d}{I_{yy}} \left(C_{m\dot{\rho}} \cdot \dot{\rho} + C_{m\alpha} \alpha \right) + \frac{r \cdot P}{57.3} - \left(\frac{P.8}{57.3} \right)'$$

$$= \frac{57.3 \bar{q} S d C_{m_a}}{I_{yy}} \left(\frac{C_{m\dot{\rho}}}{C_{m_a}} + \alpha \right) + \frac{r \cdot P}{57.3} - \left(\frac{P.8}{57.3} \right)'$$

(V.C.3)

Let:

$$K_1 = \frac{57.3 \bar{q} S d}{I_{yy}} \cdot C_{m\alpha}$$

and

$$K_2 = \frac{C_{m\delta p}}{C_{m\alpha}}$$

Taking the Laplace transform of (V.C.3) and solving for a , the equation becomes:

$$\alpha = \frac{-1}{\frac{-s^2}{K_1} + 1} \cdot \left(\frac{(rP/57.3) - s \cdot \left(\frac{P \cdot \theta}{57.3}\right)}{K_1} + K_2 \cdot \delta p \right) \quad (\text{V.C.4})$$

Increasing the magnitude of C_{m_a} will decrease both K_2 and $1/K_1$ resulting in the reduction of cross-coupling effects on the angle-of-attack (α) and the influence of δp in the a .

In the section III the equation of n_{z_B} was derived:

$$\eta_{z_B} = (-\bar{q}S/W) \cdot (C_{N\delta p} \cdot \delta p + C_{N\alpha} \cdot \alpha) \quad (\text{V.C.5})$$

which involve (a). Therefore, the reduction of inertial and kinematic effects on (a), results in the reduction of the effects in the achieved body-fixed acceleration (n_{z_B}).

In the nonlinear studies the equation for the achieved inertial acceleration was derived as:

$$\eta_z = \eta_{z_B} \cdot \cos \phi + \eta_{y_B} \cdot \sin \phi \quad (\text{V.C.6})$$

It is apparent from the equations (V.C.4), (V.C.5) and (V.C.6), that an increasing of C_{m_a} results in the reduction of kinematic and inertial effects (i.e transients in the response) in the achieved inertial acceleration (n_z), which

it is desired in order to meet the requirement of time constants (τ_1 , τ_2) and percents of overshoots and undershoot, as referred in Appendix C.

D. MINIMIZATION OF THE KINEMATIC AND INERTIAL CROSS-COUPLING EFFECTS IN ELLIPTICAL AIRFRAME

As discussed in the nonlinear studies, using the pitch angular rate q as feedback and under the influence of the inertial and kinematic effects, the achieved inertial acceleration (n_z) for both airframes doesn't meet the requirements of the time constants, overshoot and undershoot, denoted for the linear autopilots, referred to in Appendix C.

Figure 4.5 and Table II show that the achieved inertial acceleration (n_z) for elliptical airframe with feedback the pitch angular rate (q) has overshoot 11.25% and $\tau_1 = 0.48$ sec, $\tau_2 = 0.41$ sec.

Figures 4.40 and Table III illustrate that the achieved inertial acceleration (n_z) for circular airframe, with feedback the (q) has overshoot 5% and $\tau = -0.46$ sec, $\tau_2 = -0.62$ sec. Hence the (n_z) for both airframes is not acceptable.

In order to minimize the inertial and kinematic cross-coupling effect, namely to have smoother transient response of n_z which will meet the requirements of time

constants and overshoot, the magnitude of C_{m_a} was increased, utilizing as feedback the angle-of-attack and its derivative.

In order to increase the magnitude of C_{m_a} the stability augmentation theory was used.

Considered as stability derivative augmentation $\alpha \rightarrow \delta_p$ and $\dot{\alpha} \rightarrow \dot{\delta}_p$ increase the magnitude of M_a and $M_a^{\dot{}}$ directly, as referred in [Ref. 6], the increases in the M_a , is essentially an increase in C_{m_a} and hence the inertial and kinematic effects on the angle-of-attack are reduced.

In the pitch control law (Figure 3.1) a SAS exists using as feedback the pitch angular rate (q). In order to design the SAS with the angle of attack (α) as feedback, the root locus and lead-lag compensation techniques were used.

1. Stability Augmentation System (SAS) With Feedback of the Pitch Angular Rate (q).

In Figure 5.1, the stability augmentation system is shown, with feedback of pitch angular rate q where the transfer function of the q/δ_p for the uncoupled pitch dynamic model, given in section II.C. The closed-loop transfer function of the above SAS is:

$$G(s) = \frac{k \left(\frac{s}{8} + 1 \right) (57.3) (-41.35 \cdot s - 7.7118)}{s \left(\frac{s}{188.4} + 1 \right) (s^2 + 0.1815s - 11.279)} \quad (\text{V.D.1-1})$$

$$1 + \frac{k \left(\frac{s}{8} + 1 \right) (57.3) (-41.35 \cdot s - 7.7118)}{s (57.3) \left(\frac{s}{188.4} + 1 \right) (s^2 + 0.1815s - 11.279)}$$

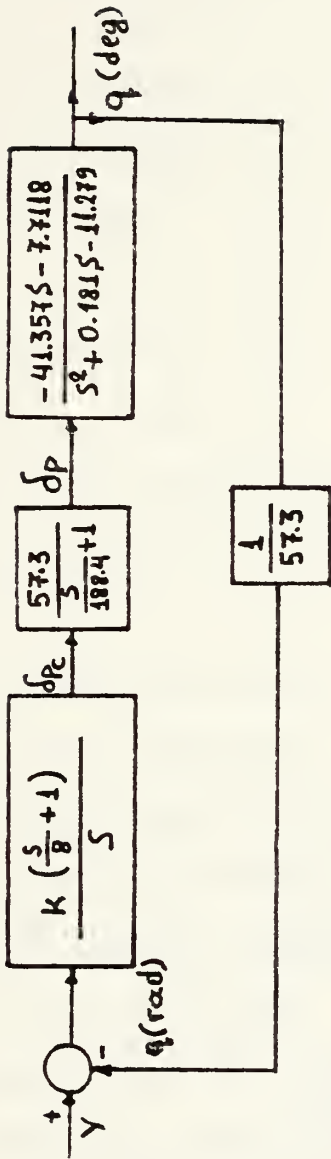


Fig. 5.1 Stability Augmentation System (SAS) with $q/\delta p$ of pitch channel; CBTT of Elliptical Airframe

Manipulating equation V.D.1-1, it results:

$$G(s) = \frac{K(-296.1837s^2 - 2424.363s - 441.8862)}{0.0053s^4 + 1.0009s^3 + 0.121s^2 - 11.28s + K(-5.169s^2 - 42.321s - 7.7118)} \quad (\text{V.D.1-2})$$

The poles and zeros of the SAS are as follows:

- a. $P_1 = -188.43$
- b. $P_2 = -3.45$
- c. $P_3 = 3.269$
- d. $P_4 = 0.0$

and

- e. $Z_1 = -8.0$
- f. $Z_2 = -0.186$

The other two zeros are at infinity.

The root locus of the system is shown in Figure (5.2).

The K was selecting at the value of -3.07 , because at this value, the system has two dominant roots at $P_{1,2} = -9.212 \pm j7.606$ which dominate the response of the system, having the following characteristics:

- a. $\theta = \tan^{-1} \frac{y}{x} = \tan^{-1} \frac{7.606}{8.212} = 42.8^\circ$
- b. $\zeta = \cos \theta = 0.733$
- c. $\omega = \omega_n \sqrt{1 - \zeta^2} = \frac{x}{\zeta} \sqrt{1 - \zeta^2} = 7.613 \text{ (rad/sec)}$
- d. $\omega_n = \frac{x}{\zeta} = 11.203 \text{ (rad/sec)}$

where:

ζ : damping constant

ω : frequency of system

ω_n : natural undamped frequency

REAL AXIS(UNITS PER INCH) = 20.0000
 IMAG AXIS(UNITS PER INCH) = 10.0000
 ROOTLOC/BIPOP ANALYSIS OF CBTT AUTOPILOT
 ELLIPTICAL AIRFRAME

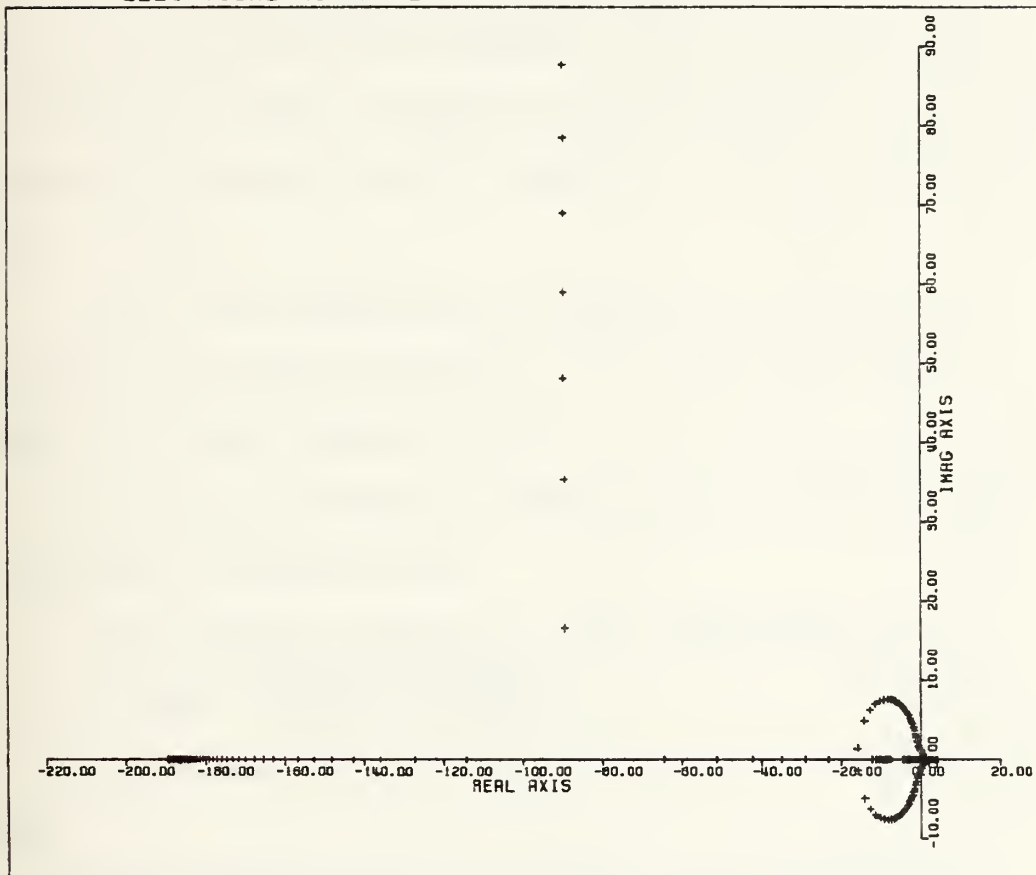


Fig. 5.2 Root locus of SAS with q/δ_p , of pitch channel; CBTT of Elliptical airframe

2. SAS with Feedback of the Angle of Attack (α) and rate of angle of attack ($\dot{\alpha}$)

The SAS with feedback the pitch angular rate q (Figure 5.1) and $K = -3.07$, is stable and the dominant roots gives damping ratio $\zeta = 0.73$ in the response of the system.

To minimize the coupling effects the angle of attack (α) was selected as feedback in the previous SAS. It is desired the SAS to have the same behavior as before, for purposes of stability and response of whole the pitch channel.

Pole zero cancellation technique is used, to obtain the same poles and zeros, as in the case with feedback the pitch angular rate q .

For above purposes, a compensator was used in the SAS, as shown in Figure 5.3.

The transfer function of the compensator is:

$$G(s) = \frac{-41.357 \cdot s - 7.7118}{-0.02 \cdot s - 41.357} \quad (\text{V.D.2-1})$$

The closed loop transfer function of the SAS is as follows:

$$G_T(s) = \frac{\left(\frac{-41.357s - 7.7118}{-0.02s - 41.357} \right) \cdot \left(\frac{K \left(\frac{s}{\delta} + 1 \right)}{s} \right) \cdot \left(\frac{57.3}{\frac{s}{188.4} + 1} \right) \cdot \left(\frac{-0.02s - 41.357}{s^2 + 0.181s - 11.279} \right)}{1 + \left(\frac{1}{57.3} \right) \left(\frac{-41.357s - 7.7118}{-0.02s - 41.357} \right) \cdot \left(\frac{K \left(\frac{s}{\delta} + 1 \right)}{s} \right) \left(\frac{57.3}{\frac{s}{188.4} + 1} \right) \left(\frac{-0.02s - 41.357}{s^2 + 0.181s - 11.279} \right)}$$

(V.D.2-2)

where the transfer function $\frac{a}{\delta p} = \frac{-0.02s - 41.357}{s^2 + 0.181s - 11.279}$ is derived in the section II.C.3.

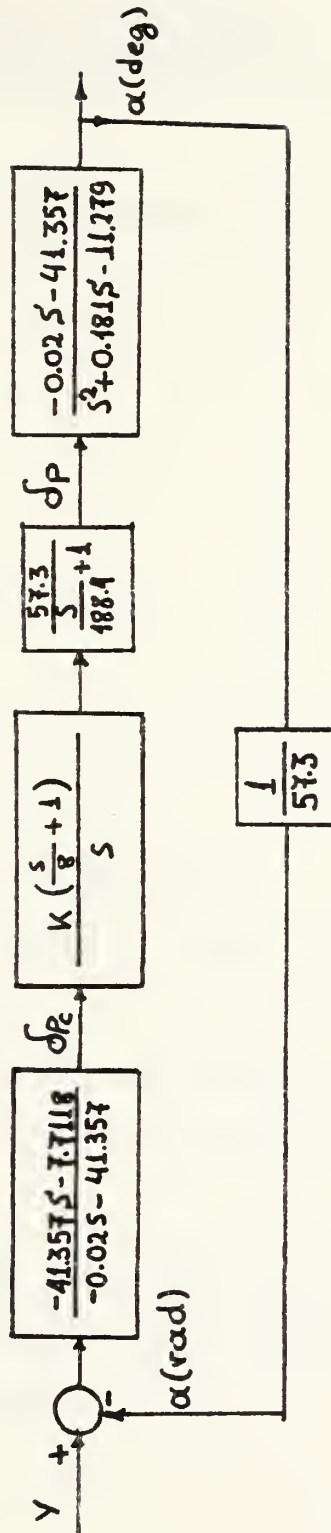


Fig. 5.3 Stability Augmentation System (SAS) with $\alpha/\delta p$, of Pitch channel; CBTT of Elliptical airframe

Rearranging and manipulating the equation

(V.D.2-2), it becomes:

$$G(s) = \frac{K(5.9231s^3 + 1229.981s^2 + 100282.449s + 18275.09)}{-0.0001s^5 + 0.2215s^4 - 41.399s^3 - 4.779s^2 - 466.466s + K(0.1034s^3 + 214.6s^2 + 1750.1s + 318.9)}$$

(V.D.2-3)

The poles and zeros of the system are:

$$P_1 = -1877.931$$

$$P_2 = -207.391$$

$$P_3 = -3.447$$

$$P_4 = -3.271$$

$$P_5 = 0.0$$

and

$$Z_1 = -2067.838$$

$$Z_2 = -8.0$$

$$Z_3 = -0.186$$

The other two zeros are at infinity.

The root locus of the system is shown in figure

5.4.

Selecting the $K = -3.07$, the system has the same dominant roots $P_{1,2} = -8.249 \pm j7.577$, as in section V.D.1.

3. Acceleration Loop

Considering the achieved acceleration loop in the Pitch channel, the modification of the SAS, effects the transmission gain of the above loop.

REAL AXIS (UNITS PER INCH) = 20.0000
 IMAG AXIS (UNITS PER INCH) = 10.0000
 ROOTLOC/BIPOLAR ANALYSIS OF CBTT AUTOPILOT
 ELLIPTICAL AIRFRAME

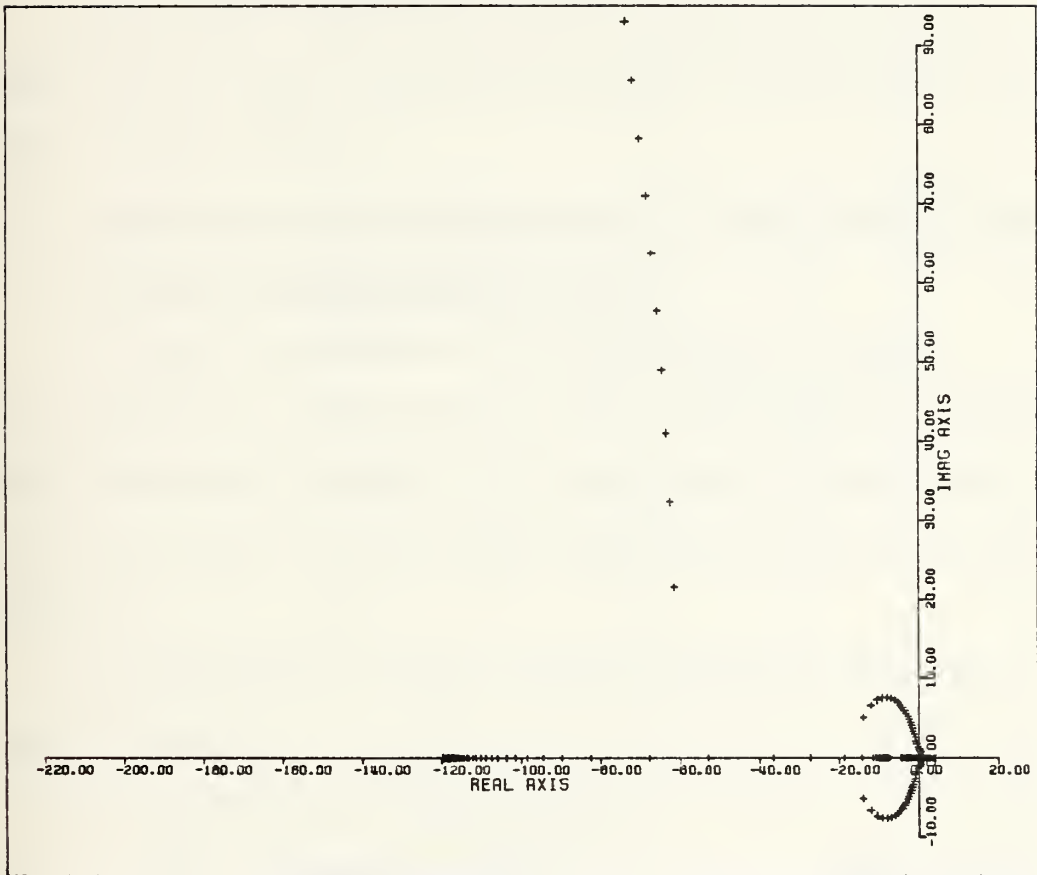


Fig. 5.4 Root locus of SAS with a/δ_p , of Pitch channels;
 CBTT of Elliptical airframe

In order to compensate the effect in the transmission path, a compensator was added as shown in Figure 5.5.

The transfer function of the compensator is the inverse of the V.D.2-1:

$$G_2(s) = \frac{1}{G(s)} = \frac{-0.02 \cdot s - 41.357}{-41.357 \cdot s - 7.7118} \quad (\text{V.D.3-1})$$

Modifying in this way, the transmission path of the acceleration loop, the gain of path, is the same as in the case of par. V.D.1.

4. Measuring of the Minimization in the Kinematic and Inertial Cross-Coupling Effect

In order to measure the minimization a CSMP program (Appendix J) was written using the equations of the nonlinear aerodynamic models, the equations of nonlinear lateral control law and the equations of the modified pitch control law.

The equations of the modified pitch control law are the following:

- a. Acceleration lag network

$$\dot{X} = -150X + 150 \eta_{zB} \quad (\text{II.C.4-2})$$

- b. Acceleration second order compensator (Figure

5.5)

$$\frac{Y}{(1.11\eta_c - X)} = \frac{(-0.008) \cdot (-0.02 \cdot s - 41.357)}{\left(\frac{s}{6} + 1\right) (-41.357 \cdot s - 7.7118)} \quad (\text{V.D.4-1})$$

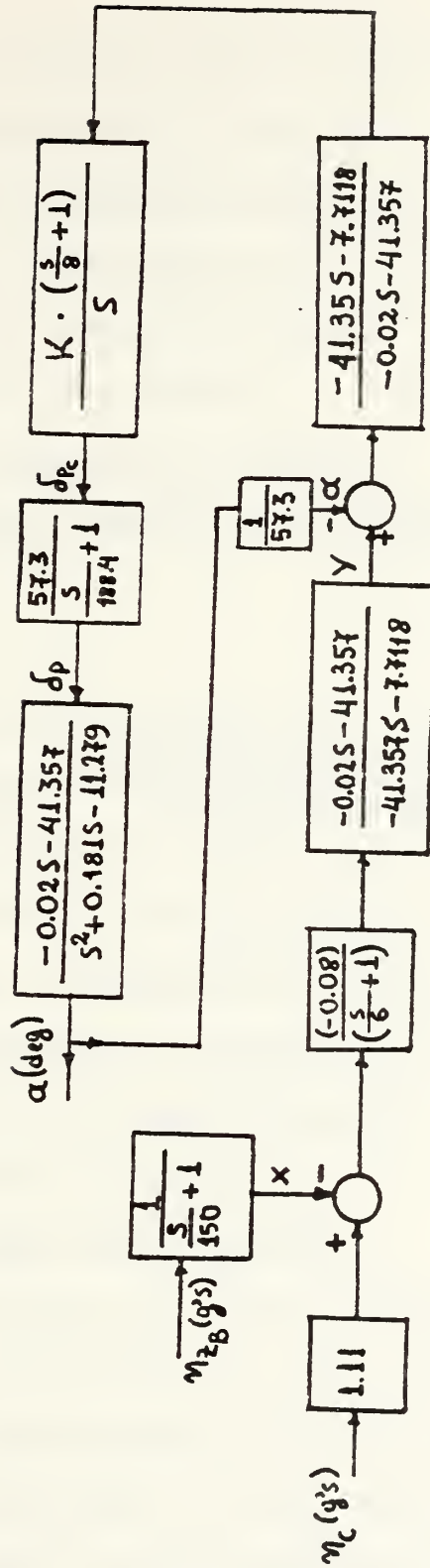


Fig. 5.5 Modified Nonlinear Pitch autopilot; CBTT of Elliptical airframe

Utilizing inverse Laplace transformation and rearranging the above equation, one has:

$$\ddot{Y} + 6.1867 \dot{Y} + 1.1188 Y = -0.000232 (1.11 \eta_c - X) - 0.4786 \cdot (1.11 \eta_c - X) \quad (\text{V.D.4-2})$$

Using space representation of a system, in which the forcing function involves derivative

[Ref. 5, pp 675-678], one obtains:

$$\dot{W}_1 = W_2 - 0.0002575 \cdot \eta_c + 0.000232 \cdot X \quad (\text{V.D.4-3})$$

$$\dot{W}_2 = -1.11887 W_1 - 6.1867 \cdot W_2 - 0.5312 \cdot \eta_c + 0.4786 \cdot X \quad (\text{V.D.4-4})$$

$$Y = W_1 \quad (\text{V.D.4-5})$$

c. Compensator of Actuator

$$\frac{\delta P_c}{(Y - \alpha | 57.3)} = \frac{K \left(\frac{s}{8} + 1 \right) (-41.3575 - 7.7118)}{s (-0.025 - 41.357)} \quad (\text{V.D.4-5a})$$

Using the method for state representation and rearranging the equation V.D.4-5 yields:

$$\delta \dot{P}_1 = \delta P_2 + K \cdot 532.382 \times 10^{-3} \cdot (Y - \alpha | 57.3) \quad (\text{V.D.4-6})$$

$$\delta \dot{P}_2 = -2067.85 \delta P_2 - K \cdot 1100.886 \times 10^6 (Y - \alpha | 57.3) \quad (\text{V.D.4-7})$$

$$\delta P_c = \delta P_1 - K \cdot 258.48 (Y - \alpha | 57.3) \quad (\text{V.D.4-8})$$

d. Equation of Actuator

$$\delta \dot{P} = -188.4 \cdot \delta P + 10795.3 \cdot \delta P_c \quad (\text{IV.B.1-4})$$

Selecting $K=3.07$, for the compensator of SAS, with feedback (a) the time constant τ_1 (i.e time constant of achieved maneuver acceleration due to the first command) is 0.45 sec, the time constant τ_2 (for second command) is 0.41 sec and the undershoot is 20.73 percent as shown in figure 5.6.

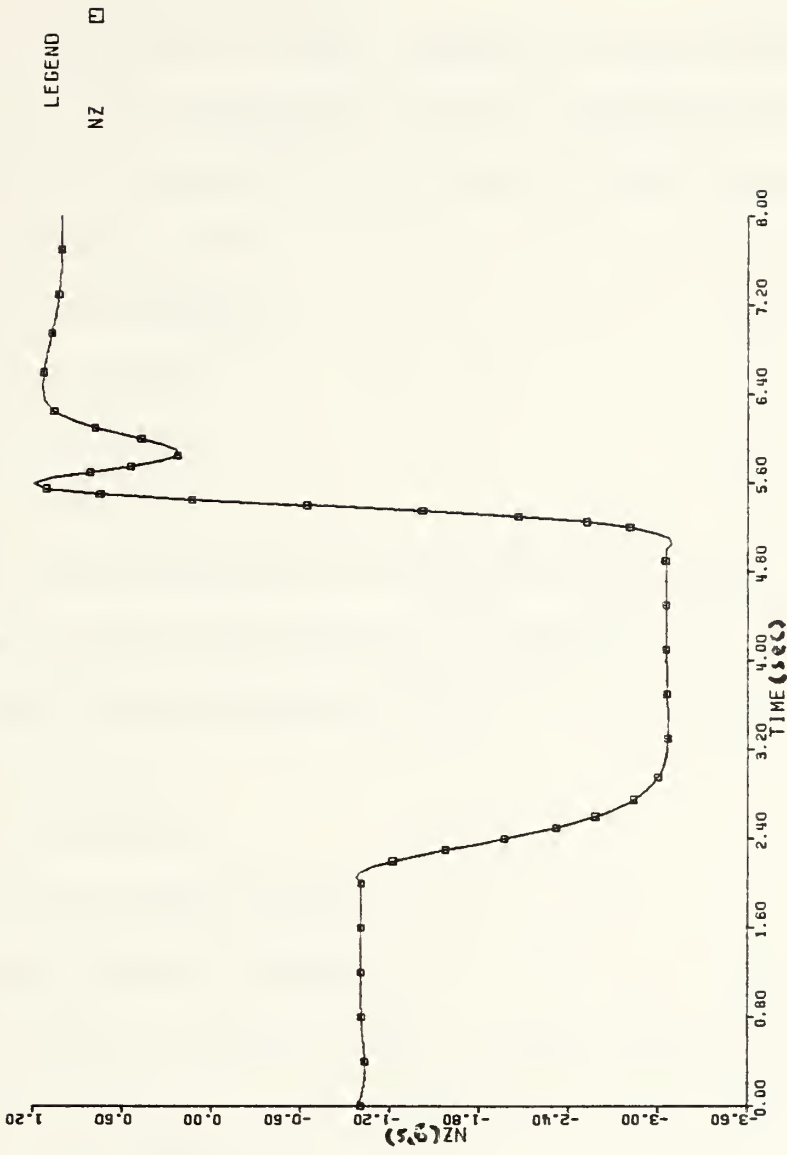


Fig. 5.6 Achieved Inertial Acceleration (n_z) vs Time (t)
 Modified Pitch channel; CBTT of Elliptical
 airframe; 2° ($0^\circ, 180^\circ$), $K = -3.07$

The above response of the inertial achieved maneuver acceleration does not have, smooth transient, because of the large undershoot.

Due to the above reason, another K was selected equal to -19.37, for minimization of the coupling effects.

With this selected K the system has the following poles, shown in figure 5.4

$$P_{1,2} = -98 \pm j96.239$$

$$P_3 = -1879.06$$

$$P_4 = -8.596$$

$$P_5 = -0.189$$

With the same zeros as section V.D.2, the dominant poles of the system are $P_{1,2}$ and the characteristics of the response are:

a. $\theta = 44.24$

b. $\zeta = 0.716$

c. $\omega = 93.775 \text{ rad/sec}$

d. $\omega_n = 134.412 \text{ rad/sec}$

It is shown in known (Ref. 6) that the ω_n can be expressed as:

$$\omega_n = \sqrt{\frac{M\alpha}{I}}$$

(V.D.4-9)

and

$$M_{\alpha} = C_{m_{\alpha}} \cdot \frac{\gamma}{2} \cdot P \cdot M^2 \cdot A \quad (\text{V.D.4-10})$$

where:

γ : specific weight of air 1.4

I: moment of inertia

P: Local pressure

M: Mach number

A: Area

Comparing the $\omega_n = 134.412$ for the $K = -19.37$, it is apparent that it is much larger than the $\omega_n = 11.203$ for $K = -3.07$ and hence according to the equations V.D.4-9 and V.D.4-10, the C_{m_a} increases essentially, resulting in minimization of kinematic and inertial cross coupling effects.

Figure 5.7 shows, that with $K = -19.37$ and feedback in SAS the (a), the achieved inertial maneuver acceleration has $\tau_1 = -.49$ sec, $\tau_2 = -.38$ sec and overshoot about 0%.

The above analysis illustrates that the selection of $K = -19.37$, instead of $K = -3.07$, keeps the damping ratio about constant $\zeta = 0.71$ ($\zeta = 0.73$ for $K = -3.07$) and increases the ω_n , which essentially increases the C_{m_a} , resulting in very smooth response of the achieved maneuver acceleration.

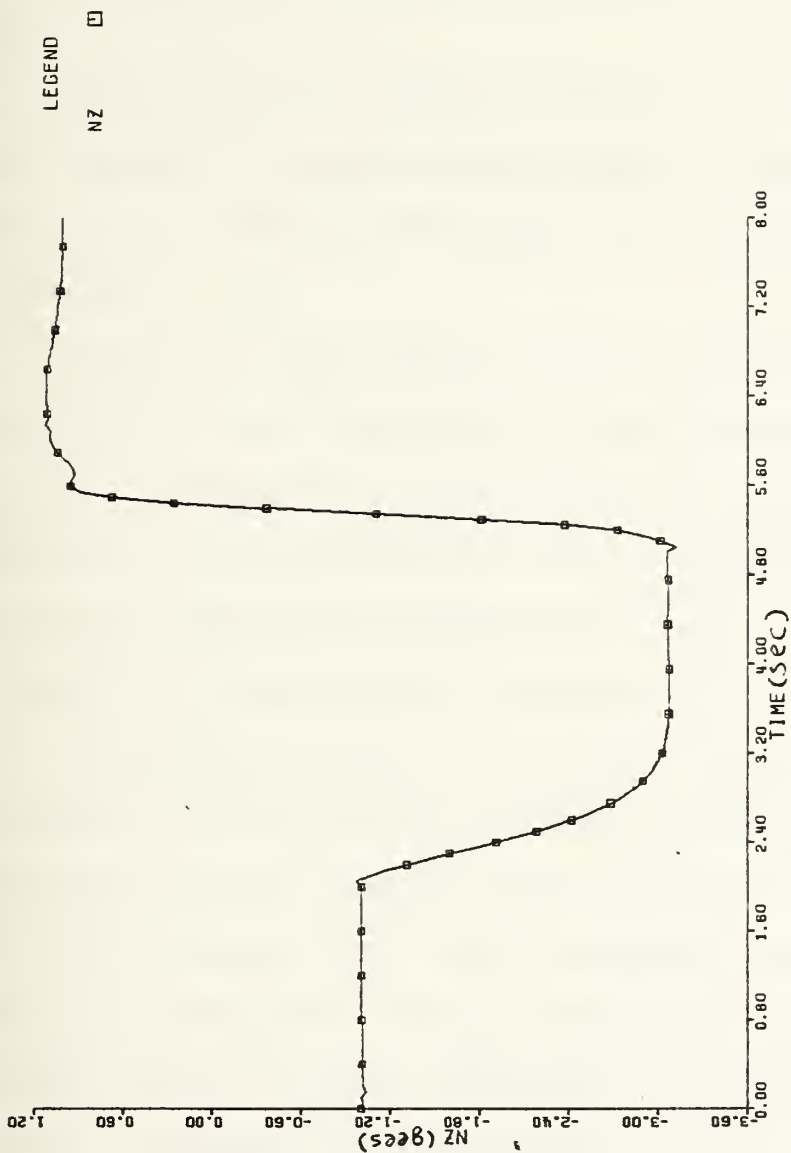


Fig. 5.7 Achieved Inertial Acceleration (n_z) vs Time (t)

Modified Pitch channel; CBTT of Elliptical
 airframe; 2° ($0^\circ, 180^\circ$), $K = -19.37$

Using the same particular compensators in the Pitch channel shown in Figure 5.5 and feedback the rate of angle of attack ($\dot{\alpha}$), the Pitch channel becomes uncontrollable for both selection of $K = -3.07$ and $K = -19.37$, because the pitch tail incidence exceeds the limits of $\pm 10^\circ$.

Also, selecting the $K = -19.37$ in SAS of Figure 5.1 with feedback the pitch angular rate q the Pitch channel becomes uncontrollable again, due to the exceeding of the limits in δ_p .

Therefore, for minimization of the kinematic and inertial effects (i.e improving of the transient response of the achieved maneuver acceleration) for this particular airframe and flight conditions, the C_{m_a} was increased, using the aforementioned compensators in the pitch control law (Figure 5.5) and feedback the angle-of-attack (α).

Comparing the achieved inertial acceleration (n_z) with feedback (q) in the Pitch channel (Figure 4.41) and the achieved inertial acceleration (n_z) with feedback (α) and $K = -19.37$ (Figure 5.7), it is concluded that for these particular airframes and flight conditions the feedback of angle-of-attack (α) is more desirable, than the feedback of (q) and ($\dot{\alpha}$), because in the achieved inertial acceleration has been reduced the kinematic and inertial effects, meeting with this way the requirement of the time constants and overshoot, denoted in the linear studies.

E. MINIMIZATION OF KINEMATIC AND INERTIAL COUPLING IN ELLIPTICAL AIRFRAME

Making a comparison in Figure 5.8, which shows the kinematic cross-coupling $(-p\beta)$ into $\dot{\alpha}$, in the pitch channel with feedback pitch angular rate (q) and Figure 5.10 which shows the $-p\beta$ in the modified pitch channel (Figure 5-5) with feedback the angle-of-attack, it is concluded (Table IV) that the kinematic coupling is increased from $(-0^{\circ}.988-5^{\circ}.877)$ to $(-2^{\circ}.124-7^{\circ}.383)$, when the kinematic coupling effects are reduced by the modified pitch channel.

Figure 5.9 shows the inertial coupling (pr) into \dot{q} in the nonlinear Pitch channel, with feedback the pitch angular rate (q) .

Figure 5.11 shows the inertial coupling for the modified Pitch autopilot with feedback the angle of attack (a) (Figure 5.5).

Comparing the above figures, it is concluded (Table IV) that the inertial coupling is increased from $(-1^{\circ}.692-168^{\circ}.317)$ to $(-20^{\circ}.373 - 181^{\circ}.415)$, when the inertial coupling effects are reduced by the modified pitch channel discussed in previous section.

Hence, the minimization of the kinematic and inertial effect does not mean necessarily minimization of the cross-couplings themselves.

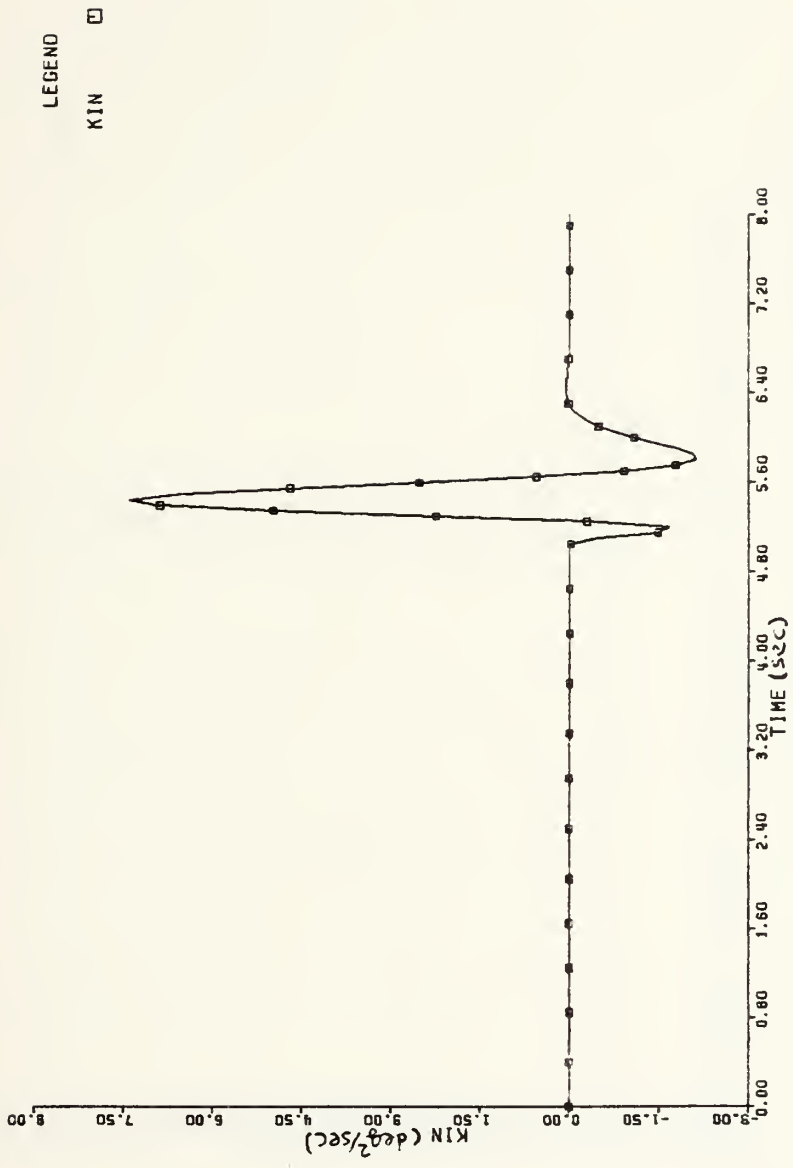


Fig. 5.8 Kinematic Coupling (-P.β) vs Time (t)
CBTT of Elliptical airframe; 2(0°, 180°)

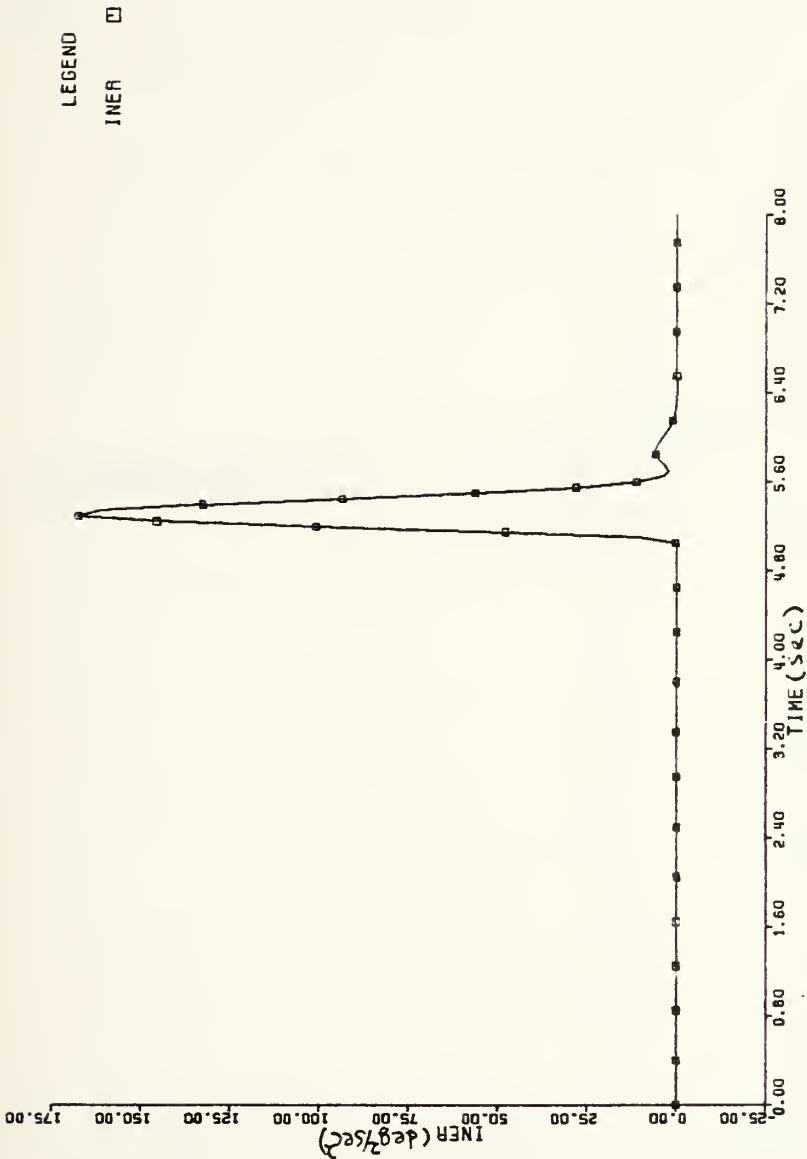
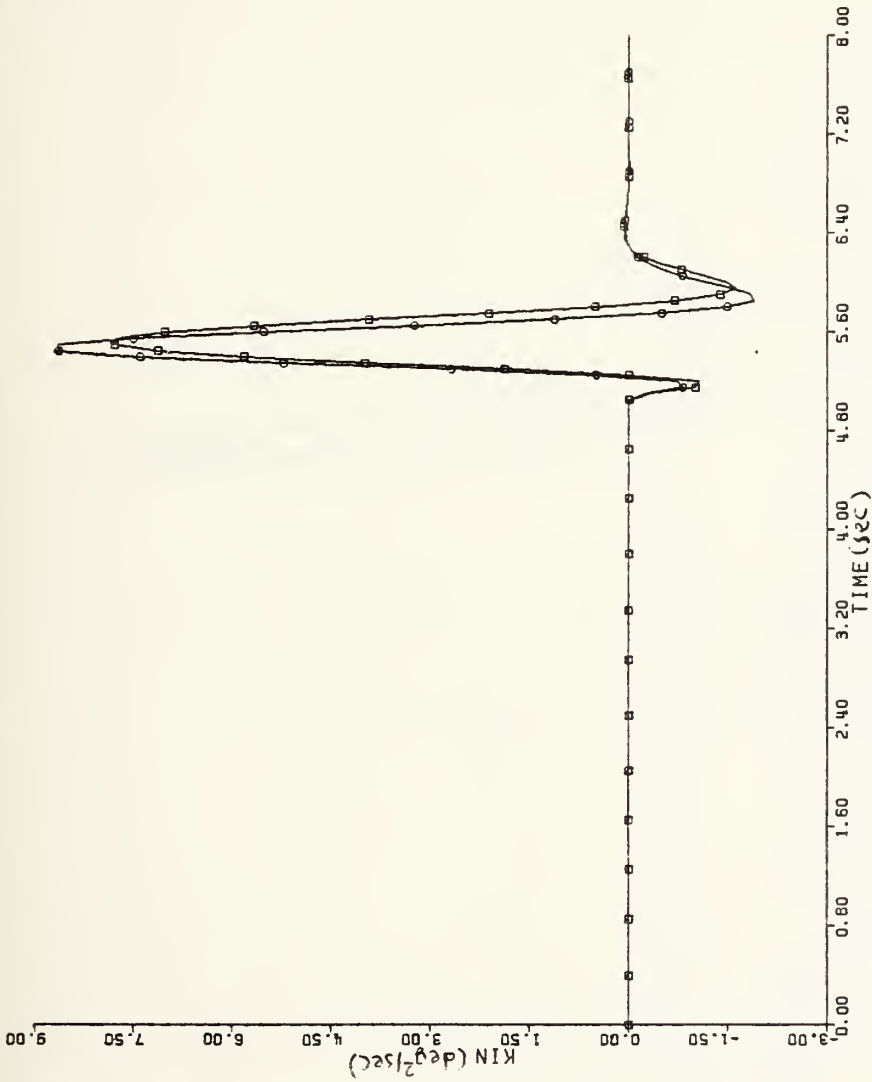


Fig. 5.9 Inertial Coupling (P.r) vs Time (t)
CBTT of Elliptical airframe; 2(0°, 180°)



LEGEND
 KIN □ K1 3.0700
 ○ K1 19.4800

Fig. 5.10 Kinematic Coupling (-P.β) vs Time (t)
 CBTT of Elliptical airframe; Modified
 Pitch channel for minimization of coupling
 effect

LEGEND

INER	□	K1	3.0700
	○	K1	19.4800

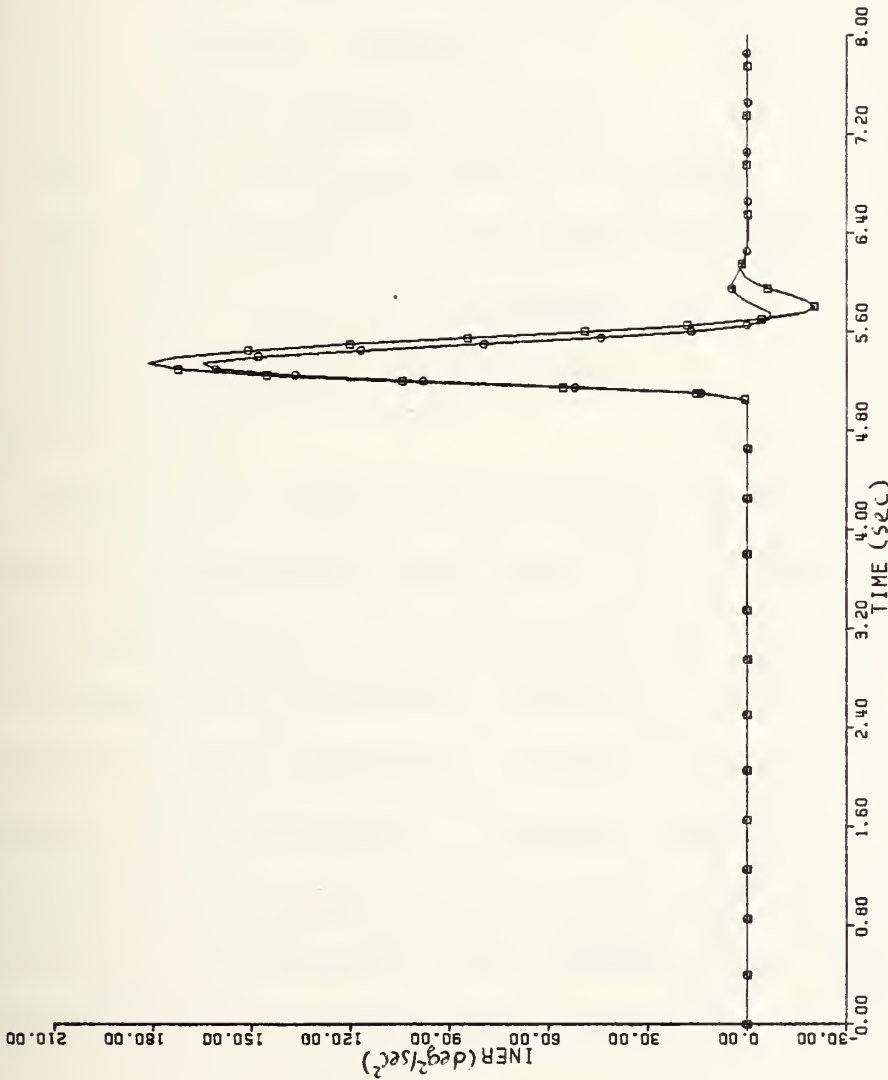


Fig. 5.11 Inertial Coupling (P.R) vs Time (t)
 CBTT of Elliptical airframe;
 Modified Pitch channel for minimization
 of the coupling effect

For minimization of the kinematic and inertial cross coupling, the same modified nonlinear pitch control law was used as that of section IV.D (Figure 5.5), except the acceleration compensator which was removed from the transmission path of the n_c as shown in Figure 5.12.

For purposes of analysis a CSMP program (Appendix J) was written, using the following equation for the nonlinear pitch control law and the same equation for lateral control law and dynamic models, as in section IV.B and IV.C.

$$\dot{X} = -150X + 150 \cdot \eta_{zB} \quad (\text{IV.B.1-1})$$

$$\dot{Y} = -6 \cdot Y - 0.5305 \eta_c + 0.48 \cdot X \quad (\text{IV.B.1-2})$$

$$\delta \dot{P}_1 = \delta P_2 + K \cdot 532.382 \times 10^3 \cdot (Y - \alpha/57.3) \quad (\text{V.D.4-6})$$

$$\delta \dot{P}_2 = -2067.85 \cdot \delta P_2 - K \cdot 1100.886 \times 10^6 (Y - \alpha/57.3) \quad (\text{V.D.4-7})$$

$$\delta P_c = \delta P_1 - K \cdot 258.48 (Y - \alpha/57.3) \quad (\text{V.D.4-8})$$

$$\delta \dot{P} = -188.4 \cdot \delta P + 10795.3 \cdot \delta P_c \quad (\text{IV.B.1-4})$$

where $K = 19.37$.

Figure 5.13 shows the minimized kinematic coupling and Figure 5.14 shows the minimized inertial coupling. Figures 5.13, 5.14 and table IV illustrate that the minimization of the kinematic and inertial coupling is 264% and 195.26% respectively from its values in the nonlinear CBTT autopilot for elliptical airframe. Figure 5.15 shows the achieved inertial acceleration (n_z), with the Pitch channel modified for minimization of kinematic and inertial coupling (Figure 5.12). From this figure it is concluded

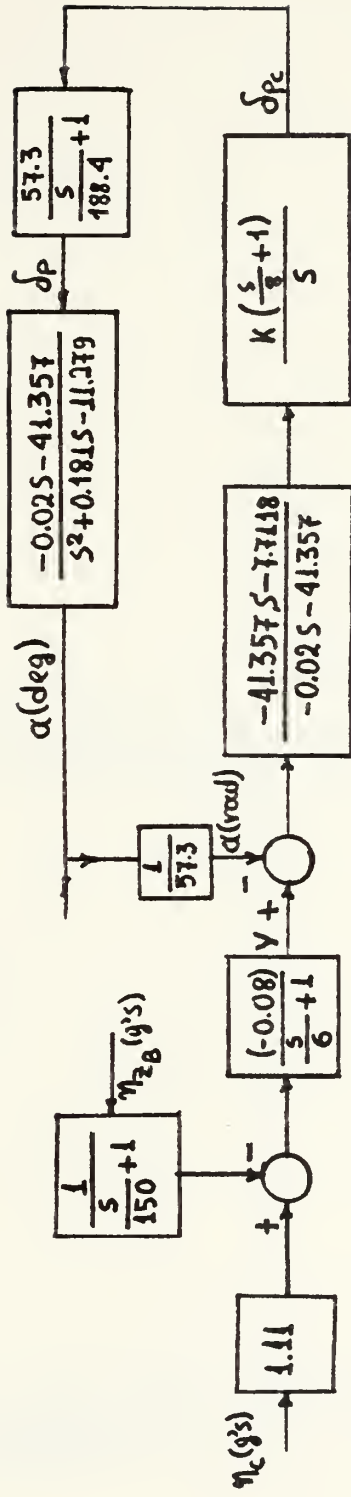


Fig. 5.12 Modified pitch control law for minimization of kinematic and inertial cross-coupling; CBTT of Elliptical airframe

LEGEND

KIN □

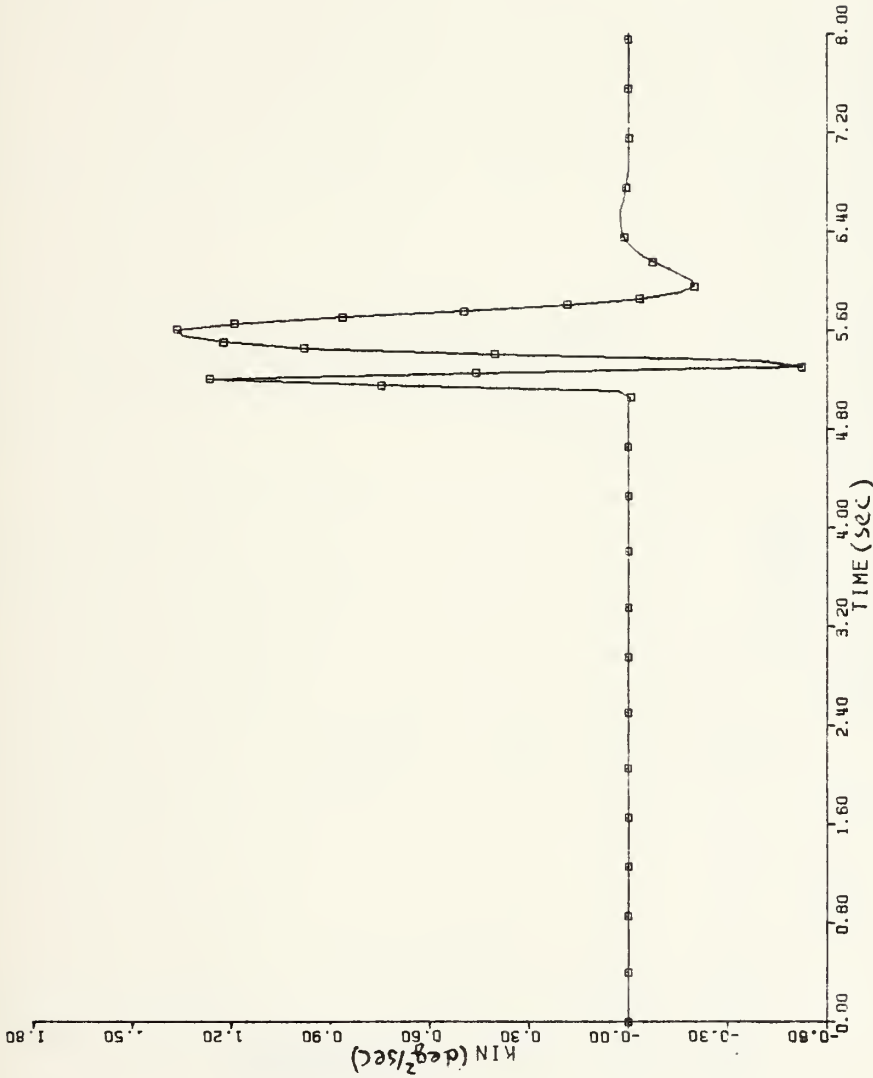


Fig. 5.13 Kinematic coupling (-P.β) vs Time (t)
Modified Pitch channel for minimization
of kinematic coupling; CBTT of Elliptical
airframe; 2 (0°, 180°)

LEGEND

INER □

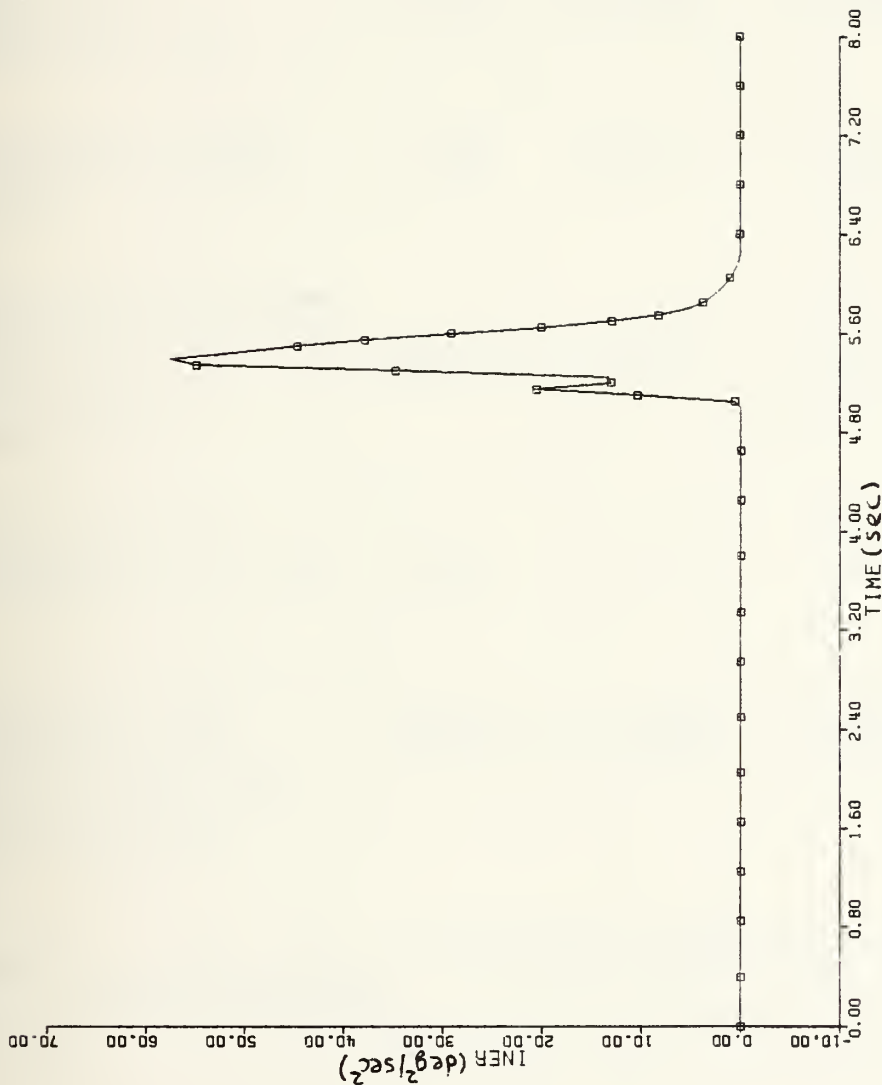


Fig. 5.14 Inertial coupling (P.r) Vs Time (t)
Modified Pitch channel for minimization
of inertial coupling; CBTT of Elliptical
airframe

TABLE IVKINEMATIC AND INERTIAL CROSS-COUPLING FOR
ELLIPTICAL AIRFRAME

CONDITION	INERTIAL (deg/sec ²)		KINEMATIC (deg/sec ²)	
	MIN	MAX	MIN	MAX
Elliptical airframe with cross- coupling (section IV.C)	-1.692	168.847	-0.9881	5.877
Elliptical ideal airframe (section IV.E)	-1.698	167.37	-2.124	7.383
Elliptical airframe with modified Pitch autopilot K = -19.37 (section V.1)	-20.373	181.415	-1.88	8.644
Modified Pitch autopilot K = -30.4 (section V.D.)	-7.263	169.371	-1.956	8.711
Modified Pitch autopilot for minimization of cross couplings (section V.E) K = -19.37	-0.0577	57.5322	-0.523	1.363

Note: K is the gain of the added compensator in SAS of the Pitch autopilot.

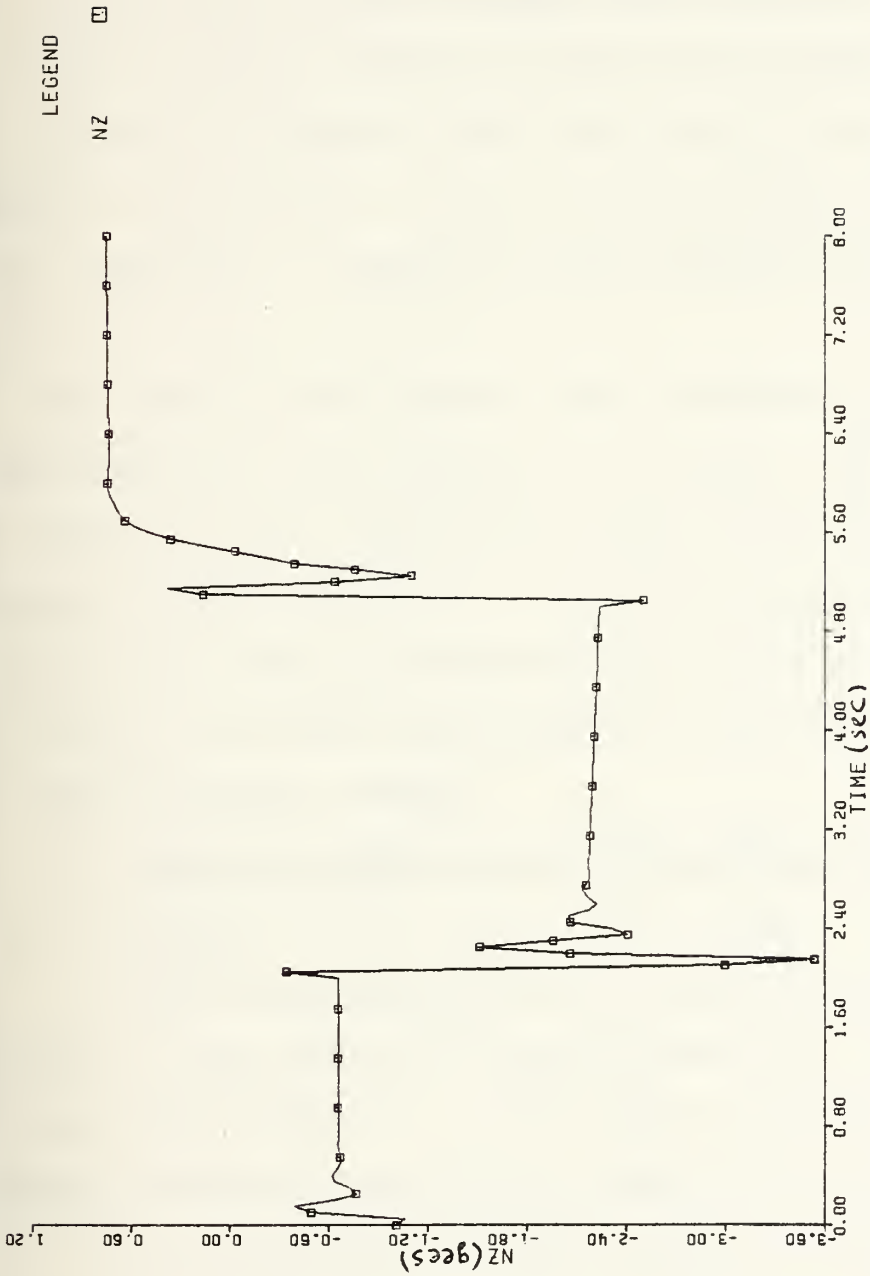


Fig. 5.15 Achieved Inertial Acceleration (n_z) vs Time (t)
 Modified Pitch channel for minimization of
 couplings; CBTT of Elliptical airframe

that the kinematic and inertial effects (i.e transient in achieved acceleration response) is increased.

F. MINIMIZATION OF THE KINEMATIC AND INERTIAL
CROSS-COUPLING EFFECTS IN CIRCULAR AIRFRAME

As shown in Figures 4.28, 4.40 and 4.42 the achieved maneuver acceleration in the circular airframe has very smooth response, in regards to the overshoot or undershoot on it.

The effect of the inertial and kinematic cross-coupling in the nonlinear aerodynamic model is that the response of the inertial achieved acceleration has a slowing transient starts at 3.5 seconds, as discussed in section IV.G. Hence, minimization of the effects means in the circular airframe improvement of time constant during the second guidance command.

1. Stability Augmentation System (SAS) with Feedback the q.

Using the same method for minimization, as in section V.D, the SAS of the pitch channel for the circular airframe with feedback q is, as shown in Figure 5.16. The transfer function of the q/δ_p is given in section II.C.

The closed-loop transfer function of the above SAS is:

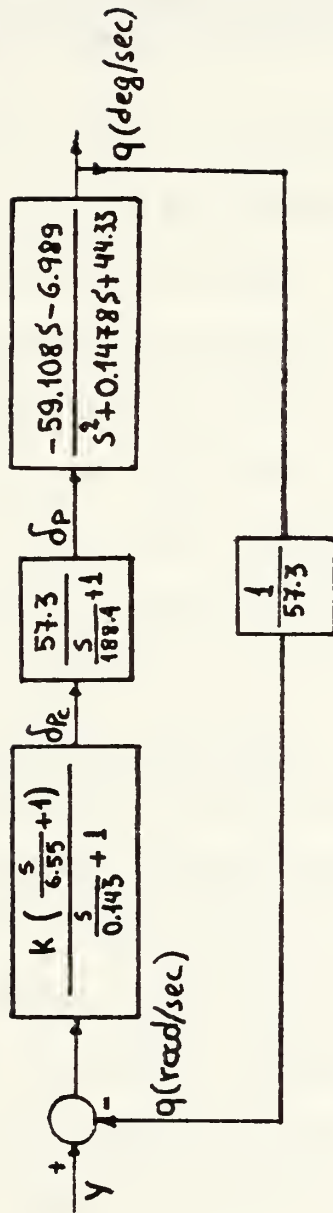


Fig. 5.16 Stability Augmentation System SAS with q/δ_p CBTT of Circular airframe

$$Z(s) = \frac{k \cdot \left(\frac{s}{6.55} + 1\right) 57.3 (-59.1088s - 6.9845)}{\left(\frac{s}{0.143} + 1\right) \left(\frac{s}{188.4} + 1\right) (s^2 + 0.14781s + 44.33)} \quad (\text{V.F.1-1})$$

$$1 + \frac{k \cdot \left(\frac{s}{6.55} + 1\right) (57.3) (-59.1088s - 6.9845)}{(57.3) \left(\frac{s}{0.143} + 1\right) \left(\frac{s}{188.4} + 1\right) (s^2 + 0.1478s + 44.3316)}$$

Rearranging equation V.F.1-1, one obtains:

$$Z(s) = \frac{k (20.38 \cdot s^3 + 30700.25s^2 + 203827.6s + 23672.8)}{0.037 \cdot s^4 + 7.004s^3 + 3.679 \cdot s^2 + 310.39 \cdot s + 44.33 + k \cdot (-9.024 \cdot s^2 - 60.179 \cdot s - 6.989)} \quad (\text{V.F.1-2})$$

The poles and zeros of the SAS are: (1)

$$P_1 = -188.438; \quad (2) P_{2,3} = -0.0739 \pm j6.657; \quad (3) P_4 = -0.143;$$

$$(4) Z_1 = -6.55 \text{ and } (5) Z_2 = -0.118. \quad \text{The other two zeros}$$

are at infinity. The root locus of the SAS is shown in Figure 5.17. The selected value of K is -15.6 and the

dominant roots are $P_{1,2} = -10.736 \pm j7.536$ (Figure 5.17).

With those dominant roots, the response of the system has θ equals to 35.06 degrees; ζ equals to 0.818; ω equals to 7.545 rad/sec and ω_n equals to 13.125 rad/sec.

2. SAS with Feedback of the a

For minimization of inertial and kinematic effect in the circular airframe, the same technique was used (i.e pole-zero cancellation technique) as in section V.D.2 and the resulted pitch control law with feedback of angle-of-attack (a), is shown in Figure 5.18.

The transfer function of the added compensator in the SAS is given by equation V.D.2-2.

REAL AXIS (UNITS PER INCH) = 20.0000
 IMAG AXIS (UNITS PER INCH) = 10.0000
 ROOTLOC/BIPOP ANALYSIS OF CBTT AUTOPILOT
 CIRCULAR AIRFRAME

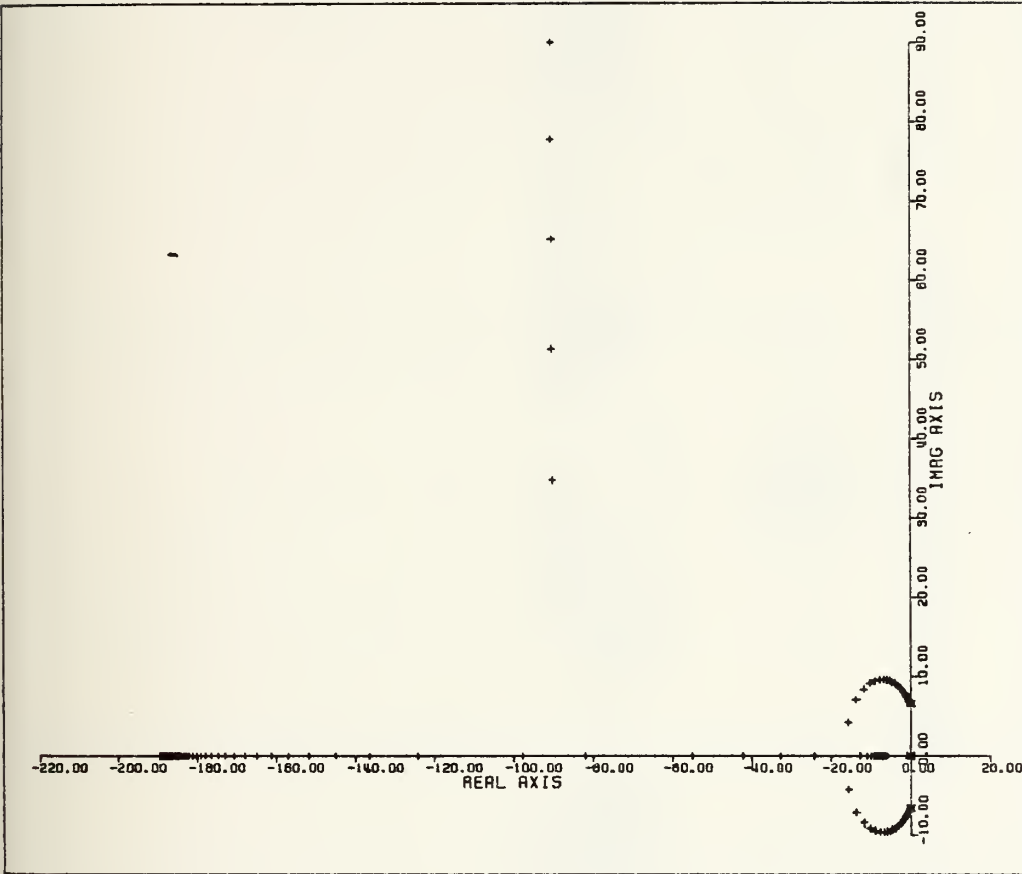


Fig. 5.17 Root locus of SAS with q/δ_p ; CBTT of
 Circular airframe

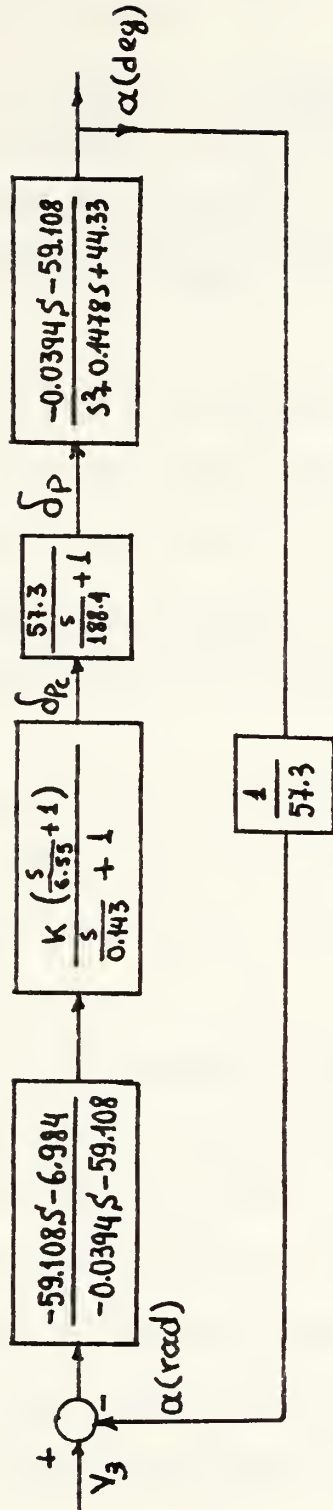


Fig. 5.18 Stability augmentation system SAS with a/δ_p ; CBTT of Circular airframe

The closed loop transfer function of the referred before system is given by equation V.D.2-3:

$$z_2 = \frac{\left(\frac{k \left(\frac{s}{6.55} + 1 \right)}{\left(\frac{s}{0.143} + 1 \right)} \right) \cdot \left(\frac{-59.1s - 6.99}{-0.039s - 59.1} \right) \cdot \left(\frac{57.3}{\frac{s}{188.4} + 1} \right) \cdot \left(\frac{-0.039s - 59.1}{s^2 + 0.148s + 44.33} \right)}{1 + \frac{k \cdot \left(\frac{s}{6.55} + 1 \right) \cdot 57.3 \cdot (-59.1s - 6.99) \cdot (-0.039s - 59.1)}{57.3 \left(\frac{s}{0.143} + 1 \right) \cdot (-0.039s - 59.1) \left(\frac{s}{188.4} + 1 \right) (s^2 + 0.148s + 44.33)}}$$

(V.D.2-3)

where the transfer function a/δ_p is given in the section II.C.3, rearranging and minor manipulating the above equation, one obtains equation V.D.2-4:

$$Z_2(s) = \frac{k \cdot (20.38s^3 + 30700.25s^2 + 203827.6s + 23672.8)}{-0.0015s^5 - 2.47s^4 - 414.34s^3 - 229.7s^2 - 18349s - 2620.4 + k(0.36s^3 + 535.78s^2 + 3557s + 413)}$$

(V.D.2-4)

The poles and zeros of the modified SAS are,

$P_1 = -1499.623$, $P_2 = -188.53$, $P_{3,4} = -0.0739 \pm j6.656$, $P_5 = -0.142$, $Z_1 = -1499.6$, $Z_2 = -6.55$, $Z_3 = -0.1182$ and all other zeros at infinity.

The root locus of the system is shown in figure 5.19, it is apparent from above Figure, that for $k=-15.6$ the dominant roots are the same as those in section V.F.1.

Considering the transmission of acceleration n_c path, as in the elliptical airframe, a compensator was added in the path, for compensation of the effect in it, which is created by the added compensator in the SAS, as shown in Figure 5.20.

REAL AXIS (UNITS PER INCH) = 20.0000
 IMAG AXIS (UNITS PER INCH) = 10.0000
 ROOTLOC/BIPOLAR ANALYSIS OF CBTT AUTOPILOT
 CIRCULAR AIRFRAME

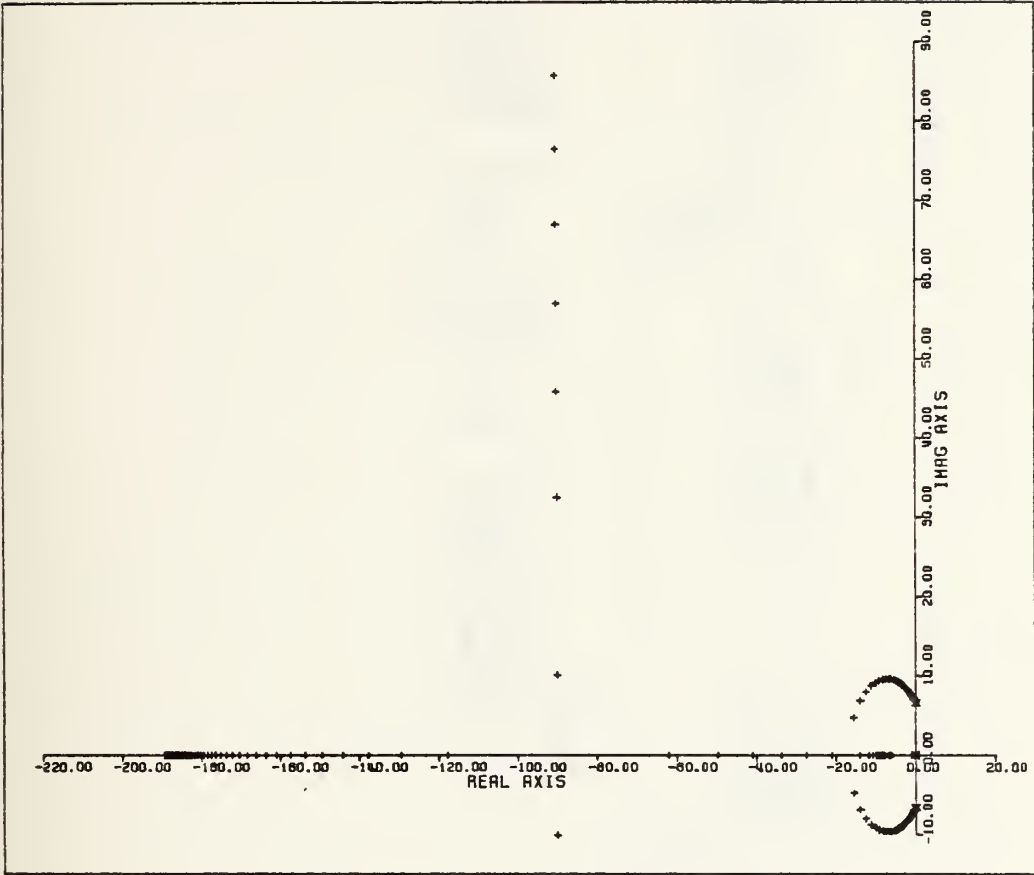


Fig. 5.19 Root locus of SAS with a/δ_p
 CBTT of Circular airframe

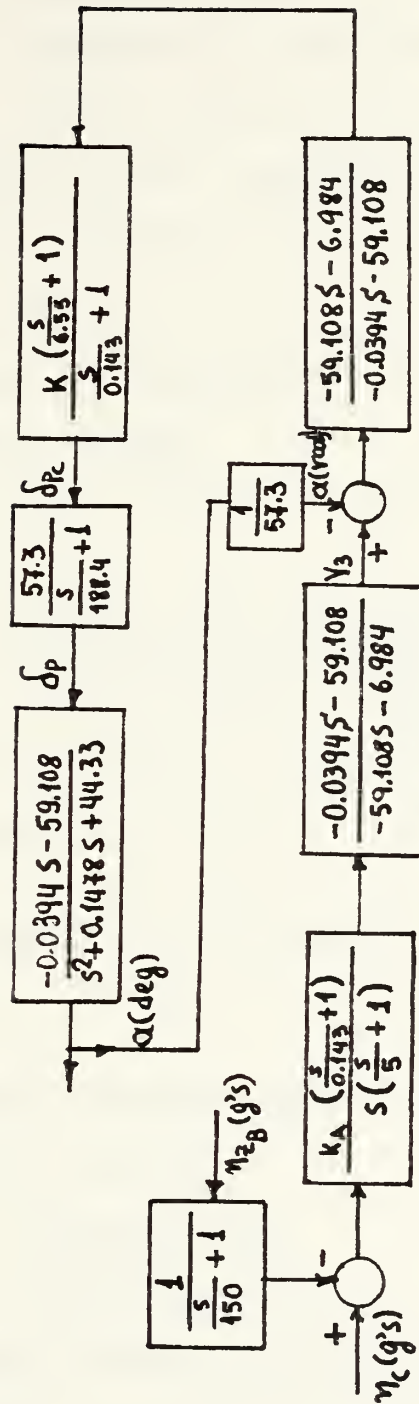


Fig. 5.20 Modified Pitch Channel for Circular airframe

3. Measuring of the Minimization in the Kinematic and Inertial Cross-Coupling Effect

A CSMP program (Appendix K) was written using equations of nonlinear lateral control law (section IV.G.2), of the aerodynamic models (section IV.4) and the following equations of the modified nonlinear pitch control law:

- a. Acceleration lag Compensator

$$\dot{X} = -150X + 150 \eta_{2B} \quad (\text{II.C.4})$$

- b. Acceleration Second-Order Compensator (Figure 3.20)

$$\frac{Y_3}{(\eta_c - X)} = \frac{K \cdot \left(\frac{S}{0.143} + 1 \right) (-0.03945 - 59.1)}{S \left(\frac{S}{5} + 1 \right) \cdot (-59.108 \cdot S - 6.9845)} \quad (\text{V.F.3-1})$$

Utilizing inverse Laplace transformation and rearranging the above equation, yields

$$\ddot{Y}_3 + 5.1183 \dot{Y}_3 + 0.591 \dot{Y}_3 = -K \cdot 0.02288 (\ddot{\eta}_c - \ddot{X}) - 34.97 (\dot{\eta}_c - \dot{X}) - 5 (\eta_c - X) \quad (\text{V.F.3-2})$$

Using state-space representation referred to in (Ref. 5: pp 675-678), one obtains:

$$\dot{W}_1 = W_2 - K_A \cdot 0.02288 (\eta_c - X) \quad (\text{V.F.3-3})$$

$$\dot{W}_2 = W_3 - K_A \cdot 34.850 (\eta_c - X) \quad (\text{V.F.3-4})$$

$$\dot{W}_3 = -0.5912 \cdot W_2 - 5.118 \cdot W_3 + K_A \cdot 173.39 (\eta_c - X) \quad (\text{V.F.3-5})$$

$$Y_3 = W_1 \quad (\text{V.F.3-6})$$

c. Compensator of Actuator in SAS

$$\frac{\delta P_c}{(Y_3 - \alpha/57.3)} = \frac{K \cdot \left(\frac{S}{6.55} + 1\right) \cdot (-59.1088 \cdot S - 6.989)}{\left(\frac{S}{0.143} + 1\right) \cdot (-0.0394 \cdot S - 59.104)} \quad (\text{V.F.3-7})$$

Utilizing, the aforementioned method for state representation and rearranging the equation V.F.3-7, it yields:

$$\delta \dot{P}_1 = \delta P_2 + K (48896.0838) \cdot (Y_3 - \alpha/57.3) \quad (\text{V.F.3-8})$$

$$\delta \dot{P}_2 = -214.473 \cdot \delta P_1 - 1500 \delta P_2 - K \cdot 7.3 \times 10^7 (Y_3 - \alpha/57.3) \quad (\text{V.F.3-9})$$

$$\delta P_c = \delta P_1 - K \cdot (32.744) (Y_3 - \alpha/57.3) \quad (\text{V.F.3-10})$$

d. Equation of Actuator

$$\delta \dot{P} = -188.4 \cdot \delta P + 10795.3 \cdot \delta P_c \quad (\text{IV.G.3-8})$$

Selecting the $K = -15.6$ and $K_{A_2} = -0.0387$ (Figure 4.26) and feedback the pitch angular rate (q), the achieved inertial acceleration n_z , has $\tau_1 = -0.34$ sec, $\tau_2 = 0.62$ sec and overshoot 5% (Figure 4.40, Table III).

This response of the n_z is unacceptable because it doesn't meet the requirement on the time constant, referred to in Appendix C.

Selecting $K = -15.6$ and $K_A = -0.0387$ (figure 5.20) and feedback the angle of attack (α) in the pitch channel the achieved inertial acceleration n_z (Figure 5.21) has $\tau_1 = -0.35$ sec, $\tau = 0.6$ sec and overshoot 7%, which is again unacceptable.



Fig. 5.21 Achieved Inertial Acceleration (nz) vs Time (t)

CBTT of Circular airframe; K = -15.6,
 $K_{A_2} = -0.0387$

It is known (Ref. 6) that:

$$\tau \sim \frac{1}{\omega_n} = \sqrt{\frac{I}{C_{m\alpha} \cdot \frac{g}{2} \rho M^2 \cdot A}} \quad (\text{V.G.3-9})$$

Hence, in order to reduce the τ_2 it is needed to increase the $C_{m\alpha}$. Selecting $K = -70.88$ and $K_A = -0.0387$ (Figure 5.20) with feedback the angle of attack (a), the dominant roots of the SAS (Figure 5.18) are $P_{1,2} = -90.55 \pm j87.95$ and the characteristics of the system response are $\theta = 44.16$ degrees, $\zeta = 0.79$, $\omega = 87.932$ rad/sec and $\omega_n = 126.212$ rad/sec. With that selected k the z decreases from 0.818 (when $K = -15.6$) to 0.72 and the ω_n increases from 13.125 rad/sec (when $K = -15.6$) to 126.212 rad/sec.

Figure 5.22 shows, the achieved inertial acceleration n_z , when $K = -70.88$, $K_{A_2} = -0.0387$ and feedback the (a). The $\tau_1 = 0.33$ sec, $\tau_2 = 0.48$ sec and overshoot 14.33 %. It is apparent that the τ_2 decreases, which is desirable but the overshoot increases, because the damping ratio ζ decreases.

In order to reduce the overshoot and to keep the time constants below the 0.5 sec, the K_A reduces to -0.0274 (Figure 5.20) and the gain K_{YP} (Figure 4.27) of the coordination branch in the nonlinear lateral control law increases from 0.458 to 1.0.

Using $K_{YP} = 1.0$ (Figure 4.27) in the coordination branch in the lateral control law, K_{A_1}



Fig. 5.22 Achieved Inertial Acceleration (n_z) vs Time (t)
 CBTT of Circular airframe; $K = -70.88$,
 $K_{A_2} = -0.0387$

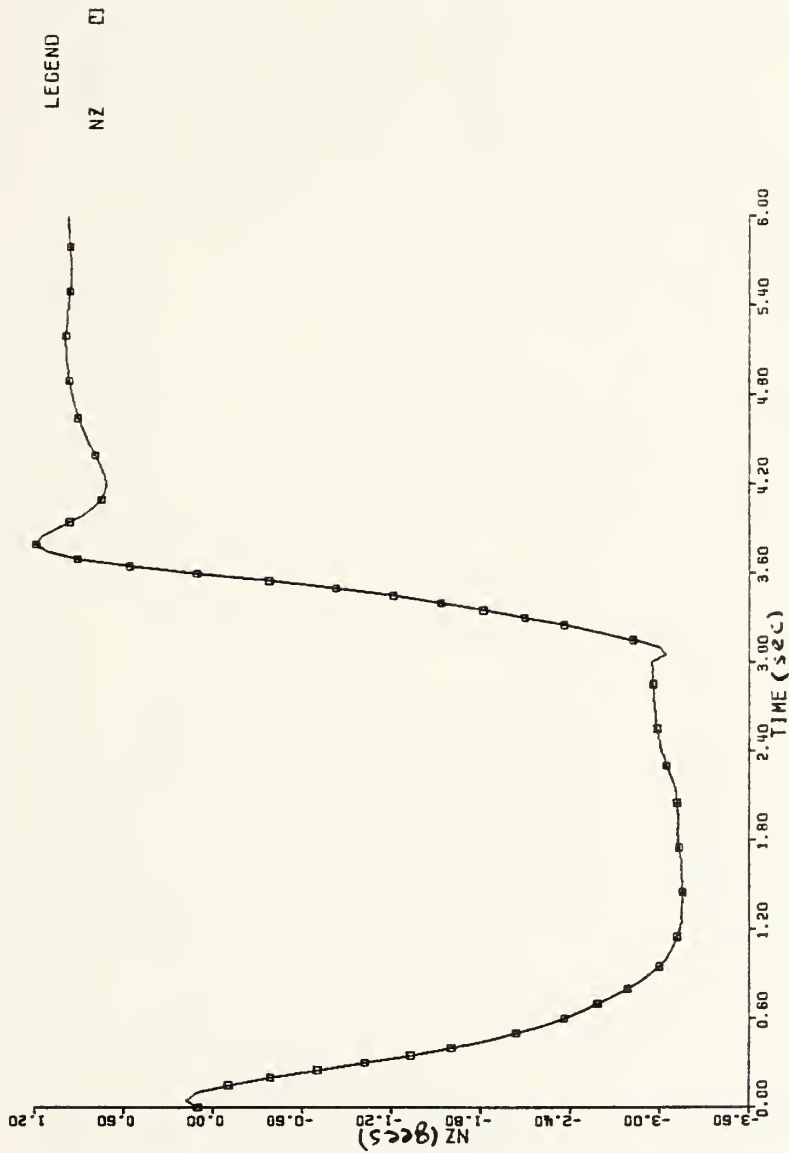


Fig. 5.23 Achieved Inertial Acceleration (n_z) vs Time (t)

CBTT of Circular airframe; $K = -15.6$,
 $K_{A_1} = -0.0274$

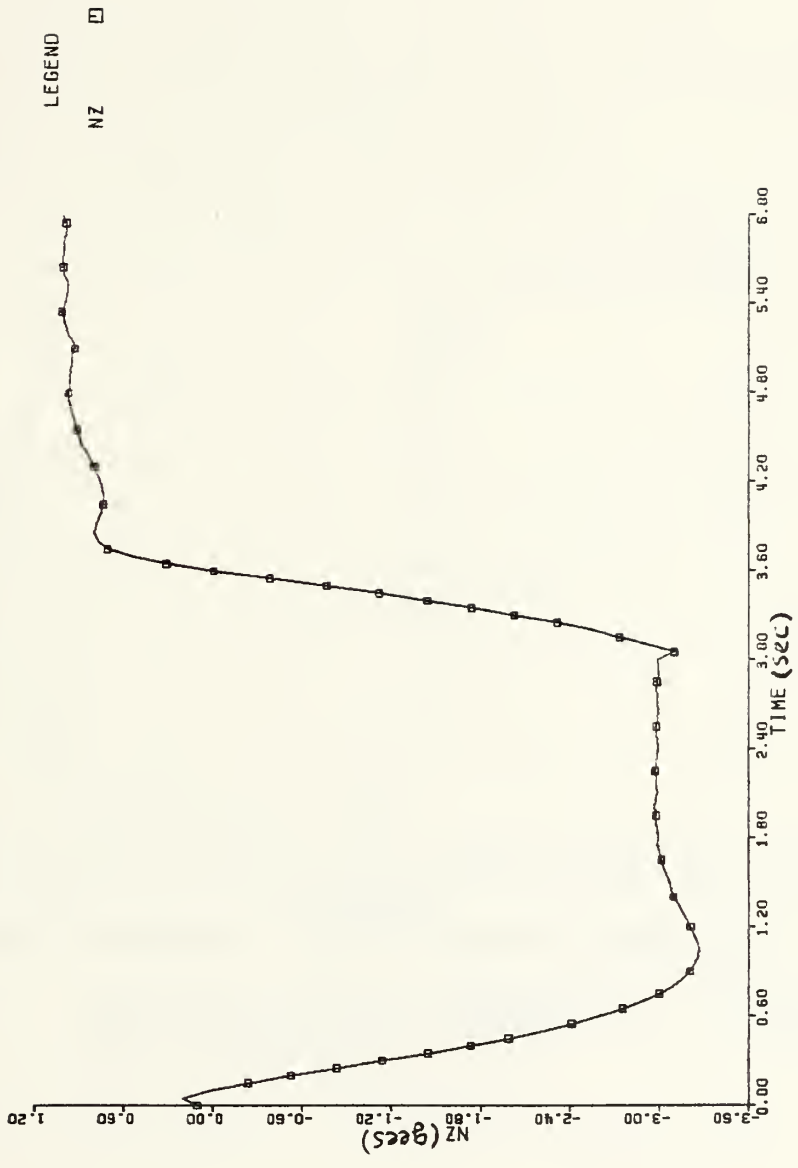


Fig. 5.24 Achieved Inertial Acceleration (n_z) vs Time (t)

CBTT of Circular airframe; $K = -70.88$,
 $K_{A1} = -0.0274$

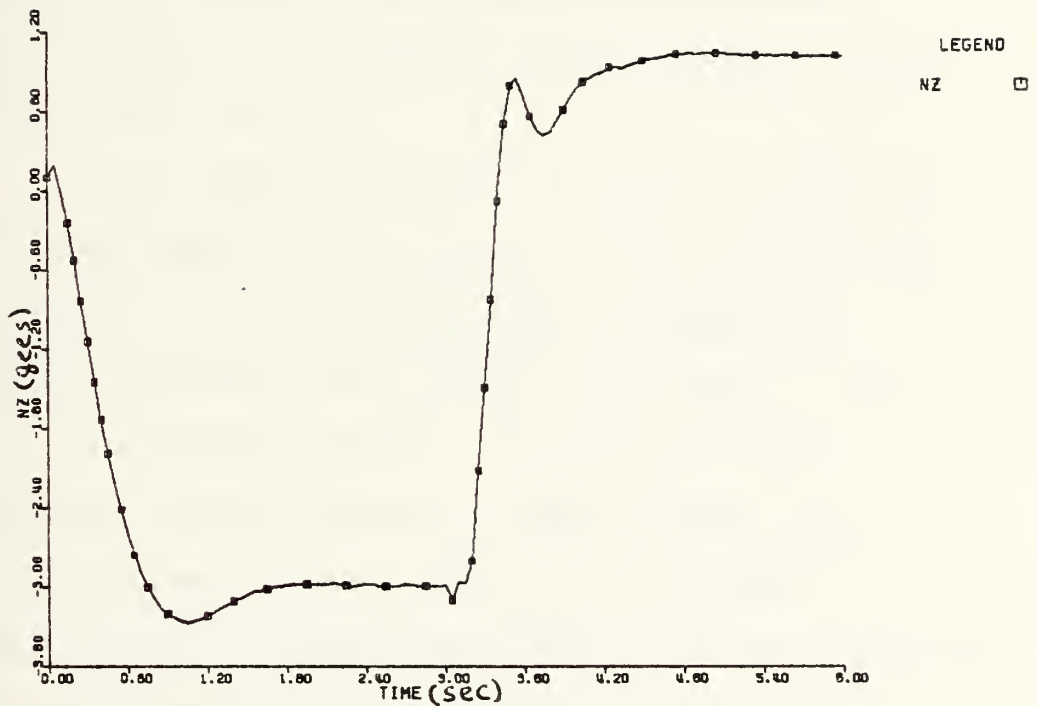


Fig. 5.25 Achieved Inertial Acceleration (n_z) vs Time (t)

CBTT of Circular airframe; $K = -70.88$,
 $K_{A_1} = -0.0274$, $K_{YP} = 1.0$

= -0.0274 in the acceleration compensator and $K = -70.88$ in the added compensator in the SAS with feedback the angle-of-attack (α) (Figure 5.20), the obtained achieved maneuver acceleration has $\tau_1 = -.43$ sec, $\tau_2 = -.37$ sec overshoot 8.9%, as shown in figure 5.25 and table V.

Using in the pitch channel with the aforementioned particular compensators, as feedback the rate of angle of attack ($\dot{\alpha}$) and making all the above selection of K_A , K and K_{YP} , the whole system becomes uncontrollable because the required tail incidence angle exceeds the limits of $\pm 10^\circ$.

Also using the selections of K , K_A , K_{YP} and feedback pitch angular rate q (Figures 4.26, 4.27), again the whole system becomes uncontrollable, because the required tail incidence angle exceeds the limit of $\pm 10^\circ$.

The above analysis illustrates that the angle-of-attack is more desirable feedback than the (q) and (α), in the nonlinear pitch control law for these particular circular airframe and flight conditions, because it reduces the kinematic and inertial coupling effect, such that the achieved inertial acceleration (n_z) meets the requirements of the time constants and overshoot, referred to in the linear studies.

TABLE V

CHARACTERISTIC OF THE INERTIAL ACHIEVED ACCELERATION (n_z)
FOR CIRCULAR AIRFRAME

CONDITION	τ_1 (sec)	τ_2 (sec)	overshoot
$K_A = 0.0387, K = -15.6$	0.35	0.6	7
$K_A = 0.0387, K = -70.88$	0.33	0.48	14.33
$K_A = 0.0274, K = -15.6$	0.435	0.51	8.6
$K_A = 0.0274, K = -70.88$			
$K_{YP} = 1$	0.43	0.37	8.9

Note: K_A : pitch autopilot acceleration gain in acceleration compensator
 τ_1 : 63 percent time constant of achieved maneuver plane acceleration due to first command
 τ_2 : 63 percent time constant of achieved maneuver plane acceleration due to second command
 K_{YP} : gain of the coordination branch
 K : gain of the added compensator is the SAS of pitch autopilot

G. MINIMIZATION OF KINEMATIC AND INERTIAL COUPLING IN
CIRCULAR AIRFRAME

As in the elliptical airframe comparing the values of the inertial and kinematic cross-coupling for the circular airframe, namely, the (P.r) and $(-p^\beta)$, referred to in table VI, it is concluded for this particular analysis that as the coupling effects in the nonlinear Pitch autopilot are reduced, the cross-couplings themselves are increased.

In order to minimize the cross-couplings, the pitch control law was modified, as shown in Figure 5.26.

For purposes of analysis, a CSMP program (Appendix K) was written, using the following equations for the nonlinear modified pitch control law, lateral control law and dynamic models, as in sections IV.G and IV.H.

$$1. \dot{X} = -150X + 150 \cdot \eta_{2B} \quad (\text{II.C.4})$$

$$2. \dot{W}_1 = W_2 - K_A \cdot 0.02288 (\eta_C - X) \quad (\text{V.F.3-3})$$

$$3. \dot{W}_2 = W_3 - K_A \cdot 34.850 (\eta_C - X) \quad (\text{V.F.3-4})$$

$$4. \dot{W}_3 = -0.591 W_2 - 5.1187 W_3 + K_A \cdot 173.385 (\eta_C - X) \quad (\text{V.F.4-5})$$

$$5. Y_3 = W_1 \quad (\text{V.F.4-6})$$

$$6. \delta \ddot{p}_c = -0.143 \cdot \delta p_c - 0.34058 (\dot{Y}_3 - \dot{\alpha}/57.3) - 2.2308 \cdot (Y_3 - \alpha/57.3) \quad (\text{V.F.4-7})$$

which is the equation IV.G.1-4, except of the feedback, which is the angle of attack (α) instead of the pitch angular rate (q).

$$7. \delta \dot{p} = -188.4 \cdot \delta p + 10795.3 \cdot \delta p_c \quad (\text{IV.G.1-5})$$

TABLE VI

KINEMATIC AND INERTIAL COUPLING FOR CIRCULAR AIRFRAME

CONDITON	INERTIAL (deg/sec ²)		KINEMATIC (deg/sec ²)	
	MIN	MAX	MIN	MAX
Circular airframe with cross- couplings (section IV.G)	-0.008	92.794	-1.132	0.012
with cross- coupling and faster response $K_A = -0.0387$, $K = -15.6$ (section V.F)	-0.0768	100.573	-2.04	0.0353
with cross- coupling and faster response $K_A = -0.0387$, $K = -70.88$ (section V.F)	-0.0212	103.553	-1.89	0.0436
with cross- coupling and slower response $K_A = -0.0274$, $K = -15.6$ (section V.F)	-0.107	118.294	-2.97	0.0387
with cross- coupling and slower response $K_A = -0.0274$, $K = -70.88$ (section V.F)	-0.0743	109.411	-2.32	0.0431
with cross- coupling slower response and increased gain in the coordinated branch $K_{yp} = 1.0$, $K_A = -0.287$ $K = -70.88$ (section V.F)	-6.0791	199.841	-0.8662	1.0541
with cross- coupling slower response and modified pitch control law as section V.G $K_A = -0.0274$	-2.264	38.386	-0.00788	-0.6021

Note: K_A , K , K_{yp} as referred in section V.F and V.G.

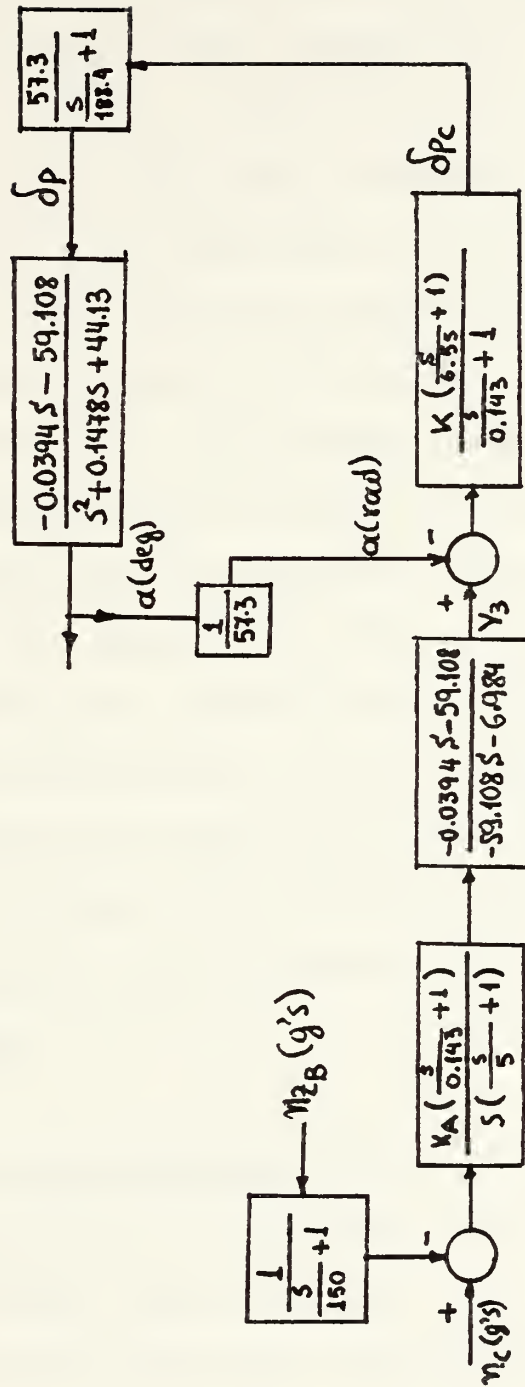


Fig. 5.26 Modified pitch Control law for minimization of cross-coupling; CBTF of Circular airframe

Figures 5.27 and 5.28 show the minimized inertial and kinematic cross-coupling, with feedback the angle-of-attack, with $K_{A_1} = -0.0274$ and $K = -70.88$. Comparing the values of the above minimized inertial and kinematic coupling, with the values of the kinematic and inertial coupling when the pitch channel has feedback the pitch angular rate (q) and $K_A = -0.0274$, as given in table VI, it is concluded that the couplings when the pitch channel has feedback angle-of-attack (α) and the aforementioned particular compensator (Figure 5.26), were reduced 228.29% for inertial and 190% for kinematic.

Also, comparing the Figure 5.25 which illustrates the achieved inertial acceleration n_z for circular airframe with minimized coupling effects and Figure 5.29 illustrated n_z for circular airframe with minimized coupling, it is concluded that as the coupling reduces, the coupling effects increases.

H. CONCLUSIONS AND RECOMMENDATIONS

The conclusions that follow are based on a single representative flight condition (Mach 3.95 and 60 kft altitude) and for the particular analysis which was done in this chapter.

1. From the studies in this chapter, it is concluded:
 - a. Transients in maneuver plane acceleration are

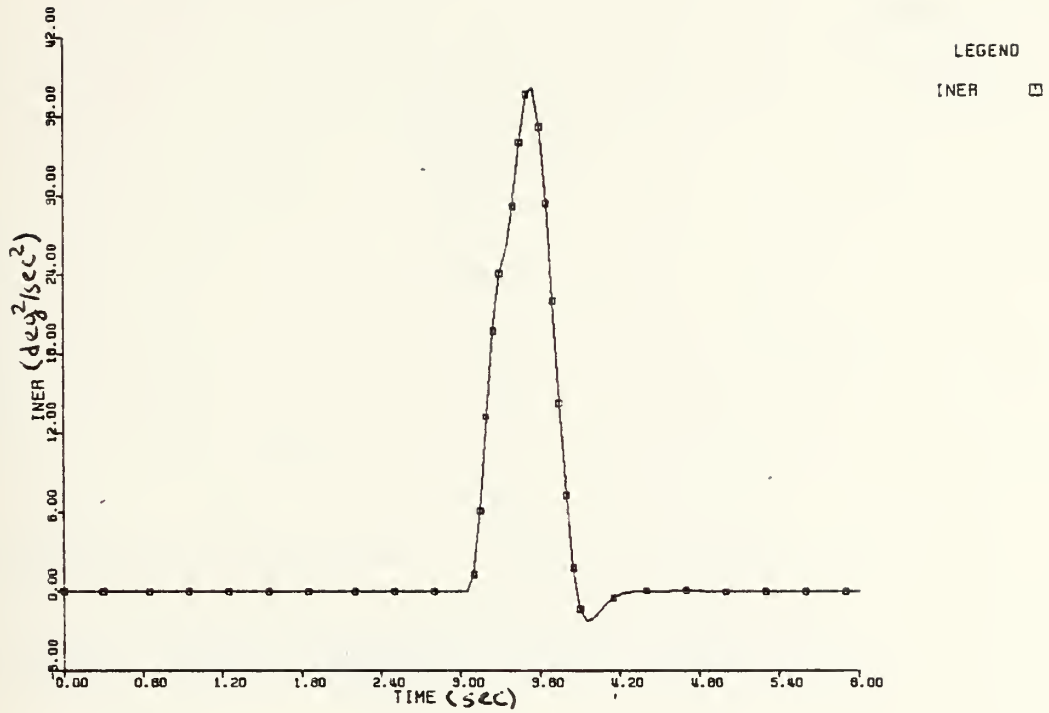


Fig. 5.27 Minimized inertial Coupling (P.r) vs Time (t)
CBTT of Circular airframe

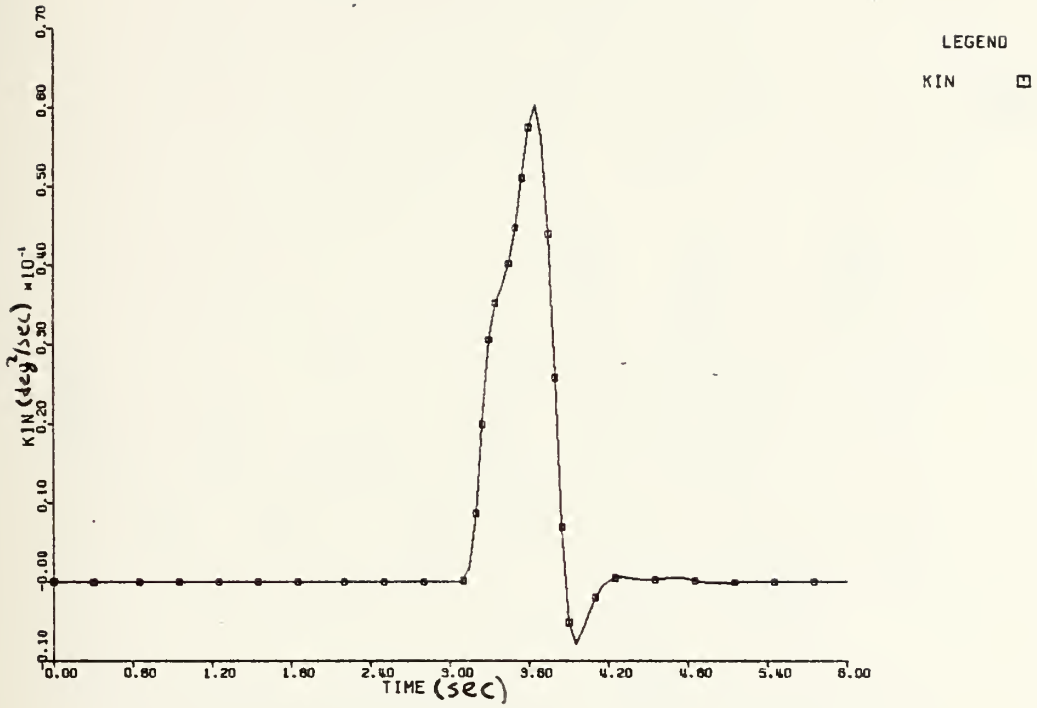


Fig. 5.28 Minimized Kinematic Coupling (-P.β) vs Time (t)
CBTT of Circular airframe

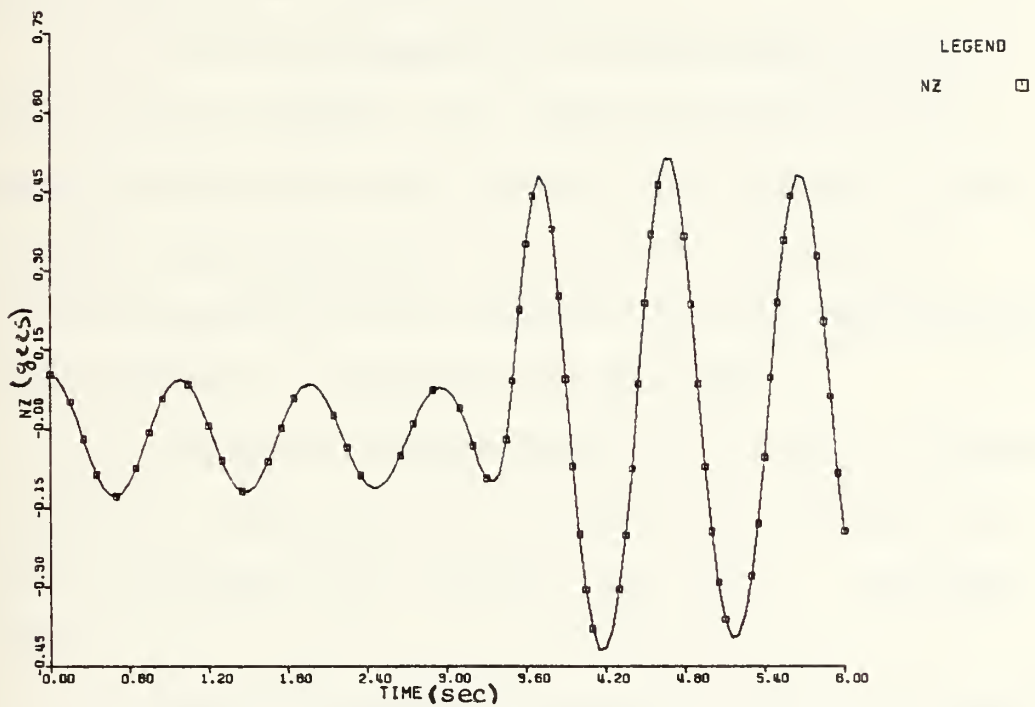


Fig. 5.29 Achieved Inertial acceleration (n_z) vs Time (t)
 Modified pitch channel for minimization of
 coupling; CBTT of Circular airframe

caused by kinematic and inertial coupling between pitch and yaw dynamics through missile roll rate. Transients are in the form of overshoots and undershoots (section V.B).

b. Using as feedback in the nonlinear pitch channel for both airframes the pitch angular rate (q), the transients in the maneuver plane exceeds the denoted requirements and the achieved maneuver acceleration is not acceptable (sections V.D and V.F).

c. Using as feedback in the nonlinear pitch channel for both airframe, the angle-of-attack (α) and modifying suitably the pitch control law (Figure 5.5 and Figure 5.20), the transients are minimized below the desired requirement and the achieved inertial acceleration (n_z) is acceptable. (sections V.D and V.F).

d. Using as feedback the rate of angle of attack ($\dot{\alpha}$), the whole system becomes uncontrollable because the pitch tail incidence (δ_p) exceeds the limits. (sections V.D, V.F).

e. Using as feedback the rate of angle of attack ($\dot{\alpha}$) and modifying suitably the pitch control law (Figure 5.26), the kinematic and inertial coupling are reduced dramatically, comparing with their values when the used feedback is the pitch angular rate. (sections V.D, and V.G)

f. Using as feedback the rate of angle of attack ($\dot{\alpha}$), in the modified pitch channel (Figure 5.26) for

minimization of kinematic and inertial coupling, the whole system becomes uncontrollable, because the pitch tail incidence (δ_p) exceeds the limits. (sections V.E and V.G)

g. Minimizing the inertial and kinematic cross-coupling effects, the values of kinematic ($-p\beta$) and inertial (p_r) coupling increase. (section V.E and V.G)

h. The above conclusions show, that for the particular airframe, flight conditions and analysis is not possible to achieve minimization of the kinematic and inertial cross-coupling effects and simultaneously minimization of the cross-couplings themselves.

2. Recommendations

Considering the studies of this work and the conclusions, it is recommended:

a. Further analysis of the minimization of the kinematic and inertial cross-coupling effects and the cross-coupling themselves in other airframes, and with other analysis to achieve simultaneous minimization.

b. Further analysis of the CBTT autopilots in other flight conditions for verification of the above results.

APPENDIX A

MISSILE SIZING AND MASS PROPERTIES

In order to provide a realistic missile based on the configuration concepts tested aerodynamically in [Ref. 1], the models have the following characteristics.

<u>Characteristic</u>	<u>Circular</u>	<u>Elliptical</u>
Length (in)	168	168
Max. Diameter	24	
Max. Major axis (in)		41.57
Max, Minor axis (in)		13.86
Weight (lbs)	2525	2475
I_{xx} (slug-ft ²)	40	110
I_{yy} (slug-ft ²)	804	790
I_{zz} (slug-ft ²)	810	853
c.g distance from L.E (in)	100.8	100.8
Reference length d (ft)	2	2
Reference area S(ft ²)	π	π

APPENDIX B

NONLINEAR AERODYNAMIC DATA

The aerodynamic data were taken from [Ref. 2]. For reference, the normal and pitching moment curves at $M = 3.95$ have been produced in fig. B.1 and B.2 for the two configurations in [Ref. 2]. The aerodynamic derivatives C_Y , C_n , C_l , with respect to sideslip angle β , yaw control δ_Y , and roll control δ_R are presented in figures B.3, B.4 and B.5 of [Ref. 2] as used in the computer simulation, namely, as piece wise linear segments for ease in interpolation.

APPENDIX C

REQUIREMENTS FOR UNCOUPLED AUTOPILOTS

The requirements for the classical design technique of the uncoupled autopilots are given in [Ref. 2] and are the following:

1. Acceleration time response

a. 63 percent time constant of 0.5 seconds for a step command of acceleration at the flight condition of interest, (i.e $M = 3.95$ and altitude 60kft) and small angles-of-attack. This response is representative of a tactical missile of this size.

b. Overshoot 10 percent

c. Zero steady state error in acceleration to reduce variations of guidance navigation gain.

2. Relative stability

Gain margins 6db, phase margins 30 deg with a goal of 12 db and 50 deg.

3. High Frequency Attenuation in Actuator Command Branch

It must be $\gg 15$ db at 100 rad/sec and zero angle-of-attack. This requirement will provide sufficient high frequency attenuation for 30 Hz actuator and for body bending modes, when high frequency filters are added. This requirement also limits autopilot speeds of response.


```
OUTPUT TIME,NZ  
PAGE XY PLOT  
OUTPUT TIME, DP  
PAGE XY PLOT  
END  
STOP  
ENDJCB  
/*
```


END
STCP
ENDJCB
/*

STCP
ENDJCE
/


```

//LICULS JOB (1207,2111), 'THESIS TOP', CLASS=C
// EXEC CSMPXV
//X.FLCTPARM CD *
//PLCT SCALE=C.55 &END
//X.SYSIN DD *
*****
** T I T L E : R C L L U N C O U P L E D C H A N N E L
** * * * * * F O R * * * * * A I R F R A M E * * * * *
** * * * * * * * * * * * * * * * * * * * * * * * * * * *
DEFINITION OF VARIABLES OF ELLIPTICAL AIRFRAME
** * * * * *
P: ROLL ANGLE CCMAND (RAD)
FC: ROLL ANGLE RATE (RAD/SEC)
F: ROLL ANGLE (RAD)
DR: ROLL TAIL INCIDENCE (DEG)
DRC: ROLL TAIL INCIDENCE (RAD)
PARAMETER Q=1650, S=3.14159, D=2.0, CLDR=0.023, IXX=110.0
FCCT=STEP(0.0)
PDCT=SQ*CLDR*DR/IXX
FDCCT=P
DRCCT=DR+188.4*57.3*DRC
DRCCT=DR/57.3
XDCT=-17.6*F+17.6*FC
YDCT=-5*X+50.333E-3*(XDCT-PDCT)+0.755*(X-P)
XDCT=-6*X+0.0782*PDCT
XDCT=-15*DRC+0.568963*(YDOT-X1DOT)+62.586*(Y-X1)
P=INTGRL(C.0, PDOT)
F=INTGRL(C.0, FDOT)
DR=INTGRL(C.0, DRDOT)
Y=INTGRL(C.0, YDOT)
X1=INTGRL(C.0, X1DOT)
DTIMER=INTGRL(0.0, DRCCT)
RANGE P, F, LRR
PRINT TIME, DR, DRR
PAGE XYPLCT
PAGE TIME, P, F
PAGE XYPLCT
END
STOP
ENDJCB
/*

```


APPENDIX G

CSMP PRCGRMS FOR LINEAR CBTT AUTOPILOTS

```

//LICLLIS JOB (1207,2111), 'THESIS', CLASS=C
// EXEC CSM PXV
//MAIN CRG=NP GVM1.1862 P
//X.FLCTPARM DD *
&PLCT SCALE=0.55 &END
//X.SYSIN DD *
*****
T I T L E : L I N E A R C B T T A U T O P I L O T S
*****
*****
DEFINITION OF VARIABLES
R : YAW NORMAL ACCELERATION (GEES)
B : SIDESLIP ANGLE(DEG)
D Y C : YAW TAIL INCIDENCE (DEG)
FC : RCLL ANGLE COMMAND (RAD)
P : RCLL ANGLE RATE (DEG/SEC)
DR : RCLL TAIL INCIDENCE (DEG)
DRC : RCLL TAIL INCIDENCE COMMAND (RAD)
PARAMETER Q=1650, K=0.48, CYDY=0.022, CYB=-0.082, CNDR=0.018
PARAMETER CNB=-0.019, CNDY=-0.053, CLDY=-0.016, CLB=-0.009
PARAMETER CLDR=0.035, S=3.14159, D=2.0, W=2525.0, IZZ=810.0
PARAMETER IXX=40.0, AE=0.17452, A=10.0
FC = STEP(0.0)
NY=G*SYE1/WDY*CY
E1=E*CYB+3*YQ*S*CD*E2/IZZ
RDCI=E*57.3*QDR*CR+CNDY*DY
E2=E*CNB+CNQ*S*CD*E4/IXX
PDCT=E*57.3*G*E3
E4=E*CLDY*DY+CLDR*DR
E3=CLDY*PA/57.3-R+K*NY
FDCT=E/P/57.3
DYDCT=-188.4*Y+188.4*Y+188.4*Y+188.4*Y+188.4*Y
YDCT=-5*Y+1.6*NY
DYCCCT=0.485*(YDCT+RDCT/57.3-0.458*AE*PDCT/57.3)
DRDCT=-188.4*CR+188.4*CR+188.4*CR+188.4*CR
XDCT=-8*X-17.6*F+17.6*F
*****

```



```

Y1DCT = -5*Y1+50.333E-3*(XCOT-PDOT/57.3)+0.755*(X-P/57.3)
X1DCT = -6*X1+0.078*PDOT/57.3
CRCCCT = -15*DRC+0.25*(Y1DCT-X1DCT)+15*(Y1-X1)
P=INTGRL(0.0,PCCT)
R=INTGRL(0.0,RCCT)
F=INTGRL(0.0,FCCT)
B=INTGRL(0.0,BCCT)
DR=INTGRL(0.0,DRDUT)
DY=INTGRL(0.0,DCCT)
Y1=INTGRL(0.0,Y1DOT)
Y1=INTGRL(0.0,X1DOT)
X1=INTGRL(C.0,X1DOT)
X1=INTGRL(0.0,LYCDUT)
DRC=INTGRL(0.0,CRCDOT)
RANGE B,F
PRINTER B,F
TIMER FIN TIME=3.25,OUTCEL=0.05
METFCC M TIME
OUTPUT X PLOT
OUTPUT TIME, F
PAGE XYPLOT
END
STCP
ENDJCB
/*

```



```

R=INTGRL(0.C,RDCT)
F=INTGRL(0.C,FDCT)
B=INTGRL(0.C,BDCT)
DR=INTGRL(0.0,DRDOT)
DY=INTGRL(C.C,DYDOT)
Y=INTGRL(0.C,YDOT)
Y1=INTGRL(C.0,Y1DOT)
X1=INTGRL(0.C,XDOT)
X1=INTGRL(0.0,X1DOT)
DYC=INTGRL(0.0,DYCDCT)
DRANGE=INTGRL(C.0,DRCDCT)
PRINT B,F
TIMER FIN TIME,B
OUTPUT X Y PLOT
PAGE X Y PLOT
PAGE X Y PLOT
END
STCP
END JCB
/*

```



```

FUNCTION CNE = (16.0,-0.035), (20.0,-0.04)
              (-4.0,0.0238), (6.0,0.0238), (10.0,0.024), ...
              (16.0,0.028), (20.0,0.031)
FUNCTION CYB = (-4.0,-0.048), (0.0,-0.042), (4.0,-0.047), ...
              (8.0,-0.052), (16.0,-0.06), (20.0,-0.065)
              (10.0,-0.04), ...
FUNCTION CNDY = (-4.0,-0.0395), (0.0,-0.045), ...
              (12.0,-0.04), (20.0,-0.045)
FUNCTION CLDY = (-4.0,0.0025), (0.0,0.0005), (4.0,-0.002), ...
              (8.0,-0.007), (12.0,-0.012), (20.0,-0.023)
              (10.0,0.01495), (20.0,0.01498), (4.0,0.015), ...
FUNCTION CLDR = (-4.0,0.0225), (0.0,0.0226), (4.0,0.0228), ...
              (10.0,0.0232), (16.0,0.027), (20.0,0.0293)
              (8.0,0.01), (16.0,0.025), (20.0,0.0325), ...
FUNCTION CNADP, -10.0 = (-4.0,-1.035), (0.0,-0.2), (4.0,0.55), ...
              (8.0,1.45), (12.0,2.320), (16.0,3.25), (20.0,4.20), ...
              (24.0,5.3)
FUNCTION CNADP, 0.0 = (-4.0,-0.80), (0.0,0.00), (4.0,0.776), ...
              (8.0,1.60), (12.0,2.55), (16.0,3.45), (20.0,4.5), ...
              (24.0,5.55)
FUNCTION CNACP, 10.0 = (-4.0,-0.6), (0.0,0.20), (4.0,1.00), ...
              (8.0,1.88), (12.0,2.75), (16.0,3.70), (20.0,4.8), ...
              (24.0,5.80)
FUNCTION CMADP, -10.0 = (-4.0,0.5), (0.0,0.525), (4.0,0.620), ...
              (8.0,0.7), (12.0,0.80), (16.0,0.90), (20.0,1.00), ...
              (24.0,1.03)
FUNCTION CMADP, 0.0 = (-4.0,-0.085), (0.0,0.00), (4.0,0.073), ...
              (8.0,0.125), (12.0,0.19), (16.0,0.2), (20.0,0.25), ...
              (24.0,0.2)
FUNCTION CMACP, 10.0 = (-4.0,-0.620), (0.0,-0.525), (4.0,-0.495), ...
              (8.0,-0.4), (12.0,-0.395), (16.0,-0.405), (20.0,-0.495), ...
              (24.0,-0.685)
DYNAMIC
CLBA = AFGEN (CLB, A)
CLBBA = AFGEN (CNE, A)
CYBA = AFGEN (CYB, A)
CLLYA = AFGEN (CLLY, A)
CLCYA = AFGEN (CLCY, A)
CLDRA = AFGEN (CLDR, A)
CNCRA = AFGEN (CNCR, A)
CN = TWOVAR (CNADP, A, DP)
CM = TWOVAR (CMADP, A, DP)

```

```

* *
-----
COMMAND FOR ELLIPTICAL AIRFRAME

```



```
NZC= -2.0*STEP(2.0)+2.0*STEP(5.0)
NC= NZC-0.913*COS(TH)
```

```
PITCH EQUATIONS OF CCNTROL LAW
```

```
* *
```

```
XDCCT= -150.0*X+150*NZB
YDCCT= -6*Y-0.530544*NC+0.48*X
DPCDCT= -383.75E-3*YDCCT+383.75E-3*(QDOT/57.3)-3.07*(Y-Q/57.3)
DPDCT= -188.4*CP+188.4*57.3*DPC
```

```
PITCH EQUATIONS OF AERODYNAMIC MODEL
```

```
* *
```

```
NZB= -QD*S*CN/W
QDCCT=(P/57.3)*R+57.3*QD*S*D*CM/IYY
ACCT=Q+K*NZB-(P/57.3)*B
THDCT=(Q/57.3)*COS(F)-(R/57.3)*SIN(F)
X=INTGRL(-1.0,XDOT)
Y=INTGRL(-0.0105,YDOT)
DPC=INTGRL(0.01148,DPCDCT)
DP=INTGRL(0.658,DPDCT)
Q=INTGRL(0.0,QDOT)
A=INTGRL(2.41,ACCT)
TH=INTGRL(0.0636,THDCT)
```

```
ROLL-YAW EQUATIONS OF CCNTROL LAW
```

```
* *
```

```
NCSCRT
IF (TIME.LE.5.0) GO TO 10
FC= 3.14159*STEP(5.0)
Y2DOT=-4*Y2+3.356*NYB
IF (A.GT.1.0) GO TO 5
```

```
AE=1.0
AEDOT=0.0
GO TO 6
```

```
5 CCNTINUE
```

```
AE=A
AEDOT=0.0
GO TO 6
```

```
6
```

```
CCNTINUE
DYDCCT= 0.608*(Y2DOT+RDCT/57.3)-(AE/57.3)*(PDOT/57.3)
-(AEDCT/57.3)*(P/57.3)+6.08*(Y2+R/57.3)-(AE/57.3)*P/57.3)
DYDCCT= -188.4*CY+188.4*57.3*DYC
X1DCCT= -8*X1-17.6*F+17.6*FC
Y1DCCT= -5*Y1+50.333E-3*(X1DOT-PDOT/57.3)+0.755*(X1-P/57.3)
X2DOT= -6*X2+C.078*PDOT/57.3
DRCCCT= -15*DRC+1.0425*(Y1DOT-X2DOT)+62.55*(Y1-X2)
```


DRDCT= -188.4*CR+188.4*57.3*DRC

RCLL-YAW EQUATIONS OF AERODYNAMIC MODEL

NYB=QD*S*(CYBA*B+CYDYA*DY)/W
BCOT=K*(NYB)+A*P/57.3-R
RDCT= -Q*(P/57.3)+57.3*QD*S*D*(CNBA*B+CNDYA*DY+CNBRA*DR)/IZZ
PDCT=57.3*QD*S*D*(CLBA*B+CLDYA*DY+CLBRA*DR)/IXX
FCCT=P/57.3
FC=F*57.3
KIN= -P*B/57.3
INER=R*P/57.3

INTEGRATION

Y2=INTGRL(0.0,Y2DOT)
DYC=INTGRL(0.0,DYCDOT)
DY=INTGRL(0.0,CYDOT)
X1=INTGRL(0.0,X1DOT)
Y1=INTGRL(0.0,Y1DOT)
X2=INTGRL(0.0,X2DOT)
DR=INTGRL(0.0,DRDOT)
B=INTGRL(C.0,BCCI)
R=INTGRL(C.0,RCOT)
P=INTGRL(0.0,PCOT)
F=INTGRL(C.0,FCOT)

10 CCNTINUE

ACHIEVED INERTIAL ACCELERATION

NZ=NZB*COS(F)+NYB*SIN(F)

TERMINAL
RANGE KIN, INER, NZ
PRINT KIN, INER, NZ
TIMER FINITIM=8.0, OUTDEL=0.050, DELMIN=0.5E-8
OUTPLT TIME, A
PAGE XYPLCT
CLTPLT TIME, CPC
PAGE XYPLCT
OUTPUT TIME, KIN
PAGE XYPLCT
CLTPLT TIME, INER
PAGE XYPLCT


```

//LICULIS JOE (1207,2111),'TFESIS TOP.',CLASS=C
//EXEC CSMPXV
//X.FLOT Parm ID #
  &PLCT SCALE=C.45 &END
//X.SYSIN DD #
*****
TITL E N O N L I N E A R C B T T A L T O P I L C T S
      W F O R H E L L I P T I C A I R F R A M E
*****

```

```

*****
* DEFINITIONS OF VARIABLES CF NONLINEAR CBTT AUTOPILOT FOR IDEAL
* ELLIPTICAL AIRFRAME DYNAMICS
*-----

```

```

NZC : PITCH NCRMAL ACCELERATION COMMAND (GEES)
NZX : INERTIAL PITCH NORMAL ACCELERATION (GEES)
NZB : BODY-FIXED YAW NORMAL ACCELERATION (GEES)
NYB : BODY-FIXED YAW NORMAL ACCELERATION (GEES)
A : ANGLE OF ATTACK (DEG)
B : SICESLJP ANGLE (DEG)
Q : PITCH ANGLAR RATE (DEG/SEC)
R : YAW ANGLAR RATE (DEG/SEC)
P : ROLL ANGLAR RATE (DEG/SEC)
F : ROLL ANGLE (DEG)
DPC : PITCH TAIL INCIDENCE (DEG)
DPC : PITCH TAIL INCIDENCE (DEG)
DYC : YAW TAIL INCIDENCE (DEG)
DRC : ROLL TAIL INCIDENCE (DEG)
DRC : ROLL TAIL INCIDENCE (DEG)

```

```

INITIAL
PARAMETER SC=1650.0,K=0.480,S=3.141592,D=2.0,W=2475.0
PARAMETER IZZ=853.0,IYY=790.0,IXX=110.0

```

```

*****
* FUNCTIONS CF DERIVATIVES
*-----

```

```

FUNCTIGN CNB = (-4.0,0.0,0.238),(6.0,0.0,0.238),(10.0,0.024),...
FUNCTIGN CYB = (-4.0,-0.048),(0.0,-0.042),(4.0,-0.047),...
FUNCTIGN CNDY = (-4.0,-0.0395),(0.0,-0.04),(10.0,-0.04),...

```



```

FUNCTION CNB = (-4.0,0.01495),(0.0,0.01458),(4.0,0.015),...
FUNCTION CLDR = (12.5,0.015),(20.0,0.019)
FUNCTION CNADP = (-4.0,0.0225),(0.0,0.0226),(4.0,0.0228),...
FUNCTION CNADP = (10.0,0.0232),(16.0,0.027),(20.0,0.0293),...
FUNCTION CNADP = (-4.0,-1.05),(0.0,-0.2),(4.0,0.55),...
FUNCTION CNADP = (8.0,1.45),(12.0,2.320),(16.0,3.25),(20.0,4.20),...
FUNCTION CNADP = (24.0,5.3)
FUNCTION CNADP = (-4.0,-0.80),(0.0,0.00),(4.0,0.776),...
FUNCTION CNADP = (8.0,1.60),(12.0,2.55),(16.0,3.45),(20.0,4.5),...
FUNCTION CNADP = (24.0,5.55)
FUNCTION CNADP = (-4.0,-0.6),(0.0,0.20),(4.0,1.00),...
FUNCTION CNADP = (8.0,1.88),(12.0,2.75),(16.0,3.70),(20.0,4.8),...
FUNCTION CNADP = (24.0,5.80)
FUNCTION CNADP = (-4.0,0.5),(0.0,0.525),(4.0,0.620),...
FUNCTION CNADP = (8.0,0.7),(12.0,0.80),(16.0,0.90),(20.0,1.00),...
FUNCTION CNADP = (24.0,1.03)
FUNCTION CNADP = (-4.0,-0.085),(0.0,0.00),(4.0,0.073),...
FUNCTION CNADP = (8.0,0.125),(12.0,0.19),(16.0,0.2),(20.0,0.25),...
FUNCTION CNADP = (24.0,0.2)
FUNCTION CNADP = (-4.0,-0.620),(0.0,-0.525),(4.0,-0.495),...
FUNCTION CNADP = (8.0,-0.4),(12.0,-0.395),(16.0,-0.405),(20.0,-0.495),...
FUNCTION CNADP = (24.0,-0.685)

```

```

DYNAMIC
CNBA=AFGEN(CNB,A)
CYBA=AFGEN(CYB,A)
CNDYA=AFGEN(CNDY,A)
CYDYA=AFGEN(CYDY,A)
CLDRA=AFGEN(CLDR,A)
CA=IWCVAR(CNADP,A,DP)
CM=TWOVAR(CMADP,A,DP)

```

```

* * CCMAND FCR ELLIPTICAL AIRFRAME
* *

```

```

Nzc= -2.0*STEP(2.0)+2.0*STEP(5.0)
NC= Nzc-0.513*cos(TH)

```

```

* * PITCH EQUATIONS OF CONTROL LAW
* *

```

```

XDOT= -150.0*X+150*NZB
YDOT= -6*Y-C.530544*NC+0.48*X
DPCDOT= -383.75E-3*YDOT+383.75E-3*(QDOT/57.3)-3.07*(Y-Q/57.3)
DPDOT= -188.4*DP+188.4*57.3*DPC

```

```

* * PITCH EQUATIONS OF AERODYNAMIC MODEL
* *

```



```

NZB= -QD*S*CN/W
QDOT=57.3*CC*S*D*CM/IYY
ADOT=Q+K*NZB
THDOT=(Q/57.3)*COS(F)-(R/57.3)*SIN(F)
X=INTGRL(-1.0,XDOT)
Y=INTGRL(-0.0105,YDOT)
DFC=INTGRL(0.01148,DP*CDOT)
DF=INTGRL(C.658,DP*DOT)
Q=INTGRL(C.0,QDOT)
A=INTGRL(C.41,ADOT)
TH=INTGRL(C.0636,THDOT)

```

* * RCLL-YAW EQUATIONS OF CONTROL LAW -----

```

NCSRT
IF (TIME.LE.5.0) GC TC 10
FC=3.14159*STEP(5.0)
Y2DOT=-4*Y2+3.356*NYB
IF (A.GT.1.0) GO TO 5

```

```

AE=1.0
AECCT=0.0
GO TO 6

```

5 CNT INUE

```

AE=A
AEDOT=ADOT

```

6

```

DYCDDT= 0.608*(Y2DOT+RCOT/57.3)-(AE/57.3)*(FDDT/57.3) *P/57.3)
-(AEDOT/57.3)*(P/57.3))+6.08*(Y2+R/57.3)-(AE/57.3) *P/57.3)
DYDOT= -188.4*CY+188.4*57.3*DYC
X1DOT= -8*X1-17.6*F+17.6*FC
Y1DOT= -5*X1+50.333E-3*(X1DOT-PDOT/57.3)+0.755*(X1-P/57.3)
X2DOT= -6*X2+0.078*PDCT/57.3
DRCDOT= -1E*DRC+1.0425*(Y1DOT-X2DOT)+62.55*(Y1-X2)
DRDOT= -1E.4*DR+188.4*57.3*DRC

```

* * RCLL-YAW EQUATIONS OF AERODYNAMIC MODEL -----

```

NYB=QC*S*(CYBA*B+CYDYA*DY)/W
BCDT=K*(NYB)+A*P/57.3-R
RDOT=-Q*(P/57.3)+57.3*QD*S*D*(CNBA*B+CNDYA*DY)/IZZ
PCDT=57.3*CC*S*D*CLDRA*DR/IXX
FC=F*57.3
KIN=-P*B/57.3
INER=R*P/57.3

```


* *
INTEGRATION
* *

Y2=INTGRL(C.0, Y2DOT)
DYC=INTGRL(0.0, DYCDOT)
DY=INTGRL(0.0, DYDOT)
X1=INTGRL(C.0, X1DOT)
Y1=INTGRL(0.0, Y1DOT)
X2=INTGRL(C.0, X2DOT)
DRC=INTGRL(0.0, DRCDOT)
DR=INTGRL(C.0, DRDOT)
B=INTGRL(C.0, BCOT)
R=INTGRL(0.0, RDOT)
P=INTGRL(0.0, PCOT)
F=INTGRL(C.0, FDOT)

10 CONTINUE

* *
ACHIEVED INERTIAL ACCELERATION
* *

NZ=NZB*COS(F)+NYB*SIN(F)

TERMINAL
RANGE KIN, INNER
PRINT KIN, INER
TIMER FIN, TIME, KIN
OUTPUT XYPLCT
OUTPUT TIME, INNER
OUTPUT XYPLCT
OUTPUT TIME, NZ, NZB, NYB
OUTPUT XYPLCT
OUTPUT TIME, Q, P, R, FD
PAGE XYPLCT
END
STOP
ENDJCB
/*

OUTDEL=0.05, DELMIN=0.5E-8


```

FUNCTION CLB = (-4.0,0.0035),(0.0,0.0),(4.0,-0.0029),(4.0,-0.0029),...
(6.0,-0.0040),(8.0,-0.0065),(12.0,-0.011),...
(20.0,-0.02)
FUNCTION CNB = (-4.0,-0.025),(0.0,-0.027),(4.0,-0.025),...
(6.4,-0.024),(8.0,-0.021),(12.0,-0.016),...
(20.0,-0.005)
FUNCTION CYB = (-4.0,-0.069),(0.0,-0.065),(4.0,-0.068),...
(5.9,-0.07),(12.0,-0.088),(20.0,-0.11)
FUNCTION CNDY = (-4.0,-0.05),(0.0,-0.05),(6.2,-0.050),...
(8.0,-0.0515),(12.0,-0.055),(20.0,-0.062)
FUNCTION CLDY = (-4.0,0.007),(0.0,0.007),(4.0,-0.0050),...
(8.0,-0.0120),(12.0,-0.0200),(20.0,-0.0375)
FUNCTION CYDY = (-4.0,0.021),(0.0,0.021),(4.0,0.021),...
(6.4,0.0212),(8.0,0.022),(12.0,0.0241),...
(20.0,0.028)
FUNCTION CLDR = (-4.0,0.0323),(0.0,0.0310),(4.0,0.0325),...
(8.0,0.0342),(10.0,0.0351),(12.0,0.0369),...
(20.0,0.0435)
FUNCTION CNDR = (-4.0,-0.007),(0.0,0.0),(4.0,0.0065),...
(8.0,0.0140),(10.5,0.019),(16.0,0.0345),...
(20.0,0.0435)
FUNCTION CNACP, -10.0 = (-4.0,-0.90),(0.0,-0.35),(4.0,0.20),...
(8.0,0.82),(10.0,1.2),(12.0,1.48),(16.0,2.20),...
(20.0,3.75)
FUNCTION CNACP, 0.0 = (-4.0,-0.55),(0.0,-0.05),(4.0,0.58),...
(8.0,1.25),(12.0,1.92),(16.0,2.70),(20.0,3.5),...
(24.0,4.30)
FUNCTION CNACP, 10.0 = (-4.0,-0.15),(0.0,0.45),(4.0,1.05),...
(8.0,1.70),(12.0,2.40),(16.0,3.10),(20.0,4.0),...
(24.0,4.90)
FUNCTION CMADP, -10.0 = (-4.0,1.095),(0.0,0.88),(4.0,0.670),...
(8.0,0.42),(10.0,0.29),(12.0,0.20),(16.0,-0.050),...
(20.0,-0.30),(24.0,-0.60)
FUNCTION CMADP, 0.0 = (-4.0,0.23),(0.0,0.02),(4.0,-0.20),...
(8.0,-0.44),(12.0,-0.71),(16.0,-1.05),(20.0,-1.40),...
(24.0,-1.95)
FUNCTION CMACP, 10.0 = (-4.0,-0.55),(0.0,-0.82),(4.0,-1.10),...
(8.0,-1.40),(12.0,-1.80),(16.0,-2.2),(20.0,-2.75),...
(24.0,-3.45)

```

```

DYNAMIC
CLBA=AFGEN(CLB,A)
CNBA=AFGEN(CNB,A)
CYBA=AFGEN(CYB,A)
CLCYA=AFGEN(CLDY,A)
CLCYA=AFGEN(CLDY,A)
CLCYA=AFGEN(CLDY,A)
CLDRA=AFGEN(CLDR,A)
CNLRA=AFGEN(CNDR,A)

```



```
CN=TWCVAR(CNACP,A,DP)
CM=TWKVAR(CMACP,A,DP)
```

```
* *
COMMAND FOR CIRCULAR AIRFRAME -----
```

```
NZC= -2.0*STEP(0.0)+2.0*STEP(3.0)
NC=  NZC -COS(TH)
```

```
* *
PITCH EQUATIONS OF CCNTRCL LAW -----
```

```
XDCT= -150.0*X+150*NZB
Y3DCT= Y4-958.C4E-3*(NC-X)
Y4DOT= -5*Y4+4.653*(NC-X)
DFDCT= -0.143*DPC-340.58E-3*Y3DOT+340.58E-3*(QDCT/57.3)- ...
DPCCT= -188.4*CP+188.4*57.3*DPC
```

```
* *
PITCH EQUATIONS OF AERCCYDYNAMIC MODEL -----
```

```
NZB= -QD*S*CN/W
QCCT=(P/57.3)*R+57.3*QD*S*D*CM/IYY
ALCCT=Q+K*NZB-(P/57.3)*B
THDCTI=(Q/57.3)*COS(F)-(R/57.3)*SIN(F)
X=INTGRL(C.0,XCCT)
Y3=INTGRL(0.0,Y3DCT)
Y4=INTGRL(0.0,Y4DCT)
DPC=INTGRL(0.0,DPCDCT)
DF=INTGRL(0.0,DFDCT)
A=INTGRL(0.0,ACCT)
TF=INTGRL(0.0,THDCT)
```

```
* *
RCLL-YAW EQUATIONS OF CCNTRCL LAW -----
```

```
NCSORT
IF (TIME.LE.3.0) GO TO 10
FC= 2.14159*STEP(3.0)
Y2CCT=-5*Y2+1.6*NYB
IF (A.GT.1.0) GC TO 5
  AE=1.0
  AEDOT=0.0
  GC TO 6
  AE=A
```

```
5 CONTINUE
```



```

AEDOT=ADOT
6 CCNTINUE
CYCCCT= 0.485*(Y2DJT+RDCT/57.3-0.458*((AE/57.3)*PDCT/57.3 + *P/57.3)
      + (AEDOT/57.3)*P/57.3)+4.85*(Y2+R/57.3-0.458*(AE/57.3)*P/57.3)
DYDCT= -188.4*CY+188.4*57.3*DYC
X1DCT= -8*X1-17.6*F+17.6*FC
Y1DCT= -5*Y1+5C.33E-3*(X1DCT-PDCT/57.3)
X2DCT= -6*X2+C.078*PDCT/57.3
CRCCCT= -15*DRC+0.25*(Y1DCT-X2DCT)+15*(Y1-X2)
DRDCT= -188.4*DR+188.4*57.3*DRC

```

```

* *
* RCLL-YAW EQUATICNS OF AERCDYNAMIC MODEL
* *

```

```

NYB=GD*S*(CYBA*B+CYDYA*CY)/W
BDCT=K*NYB+A*P/57.3-R
RDCT= -Q*P/57.2+(57.3*QD*S*D*(CNBA*B+CNDYA*DY+CNDR*DR))/IZZ)
PDCT=57.3*QD*S*D*(CLBA*B+CLUYA*DY+CLDRA*DR)/IXX
FLCT=P/57.3
FC=F*57.3
KIN= -(R*B/57.3)
INER=R*P/57.3

```

```

* *
* INTEGRATION
* *

```

```

Y2=INTGRL(0.0,Y2DCT)
CYC=INTGRL(0.0,CYCDOT)
DY=INTGRL(0.0,DYDCT)
X1=INTGRL(0.0,X1DCT)
Y1=INTGRL(0.0,Y1DCT)
X2=INTGRL(0.0,X2DCT)
DR=INTGRL(0.0,DRDCT)
B=INTGRL(0.0,BDCT)
P=INTGRL(0.0,PDCT)
F=INTGRL(0.0,FLCT)

```

```

10 CCNTINUE

```

```

* *
* ACPIEVED MANUEVER ACCELERATION
* *

```

```

NZ=NZB*COS(F)+NYB*SIN(F)

```

```

* *
* TERMINAL
* RANGE NZ,NZB,NYB,A,B,Q,R,P,FD,DP,DY,DR
* PRINT NZ,NZB,A,B,Q,R,P,FD

```



```

TIMER FINTIME=6.0, OUTDEL=0.05, DELMIN=0.5E-8
METHOD MILINE
CLTPEUT TIME, A,B
PAGE XY PLCT
CLTPEUT TIME, DP,DY,DR
PAGE XY PLOT,NZ
CLTPEUT TIME,K IN
PAGE XY PLOT, INER
PAGE XY PLCT
ENC
STCP
ENDJCE
/*

```



```

FUNCTION CYB = (-4.0,-0.069),(0.0,-0.065),(4.0,-0.068),...
FUNCTION CNDY = (5.9,-0.07),(12.0,-0.088),(20.0,-0.11),...
FUNCTION CLDY = (8.0,-0.0515),(12.0,-0.055),(20.0,-0.062),...
FUNCTION CYDY = (-4.0,-0.021),(0.0,-0.021),(4.0,-0.021),...
FUNCTION CLDR = (20.0,-0.028),(8.0,-0.022),(12.0,-0.024),...
FUNCTION CNDR = (-4.0,-0.0323),(0.0,-0.0310),(4.0,-0.0325),...
FUNCTION CNADP = (-4.0,-0.0435),(10.0,-0.0351),(12.0,-0.0369),...
FUNCTION CNADP = (-4.0,-0.007),(10.5,-0.019),(4.0,-0.0065),...
FUNCTION CNADP = (-4.0,-0.090),(0.0,-0.090),(4.0,-0.090),...
FUNCTION CNADP = (-4.0,-0.21),(12.0,-0.148),(16.0,-0.220),...
FUNCTION CNADP = (-4.0,-0.375),(24.0,-0.375),...
FUNCTION CNADP = (-4.0,-0.55),(0.0,-0.05),(4.0,-0.58),...
FUNCTION CNADP = (-4.0,-0.92),(12.0,-0.92),(16.0,-0.92),...
FUNCTION CNADP = (-4.0,-0.15),(0.0,-0.45),(4.0,-0.15),...
FUNCTION CNADP = (-4.0,-0.40),(12.0,-0.40),(16.0,-0.40),...
FUNCTION CNADP = (-4.0,-0.095),(0.0,-0.88),(4.0,-0.670),...
FUNCTION CNADP = (-4.0,-0.30),(24.0,-0.60),...
FUNCTION CNADP = (-4.0,-0.23),(0.0,-0.02),(4.0,-0.20),...
FUNCTION CNADP = (-4.0,-0.44),(12.0,-0.71),(16.0,-1.05),(20.0,-1.40),...
FUNCTION CNADP = (-4.0,-0.55),(0.0,-0.82),(4.0,-1.10),...
FUNCTION CNADP = (-4.0,-1.40),(12.0,-1.80),(16.0,-2.2),(20.0,-2.75),...
FUNCTION CNADP = (-4.0,-3.45)

```

```

DYNAMIC
CLBA=AFGEN(CLB,A)
CNBA=AFGEN(CNB,A)
CYBA=AFGEN(CYB,A)
CLDYA=AFGEN(CLDY,A)
CNDYA=AFGEN(CNDY,A)
CYDYA=AFGEN(CYDY,A)
CLDRA=AFGEN(CLDR,A)
CN=TWQVAR(CNADP,A,DP)
CN=TWQVAR(CNADP,A,CP)

```

 COMMAND FOR CIRCULAR AIRFRAME

NZC= -2.0*STEP(0.0)+2.0*STEP(3.0)
NC= -CCS(TH)

* PITCH EQUATIONS OF CONTROL LAW

XDOT= -150.0*X+150*NZB
Y3DOT= Y4-1.3531*(NC-X)
Y4DOT= -5*Y4+6.572*(NC-X)
DPCDOT= -0.143*DPC-340.58E-3*Y3DOT+340.58E-3*(CDOT/57.3)- ...
DPDOT= -188.4*DP+188.4*57.3*DPC

* PITCH EQUATIONS OF AERODYNAMIC MODEL

NZB= -CD*S*CN/W
QDOT=(P/57.3)*R+57.3*QD*S*D*CM/IYY
ACOT=Q+K*NZB-(P/57.3)*#B
THDOT=(Q/57.3)*COS(F)-(R/57.3)*SIN(F)
X=INTGRL(0.0,XDOT)
Y3=INTGRL(C.0,Y3DOT)
Y4=INTGRL(C.0,Y4DOT)
DPC=INTGRL(0.0,DPCDOT)
DP=INTGRL(0.0,DPDOT)
Q=INTGRL(C.0,QDOT)
A=INTGRL(0.0,ADOT)
TH=INTGRL(0.0,THDOT)

* ROLL-YAW EQUATIONS OF CONTROL LAW

NCSORT
IF (TIME.LE.3.0) GC TC 10
FC= 3.14159*STEP(3.0)
Y2DOT=-5*Y2+1.6*NYB
IF (A.GT.1.0) GO TO 5

AEE=1.0
AECOT=C.0
GC TO 6

5 CONTINUE

AEDOT=ADOT

6 CONTINUE

DYCDOT= 0.485*(Y2DOT+RDOT/57.3-0.458*(AE/57.3)*PDOT/57.3 + P/57.3)
DYDOT= -188.4*DY+188.4*57.3*DYC
X1DOT= -8*X1-17.6*F+17.6*FC


```

Y1DDOT = -5*Y1+50.333E-3*(X1DDOT-PDDOT/57.3)+0.755*(X1-P/57.3)
X2DDOT = -6*X2+0.078*PDDOT/57.3
DRCCDOT = -15*RC+0.25*(Y1DDOT-X2DDOT)+15*(Y1-X2)
DRDDOT = -188.4*DR+188.4*57.3*DRC

```

ROLL-YAW EQUATIONS OF AERODYNAMIC MODEL

```

NYB=QD*S*(CYBA*B+CYDYA*DY)/W
BCOT=K*NYB+A*P/57.3-R
RDOT = -Q*P/57.3+(57.3*QD*S*D*(CNBA*B+CNDYA*DY+CNDRA*DR)/I ZZ)
PDDOT = 57.3*CC*S*D*(CLBA*B+CLDYA*DY+CLDRA*DR)/IXX
FDC = F*57.3
KIN = -(R*8/57.3)
INER = R*P/57.3

```

INTEGRATION

```

Y2=INTGRL(0.0,Y2DDOT)
DYC=INTGRL(0.0,DYCCDOT)
DX1=INTGRL(0.0,X1DDOT)
Y1=INTGRL(0.0,Y1DDOT)
X2=INTGRL(0.0,X2DDOT)
DR=INTGRL(0.0,DRDDOT)
B=INTGRL(0.0,BDDOT)
R=INTGRL(0.0,RDDOT)
P=INTGRL(0.0,PDDOT)
F=INTGRL(0.0,FDDOT)

```

10 CONTINUE

ACHIEVED MANUEVER ACCELERATION

NZ=NZB*CCS(F)+NYB*SIN(F)

```

TERMINAL
RANGE NZ,NZB,NYB,A,B,C,R,P,FD,DP,DY,DR,INER,KIN
PRINT NZ,NZB,NYB,A,B,Q,R,P,FD,DP,DY,DR
TIMER FIN TIME=6.0,OUTDEL=0.05,DELMIN=0.5E-12
METHOD MILINE
OUTPUT TIME,A,B
OUTPUT XYPLCT
OUTPUT TIME,DP,DY,DR
PAGE XYPLCT

```



```
* * * * *  
OUTPUT TIME,NZ,NZB,NYB  
PAGE XYPLCT  
OUTPUT TIME,KIN  
PAGE XYPLCT  
OUTPUT TIME,INER  
PAGE XYPLCT  
OUTPUT TIME,Q,R,P,FD  
PAGE XYPLCT  
END  
STOP  
ENDJCB  
/*
```



```

FUNCTION CNB = (-4.0,-0.025),(0.0,-0.027),(4.0,-0.025), ...
              (6.4,-0.024),(8.0,-0.021),(12.0,-0.016), ...
              (20.0,-0.005)
FUNCTION CYB = (-4.0,-0.069),(0.0,-0.065),(4.0,-0.068), ...
              (5.9,-0.07),(12.0,-0.088),(20.0,-0.11)
              (-4.0,-0.051),(0.0,-0.05),(6.2,-0.050), ...
FUNCTION CNDY = (-4.0,-0.0515),(12.0,-0.055),(20.0,-0.062)
              (8.0,-0.007),(0.0,0.007),(4.0,-0.0050), ...
FUNCTION CLDY = (8.0,-0.0120),(12.0,-0.0200),(20.0,-0.0375)
              (-4.0,0.021),(0.0,0.021),(4.0,0.021), ...
              (6.4,0.0212),(8.0,0.022),(12.0,0.024), ...
              (20.0,0.028)
FUNCTION CLDR = (-4.0,0.0323),(0.0,0.0310),(4.0,0.0325), ...
              (8.0,0.0342),(10.0,0.0351),(12.0,0.0369), ...
              (20.0,0.0435)
FUNCTION CNDR = (-4.0,-0.007),(0.0,0.0),(4.0,0.0065), ...
              (8.0,0.0140),(10.5,0.019),(16.0,0.0345), ...
              (20.0,0.0435)
FUNCTION CNADP1 = (-4.0,-0.90),(0.0,-0.35),(4.0,0.20), ...
              (8.0,0.82),(10.0,1.2),(12.0,1.48),(16.0,2.20), ...
              (20.0,3.75)
FUNCTION CNADP0 = (-4.0,-0.55),(0.0,-0.05),(4.0,0.58), ...
              (8.0,1.25),(12.0,1.52),(16.0,2.70),(20.0,3.5), ...
              (24.0,4.30)
FUNCTION CNADP100 = (-4.0,-0.15),(0.0,0.45),(4.0,1.05), ...
              (8.0,1.70),(12.0,2.40),(16.0,3.10),(20.0,4.0), ...
              (24.0,4.90)
FUNCTION CMADP1 = (-4.0,1.095),(0.0,0.88),(4.0,0.670), ...
              (8.0,0.42),(10.0,0.29),(12.0,0.20),(16.0,0.050), ...
              (20.0,-0.30),(24.0,-0.60)
FUNCTION CMADP0 = (-4.0,0.23),(0.0,0.02),(4.0,-0.20), ...
              (8.0,-0.44),(12.0,-0.71),(16.0,-1.05),(20.0,-1.40), ...
              (24.0,-1.95)
FUNCTION CMADP100 = (-4.0,-0.55),(0.0,-0.82),(4.0,-1.10), ...
              (8.0,-1.40),(12.0,-1.80),(16.0,-2.2),(20.0,-2.75), ...
              (24.0,-3.45)

```

```

DYNAM IC
CLBA=AFGEN(CLB,A)
CNBA=AFGEN(CNB,A)
CYBA=AFGEN(CYB,A)
CLDYA=AFGEN(CLDY,A)
CNDYA=AFGEN(CNDY,A)
CLDRA=AFGEN(CLDR,A)
CNDRA=AFGEN(CNDR,A)
CN=TWQVAR(CNADP,A,DP)
CM=TWQVAR(CMADP,A,CP)

```


* * COMMAND FOR CIRCULAR AIRFRAME -----

NZC= -2.0*STEP(0.0)+2.0*STEP(3.0)
 NC= NZC -COS(TH)

* * PITCH EQUATIONS OF CONTROL LAW -----

XDOT= -150.0*X+150*NZB
 Y3DOT= Y4-1.3531*(NC-X)
 Y4DOT= -5*Y4+6.572*(NC-X)
 DPCDOT= -0.143*DPC-340.58E-3*Y3DOT+340.58E-3*(QDOT/57.3)- ...
 DPDOT= -188.4*DP+188.4*57.3*DPC

* * PITCH EQUATIONS OF AERODYNAMIC MODEL -----

NZB= -QD*S*CN/W
 QDOT= 57.3*CC*S*D*CM/IYY
 ACOT= Q+K*NZB
 THDOT= (Q/57.3)*COS(F) - (R/57.3)*SIN(F)
 X= INTGRL(C.0, XDOT)
 Y3= INTGRL(C.0, Y3DOT)
 Y4= INTGRL(C.0, Y4DOT)
 DPC= INTGRL(C.0, DPCDOT)
 DP= INTGRL(C.0, DPDOT)
 Q= INTGRL(C.0, QDOT)
 A= INTGRL(C.0, ACOT)
 TH= INTGRL(C.0, THDOT)

* * RCLL-YAW EQUATIONS OF CONTROL LAW -----

NCSORT
 IF (TIME, LE, 3.0) GC TC 10
 FC= 3.14159*STEP(3.0)
 Y2DOT= -5*Y2+1.6*NYB
 IF (A, GT, 1.0) GO TO 5

AE=1.0
 AEDOT=0.0
 GC TO 6

5 CCNTINUE
 AE=A
 AEDOT=ADOT

6 CCNTINUE
 DYCDOT= 0.485*(Y2DCT+RCOT/57.3-0.458*(AE/57.3)*PDOT/57.3 + ...


```

(AE/57.3)*P/57.3)+4.85*(Y2+R/57.3-0.458*(AE/57.3)*P/57.3)
DYDOT = -188.4*DY+188.4*57.3*DYC
X1DOT = -8*X1-17.6*F+17.6*FC
Y1DOT = -5*Y1+50.333E-3*(X1DOT-PDOT/57.3)+0.755*(X1-P/57.3)
X2DOT = -6*X2+0.078*PDOT/57.3
DRCDOT = -15*DRC+0.25*(Y1DOT-X2DOT)+15*(Y1-X2)
DRDOT = -188.4*DR+188.4*57.3*DRC

```

** RCLL-YAW EQUATIONS OF AERODYNAMIC MODEL

```

NYB=QD*S*(CYBA*B+CYDYA*DY)/W
BCOT=K*NYB+A*P/57.3-R
RDOT = -Q*P/57.3+(57.3*QD*S*D*(CNBA*B+CNDYA*DY+CNDR*A*DR)/I ZZ)
PDOT = 57.3*CC*S*D*(CLBA*B+CLDYA*DY+CLDRA*DR)/I XX
FC=F*57.3
KIN = -(R*B/57.3)
INER = R*P/57.3

```

** INTEGRATION

```

Y2=INTGRL(C.0,Y2DOT)
DYC=INTGRL(C.0,DYCDOT)
DY=INTGRL(C.0,CYDOT)
X1=INTGRL(C.0,X1DOT)
Y1=INTGRL(C.0,Y1DOT)
X2=INTGRL(C.0,X2DOT)
DRC=INTGRL(C.0,DRCDOT)
DR=INTGRL(C.0,DRDOT)
B=INTGRL(C.0,BDOT)
R=INTGRL(C.0,RDOT)
P=INTGRL(C.0,PDOT)
F=INTGRL(C.0,FCOT)
10 CONTINUE

```

** ACHIEVED MANUEVER ACCELERATION

NZ=NZB*COS(F)+NYB*SIN(F)

```

TERMINAL
RANGE NZ,NZB,NYB,A,B,Q,R,P,FD,DP,DY,DR,KIN,INER
PRINTER NZ,NZB,NYB,A,B,Q,R,P,FD,DP,DY,DR
TIMER FIN TIME=6.0,OUTDEL=0.05,DELMIN=0.5E-12
METHOD MILINE
OUTPUT TIME,A,B

```



```

** ** ** ** **
PAGE XYPLCT, DP, DY, DR
OUTPUT TIME, NZ, NZ B
PAGE XYPLCT, KIN
OUTPUT TIME, INER
PAGE XYPLCT, QR, P, FD
PAGE XYPLCT
END
STOP
ENDJCB
/*

```


* FUNCTIONS OF DERIVATIVES

```

FUNCTION CLB = (-4.0,0.0,0.12), (4.0,-0.0,0.01), (10.0,-0.0,0.027), ...
              (16.0,-0.0,0.035), (20.0,-0.0,0.04)
FUNCTION CNB = (-4.0,0.0,0.238), (6.0,0.0,0.238), (10.0,0.0,0.24), ...
              (16.0,0.0,0.28), (20.0,0.0,0.31)
FUNCTION CYB = (-4.0,-0.0,0.48), (0.0,-0.0,0.42), (4.0,-0.0,0.47), ...
              (8.0,-0.0,0.52), (16.0,-0.0,0.06), (20.0,-0.0,0.065)
FUNCTION CNDY = (-4.0,-0.0,0.395), (0.0,-0.0,0.04), (10.0,-0.0,0.04), ...
              (12.0,-0.0,0.04), (20.0,-0.0,0.045)
FUNCTION CLDY = (-4.0,0.0,0.0025), (0.0,0.0,0.0005), (4.0,-0.0,0.002), ...
              (8.0,-0.0,0.007), (12.0,-0.0,0.012), (20.0,-0.0,0.023)
FUNCTION CYDY = (-4.0,0.0,0.01495), (0.0,0.0,0.01498), (4.0,0.0,0.015), ...
              (12.0,0.0,0.015), (20.0,0.0,0.019)
FUNCTION CLDR = (-4.0,0.0,0.225), (0.0,0.0,0.226), (4.0,0.0,0.228), ...
              (10.0,0.0,0.232), (16.0,0.0,0.27), (20.0,0.0,0.293)
FUNCTION CNDR = (-4.0,-0.0,0.034), (0.0,0.0,0.0), (5.2,0.0,0.05), ...
              (8.0,0.0,0.01), (16.0,0.0,0.025), (20.0,0.0,0.325)
FUNCTION CNACP = (-4.0,-1.05), (0.0,-0.2), (4.0,0.55), ...
              (8.0,1.45), (12.0,2.320), (16.0,3.25), (20.0,4.20), ...
              (24.0,5.3)
FUNCTION CNACDF = (-4.0,-0.80), (0.0,0.0,0.0), (4.0,0.776), ...
              (8.0,1.60), (12.0,2.55), (16.0,3.45), (20.0,4.5), ...
              (24.0,5.55)
FUNCTION CNACCP = (-4.0,-0.6), (0.0,0.20), (4.0,1.00), ...
              (8.0,1.88), (12.0,2.75), (16.0,3.70), (20.0,4.8), ...
              (24.0,5.80)
FUNCTION CMACP = (-4.0,0.5), (0.0,0.525), (4.0,0.620), ...
              (8.0,0.7), (12.0,0.80), (16.0,0.90), (20.0,1.00), ...
              (24.0,1.03)
FUNCTION CMADCP = (-4.0,-0.085), (0.0,0.0,0.0), (4.0,0.073), ...
              (8.0,0.125), (12.0,0.19), (16.0,0.2), (20.0,0.25), ...
              (24.0,0.2)
FUNCTION CMACCP = (-4.0,-0.620), (0.0,-0.525), (4.0,-0.495), ...
              (8.0,-0.4), (12.0,-0.395), (16.0,-0.405), (20.0,-0.495), ...
              (24.0,-0.685)

```

```

DYNAMIC
CLBA = AF GEN (CLB, A)
CNBA = AF GEN (CNB, A)
CYBA = AF GEN (CYB, A)
CLDYA = AF GEN (CLDY, A)
CYDYA = AF GEN (CYDY, A)
CLDRA = AF GEN (CLDR, A)
CNDRA = AF GEN (CNDR, A)
CA = TVCVAR (CNACP, A, DP)
CN = TVCVAR (CMACDF, A, DP)

```


* * *
 CCMAND FOR ELLIPTICAL AIRFRAME

NZC= -2.0*STEP(2.0)+2.0*STEP(5.0)
 NC= 0.940*NZC-0.913*COS(TH)

* * *
 EQUATIONS OF MODIFIED PITCH CONTROL LAW

XDCI= -150.0*X+150*NZB
 W1COT=W2-0.000232*(1.1053*NC-X)
 W2COT= -1.118E7*W1-6.18675*W2-0.47853*(1.1053*NC-X)
 Y=W1
 DP1DCI= DP2+K1*532.38182E3*(Y-ADOT/57.3)
 DP2DCI= -2067.85*DP2-K1*1.1008861E9*(Y-ADOT/57.3)
 LPC=CP1-K1*258.48*(Y-ADCI/57.3)
 DPCCT= -188.4*CP+188.4*57.3*DPC

* * *
 PITCH EQUATIONS OF AERODYNAMIC MODEL

NZE= -QD*S*CN/W
 CCCI=(P/57.3)*R+57.3*QD*S*D*CM/IYY
 ADCCT=Q+K*NZB-(P/57.3)*B
 TFDCT=(Q/57.3)*COS(F)-(R/57.3)*SIN(F)
 X=INTGRL(-1.0,XCOT)
 W1=INTGRL(0.0,20593368,W1DOT)
 W2=INTGRL(0.0,W2DOT)
 DP1=INTGRL(0.0,C1148,DP1DCT)
 DP2=INTGRL(0.0,DP2DOT)
 DF=INTGRL(0.658,DFDOT)
 Q=INTGRL(C.0,CCOT)
 A=INTGRL(2.41,ADOT)
 TH=INTGRL(0.0,636,THDCT)

* * *
 ROLL-YAW EQUATIONS OF CONTROL LAW

NCSCRT
 IF (TIME.LE.5.C) GO TO 10
 FC= 3.14159*STEP(5.0)
 Y2COT=-4*Y2+3.356*NYB
 IF (A.GT.1.0) GO TO 5
 AE=1.0
 AEDOT=0.0
 GO TO 6


```

5 CCN INUE
  AE=A
  AEDOT=0.0
6 CCN INUE
  DYDCCT= 0.608*(Y2DOT+RDCT/57.3-(AE/57.3)*(PDOT/57.3)
    -(AEDCT/57.3)*(P/57.3))+6.08*(Y2+R/57.3-(AE/57.3)*P/57.3)
  DYCCCT= -188.4*CY+188.4*57.3*DYC
  XIDCCT= -8*X1-17.6*F+17.6*FC
  Y1CCT= -5*Y1+50.333E-3*(X1DOT-PDOT/57.3)+0.755*(X1-P/57.3)
  X2DCCT= -6*X2+C.078*PDOT/57.3
  DRCCCT= -15*DRC+1.0425*(Y1DOT-X2DOT)+62.55*(Y1-X2)
  URCCCT= -188.4*DR+188.4*57.3*DRC
*
* RCLL-YAW EQUATICNS OF AERODYNAMIC MODEL
*
  NYB=QD*S*(CYBA*B+CYDYA*DY)/W
  BCCT=K*(NYB)+A*P/57.3-R
  RCCT= -Q*(P/57.3)+57.3*QC*S*D*(CNBA*B+CNDYA*DY+CNRA*DR)/IZZ
  FCCT=P/57.3
  FD=F*57.3
  KIN= -(P/57.3*B)
  INER=R*P/57.3
*
* INTEGRATION
*
  Y2=INTGRL(0.0,Y2DOT)
  DY=INTGRL(0.0,CYCDOT)
  DY=INTGRL(0.0,CYDOT)
  X1=INTGRL(0.0,X1DOT)
  Y1=INTGRL(0.0,Y1DOT)
  X2=INTGRL(0.0,X2DOT)
  DRC=INTGRL(0.0,DRCDOT)
  DR=INTGRL(0.0,DRDOT)
  B=INTGRL(0.0,BCOT)
  R=INTGRL(0.0,RCOT)
  P=INTGRL(C.0,PCOT)
  F=INTGRL(0.0,FCOT)
10 CCN INUE
*
* AC FIEVED INERTIAL ACCELERATION
*
  NZ=NZE*CO S(F)+NYB*SIN(F)
  TERMINAL

```



```
RANGE NZ, KIN, INER  
PRINT NZ, KIN, INER  
TIMER FIN TIME=8.0, OUTDEL=0.050, DELMIN=0.5E-8  
METFCD MILNE  
CLTPUT TIME, KIN  
PAGE XYPLCT  
OUTPUT TIME, INER  
END  
STCP  
ENDJCB  
/ #
```



```

FUNCTION CNB = (-4.0,-0.025),(0.0,-0.027),(4.0,-0.025), ...
              (6.4,-0.024),(8.0,-0.021),(12.0,-0.016), ...
              (20.0,-0.005)
FUNCTION CYB = (-4.0,-0.069),(0.0,-0.065),(4.0,-0.068), ...
              (5.9,-0.07),(12.0,-0.088),(20.0,-0.11)
              (-4.0,-0.05),(0.0,-0.05),(6.2,-0.050), ...
FUNCTION CNDY = (8.0,-0.0515),(12.0,-0.055),(20.0,-0.062)
              (-4.0,-0.007),(0.0,0.0007),(4.0,-0.0050), ...
FUNCTION CLDY = (8.0,-0.0120),(12.0,-0.0200),(20.0,-0.0375)
              (-4.0,0.021),(0.0,0.021),(4.0,0.021), ...
              (6.4,0.0212),(8.0,0.022),(12.0,0.0241), ...
              (20.0,0.028)
FUNCTION CLDR = (-4.0,0.0323),(0.0,0.0310),(4.0,0.0325), ...
              (8.0,0.0342),(10.0,0.0351),(12.0,0.0369), ...
              (20.0,0.0435)
FUNCTION CNDR = (-4.0,-0.007),(0.0,0.0),(4.0,0.0065), ...
              (8.0,0.0140),(10.5,0.019),(16.0,0.0345), ...
              (20.0,0.0435)
FUNCTION CNADP, -10.0 = (-4.0,-0.90),(0.0,-0.35),(4.0,0.20), ...
              (8.0,0.82),(12.0,1.48),(16.0,2.20),(20.0,2.97), ...
              (24.0,3.75)
FUNCTION CMADP, 0.0 = (-4.0,-0.55),(0.0,-0.05),(4.0,0.58), ...
              (8.0,1.25),(12.0,1.92),(16.0,2.70),(20.0,3.5), ...
              (24.0,4.30)
FUNCTION CMADP, 10.0 = (-4.0,-0.15),(0.0,0.45),(4.0,1.05), ...
              (8.0,1.70),(12.0,2.40),(16.0,3.10),(20.0,4.0), ...
              (24.0,4.90)
FUNCTION CMADP, -10.0 = (-4.0,0.1095),(0.0,0.88),(4.0,0.670), ...
              (8.0,0.42),(12.0,0.20),(16.0,-0.050),(20.0,-0.30), ...
              (24.0,-0.60)
FUNCTION CMADP, 0.0 = (-4.0,0.23),(0.0,0.02),(4.0,-0.20), ...
              (8.0,-0.44),(12.0,-0.71),(16.0,-1.05),(20.0,-1.40), ...
              (24.0,-1.95)
FUNCTION CMADP, 10.0 = (-4.0,-0.55),(0.0,-0.82),(4.0,-1.10), ...
              (8.0,-1.40),(12.0,-1.80),(16.0,-2.2),(20.0,-2.75), ...
              (24.0,-3.45)

```

```

DYNAMIC
CLBA=AFGEN(CLB,A)
CLBA=AFGEN(CNB,A)
CYBA=AFGEN(CYB,A)
CLDYA=AFGEN(CLDY,A)
CYDYA=AFGEN(CYDY,A)
CLDRA=AFGEN(CLDR,A)
CNDRA=AFGEN(CNDR,A)
CA=TWQVAR(CMADP,A,CP)
CM=TWCVAR(CMADP,A,CP)

```


* * CCMAND FCF CIRCULAR AIRFRAME -----

NZC= -2.0*STEP(0,0)+2.0*STEP(3.0)
 NZC= NZC -CGS(TH)

* * PITCH EQUATIONS OF CONTROL LAW -----

XCOI= -150.0*X+150*NZB
 W1DOT= W2-KA*0.02288*(NC-X)
 W2DOT= W3-KA*34.850*(NC-X)
 W3DOT= -0.591237*W2-5.11827*W3+KA*173.385*(NC-X)
 Y2= W1
 DFI1DOT= DP2+K1*48896.08381*(Y3-A/57.3)
 DP2DOT= -214.4733*DP1-1499.9535*DP2-K1*73.334853E6*(Y3-A/57.3)
 DP1= DP1-K1*32.7439*(Y3-A/57.3)
 DPDOT= -188.4*CP+188.4*57.3*DPC

* * PITCH EQUATIONS OF AERODYNAMIC MODEL -----

NZB= -QD*S*CN/W
 QDOT= (P/57.3)*R+57.3*CC*S*D*CM/IYY
 ADOT= Q+K*NZB-(P/57.3)*B
 THDOT= (Q/57.3)*COS(F)-(R/57.3)*SIN(F)
 X= INTGRL(C.0,XDOT)
 W1= INTGRL(C.0,W1DOT)
 W2= INTGRL(C.0,W2DOT)
 W3= INTGRL(C.0,W3DOT)
 DP1= INTGRL(C.0,DP1DOT)
 DP2= INTGRL(C.0,DP2DOT)
 Q= INTGRL(C.0,QDOT)
 A= INTGRL(C.0,ADOT)
 TH= INTGRL(C.0,THDOT)

* * RCLL-YAW EQUATIONS OF CONTROL LAW -----

NCSORT
 IF (TIME.LE.3.0) GO TO 10
 FCF= 3.14159*STEP(3.0)
 Y2DOT= -5*Y2+1.6*NYB
 IF (A.GT.1.0) GO TO 5
 AE= 1.0
 AEDOT= C.0
 GC TO 6


```

5 CCNTINUE
  AE=A
  AEDOT=ADCT
6 CCNTINUE
  DYCDOT= 0.485*(Y2DCT+RDOT/57.3-((AE/57.3)*PDOT/57.3+(AE/57.3)*P/57.3)
  (AEDOT/57.3)*P/57.3)+4.85*(Y2+R/57.3)*DYC
  DYDOT= -188.4*DY+188.4*57.3*DYC
  X1DOT= -8*X1-17.6*F+17.6*FC
  Y1DOT= -5*Y1+50.333E-3*(X1DOT-PDOT/57.3)+0.755*(X1-P/57.3)
  X2DOT= -6*X2+0.078*PDOT/57.3
  DRCDOT= -15*CR+0.25*(Y1DOT-X2DOT)+15*(Y1-X2)
  DRDOT= -188.4*DR+188.4*57.3*DRC

* RCLL-YAW EQUATIONS OF AERODYNAMIC MODEL -----
*
NYB=QD*(CYBA*B+CYDYA*DY)/W
BCOT=K*NYB+A*P/57.3-R
RCOT=-Q*F/57.3+(57.3*QD*S*D*(CNBA*B+CNDYA*DY+CNDRADR)/I ZZ)
PDOT=57.3*QD*S*D*(CLBA*B+CLDYA*DY+CLDRA*DR)/IXX
FCOT=P/57.3
FD=F*57.3
KIN=-R*B/57.3
INER=R*P/57.3

* INTEGRATION -----
*
Y2=INTGRL(C.0,Y2DOT)
DYC=INTGRL(C.0,DYCDOT)
DY=INTGRL(C.0,DYDOT)
X1=INTGRL(C.0,X1DOT)
Y1=INTGRL(C.0,Y1DOT)
X2=INTGRL(C.0,X2DOT)
DRC=INTGRL(C.0,DRCDOT)
DR=INTGRL(C.0,DRDOT)
B=INTGRL(C.0,BCOT)
R=INTGRL(C.0,RCOT)
P=INTGRL(C.0,PDOT)
F=INTGRL(C.0,FCOT)
10 CONTINUE

* ACHIEVED INERTIAL MANEUVER ACCELERATION -----
*
NZ=NZB*COS(F)+NYB*SIN(F)

* TERMINAL RANGE NZ

```



```
PRINT NZ  
TIMER FIN TIME=6.0, OUTDEL=0.05, DELMIN=0.5E-12  
METHOD MILAE  
OUTPUT TIME, KIN  
PAGE XYPLCT  
OUTPUT TIME, INER  
PAGE XYPLCT  
END  
STOP  
ENDJCB  
/*
```


APPENDIX K

CSPM PROGRAMS FOR MINIMIZATION OF KINEMATIC AND INERTIAL COUPLING

```

//LICLLIS JOB (0207,2111), 'THESIS TCP.', CLASS=G
// EXEC CSMPXV
// * MAIN ORG=NPGVM1.1862P
//X.FLOTPARM DD *
&PLCT SCALE=0.5 &END
//X.SYSIN DD *
*****
T I N O F I N E A R C B T T A U T O P I L C I S
E L L I Z E D I N E C O U P L I N G
N I N D I A
*****

```

DEFINITIONS OF VARIABLES OF NONLINEAR CBTT AUTOPILOT FOR ELLIP. ARF
 WITH MODIFIED PITCH CONTROL LAW FOR MINIMIZATION OF THE KINEMATIC
 INERTIAL CROSS-COUPLING.

```

N Z C : P I T C H N C R M A L A C C E L A R A T I O N C O M M A N D ( G E E S )
N Z E : I N E R T I A L P I T C H N C R M A L A C C E L A R A T I O N ( G E E S )
N Y B : B O D Y - F I X E D Y A W N C R M A L A C C E L A R A T I O N ( G E E S )
N A : A N G L E O F A T T A C K ( D E G )
B : S I D E S L I P A N G L E ( D E G )
Q : P I T C H A N G U L A R R A T E ( D E G / S E C )
R : Y A W A N G U L A R R A T E ( D E G / S E C )
P : R O L L A N G L E ( D E G )
F : R O L L A N G L E ( D E G )
D P C : P I T C H T A I L I N C I D E N C E C O M M A N D ( R A D )
D Y C : Y A W T A I L I N C I D E N C E ( D E G )
D R C : Y A W T A I L I N C I D E N C E C O M M A N D ( R A D )
D R C : R O L L T A I L I N C I D E N C E ( D E G )
D R C : F O L L T A I L I N C I D E N C E C O M M A N D ( R A D )

```

INITIAL
 PARAMETER QD=1650.0, K=0.480, S=3.141592, D=2.0, W=2475.0
 PARAMETER IZZ=853.0, IYY=790.0, IXX=110.0, KI=19.37

FUNCTIONS OF DERIVATIVES

**

```

FUNCTION CLB = (-4.0,0.012), (4.0,-0.01), (10.C,-0.027), ...
              (16.0,-0.035), (20.0,-0.04)
FUNCTION CNB = (-4.0,0.0238), (6.0,0.0238), (10.C,0.024), ...
              (16.C,0.028), (20.0,0.031)
FUNCTION CYB = (-4.0,-0.048), (0.0,-0.042), (4.0,-0.047), ...
              (8.0,-0.052), (16.0,-0.06), (20.0,-0.065), ...
              (-4.0,-0.052), (0.0,-0.04), (10.0,-0.04), ...
              (-4.0,-0.04), (20.0,-0.045)
FUNCTION CLDY = (-4.0,0.0025), (0.0,0.0005), (4.0,-0.002), ...
              (8.0,-0.007), (12.0,-0.012), (20.0,-0.023), ...
              (-4.0,0.007), (12.0,-0.012), (20.0,0.01498), (4.0,0.015), ...
              (-4.0,0.015), (20.0,0.019)
FUNCTION CLDR = (-4.0,0.0225), (0.0,0.0226), (4.0,0.0228), ...
              (10.0,0.0232), (16.0,0.027), (20.0,0.0293), ...
              (-4.0,-0.004), (0.0,0.0), (5.2,0.005), ...
              (8.0,0.01), (16.0,0.025), (20.0,0.0325), ...
              (-4.0,-1.05), (0.0,-0.2), (4.0,0.55), ...
              (-4.0,-1.05), (12.0,2.320), (16.0,3.25), (20.0,4.20), ...
              (24.0,5.3)
FUNCTION CNACP,0.0 = (-4.0,-0.80), (0.0,0.00), (4.0,0.776), ...
              (12.0,2.55), (16.0,3.45), (20.0,4.5), ...
              (24.0,5.55)
FUNCTION CNACFP,10.0 = (-4.0,-0.6), (0.0,0.20), (4.0,1.00), ...
              (12.0,2.75), (16.0,3.70), (20.0,4.8), ...
              (24.0,5.80)
FUNCTION CMACP,-10.0 = (-4.0,0.5), (0.0,0.525), (4.0,0.620), ...
              (8.0,0.7), (12.0,0.80), (16.0,0.90), (20.0,1.00), ...
              (24.0,1.03)
FUNCTION CMADP,0.0 = (-4.0,-0.085), (0.0,0.00), (4.0,0.073), ...
              (8.0,0.125), (12.0,0.19), (16.0,0.2), (20.0,0.25), ...
              (24.0,0.2)
FUNCTION CMACFP,10.0 = (-4.0,-0.620), (0.0,-0.525), (4.0,-0.495), ...
              (8.0,-0.4), (12.0,-0.395), (16.0,-0.405), (20.0,-0.495), ...
              (24.0,-0.685)

```

```

DYNAMIC
CLBA=AFGEN(CLE,A)
CNBA=AFGEN(CNE,A)
CYBA=AFGEN(CYB,A)
CLLYA=AFGEN(CLLY,A)
CNDYA=AFGEN(CNLY,A)
CYCYA=AFGEN(CYCY,A)
CLDRA=AFGEN(CLCR,A)
CNCR=AFGEN(CNCR,A)
CN=TWCVAR(CMACP,A,DP)
CN=TWCVAR(CMACP,A,DP)

```


* *

COMMAND FOR ELLIPTICAL AIRFRAME

NZC= -2.0*STEF(2.0)+2.0*STEP(5.0)
NC= C.8*NZC-0.913*COS(TH)

* *

PITCH EQUATIONS OF CCNTRCL LAW

XCCI= -15C.0*X+150*NZB
YDCT= -6*Y-0.2205*NC+0.48*X
DP1DCT= DP2+K1*532.38182E3*(Y-A/57.3)
DP2DCT= -2067.85*DP2-K1*1.1008861E9*(Y-A/57.3)
CPC=CPI-K1*258.48*(Y-A/57.3)
DPCCT= -188.4*CP+188.4*57.3*DPC

* *

PITCH EQUATIONS OF AERCDYNAMIC MODEL

NZB= -QD*S*CM/W
QCCT=(P/57.3)*R+57.3*QD*S*D*CM/IYY
ACCT=Q+K*NZB-(P/57.3)*8
TFCCT=(Q/57.3)*COS(F)-(R/57.3)*SIN(F)
X=INTGRL(-1.0,XCCT)
Y=INTGRL(C.042C593368,YDCT)
DF1=INTGRL(0.C1148,DP1DCT)
DP2=INTGRL(0.C,DP2DCT)
DP=INTGRL(0.658,DPDCT)
Q=INTGRL(0.0,QCCT)
A=INTGRL(2.41,ACCT)
TF=INTGRL(0.0,36,THDCT)

* *

RCLL-YAW EQUATIONS OF CCNTRCL LAW

NCSRT
IF (TIME.LE.5.C) GO TO 10
FC= 3.14159*STEP(5.0)
Y2DCT=-4*Y2+3.256*NYB
IF (A.GT.1.0) GO TO 5

AE=1.0
AEDOT=0.0
GC TO 6

5 CCNT INUE
AE=A

6 CCNT INUE
AEDOT=0.0


```

CYCDOCT= 0.608*(Y2DOOT+RDCT/57.3-(AE/57.3)*(P/57.3)*(P/57.3)+6.08*(Y2+R/57.3-(AE/57.3)*P/57.3)
DYCDOCT= -188.4*DY+188.4*57.3*DYC
XYCDOCT= -8*X1-17.6*F+17.6*FC
Y1CDOCT= -5*Y1+5C.333E-3*(X1DOOT-PDOOT/57.3)+0.755*(X1-P/57.3)
X2DOOT= -6*X2+C.078*PDOOT/57.3
XZDOCT= -15*DRCT+1.0425*(Y1DOOT-X2DOOT)+62.55*(Y1-X2)
YDOCT= -188.4*CR+188.4*57.3*DRC

```

** RCLL-YAW EQUATIONCS OF AERODYNAMIC MODEL -----

```

NYB=CD*S*(CYBA*B+CYDYA*CY)/W
RDCT=K*(NYB)+A*P/57.3-R
PLCCT=57.3*QD*S*D*(CLBA*B+CLDYA*DY+CLDRA*DR)/IXX
FCCT=F*57.3
KIN=-(P/57.3*E)
INER=R*P/57.3

```

** INTEGRATION -----

```

Y2=INTGRL(0.0,Y2DOOT)
CYC=INTGRL(0.0,CYCDOOT)
DY=INTGRL(0.0,DYDOOT)
Y1=INTGRL(0.0,X1DOOT)
Y1=INTGRL(0.0,Y1DOOT)
X2=INTGRL(0.0,X2DOOT)
DR=INTGRL(0.0,DRDOOT)
B=INTGRL(0.0,ECCT)
R=INTGRL(0.0,RCCT)
P=INTGRL(0.0,PCCT)
F=INTGRL(C.0,FCCT)
10 CCNTINUE

```

** ACHIEVED INERTIAL ACCELERATION -----

```

NZ=NZ* $\cos(F)$ +NYB*SIN(F)
TEFMINAL
RANGE NZ,KIN,INER
PRINT NZ,KIN,INER
TIMER FIN TIME=8.0,OUTDEL=0.050,DELMIN=0.5E-8
METHCD MILNE

```


CLTPUT TIME,KIN
PAGE XYPLCT
CLTPUT TIME,INER
PAGE XYPLCT
CLTPUT TIME,NZ
PAGE XYPLCT
EAC
STCP
ENDJCE
/*


```

FUNCTION CNB = (-4.0,-0.025),(0.0,-0.027),(4.0,-0.025), ...
(6.4,-0.024),(8.0,-0.021),(12.0,-0.016), ...
(20.0,-0.005)
FUNCTION CYB = (-4.0,-0.069),(0.0,-0.065),(4.0,-0.068), ...
(5.9,-0.07),(12.0,-0.088),(20.0,-0.11)
FUNCTION CNDY = (-4.0,-0.05),(0.0,-0.05),(6.2,-0.050), ...
(8.0,-0.0515),(12.0,-0.055),(20.0,-0.062)
FUNCTION CLDY = (-4.0,-0.007),(0.0,0.007),(4.0,-0.0050), ...
(8.0,-0.0120),(12.0,-0.0200),(20.0,-0.0375)
FUNCTION CYDY = (-4.0,0.021),(0.0,0.021),(4.0,0.021), ...
(6.4,0.0212),(8.0,0.022),(12.0,0.024), ...
(20.0,0.028)
FUNCTION CLDR = (-4.0,0.0323),(0.0,0.0310),(4.0,0.0325), ...
(8.0,0.0342),(10.0,0.0351),(12.0,0.0369), ...
(20.0,0.0435)
FUNCTION CNDR = (-4.0,-0.007),(0.0,0.0),(4.0,0.0065), ...
(8.0,0.0140),(10.5,0.019),(16.0,0.0345), ...
(20.0,0.0435)
FUNCTION CNADP,-10.0=(-4.0,-0.90),(0.0,-0.35),(4.0,0.20), ...
(8.0,0.82),(12.0,1.48),(16.0,2.20),(20.0,2.97), ...
(24.0,3.75)
FUNCTION CNADP,0.0=(-4.0,-0.55),(0.0,-0.05),(4.0,0.58), ...
(8.0,1.25),(12.0,1.92),(16.0,2.70),(20.0,3.5), ...
(24.0,4.30)
FUNCTION CNADP,10.0=(-4.0,-0.15),(0.0,0.45),(4.0,1.05), ...
(8.0,1.70),(12.0,2.40),(16.0,3.10),(20.0,4.0), ...
(24.0,4.90)
FUNCTION CMADP,-10.0=(-4.0,0.1095),(0.0,0.88),(4.0,0.670), ...
(8.0,0.42),(12.0,0.20),(16.0,-0.050),(20.0,-0.30), ...
(24.0,-0.60)
FUNCTION CMADP,0.0=(-4.0,0.23),(0.0,0.02),(4.0,-0.20), ...
(8.0,-0.44),(12.0,-0.71),(16.0,-1.05),(20.0,-1.40), ...
(24.0,-1.95)
FUNCTION CMADP,10.0=(-4.0,-0.55),(0.0,-0.82),(4.0,-1.10), ...
(8.0,-1.40),(12.0,-1.80),(16.0,-2.2),(20.0,-2.75), ...
(24.0,-3.45)

```

```

DYNAMIC
CLBA=AFGEN(CLB,A)
CNBA=AFGEN(CNB,A)
CYBA=AFGEN(CYB,A)
CLDYA=AFGEN(CLDY,A)
CYDYA=AFGEN(CNDY,A)
CLDRA=AFGEN(CLDR,A)
CNDRA=AFGEN(CNDR,A)
CN=TWCVAR(CNADP,A,DP)
CM=TWCVAR(CMADP,A,DP)

```



```

* COMMAND FOR CIRCULAR AIRFRAME
NZC= -2.0*STEP(0.0)+2.0*STEP(3.0)
NCC= NZC -CCS(TH)

* PITCH EQUATIONS OF CONTROL LAW
XCOT= -150.0*X+150*NZB
W1DOT= W2-KA*0.02288*(NC-X)
W2DOT= W3-KA*34.850*(NC-X)
W3DOT= -0.591237*W2-5.11827*W3+KA*173.385*(NC-X)
Y2= W1
DPCDOT= -0.143*DP C-34 C.58E-3*Y3DOT+34 C.58E-3*(ADOT/57.3)- ...
DPDOT= -188.4*DP+188.4*57.3*DPC

* PITCH EQUATIONS OF AERODYNAMIC MODEL
NZB= -QD*S*CN/W
QDOT= (P/57.3)*R+57.3*CC*S*D*CM/IYY
ADOT= Q+K*NZB-(P/57.3)*B
X= INTGRL(0.0,XDOT)
W1= INTGRL(C.0,W1DOT)
W2= INTGRL(C.0,W2DOT)
W3= INTGRL(C.0,W3DOT)
DP1= INTGRL(C.0,DP1DOT)
DP2= INTGRL(C.0,DP2DOT)
DP= INTGRL(C.0,DPDOT)
Q= INTGRL(C.0,QDOT)
A= INTGRL(C.0,ACDOT)

* ROLL-YAW EQUATIONS OF CONTROL LAW
NCSORT
IF (TIME.LE.3.0) GO TO 10
FC= 3.14159*STEP(3.0)
Y2DOT= -5*Y2+1.6*N YB
IF (A.GT.1.0) GO TO 5
  AEDOT= C.0
  GC TO 6
5 CCNTINUE
  AECOT= ADCT
6 CCNTINUE
  AECOT= 0.485*(Y2DOT+RDOT/57.3-((AE/57.3)*PDOT/57.3 +
  (AECOT/57.3)*P/57.3))+4.85*(Y2+R/57.3-(AE/57.3)*P/57.3)
DYDOT= -188.4*DY+188.4*57.3*DYC

```



```

X1DDOT = -8*X1-17.6*F+17.6*FC
Y1DDOT = -5*Y1+50.333E-3*(X1DDOT-PDOT/57.3)+0.755*(X1-P/57.3)
X2DDOT = -6*X2+0.078*PDOT/57.3
DRCDDOT = -15*DRC+0.25*(Y1DCT-X2DDOT)+15*(Y1-X2)
DRDDOT = -188.4*DR+188.4*57.3*DRC

```

* RCLL-YAW EQUATIONS OF AERODYNAMIC MODEL

```

NYB=QD*S*(CYBA*B+CYDA*DY)/W
BDDOT=K*NYB+A*P/57.3-R
RDDOT = -Q*P/57.3+(57.3*QD*S*D*(CNBA*B+CNDYA*DY+CNDRA*DR)/I ZZ)
PDDOT = 57.3*CD*S*D*(CLBA*B+CLDYA*DY+CLDRA*DR)/IXX
FC=F*57.3
KIN = -R*B/57.3
INER = R*P/57.3

```

* INTEGRATION

```

Y2=INTGRL(C.0, Y2DDOT)
DYC=INTGRL(C.0, DYCDOT)
DY=INTGRL(C.0, CYDDOT)
X1=INTGRL(C.0, X1DDOT)
Y1=INTGRL(C.0, Y1DDOT)
X2=INTGRL(C.0, X2DDOT)
DR=INTGRL(C.0, DRDDOT)
B=INTGRL(C.0, BDDOT)
R=INTGRL(C.0, RDDOT)
P=INTGRL(C.0, PDDOT)
F=INTGRL(C.0, FDDOT)

```

```

10 CONTINUE
THDDOT=(Q/57.3)*COS(F)-(R/57.3)*SIN(F)
TH=INTGRL(C.0, THDDOT)
NZ=NZB*COS(F)+NYB*SIN(F)

```

```

TERMINAL
RANGE NZ, INER, KIN
PRINT NZ, INER, KIN
TIMER FIN TIME=6.0, OUTDEL=0.05, DELMIN=0.5E-12
METHOD MILLER, KIN
METPU TIME, KIN
PAGE XYPLCT
OUTPU TIME, INER
PAGE XYPLCT
OUTPU TIME, NZ
PAGE XYPLCT
END
STOP

```


END JCB
/*

LIST OF REFERENCES

1. Graves, E.B., Aerodynamic Characteristics of a Mono Planar Missile Concept with Bodies of Circular and Elliptical Cross Sections, NASA TM 74079, December 1977.
2. Arrow, A, An Analysis of Aerodynamic Requirements for Coordinated Bank-To-Turn Autopilots NASA Contractor Report 3644, November 1982.
3. Riedel, F.W., Bank-To-Turn Control Technology Survey for Homing Missiles, NASA CR-3325, September 1983.
4. Reichert, R.T., Homing Performance Comparison of Selected Airframe Configurations Using Skid-to-turn and Bank-to-turn Steering Policies, NASA CR-3420, May 1981.
5. Ogata, Katshuhiko, Modern Control Engineering, 1970.
6. McRuer, Ashkenas and Graham, Aircraft Dynamic and Automatic Control, 1972.

BIBLIOGRAPHY

Dorf, R.C., Modern Control Systems, 1974.

Garnell, P., Guided Weapon Control Systems, 1980.

Kuo, Benjamin, Automatic Control System, 1982.

Roskam, Jan, Flight dynamics of Rigid and Elastic Airframes, 1976.

INITIAL DISTRIBUTION LIST

	No. Copies
1. Defense Technical Information Center Cameron Station Alexandria, Virginia 22314	2
2. Library, Code 0142 Naval Postgraduate School Monterey, California 93943	2
3. Department Chairman, Code 67 Department of Aeronautical Engineering Naval Postgraduate School Monterey, California 93943	1
4. Professor D.J. Collins, Code 67Co Department of Aeronautical Engineering Naval Postgraduate School Monterey, California 93943	3
5. Hellenic General Naval Staff 2nd Branch, Education Department Stratopedon Papagou Athens, GREECE	3
6. G.E.T.E.N Stratopedon Papagou Athens, GREECE	2
7. LT Lioulis Ioannis H.N PANAGIA ODIGITRIAS,7, PIRAEUS Athens, GREECE	5
8. Maj. Tiago DA Silva Ribeiro Centro Tecnico Aeroespacial Rua Pauraibuna S/N 12200 SAO Jose Dos Campos-SP SAO PAULO, BRAZIL	1
9. LT Chorianopoulos Man SMC 1863 Naval Postgraduate School Monterey, California 93943	1
10. LT Kyritsis-Spyromillos P. SMC 1154 Naval Postgraduate School Monterey, California 93943	1

207147

Thesis
L674
c.1

Lioulis

Design and analysis
of Coordinated Bank-
To-Turn (CBTT) auto-
pilots for Bank-TO-
Turn (BTT) missiles.

MAY 14 85
10 JAN 86

33034
33139

207147

Thesis
L674
c.1

Lioulis

Design and analysis
of Coordinated Bank-
To-Turn (CBTT) auto-
pilots for Bank-TO-
Turn (BTT) missiles.



